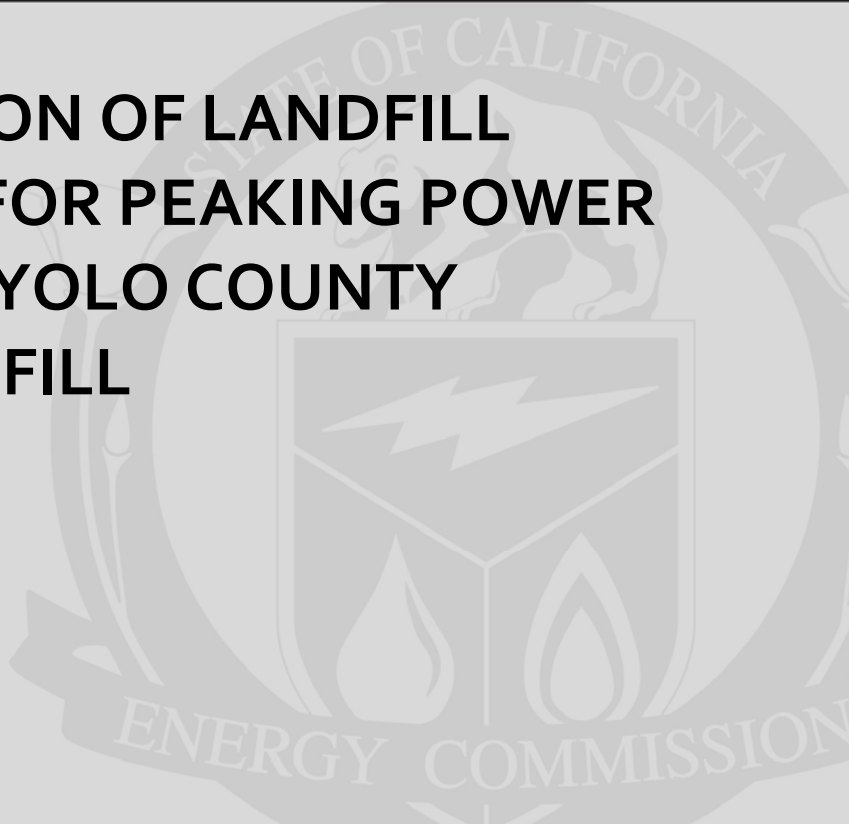**Energy Research and Development Division**
FINAL PROJECT REPORT

DEMONSTRATION OF LANDFILL TECHNOLOGY FOR PEAKING POWER POTENTIAL AT YOLO COUNTY CENTRAL LANDFILL

PREPARED BY:

Primary Author(s):
  Ramin Yazdani
  Don Augenstein
  Dr. Paul Imhoff
  Dr. Morton Barlaz

Yolo County Planning and Public Works
44090 County Road 28H
Woodland, CA 95766

Contract Number: 500-00-034

Prepared for:

California Energy Commission

Hassan Mohammed
Contract Manager

Linda Spiegel
Office Manager
Energy Generation Research Office

Laurie ten Hope
Deputy Director
ENERGY RESEARCH AND DEVELOPMENT DIVISION

Robert P. Oglesby
Executive Director

ACKNOWLEDGEMENTS

PREFACE

The California Energy Commission Energy Research and Development Division supports public interest energy research and development that will help improve the quality of life in California by bringing environmentally safe, affordable, and reliable energy services and products to the marketplace.

The Energy Research and Development Division conducts public interest research, development, and demonstration (RD&D) projects to benefit California.

The Energy Research and Development Division strives to conduct the most promising public interest energy research by partnering with RD&D entities, including individuals, businesses, utilities, and public or private research institutions.

Energy Research and Development Division funding efforts are focused on the following RD&D program areas:

- Buildings End-Use Energy Efficiency

- Energy Innovations Small Grants

- Energy-Related Environmental Research

- Energy Systems Integration

- Environmentally Preferred Advanced Generation

- Industrial/Agricultural/Water End-Use Energy Efficiency

- Renewable Energy Technologies

- Transportation

Demonstration of Landfill Technology for Peaking Power Potential at Yolo County Central Landfill is the final report for the SMUD ReGen Program (contract number 500-00-034) conducted by Yolo County Planning and Public Works Division of Integrated Waste Management. The information from this project contributes to Energy Research and Development Division's Renewable Energy Technologies Program.

For more information about the Energy Research and Development Division, please visit the Energy Commission's website at www.energy.ca.gov/research/ or contact the Energy Commission at 916-327-1551.

ABSTRACT

In this project a landfill with a new gas control system consisting of a permeable layer made of shredded tires plus a biocover was designed, constructed, and monitored to provide peaking power. The gas collection system was operated at variable diurnal extractions by operating on a 12-hour on-off extraction cycle. Gas output, gas composition (both collected and sampled from the landfills), and landfill surface gas emissions were monitored during the diurnal gas extraction. Computer modeling was performed to assist in designing this system and to analyze the effects of various changes in the design. Field and laboratory tests were conducted to validate the computer model for various operating conditions. The biocover material was characterized in laboratory and field tests. Field tests showed that various biocover configurations controlled fugitive methane emissions by promoting methane oxidation. However, biocovers did not perform as well in the wet season relative to the dry season rate of the biocover.

Field-scale experiments were conducted to assess the performance of two methanotrophic biocovers (compost wood chip mixture and green waste) under varying climatic conditions and a landfill gas collection vacuum. The green waste biocover performed better at oxidizing methane and reducing surface emissions than a compost mixed with woodchips, although there were greater emissions in the wet season than in the dry season due to surface cracks. A permeable horizontal tire layer beneath the surface helped distribute gas and limit fugitive methane emissions whether or not the landfill was operated in the "peaking" mode. The increase in surface methane emissions was limited to one percent without considering the biocover methane oxidation, which had been predicted by computer simulations during peaking operation.

TABLE OF CONTENTS

LIST OF FIGURES

LIST OF TABLES

EXECUTIVE SUMMARY

Introduction

Landfill gas (LFG) has an economic value in addition to its value as a carbon dioxide (CO_2)-neutral source of renewable energy when it is converted to electrical energy. Landfill gas can be used as a replacement for natural gas in distributed power generation systems and other applications, with a total landfill gas electric power generation potential of about 5 gigawatts of energy (GWe). Although LFG utilization has increased ten-fold in the past 15 years, only about 20 percent of its potential is actually used for electricity generation; a similar amount of the captured landfill gas is flared. The reasons for this low utilization rate are the unpredictability and variability of LFG available for fuel generation and the lower value for baseload power sold to the grid, which worsens the economics and increases the financial risk of developing and operating LFG recovery systems.

Today, LFG converted to electricity is collected at constant rates for fueling baseload power generation, which is the lowest value electricity. By comparison, pipeline gas-fired power plants can be operated as peaking power plants in response to the much higher value of peaking electricity. Other constraints are the availability of grid transmission at peaking power times and the transmission losses during power wheeling (up to 40 percent in sending power from Utah to California). These constraints make distributed peaking power generation highly advantageous. Landfill gas is generated from landfills near major population centers, significantly offsetting grid congestion. Finally, LFG is a renewable, green power source that is desired by many consumers even at premium prices. Few renewable energy sources can provide peaking power. Converting LFG systems from baseload to peaking power would improve the economics, allowing landfill gas energy systems to be profitable with less need for government subsidies or new regulatory drivers. This could greatly increase LFG use and result in a major reduction of greenhouse gases emitted in the United States, since landfill gas accounts for only five percent of total United States' fossil fuel CO_2 emissions. The economic drivers associated with peaking power operations could encourage rapid implementation of this technology, even within the next decade.

The peaking power technology used to convert landfill gas to electricity is to selectively remove methane gas at times of peak energy demand, with methane being "stored" within a permeable zone in the landfill at other times. Demonstrating that variable diurnal gas extraction is feasible without undue air intrusion or increased air emissions would allow widespread application of this technology.

Project Purpose

The overall objective of this project was to evaluate the feasibility of operating landfills in a peaking-power mode. This required varying the extraction rate of landfill gas during a 24 hour cycle, from zero to two-fold over the average rate of production.

Preliminary modeling indicated that peaking power operations should result in only minor increases in methane emissions (not accounting for biocover methane oxidation) if a horizontal tire layer is installed, and that the construction of a horizontal tire layer can *increase* the methane

12

collection efficiency by 50 percent over conventional (constant) pumping conditions without a tire layer. The horizontal tire layer was also expected to significantly *decrease* the intrusion of oxygen into the landfill.

Another goal of the project was demonstrating the use of a surface permeable layer and biocover instead of a soil and synthetic liner cover to control greenhouse gas emissions by natural oxidation of fugitive methane emissions.

Project Results

The usual approach to landfill gas recovery has been to use deep vertical wells attached to a network of pipes with a blower that provides vacuum. The profile of surface flux leads to landfill gas emissions away from the wells, resulting in inefficient landfill gas collection in the range of 60 to 85 percent.

In this project a landfill with a new gas permeable layer and gas extraction system with a biocover was designed, constructed, and operated at Yolo County Central Landfill using variable extraction rates on a 12-hour on-off cycle. Landfill gas composition and landfill gas emissions were measured at two pumping rates: 15 and 65 standard cubic feet per minute. This study examined the influence of various operational parameters on fugitive methane emissions and composition of the collected landfill gas. These model results were compared with field tests conducted in the peaking power test cell. The comparison of the computer simulations with field data collected to date suggested that the model is a reasonable representation of conditions in the field and supported the results obtained from the modeling exercise.

Modeling helped guide the design of the peaking power landfill test cell by estimating the influence of different operational parameters. Several important simulation cases were evaluated:

- The influence of biocover permeability on methane emission and oxygen intrusion.

- The effect of the pumping rate on methane emissions and oxygen intrusion into the landfill.

- The effect of the permeable layer near the landfill surface, specifically the depth and width of the tire layer on methane emissions and peaking power operation.

The project approach was to:

- Evaluate the feasibility of operating landfills in a peaking power mode.

- Operate and monitor the performance of the constructed permeable layer and gas extraction system in a landfill with biocover.

- Operate under the on-peaking and off-peaking mode for several months.

- Use collected data to compare performance of the cell to the performance predicted by a computer model.

The feasibility of peaking power operations was further evaluated in terms of its influence on methane emission and oxygen intrusion. It was estimated that substantial efficiency improvements over conventional extraction could be gained by combining a low permeability surface over an upper near-surface highly conductive layer with extraction by the deep well(s). This layer enabled essentially uniform pressure across the entirety of the conductive or permeable layer of the landfill. It greatly reduced fugitive emissions far from vertical wells. This method resulted in constant gas composition and high landfill gas quality (methane content) due to two factors: landfill gas mixing in passage through the waste to reach the deep well, and diffusion and dispersion results from the long transit time as it travels toward the extraction system.

From this analysis it seemed possible to *increase* the amount of landfill gas collected during peak energy demands above the assumptions in the base case simulations. The ratio of overpull to underpull pumping might be increased from two up to five with less than one percent increase in methane emissions above constant pumping conditions, which would be oxidized by the biocover construction as demonstrated in the field and laboratory experiments. In addition, it was clear that peaking power operation with a horizontal tire layer should result in both *increased* methane collection efficiencies and *reduced* methane emissions when compared to cases with standard vertical gas collection wells without horizontal tire layers.

The predicted trends in gas composition were in excellent agreement with measured trends in the field. This suggested that the computer model was a useful tool for evaluating the effects of various operational conditions on peaking power operations. Differences between model predictions and field measurements of methane concentration in the pumping well suggested leakage into the well through side slopes where the surface permeable layer was terminated. This could be mitigated by extending this surface permeable layer on all side slopes.

From these analyses, some of the more significant conclusions were:

Operating the landfill in peaking power mode resulted in only a one percent increase in methane emissions over normal (constant gas extraction) operations. This difference was likely too small to measure in the field and was consistent with field measurements using flux chambers. These simulations did not account for the oxidation of fugitive methane in the biocover, which may reduce fugitive methane emissions even more. Simulations indicated that molecular diffusion is the dominant mechanism controlling upward methane fluxes through the biocover.

When the time-averaged pumping rate was kept constant, it was possible to increase the ratio of overpull/underpull from two to five with minimal effect on oxygen intrusion or methane emissions. Thus, significantly greater overpull might be used to generate more electricity during daytime hours with minimal effect on methane collection efficiency.

The permeable horizontal tire layer near the top of the landfill worked as a distributor so that all the gases flowing through the layer became uniform. This feature would help to reduce fugitive methane emissions even if the landfill is not operated in peaking-power mode.

The original landfill design called for a horizontal tire layer near the top of the landfill that completely covered the landfill width. Simulations indicated that the tire layer could be considerably smaller while still mitigating fugitive methane emissions from peaking power operations. Lost capacity in the landfills from including a permeable layer could therefore be minimized by reducing the area covered by the tire layer.

Operating the pumping well in peaking power mode (with the tire layer at the top of the landfill) did *not* result in significant increases in methane emissions from the landfill. Fifteen and one-half percent of the methane generated escaped from the landfill when the landfill was operated at a constant pumping rate equal to the landfill gas generation rate. Only 16.1 percent of the methane generated escaped from the landfill during peaking power operations, when the pumping well was operated for 12 hours in overpull (pumping rate equal to 1.5 times the landfill gas generation rate) followed by 12 hours in underpull (pumping rate equal to 0.5 times the landfill gas generation rate). Significantly smaller amounts of methane would be predicted to escape into the atmosphere if the effect of methane oxidation in the biocover were included in the analysis.

Field and laboratory experiments were conducted to determine methane (CH_4) oxidation rates. In-field static chambers were used to sample emissions during rainy and dry seasons. The results of the landfill gas surface emissions testing showed that a maximum oxidation rate of 664.2 grams CH_4/meter^2 per day was achieved. This average CH_4 oxidation rate was comparable to reported oxidation rates for biocovers and higher than oxidation rates reported for soil covers. In laboratory columns, methane oxidation decreased as the flux or pressure gradient increased. The CH_4 flux exceeded the oxidation capacity of the laboratory experiments, presumably because there was insufficient retention time in regions where CH_4 and oxygen (O_2) mixed.

The addition of moisture to the laboratory columns was inhibitory for O_2 diffusion in the compost as evidenced by the reduced O_2 concentrations at depth in the water addition columns. This observation was consistent with the field methane emissions tests where the effect of climate was also significant. In the rainy season tests, there was a statistically significant decrease in CH_4 emissions when the gas system vacuum was increased for the covers with the highest emissions (0.91 meters compost plus wood chips, 0.31 meters compost and soil). In contrast, there was no change in CH_4 emissions associated with reduced gas collection system vacuum during the dry season tests. Thus, when the biocover was very wet its oxidative performance may be reduced and greater fugitive methane emissions might be expected.

These results suggested that it would be prudent to operate the gas system to maximize methane collection during periods when cover soils are saturated with moisture, since in this state CH_4 oxidation will likely be reduced. Further field tests are required to more precisely determine the extent to which reductions in gas collection vacuum for peaking power operations may be possible when the cover is saturated.

Project Benefits

California's landfilled waste tonnage for 2006 was about 42 million tons according to the California Integrated Waste Management website. The authors estimated that each ton of waste could fuel 0.25 megawatt-hours (MWh) or four tons of waste would yield one MWh. This estimate was based on the assumption that the recovery yield of methane with use of the highly efficient permeable layer would be 3,000 cubic feet per ton of "gate waste" as received at the landfill and that the heat rate of the GenSet prime mover was 12,000 British thermal units per kilowatt-hour.

If half of California's landfills or 20 million tons of waste were to operate under a peaking power mode, the total amount of power generated would be five million MWh. Assuming that this power was recovered over half days throughout the year (4,380 hours per year), the contribution of the "peaking landfill" would be 1,141 MW or about 1,100 MWe. While this comprises a relatively small number in the mix of total generation, it would provide over 10 percent of the daytime excess of power requirement over minimum nighttime use. This would be enough daytime power increment to satisfy the total electrical needs of four million Californians (out of a population near 40 million in 2012).

Economic benefits are difficult to determine. If the sale price were between 10 cents per kilowatt hour and 15 cents per kilowatt hour, however, the authors estimated that the gross revenue from peaking power would be between $500 million and $750 million per year for California.

The fueling of peaking power relative to constant rate baseload generation might not have much of an effect "up or down" on greenhouse gas emissions, all other things being equal. Natural gas fueled peaking plants tend to be older and less efficient, so the avoided CO_2 emissions from substituting landfill gas-fueled peaking power for natural gas-fueled peaking plants would be better than its substitution for conventional baseload power. Offsetting this is the fact that the peaking approach might lead to some limited, additional CO_2 emissions relative to constant-rate baseload power generation. The modeling and field data from this project showed that peaking may increase the incremental emissions but the biocover used will eliminate this increase in methane emissions relative to conventional generation.

This project's most promising result for abating greenhouse gases was the overall design incorporating permeable layers. Based on modeling and field measurements, the permeable layers could reduce emissions whether the extraction is for conventional baseload power or for peaking. Thus the permeable layer itself is worth pursuing on its own merits independent from peaking power

Chapter 1:
Introduction

Global warming is the direct consequence of the increase in the atmospheric concentration of greenhouse gases, including methane (CH_4), carbon dioxide (CO_2), ozone, nitrous oxide (NO_x), and chlorofluorocarbons (US EPA 2007). CH_4 is the most abundant hydrocarbon present in the atmosphere with an average concentration of 1.7 parts per million (ppm) (Le Mer and Roger 2001). It has 21 times the global warming potential of CO_2 by mass during a 100-year time period (U.S. EPA 2007) and atmospheric CH_4 has increased by a factor of 2 during the last century.

Methane is emitted to the atmosphere both from natural and anthropogenic sources. Natural sources include wetlands, tundra, bogs, swamps, termites, and wildfires. Major anthropogenic sources include landfills, natural gas and oil production and processing, coal mining and agriculture. In the United States, landfills are estimated to be the largest source of anthropogenic CH_4, accounting for 24 percent of anthropogenic CH_4 emissions (U.S. EPA 2007). A reduction in CH_4 emissions is a key objective of the U.S. Climate Change Action Plan (U.S. EPA 1999).

CH_4 and CO_2, which comprise more than 99 percent of landfill gas (LFG), are produced during the anaerobic decomposition of refuse in landfills. Unlike other greenhouse gases, CH_4 can be used to produce energy as it is the main component (95 percent) of natural gas. Despite its potential as a fuel resource, effective storage and collection of CH_4 can be a major challenge.

The major control on CH_4 emissions from landfills is to collect LFG and burn it in a flare or utilize it for energy recovery. Gas recovery systems can be an effective strategy to mitigate CH_4 emissions from landfills. Field studies have shown that CH_4 emissions decreased more than three orders of magnitude adjacent to recovery systems (Bogner et al. 1993). Reductions of 75 to 90 percent of the emitted CH_4 through the use of LFG recovery systems have been reported (Mosher et al. 1996).

CH_4 may also be oxidized in landfill covers by methanotrophic bacteria (Whalen et al. 1990; Kightley et al. 1995; Czepiel et al. 1995; Chanton and Liptay 2000; Borjesson et al. 2001). Reported values of CH_4 oxidation vary widely based on cover types, climatic conditions and presumably based on the LFG flow rate. Field studies show that CH_4 emissions fluctuate daily and seasonally and are affected by climate (Jones and Nedwell 1993; Borjesson and Svensson 1997; Kjeldsen et al. 1997). Landfill covers had been reported to oxidize CH_4 from about 7 percent to 50 percent of the total amount (Kightley et al. 1995; Gardner and Manley 1993). Czepiel et al. (1996) calculated 10 percent CH_4 oxidation in a landfill in the northeastern United States during a 12-month period in which temperature fluctuations were considered. Recently Barlaz et al. (2004) reported a mean CH_4 oxidation of 55 percent and 21 percent in a biologically active cover constructed of compost and soil, respectively. These values are conservative as a measure of methane oxidation is only possible when oxidation is less than 100 percent. In the referenced study, many tests had no measurable emission, implying 100 percent oxidation.

Moreover, nearly 100 percent oxidation had been reported in the literature (Kjeldsen et al. 1997). Even consumption of atmospheric CH_4 is possible under certain conditions (Bogner et al 1995; Borjesson et al. 1998; Barlaz et al. 2004).

When CH_4 is converted to electrical energy, it has an economic value in addition to its value as a CO_2-neutral source of renewable energy. Additionally, relating to the United States' energy security, landfill gas is usable as a replacement or extender of natural gas in distributed power generation systems and other applications, with a total LFG electric power generation potential of about 5 gigawatts of energy (GWe). This is almost 1 percent of current United States' generation capacity, potentially abating over 40 million tons of CO_2 annually from coal, or from burning 200,000 barrels of oil per day. An even greater amount of greenhouse gas is abated by the reduction of LFG methane emissions, estimated equivalent to about 200 million tons CO_2 (based on the EIA 1998 value of 9.8 Tg LFG methane emissions, 21-fold CH_4/CO_2 potency, and as detailed in Augenstein 2000 for the U.S. Department of Energy [DOE]). Landfill gas is also the fastest growing renewable source of energy in the United States, approaching 1,000 megawatts of energy (MWe). To the extent that the electricity can be sold during periods of peak demand, the CH_4 is most valuable.

Although landfill gas utilization increased ten-fold in the past 15 years, at present only about 20 percent of LFG potential is actually used for electricity generation or otherwise, with about an equal amount of the captured LFG being flared. Among reasons there is not greater beneficial use of already collected and available LFG, which is presently flared, are the unpredictability, variability, low rates, and long-term nature of landfill gas recovery (see for example Vogt and Augenstein 1997). All of these tend to worsen the economics and increase the risk of landfill gas recovery and utilization. As examples the unpredictable gas recovery makes projecting of landfill gas energy equipment more risky, generally resulting in under-sizing, leading to reduced landfill gas methane gas utilization, or over-sizing, and cost of idle equipment.

Landfill gas converted to electricity is collected at constant rates, fueling baseload power generation, the lowest value electricity. By comparison, pipeline gas-fired power plants can frequently serve as peaking power plants, due to the much higher value of peaking electricity, (even if the plant is idle for part of the time). Another constraint is the availability of grid transmission at peaking power times, and the transmission losses during power wheeling (up to 40 percent in sending power from Utah to California), making distributed peaking power generation highly advantageous. LFG is generated from landfills near the major population centers, significantly offsetting grid congestion. Finally, landfill gas is a renewable, green power source, desired by many consumers even at a premium. Few renewable energy sources can provide peaking power. Converting LFG systems from baseload to peaking power would improve economics, and allow LFG energy systems to be profitable with less need for government subsidy (i.e. IRS section 29 Tax Credits) or new regulatory drivers. This could greatly increase LFG use and result in a major decrease in greenhouse gases emitted in the United States, far in excess of just its renewable energy generation, approaching 5 percent of total United States' fossil CO_2 emissions. These economic drivers would also allow for rapid implementation of this technology, even within the next decade.

This technology would be applicable to both existing and new landfills, and appears useful in conjunction with the so-called "Controlled Bioreactor Landfill" technology developed by Yolo County and other investigators over the past decade (Augenstein et al. 2000; Augenstein et al. 2003). The Controlled Bioreactor Landfill technology, with funding from the California Energy Commission, California Integrated Waste Management Board, and the U.S. DOE National Energy Technology Laboratory, is described in more detail in Energy Commission PEIR Project 2.1 *Accelerated Anaerobic Composting for Energy Generation at Yolo County Central Landfill*. Landfill design modifications may also increase feasibility of peaking power and offer other advantages as well.

One promising idea for improving landfill gas to electricity is to selectively remove methane gas at times of peak energy demand, with methane being "stored" within a permeable zone in the landfill at other times. This project is to demonstrate that variable diurnal gas extraction is feasible in practice without undue air intrusion or increased air emissions, allowing widespread application of this technology.

1.1   Background and Overview

The usual approach to LFG recovery has been to use deep wells attached to a network of pipes with a blower that provides vacuum. To illustrate performance of conventional systems, gas flow dynamics with "conventional" well (or trench) extraction are shown qualitatively in Figure 1-1. Arrows in Figure 1-1 denote directions of gas fluxes, through (in and out of) a waste landfill surface, and within the waste. Gas flow velocity is denoted qualitatively by lengths of the arrows. Note the gas escaping to the atmosphere far from the wells. It is principally because of this LFG emission and loss far from the wells that gas capture is typically only 60 to 85 percent (SWANA 1994 on Landfill Gas Modeling and Recovery, 1994). Although this inefficiency exists, and is acknowledged by the U.S. Environmental Protection Agency (EPA) (Peer et al. 1991; ICF 2002) and California Air Resources Board, it has been in most cases accepted. The profile of surface flux is well recognized to lead to LFG emissions away from the wells under most circumstances. Note also that there is normally entrainment of gas, whether LFG or atmospheric air, through the surface area most proximate to, or over, deep collection. Both LFG emission far from wells, and air entrainment proximate to subsurface collection, are well recognized as deleterious to collection efficiency. A "tradeoff" exists between extracting or "pulling" at too high a flow rate and entraining excessive atmospheric air, and pulling too little and recovering less LFG.
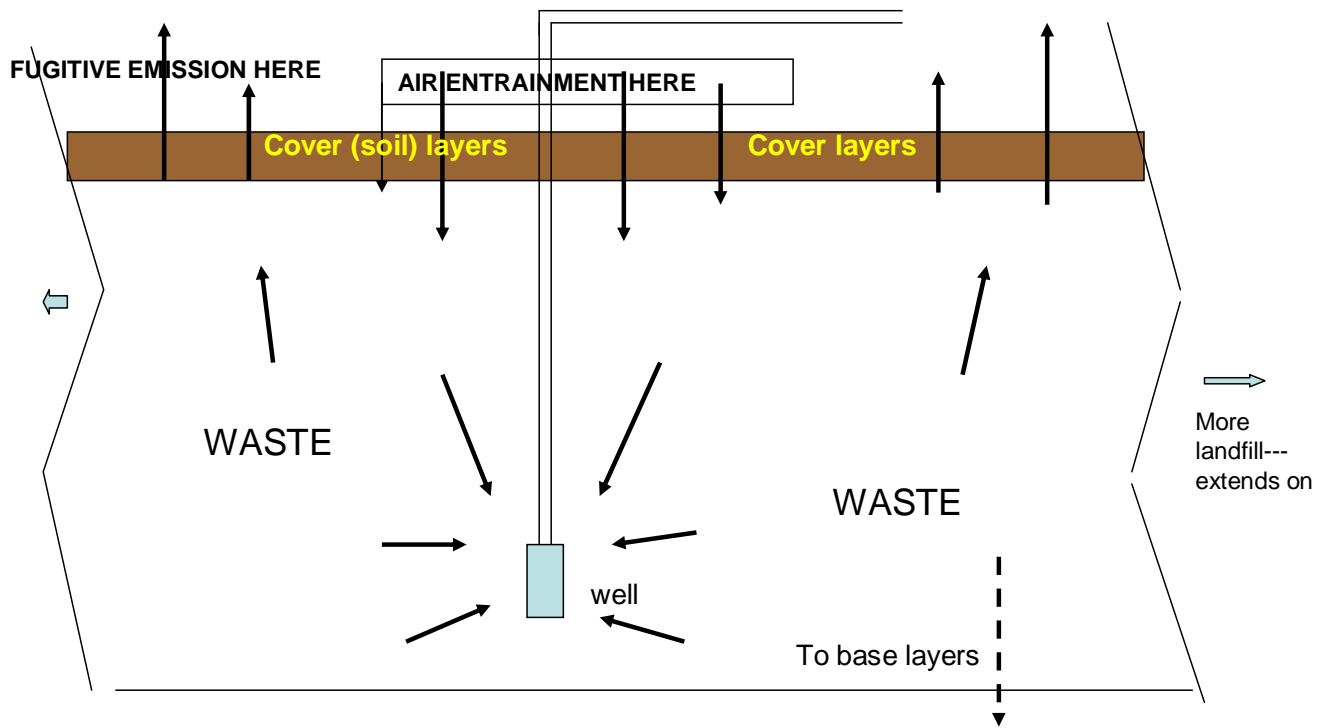
Figure 1-1. Conventional landfill gas (LFG) extraction and gas flows

Photo Credit: Yolo County Planning & Public Works Department

This investigation demonstrates substantial improvements over conventional extraction can be gained by combining a low permeability surface over an upper near-surface highly conductive layer with extraction by the deep well(s). A schematic is shown in Figure 1-2 below. Conductive or permeable layer (shred tires, rubble, gravel, etc.) that can be incorporated in landfills will normally be from three to five orders of magnitude more permeable than typical landfilled waste. This enables essentially uniform pressure across the entirety of the conductive or permeable layer "footprint", and can enable a uniform vertical pressure gradient through the surface layers of the landfill. This will in turn greatly reduce irregularities in vertical gas flow at the landfill surface. In other words, it will greatly reduce the air entrainment near vertical wells, and fugitive emission far from vertical wells, shown in Figure 1-1, that substantially impede efficiency of "conventional" extraction. Close control of extraction is possible through monitoring of LFG composition in the conductive layer over the well.

By placing deep wells beneath the permeable layer, a further advantage is obtained in terms of reducing variations in LFG composition. The extraction from the large deep void LFG volume in the landfill, in combination with re-entrainment of LFG emitted far from the wellhead of the vertical well, gives constant gas composition and high LFG quality (methane content) from the large deep reservoir comprised of the voluminous total of deep voids. The composition of this deep void gas will be constant or very slowly changing. The improved stability of extracted LFG composition is due to two factors:

LFG mixing in passage through the waste to reach the deep well(s). Even if composition of gas entering the entrainment area may vary somewhat over hours or days, the multiple flow paths and associated dispersive and diffusional mixing as the gas moves toward the deep extraction zone will "time average" the concentration and minimize variations.

Given the long transit time of gas from the entrainment area over the extraction zone to the deep extraction zone, diffusion will tend to further even out the composition variations. A near-constant composition of gas from the deep well extraction ideally suits the gas for all of the common LFG energy uses.
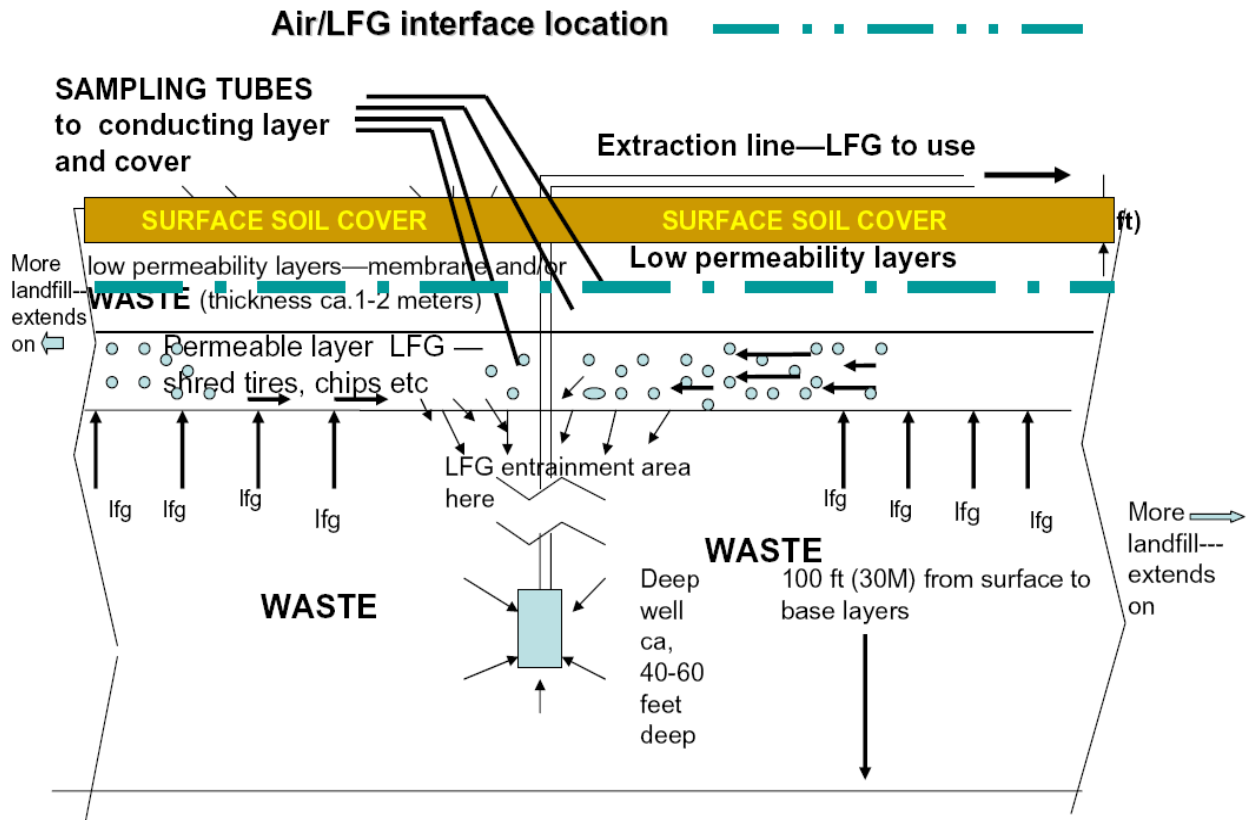
Figure 1-2. Landfill gas extraction and gas flow using permeable layers

Photo Credit: Yolo County Planning & Public Works Department

Electric power in the United States is used much more (a factor of 2 or more) during the day compared to late night. By extracting LFG to fuel electric power predominantly during the time of highest electric power need, the peaking landfill addresses this problem. An example profile of gas extraction generally appears as shown in Figure 1-3. In Figure 1-3, the ratio of "high" to "low" power need and "overpull, i.e. the excess of Qext over Qgen, will be choices that are specific to given sites and regions.
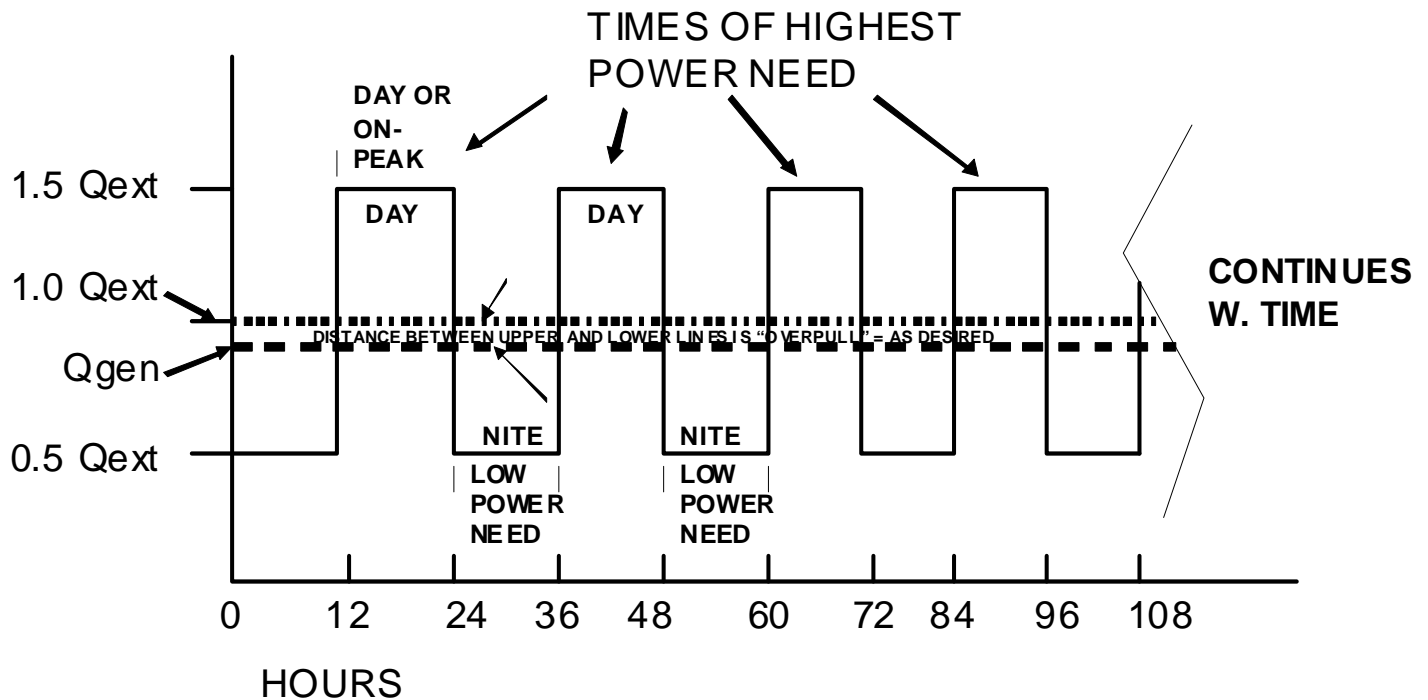
Where

Qext = Time (long term) average extraction rate;
Qgen = Underlying total LFG generation;
Overpull is the extra extraction in excess of generation.

Figure 1-3. Typical LFG extraction profile vs. time for "peaking"

Photo Credit: Yolo County Planning & Public Works Department

1.2   Project Objectives

The objective of this study was to demonstrate the ability to operate landfill gas extraction and utilization systems on a diurnal basis for peaking power production. As described in the following section, this included design, construction, operation, field tests of fugitive methane emissions, characterization of cover properties and mathematical modeling to simulate gas movement as a function of the imposed gas collection system vacuum field. The key issues were how to carry out such a variable rate extraction without increasing landfill gas fugitive emissions while also avoiding air intrusion into the landfill, which could affect overall gas production and recovery.

The project team explored different ways to optimize the utilization of CH_4 generated during waste decomposition by capturing CH_4 during times of peak power demand and storing the LFG in the landfill during the off peak periods. Gas recovery was controlled by adjusting the vacuum on the LFG collection system. To evaluate this peak power recovery concept, it was important to demonstrate that emissions to the atmosphere did not increase when the LFG collection system vacuum was reduced, thereby increasing the pressure gradient between the landfill and atmosphere.

22

1.3   Report Organization

This report is organized into the main sections of project design and construction, outcome, and conclusions and recommendations. The design and construction sections cover project approach. The outcome section discusses monitoring and data analysis. The conclusion and recommendation section discusses project conclusions and commercialization potential and benefits to California.

Section 2 discusses the project design, preliminary modeling, and assessment of biocover material. Section 2.1 of this report discusses design of the peaking well and peaking power operation. Section 2.2 describes the initial work to develop a computer model to evaluate the feasibility of operating landfills in a peaking-power mode and was used to guide the design and construction of the peaking power test cell. In Section 2.3, tests were conducted to understand the movement of water and landfill gases in biocover materials by measurement of pneumatic and hydraulic parameters of the biocover under laboratory conditions.

Section 4 discusses the laboratory and field results as well as computer modeling validation. Section 4.1 describes field measurements of methane emissions from a series of different covers. Parallel laboratory work to evaluate methane oxidation under several flow regimes designed to represent field conditions for the peak power gas collection plan is also presented in this section. Sections 4.2 and 4.3 discuss the operation and monitoring of the peaking power cell, and uses the collected data to validate and compare to the computer model.

Chapter 2:
Project Approach

2.1 Overview

In this section key design parameters for the peaking well and methods for monitoring gas composition within the gas extraction zones are discussed.

2.2 Design of Peaking Well

The preliminary modeling of "landfill peaking power" performance was carried out by Professor Paul Imhoff (Section 2.2) and his graduate students at the University of Delaware in order to assist in the design of this project. Parameters were chosen that were as close as possible to expectations for conventional landfills. For a peaking landfill with gas extraction profile as shown in Figure 1-3, the recovery of methane remained over 95 percent and the methane content of recovered gas varied by less than 1 percent over the 24 cycle of recovery. A parallel analysis (not shown) was carried out by HGC Corporation of Tucson, Arizona, using a U.S. DOE (Los Alamos National Laboratory) reservoir fluid flow model adapted to gas flow in a landfill. The HGC analysis results were close-to-identical to those of the University of Delaware, i.e. collection of about 95 percent of generated gas with close to constant composition over a 24-hour extraction profile as shown in Figure 1-3. These results suggested that the peaking landfill design approach can perform well.

A schematic of the design for the peaking landfill is shown in Figure 2-1. The key elements of the peaking landfill will generally include:

- A low-permeability but porous surface cover of relatively constant thickness and gas flow resistance.

- Below and parallel to this top surface, a layer highly conductive of gas.

- Beneath the surface, a gas extraction zone or zones. Gas extraction occurs from a locus that would normally be the perforated area of a gas well which gas is extracted.

Sampling sensors or tubes, that allow detection of gas composition as desired within the cover and highly conductive layer.

Combining conductive layers, surface permeable layers, and peaking can allow the transient LFG storage in the landfill to increase or decrease with highest efficiency. Here, efficiency is defined as capture of the highest fraction of generated gas during the full peaking cycle while keeping both fugitive emission and air entrainment into the landfill to the minimum necessary. As gas is extracted at lesser or greater amounts than the underlying generation (See Figure 1-3) an interface between LFG and entrained air or resultant nitrogen moves up and down under the cover as shown in Figure 2-1.

In designing the peaking landfill to deliver gas at variable rates in response to energy needs, constraints on the "peaking landfill" are: (a) the gas composition must remain suitable, i.e. high

enough methane content for energy uses; (b) the gas composition should vary as little as possible to facilitate energy uses; (c) losses of "fugitive methane" and atmospheric emissions must be kept as low as possible.

Key design features and constraints are summarized below:

- Composition of gas flowing to use will be monitored and adjusted to achieve a desired gas methane content suitable for energy. The gas compositions in the highly conductive layer and the cover will also be monitored by the tubes or sensors, examples shown in Figure 2-1, to give quick feedback

- For energy uses, the extracted gas composition should remain as close to constant as possible. The concentration of methane in the top cover and highly conductive layer may vary. However, considerable averaging out of the gas composition in the entrainment occurs due to: (a) the mixing due to gas flow along differing paths or flow streamlines in the entrainment zone on the way to the extraction; (b) diffusional mixing in the entrainment zone; (c) dispersive mixing due to gas passage through pockets of greater or lesser permeability in the entrainment zone; and (d) in typical landfills there is a large volume of gas stored deep within the landfill. The consequence of factors of (a) through (d) is that a gas stream of near-constant composition can be withdrawn at extraction rates which vary in accordance with fuel energy (or "peaking fuel") needs.

- The losses, (i.e. emissions of LFG to the atmosphere), should be kept as low as possible. To this end, there is "overpull" or recovery of gas at a rate in excess of its generation. The degree of overpull needed will be determined by testing and modeling.
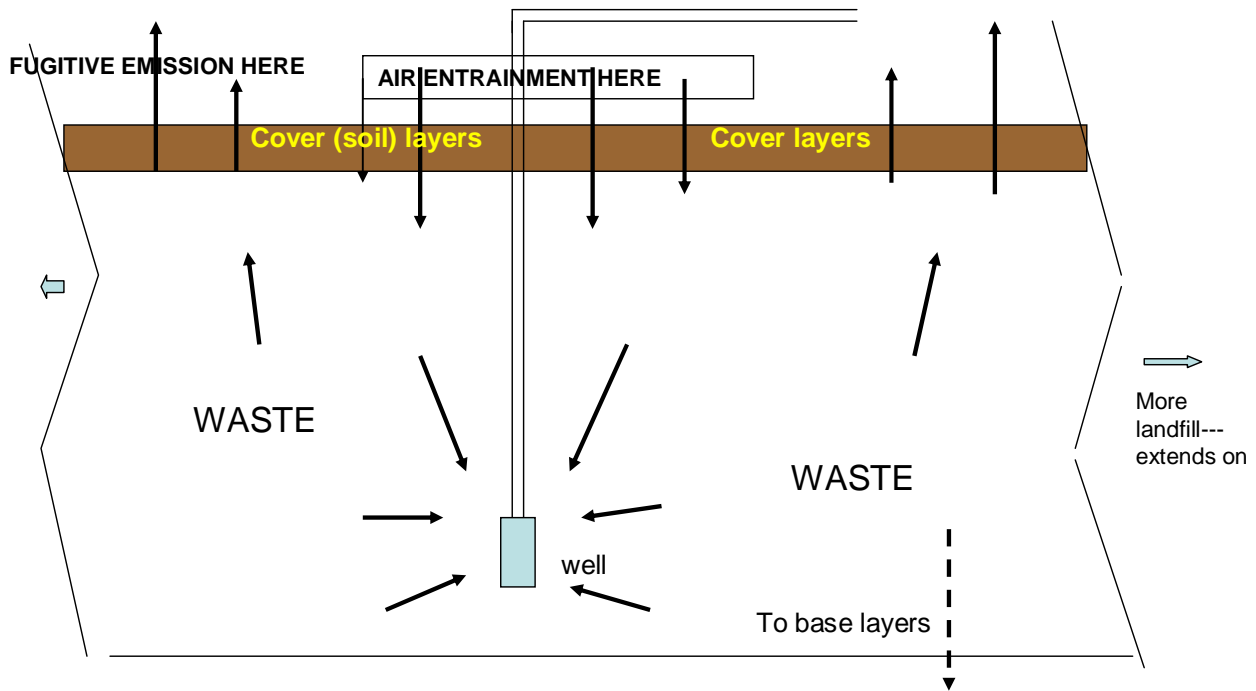
Figure 2-1: Schematic of peaking landfill with components and LFG flows

Photo Credit: Yolo County Planning & Public Works Department

2.3 Design of Peaking Power System

Detailed drawings of construction, instrumentations, and piping placement were prepared at the beginning of the project. They are presented in Appendix A. The peaking landfill field test has made use of a 340 x 195 x 40 foot deep section in the landfill's module D-Phase II. A top view of this module is shown in Figure 2-2. Within the section is a flat, circular well (called a "pancake" well) with a diameter of 25 feet. The cross-section is shown at different scales in Figure 2-3 and Figure 2-4.

A valving arrangement was designed as shown in Figure 2-5. It is assumed that constant or close to constant extraction vacuum V can be applied at the outlet to the left of Figure 2-5. If necessary, a pressure/vacuum regulator can be placed to control the extraction vacuum.

With this outlet valving arrangement of Figure 2-5, LFG flows can be straightforwardly pre-set so that: (a) with solenoid Valve 1 open, LFG flow is 1.5 x the time averaged extraction flow Qext; (b) With the solenoid Valve 1 closed, outlet gas flow is 0.5 x the time averaged extraction flow.

This particular valve setting described above will give the specific extraction flows shown in Figure 1-3. As noted earlier, adjustment of valves can enable other desired ratios of day/night flow.

26

The extraction is however subject to constraints that time average extraction Qext will exceed Qgen and meet other constraints including those on emissions.

Top view of cell footprint, showing (at lower left) peaking area (permeable layer textured [   ]) footprint and well.

SHALLOW "PANCAKE" WELL –shred tire layer extraction zone above well

4-inch HDPE pipe

Pre-existing deeper wells

X X

X

Vacuum draws gas to extraction system—see detail that follows of valves and operation

Approximate permeable layer footprint (inside brown boundary) 340 ft x 195 ft

300

200   400

SCALE 1" =30

Figure 2-2. Top view of well design and permeable layer components

Photo Credit: Yolo County Planning & Public Works Department

Schematic (not to scale) of gas well, permeable layer and some notes on design. Dimension arrows in blue.

LANDFILL CELL SURFACE

3 ft deep highly conductive layer

2' depth   6 Ft approximately   Soil and waste layers

to side slope and extraction

Approx 320 ft

Cell extends on at least 60 feet to any side slope

6 ft   3'depth

2-inch PVC pipe for extraction

? 25 ft

"Pancake" well is 3 ft deep and about 25 feet wide and filled with shredded tires.

22 feet approx. from permeable to base layers

Note. This new flat "pancake" profile well is different from standard design, but meets needs of controllability for capture and peaking. See the blown-up detail and notes in the next sketch.

Figure 2-3: Well design and permeable layer components

Photo Credit: Yolo County Planning & Public Works Department

Design detail of "peaking landfill" section with gas well cross-section.

Landfill surface

SOIL 1 to 3 feet depth

3 feet tire shreds

Cover of soil (1 foot or more depth) with balance of waste.

WASTE to make cover total of 6 feet

HIGHLY CONDUCTIVE (SHRED TIRE) LAYER

Pancake well with enough diameter (25 feet) to minimize pressure gradient of gas flowing to it. at acceptable extraction vacuum

6 ft   WASTE

LANDFILL EXTENDS ON

Well extraction zone   3 feet tire shreds

LFG flow in 4-inch HDPE extraction pipe

Pipe perforated only within tire shred extraction zone. Total area of well pipe perforations recommended at 60 square inches

40 ft to base

Well features shown, and reasons:

--Note 1: The well requires an adequate extraction area interface between tire shreds and waste, 300 or more ft² tire shred to waste interface (important to have enough area). The interface is > 1000 ft2 here.
--Note 2: As long as air infiltration of the LCRS is largely prevented differing well shapes (vertical pipe or horizontal) should give acceptable performance, defined as either (a) constant high (>50%) methane content and low ppm scans at constant or even variable (peaking) extraction rates. The preexisting vertical wells could be used in flat well-vertical well comparisons.
--Note 3: Extraction should only occur from the well below the permeable layer, not the permeable layer. So the well pipe perforations should be only within tire shreds within the well extraction
–Note 4 Extraction pipe needs to accommodate extraction pipe flexing and settlement. The well pipe is standard HDPE pipe.

Figure 2-4. Cross-section of the peaking power well and horizontal tire layer

Photo Credit: Yolo County Planning & Public Works Department

28

Figure 2-5. Schematic of peaking landfill valve and operational strategy

Photo Credit: Yolo County Planning & Public Works Department

2.4 Preliminary Modeling

Preliminary modeling was performed to help with the design of the project and to evaluate the feasibility of operating landfills in a peaking power mode.

2.4.1 Objectives

The overall objective of Part 1 of the modeling study was to evaluate the feasibility of operating landfills in a peaking-power mode. More specifically, the modeling will help to guide the design of the peaking power landfill test cell constructed at the Yolo County Central Landfill. To achieve these objectives, five different cases were simulated:

Case 1: evaluate the influence of anisotropy in gas permeability of the refuse on methane emissions.

Case 2: evaluate the effect of the horizontal tire layer beneath the landfill cover on the methane emissions and oxygen intrusion into the landfill.

Case 3: evaluate the effect of the depth of tire layer on methane emissions and peaking power operation.

Case 4: evaluate the effect of the depth of the pancake well on methane emissions and peaking power operation.

Case 5: evaluate the effect of biocover thickness on methane emissions and peaking power operations.

2.4.2 Methodology

2.4.2.1 Numerical Simulator

To simulate landfill gas migration, a multiphase and multi-component simulator was used, T2VOC. T2VOC is an extended version of the TOUGH2 (Transport of Unsaturated Groundwater and Heat) computer code that has been broadly used to simulate geothermal reservoirs, contamination of nuclear waste disposal sites, environmental pollution assessment and remediation, and hydrology of unsaturated and saturated zones. TOUGH2 and T2VOC belong to the MULKOM family of codes, developed in the Earth Sciences Division of Lawrence Berkeley National Laboratory. The main distinguishing feature of T2VOC is the capability to simulate multiphase contamination and remediation processes involving non-aqueous phase liquids. T2VOC uses a general integral finite difference formulation, and it consists of multiphase, multi-component mass and energy balance equations. A brief description of governing equations used in T2VOC is presented in this section.

The mass balance equations for component κ for an arbitrary flow region V_n with surface area Γ_n is given by

$$\frac{d}{dt}\int_{V_n} M^\kappa dV_n = \int_{\Gamma_n}(F^\kappa \bullet \mathbf{n})d\Gamma_n + \int_{V_n}q^\kappa dV_n$$

where M^κ is the mass of component κ per unit porous medium volume, F^κ is the mass flux of component κ into V_n, n is inward unit normal vector, and q^κ is the rate of mass generation of component κ per unit volume. The left-hand side represents the change of mass in the volume V_n per unit time, and the right-hand side terms describe the fluxes through the boundaries of the region and the sink or source in the volume.

The phase fluxes follow a multiphase extension of Darcy's law and are given by

$$F_g^\kappa = -k_0(1+\frac{b}{P_g})\frac{k_{rg}\rho_g}{\mu_g}X_g^\kappa(\nabla P_g - \rho_g g)+J_g^\kappa$$

where k_0 is the absolute permeability at large gas pressures and is equal to the single-phase liquid permeability, b is the Klinkenberg b-factor, which describes gas slippage that effectively increases gas permeability at low pressures, and J_g^κ is the diffusive mass flux of component κ in the gas phase. In T2VOC the diffusion of each component occurs only in the gas phase. The diffusive mass fluxes of water vapor and organic chemical vapor are calculated by

$$J_g^\kappa = -\phi S_g \tau_g D_g^\kappa \rho_g \nabla X_g^\kappa$$

where D_g^κ is the multicomponent molecular diffusion coefficient of component κ in the gas phase when no porous medium is present, and τ_g is the gas phase tortuosity computed from

the Millington and Quirk (1961) model, $\tau_g = \phi^{1/3} S_g^{7/3}$. The multicomponent diffusivities for water and chemical vapor in the gas phase are calculated from the binary diffusivities by the Wilke method (API 1977), and the binary air-water and air-chemical diffusivities are functions of temperature and pressure (Vargaftik 1975; Walker et al. 1981)

$$D_g^{ij} = D_g^{ijR} (P_R / P_g)(T / T_R)^{\theta_{ij}}$$

where D_g^{ijR} is the experimentally determined i-j binary diffusivity at reference temperature of T_R and pressure P_R, and θ_{ij} is an experimentally determined constant.

The multiphase extension of Darcy's law also includes the effects of relative permeabilities and capillary pressure between phases. Several multiphase relative permeability and capillary pressure models are available in T2VOC. In this study the van Genuchten–Mualem model (Mualem 1976; van Genuchten 1980) was used, and it is given by

$$k_{rl} = \sqrt{S^*} \{1 - (1 - [S^*]^{1/\lambda})^\lambda\}^2$$

$$k_{rg} = \begin{cases} 1 - k_{rl} & if \ S_{gr} = 0 \\ (1 - \hat{S})^2 (1 - \hat{S}^2) & if \ S_{gr} > 0 \end{cases}$$

$$P_{cap} = -P_0([S^*]^{-1/\lambda} - 1)^{1-\lambda}$$

with

$$S^* = (S_l - S_{lr})/(S_{ls} - S_{lr}), \ \hat{S} = (S_l - S_{lr})/(1 - S_{lr} - S_{gr})$$

$$P_0 = \rho_w g / \alpha$$

where S_{lr} is the irreducible water saturation, S_{ls} is the satiated water saturation, and S_{rg} is the irreducible gas saturation. The parameter λ is a pore-size distribution index that determines the shape of the functions, and α is a capillary strength parameter. The second equation of gas relative permeabilities is due to Corey (1954).

Description of Model Domain and Initial and Boundary Conditions

In this study the project team simplified and idealized a complicated three-dimensional landfill system in order to evaluate peaking power operations for a hypothetical landfill. In these simulations, the authors focused on a region where a pumping well is centrally positioned. Considering the characteristics of gas flows, a two-dimensional axisymmetric, radial domain was selected. On March 27, 2006, Figure 2-6, which shows a schematic of the model domain, was presentation to SMUD. The general properties of each layer utilized in the base case simulations are given in Figure 5.2-1. For capillary pressure and relative permeability relationships, the van Genuchten–Mualem model (Mualem 1976; van Genuchten 1980) is used, and the parameters are also presented in Figure 2-6. The discretization used in the simulations is shown in Figure 2-7.

The pumping rate, Q, in the system was varied in the simulations to reflect peaking power operations. For base-case simulations, the pumping rate was set equal to 1.5 times the landfill gas generation rate to represent "overpull" conditions during peak energy demand periods, and set to 0.5 times the landfill gas generation rate to represent "underpull" when energy demands are less. During the daytime the pump is operated for 12 hours in the overpull condition, and during the night it is operated for 12 hours in the underpull condition. All simulations in this study were based on this pumping sequence.

To describe fluid flows across the boundaries of the domain, two conditions were applied. The first is for the top grid blocks, which were designated as the atmosphere. The top surface was a Dirichlet boundary condition, and for this condition the top grid cells were specified as "inactive" in the code, which is a specific device supported in T2VOC. For the inactive elements no mass and energy balance equations are set up, and temperature and atmospheric conditions are kept constant. However, inactive elements appear in flow connections and initial condition specifications like all other elements. Thus, mass flux between adjacent cells can be calculated. The second boundary condition was a no flux boundary condition for the lateral and bottom borders of the simulation domain.

Various cases were simulated to explore different setup conditions and the sensitivity of important model parameters. Each case required changes in the grid size, gas generation rate, or formation properties; however, most of the initial and boundary conditions were fixed as shown in Table 2-1. In addition, several assumptions were made to complement the lack of field data and to simplify the simulations. First, the project team assumed isothermal conditions within the landfill. Second, the generation rate of landfill gas was steady since the simulation period was too short to account for the decrease in the rate of landfill gas generation associated with waste stabilization. Third, the thermodynamic properties of all solid materials and the gas generation rate were uniform throughout the domain. Fourth, no chemical and biological degradation processes were explicitly considered: instead, a constant landfill gas generation rate was specified for each grid block in the domain. In future simulations, the authors plan to include the influence of methane oxidation within the top biocover.

Table 2-1. General properties of model domain for all simulations

		Trash	Tire	Soil
Density (kg/ m^3)		714	476	1,700
Porosity		0.40	0.50	0.35
Aqueous phase saturation		0.21	0.21	0.15
Intrinsic Horizontal Permeability (m^2)		3.0e-12	2.96e-8	1.0e-12
Intrinsic Vertical Permeability (m^2)		3.0e-12	2.96e-9	1.0e-13
van Genuchten – Mualem parameters (for relative permeability function)	λ	0.11	0.11	0.457
	S_{lr}	0.21	0.21	0.15
	S_{ls}	1.00	1.00	1.00
	S_{gr}	0.005	0.005	0.10
van Genuchten parameters (for capillary pressure Function)	λ	0.11	0.11	0.457
	S_{lr}	0.20	0.20	0.14
	$1/P_0$	5.097e-4	5.097e-4	5.105e-4
	P_{max}	1.0e5	1.0e5	1.0e7
	S_{ls}	1.00	1.00	1.00

Data collected by Yolo County project team
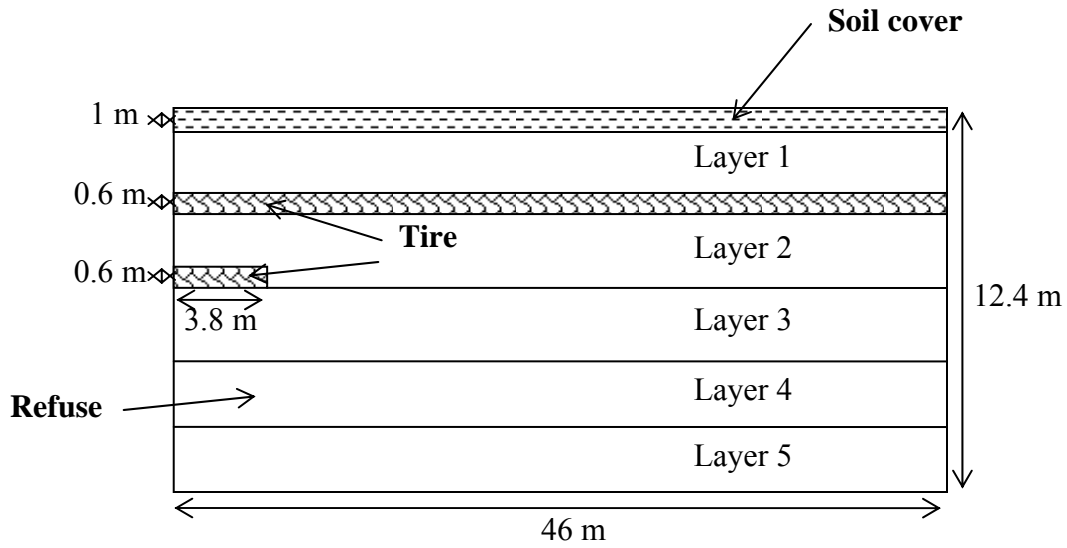
Figure 2-6. Schematic profile of model domain presented to SMUD March 7, 2006. A radially symmetric domain was used for all simulations.

Photo Credit: Yolo County Planning & Public Works Department
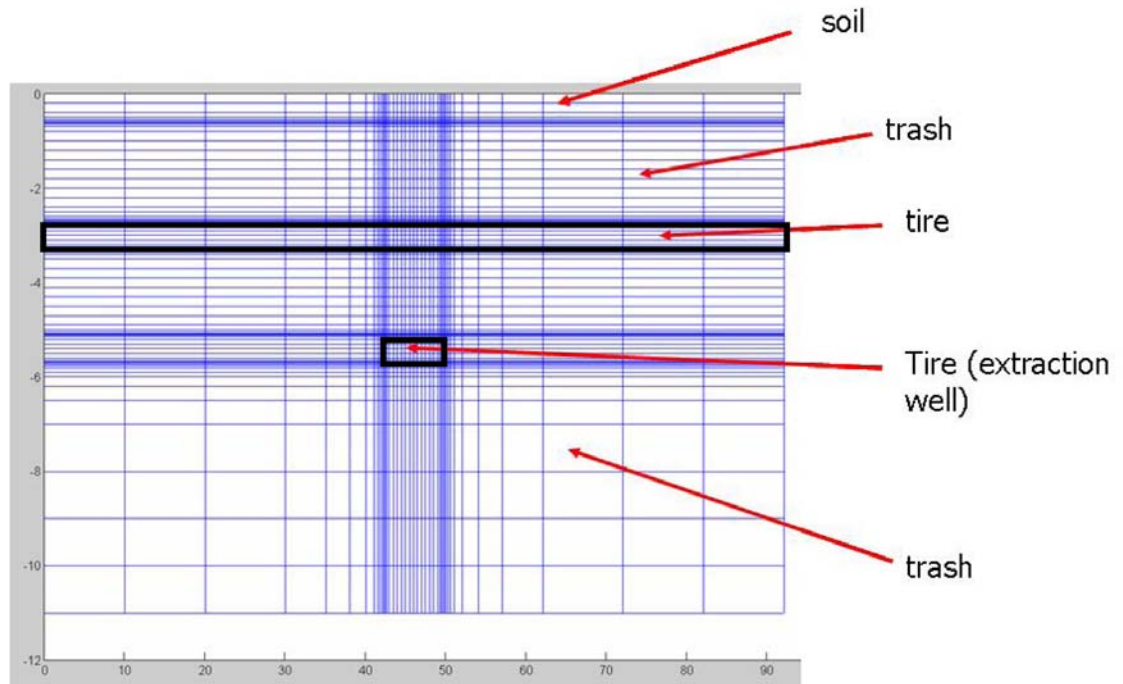
*Note that the Scale is Exaggerated in the Vertical Direction

Figure 2-7. Domain discretization

Photo Credit: Yolo County Planning & Public Works Department

Table 2-2. Initial and boundary conditions used in base-case simulations

Landfill depth (m)		12.4
Landfill diameter (m)		46
Tire layer depth (m)		3.1
Pancake depth (m)		5.5
Biocover thickness (m)		1.0
Atmosphere temperature (℃)		25
Atmosphere pressure (Pa)		101300
Landfill gas generation (m^3/ton/year) (55 % of methane and 45 % of carbon dioxide)		25
Parameters for binary air-methane diffusivity	D_g^{ijR} (m^2/s)	1.6e-5
	T_R (K)	293.2
	P_R (Pa)	1.013e5
	θ_{ij}	1.6

The modeling process was divided into three parts. It began with generating a grid that was pre-determined to effectively describe the system. Next, a natural state that corresponds to the condition prior to peaking power operation was calculated. In this natural state the system is in steady-state, which means thermodynamic conditions and the mass fraction of each component are time-independent in the whole domain. The pumping rate under these conditions is set equal to the landfill gas generation rate. Using these steady-state conditions as the initial conditions of the subsequent simulation, one important parameter was changed: time-dependent pumping rates in the pancake well were specified. New time-dependent sink terms in the pancake layer were introduced to act as a peaking power pumping well. After this change, the simulation was run for until steady diurnal changes in the system were achieved.

2.4.3 Results

2.4.3.1 Preliminary Computational Experiments

Figure 2-8 shows the methane emission rate from the landfill versus simulation time once time-dependent pumping within the pancake well was initiated at the end of Day 1. Based on the output of this simulation, the system satisfies the steady-state condition at the end of Day 9. Thus, all simulation results were calculated and presented for the 24-hour period beginning on Day 10.

Case 1: Effect of Anisotropy of Waste Permeability

Because landfills are very complicated, heterogeneous, and anisotropic systems, the way the gas permeabilities are specified for the waste can result in significant differences between simulations. Because the domain was assumed to be uniform, the effect of anisotropy was evaluated, changing the ratio of horizontal gas permeability to vertical gas permeability. In general, it has been typically assumed that the horizontal gas permeability is between 3 and 10 times larger than the vertical gas permeability for solid waste.

In Figure 2-9 the effect of the horizontal to vertical gas permeability on methane emissions from the landfill surface is shown. Methane emissions are plotted for the 24 hour period beginning on Day 10 (see Figure 2-8). It is clear that for peaking power operations with the tire layer installed at the top of the landfill, the influence of anisotropy in the gas permeability on methane emissions is relatively minor. For this reason and to simulate the worse state conditions for methane emissions from landfills, in all future simulations the gas permeability was assumed to be the same in the horizontal and vertical directions.
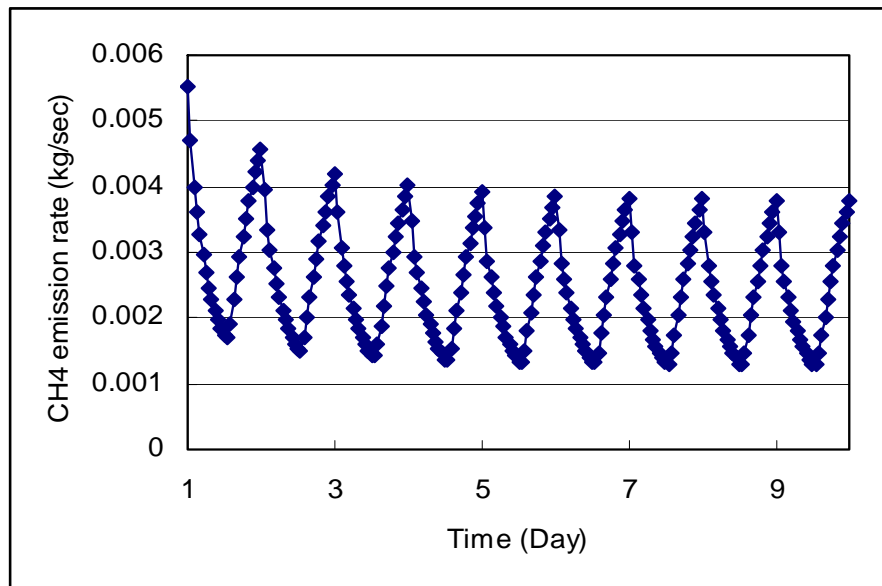
Figure 2-8. Variation of methane emission with elapsed simulation time for base case simulation

Photo Credit: Yolo County Planning & Public Works Department
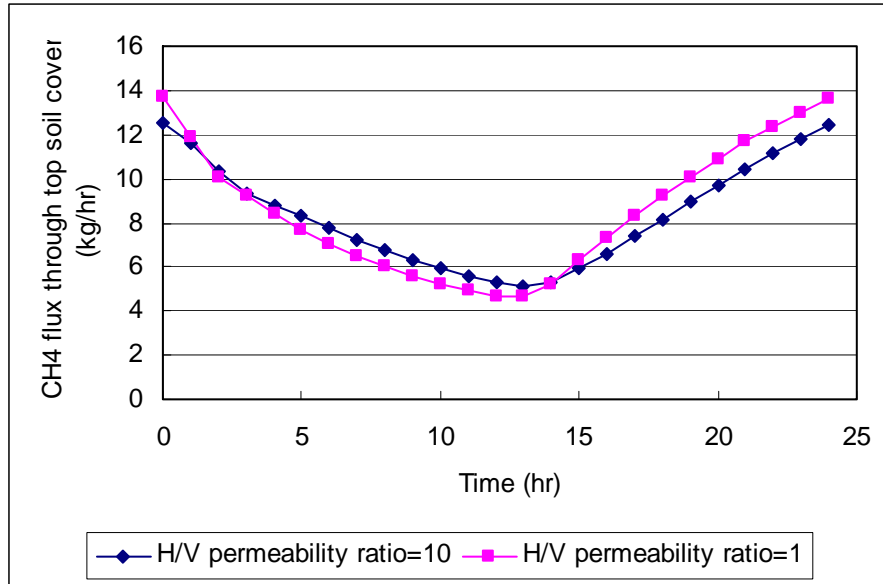
Figure 2-9. Methane fluxes from landfill at different anisotropy ratios (Horizontal [H] to Vertical [V] gas permeability) during peaking power operation

Photo Credit: Yolo County Planning & Public Works Department

Case 2: Effect of Tire Layer on Methane Emissions

One of the most important objectives was to evaluate the influence of the horizontal tire layer beneath the biocover on methane emissions. Figure 2-10 illustrates two points: (1) the effect of tire layer at constant pumping rate (without peaking power operations), and (2) the influence of tire layer on methane emissions during peaking power operation. Without peaking power operations, the installation of the horizontal tire layer at the top of the landfill reduced methane emissions by approximately 50 percent, from 17.4 to 7.9 kg/hr. Thus, the tire layer significantly improves the collection efficiency of the methane gas, which should result in increased income for landfill operators. The collection efficiency of the landfill gas would be improved even further by increasing the pumping rate to between 5 to 15 percent larger than the landfill gas generation rate. The landfill gas generation rate was assumed to be 25 cubic meter per ton per. The gas composition was assumed to be 55 percent methane and 45 percent carbon dioxide. The gas generation rate will change based on the waste composition, age, etc. The actual gas generation rate used in the simulations does not affect the results of the simulation.
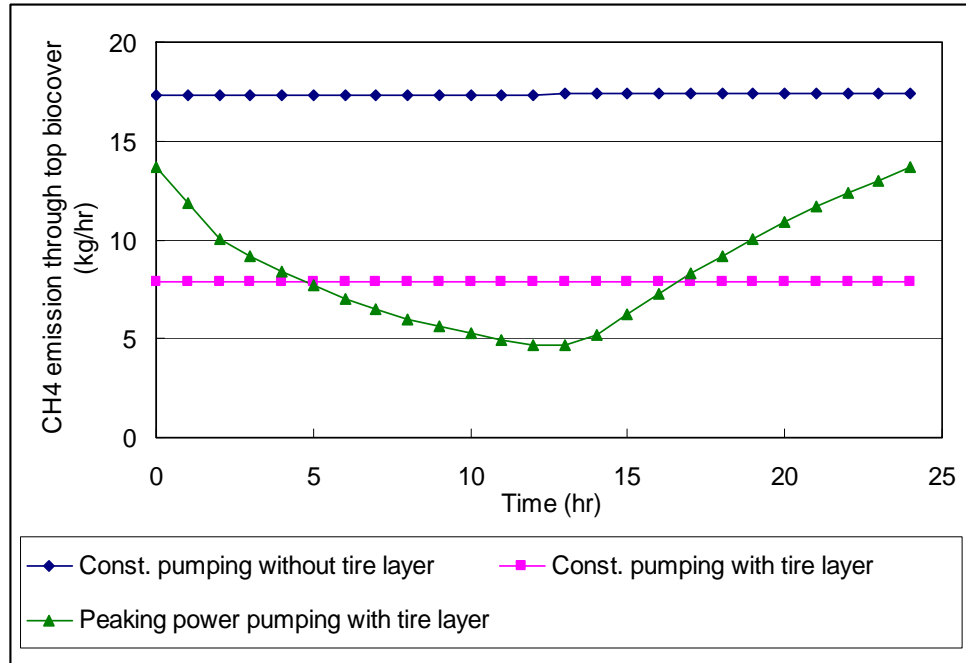
Figure 2-10. Comparison of methane fluxes with or without the tire layer at constant pumping rate and peaking power operation. Results are shown for Day 10 of the simulation.

Second, it is important to note that operating the pumping well in peaking power mode (with the tire layer at the top of the landfill) does NOT result in significant increases in methane emissions from the landfill. When the landfill was operated at a constant pumping rate equal to the landfill gas generation rate, 13.7 percent of the methane generated escaped from the landfill. During peaking power operations, when the pumping well was operated for 12 hours in overpull (pumping rate = 1.5 x landfill gas generation rate) followed by 12 hours in underpull (pumping rate = 0.5 x landfill gas generation rate), only 14.5 percent of the methane generated escaped from the landfill. Thus, the tire layer *significantly mitigated* the effect of changes in pumping rates on methane emissions. If the effect of methane oxidation in the biocover was included in the analysis, significantly smaller amounts of methane would be predicted to escape into the atmosphere.

Figure 2-11 shows the result of methane fluxes under peaking power operation with and without the tire layer shown at the top of the landfill in Figure 2-6. The emission rates with and without the tire layer are both affected by changes in the pumping rate. During the overpull period the methane fluxes are decreased, and with the start of the underpull period the fluxes increased. Even at a "strong" point that represents the state of the smallest pressure inside the landfill domain and the greatest extraction from the pumping well (see Figure 2-11), the net methane flux into the atmosphere is positive. In this case molecular diffusion is the dominant mechanism driving methane out of the landfill cover. If the tire layer is installed the methane emission is half the rate that occurs during peaking power operation without the tire layer. The percentages of methane emitted through the top biocover, which is based on the total amount of

methane generated in the domain, were 14.5 and 28.8 percent with and without tire layers, respectively, during peaking power operations. Again, the influence of the top tire layer on methane collection efficiency is dramatic.
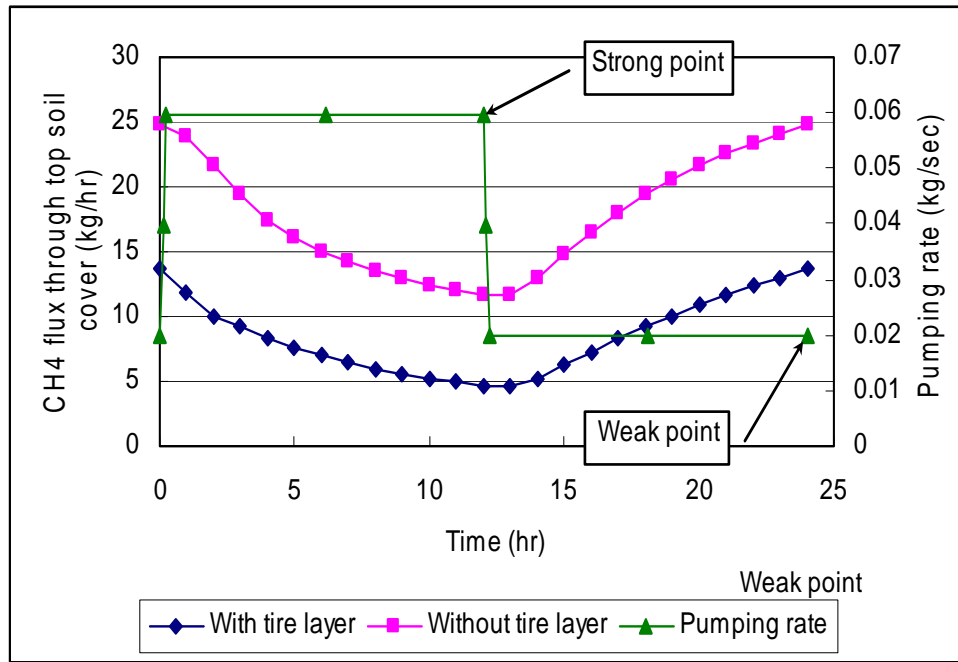
Figure 2-11. Methane fluxes from landfill as a function of time for Day 10 of the simulation during peaking power operation. Also shown is the pumping rate during this period.

Photo Credit: Yolo County Planning & Public Works Department

It is important to note that in these simulations no oxidation of the methane was assumed to occur within the top soil cover, i.e., the biocover. In reality, significant amounts of methane may be oxidized in this layer, which may appreciably reduce landfill gas emissions. The influence of methane oxidation within the biocover will be included in future simulations using data from field tests of biocover performance at the Yolo County Central Landfill.

To understand gas flow inside the landfill, pressure profiles at the "strong point" (see Figure 2-11) are presented in Figures 2-12 and 2-13. Here, the "strong point" corresponds to the time when the largest gas extraction rate is exerted at the pumping well, which is 150 percent of the landfill gas generation rate. Figure 2-12 shows the case with the horizontal tire layer installed at the top of the landfill: level contour lines are observed at the upper part of the domain. This confirms that an even vertical gas flow through the biocover was attained when the permeable tire layer was installed. At distances greater than 20 meters (m) from the well, all pressure contours are horizontal. This implies that the pumping well cannot capture distant landfill gases and it allows them to be transferred to the atmosphere. Pumping at rates greater than the landfill gas generation rate would improve capture of these gases.
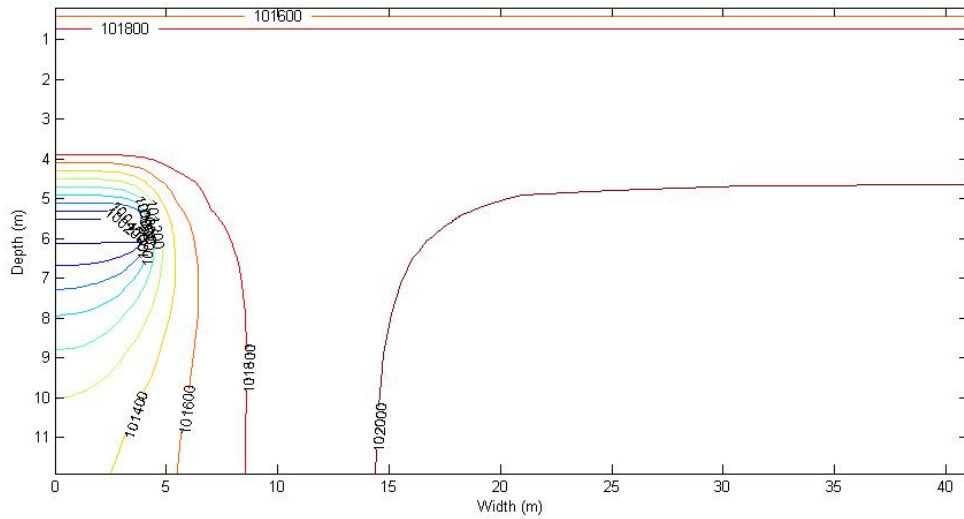
Figure 2-12. Pressure (Pa) contours through one half of the problem domain at the "strong point," with the pumping well operating at 150% of the landfill gas generation rate. Results shown with upper horizontal tire layer installed.

Photo Credit: Yolo County Planning & Public Works Department

When the tire layer was not included in the simulation domain, the constant pressure contours exhibit different features (see Figure 2-13). Up to 25 m away from the pumping well the pressure lines are distributed vertically across almost the entire depth. In other words, the lateral influence of the pumping well is extended when a tire layer is not installed at the top of the landfill. On the other hand, the vertical pressure gradients near the top of the landfill are larger than those in Figure 2-12. This indicates that the advective forces driving landfill gases out of the landfill are more significant without the tire layer, which result in greater fugitive methane fluxes.
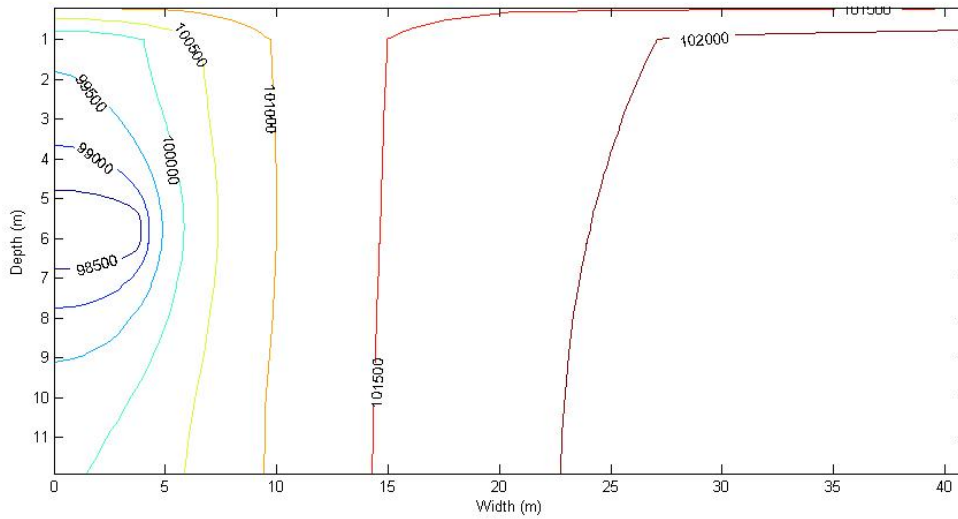
Figure 2-13. Pressure (Pa) contours through one half of the problem domain at the "strong point," with the pumping well operating at 150% of the landfill gas generation rate. Results shown without upper horizontal tire layer installed.

Photo Credit: Yolo County Planning & Public Works Department

Another important factor to examine is the extent of oxygen intrusion in the landfill. Figures 2-14 and 2-15 show the concentration of oxygen inside the landfill depending on whether the tire layer is installed or not. These profiles are at the "strong point", maximum pumping rate during peaking power, where the highest oxygen concentration is expected. When the tire layer is included, the concentration of oxygen does not vary with radial distance from the well. But with removal of the tire layer from the system high concentrations of oxygen occur at greater depths throughout the system. As discussed above, these simulations do not account for utilization of the oxygen by methane-degrading bacteria. Nevertheless, it is clear that the tire layer functions as a screen to prevent severe intrusion of oxygen through the refuse and distributes oxygen evenly above the tire layer.
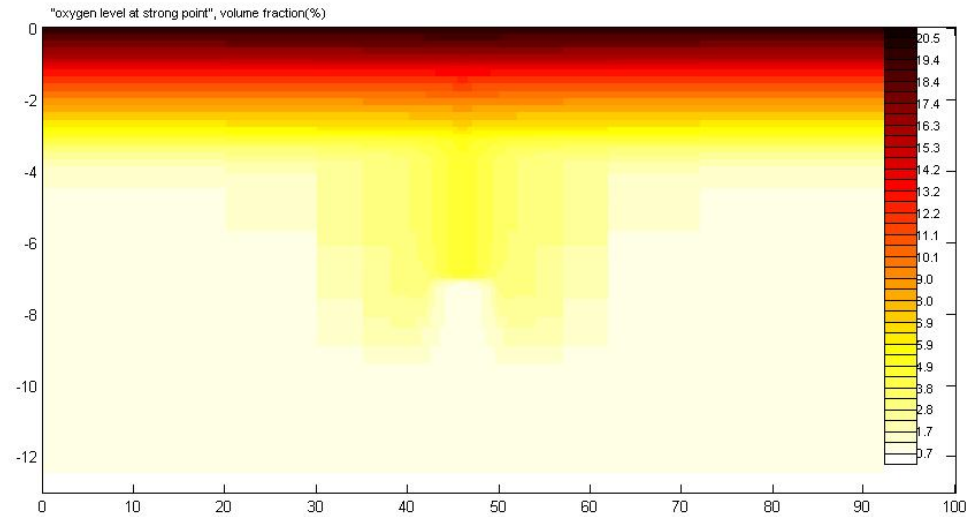
Figure 2-14. Oxygen profiles (percent by mass) throughout the problem domain at the "strong point," with the pumping well operating at 150% of the landfill gas generation rate. Results shown with upper horizontal tire layer installed.

Photo Credit: Yolo County Planning & Public Works Department
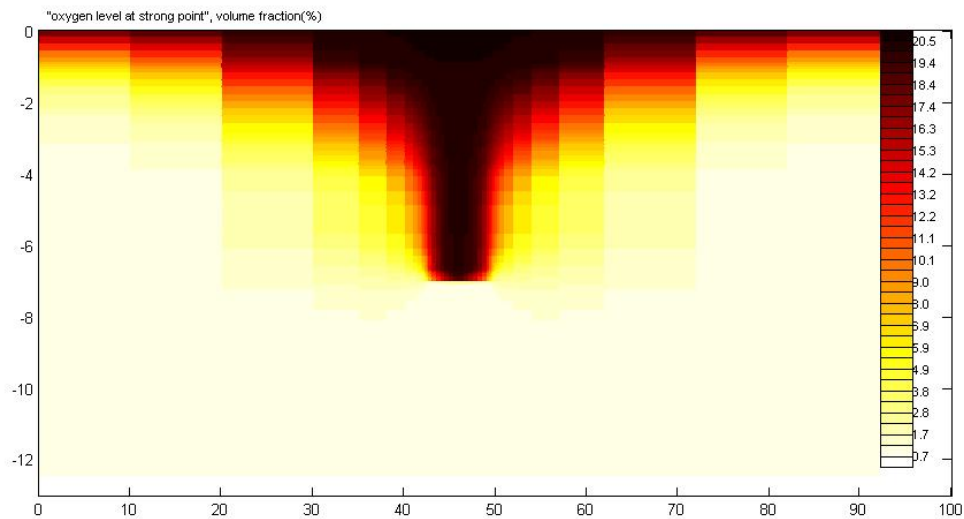
Figure 2-15. Oxygen profiles (percent by mass) throughout the problem domain at the "strong point," with the pumping well operating at 150% of the landfill gas generation rate. Results shown without upper horizontal tire layer installed.

Photo Credit: Yolo County Planning & Public Works Department

Case 3: Effect of Depth of Tire Layer

The depth of the horizontal tire layer was varied between 2.5 to 3.7 m from the top surface to evaluate the influence of "depth" on methane emissions. The results are presented in Figure 2-16 for a 24-hour period beginning on Day 10. Also shown in this figure is the maximum depth of penetration of the 4 percent oxygen concentration profile during the 24-hour simulation period. As the depth of the tire layer increases, the methane emissions decrease. The reason can be found by examining the pressure contour diagrams in Figures 2-17 and 2-18. When the tire layer is positioned at a depth of 3.7 m (Figure 2-17) the constant pressure lines around the pumping well are more densely contoured than those at 2.5-m depth (Figure 2-18). This implies two things: with an increase in depth of the tire layer, the generated landfill gas is more efficiently collected at the pumping well and the advective driving force for emitting methane gas through the biocover is decreased. On the other hand, the deeper the tire layer the greater the intrusion of oxygen into the refuse. The depth where 4 percent of oxygen concentration was detected differs by 1 m between minimum (2.5 m) and maximum (3.7 m) depths of tire layer (see Figure 2-16). Thus, the optimal depth of the horizontal tire layer is dependent upon the rate of oxygen consumption in the biocover. If the oxygen consumption rate is significant, then increasing the depth of the tire layer will allow for more efficient collection of methane while not resulting in problematic oxygen concentrations within the waste.
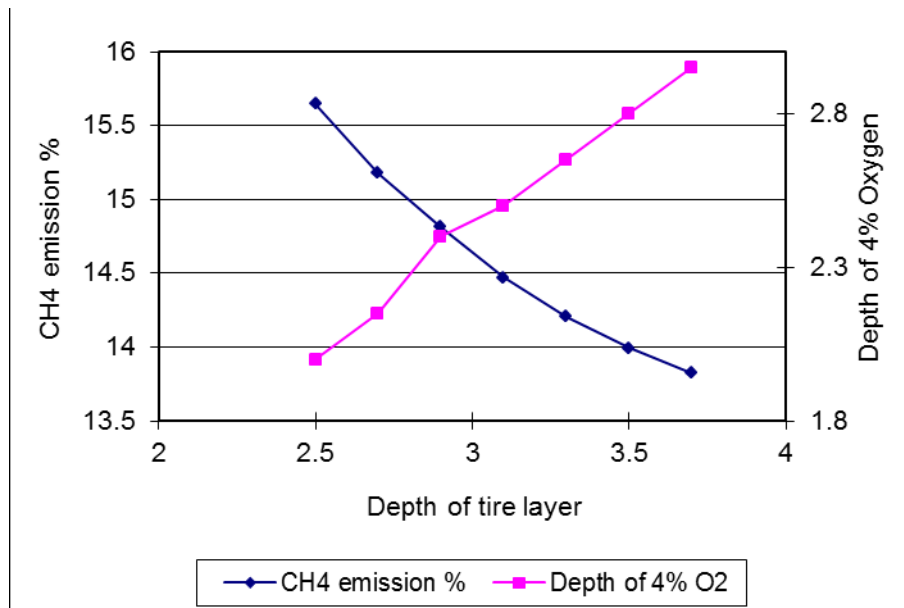
Figure 2-16. Variations of methane emissions and depth of oxygen intrusions as a function of depth of tire layer during peaking power operation. All depths are in meters.

Photo Credit: Yolo County Planning & Public Works Department

43
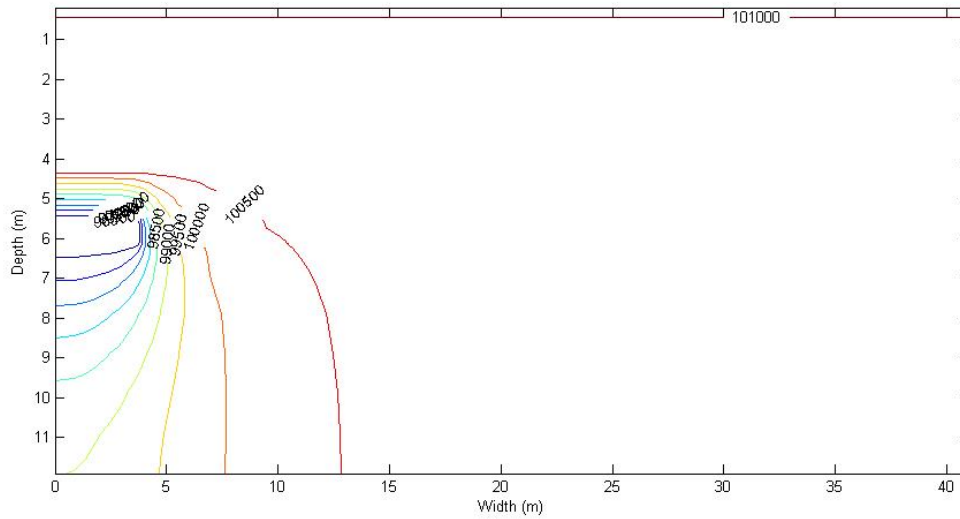
Figure 2-17. Pressure (Pa) contours through one half of the problem domain at "strong point", with the pumping well operating at 150 % of the landfill gas generation rate. Results are for conditions when upper tire layer is installed at 3.7 m depth.

Photo Credit: Yolo County Planning & Public Works Department
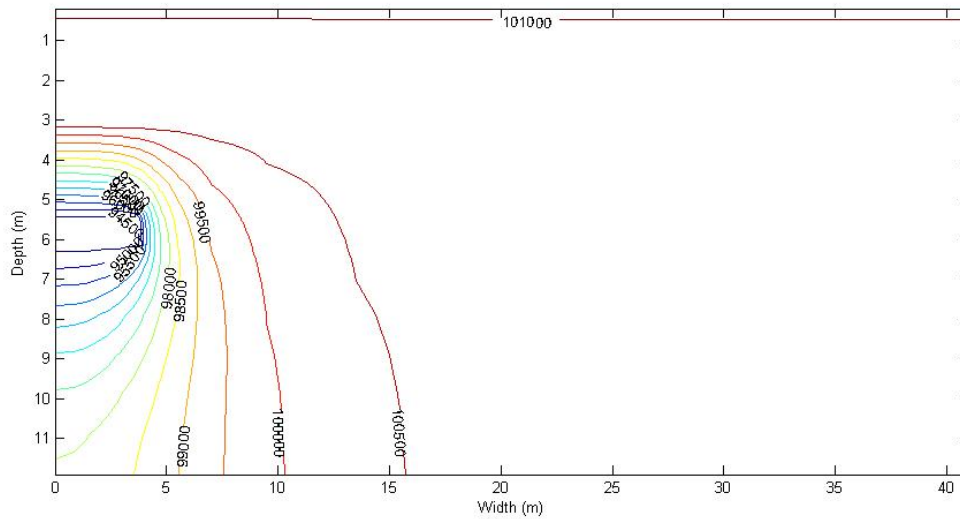
Figure 2-18. Pressure (Pa) contours through one half of the problem domain at "strong point", with the pumping well operating at 150 % of the landfill gas generation rate. Results are for conditions when upper tire layer is installed at 2.5 m depth.

Photo Credit: Yolo County Planning & Public Works Department

44

Case 4: Effect of Depth of Pancake Well

Pumping wells are usually placed at about 50 percent to 90 percent of the landfill depth (O'Leary and Walsh 1991). Well depth has been recognized as an important factor affecting gas flow rates at pumping wells (Chen et al. 2003). Well placement is also closely related to landfill gas emissions through the top cover. In this section the influence of the depth of pancake layer (i.e., the pumping well) on methane emissions was evaluated. Figure 2-19 examines variations of the total methane emissions during the 24-hour period beginning on Day 10 with depth of the pancake layer. Pancake layer depths were varied from 5.5 to 9.5 m, which corresponds to 46 percent and 79 percent of the simulated landfill depth, respectively. When the tire layer is not installed, methane emissions decrease with an increase in depth of the pancake well. But when the tire layer is included, methane emissions *do not change* with well depth. These results can be explained in connection with the pressure profiles. As was discussed in Section 2.3, the highly permeable tire layer functions to spread out the gas flow. The pressure alterations that result from different depths of the pancake well are lessened and result in no measurable changes in the rate of methane emission with corresponding changes in well depth (see Figure 2-19). In addition, it should be noted that the oxygen intrusion would be much more serious as the pancake well is placed deeper if the system did not contain the upper tire layer. As drawn in Figure 2-19, the depth of oxygen intrusion is significantly increased with increases in the depth of pancake layer when the tire layer is not included.
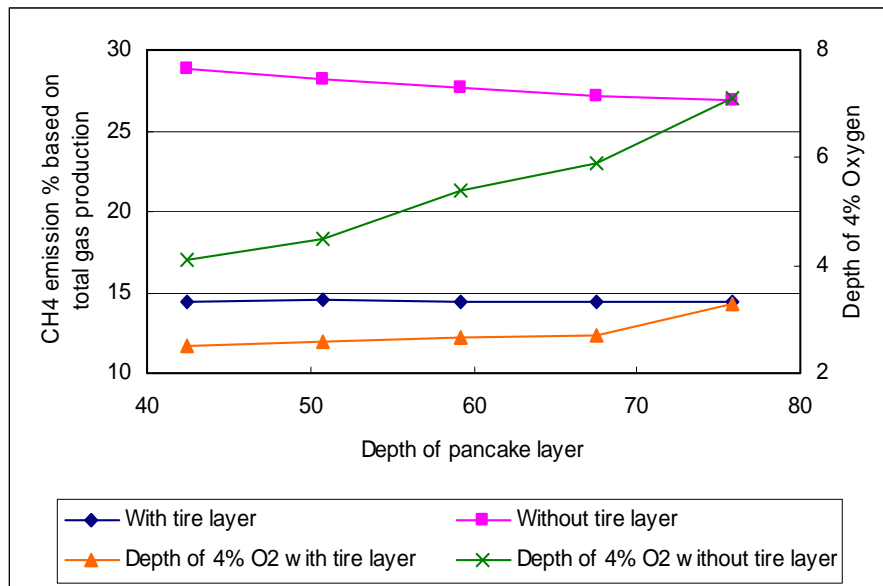
Figure 2-19: Percent change in methane emissions and depth of 4% oxygen contour as a function of depth of pancake well, shown as percent of total landfill depth.

Photo Credit: Yolo County Planning & Public Works Department

Case 5: Effect of Biocover Thickness

The biocover is the uppermost layer covering landfills; it separates landfills from the atmosphere and reduces methane emissions. The physical features of the biocover, e.g.,

tortuosity, gas permeability, and water saturation, can significantly affect the gas flow. The influence of biocover thickness on methane emissions was evaluated here, which can be controlled when the layer is constructed. The thickness was varied between 0.6 and 1.8 m, and the results are presented in Figure 2-20. Regardless of the presence or absence of the tire layer, the thicker the biocover the greater the reduction in methane emissions. But the two simulation results, with and without the tire layer, differ in the level of decrease of methane emissions. When the tire layer is not installed, methane emissions percent are reduced by about 40 percent when the biocover thickness increases from 0.6 to 1.8 m. For simulations with the tire layer, there is only a 26 percent decrease in methane emissions. These reductions result from smaller rates of gas advection and diffusion through the biocover as the thickness increases. The vertical gas permeability that mainly governs the gas flow through the top biocover is over one order of magnitude smaller than the vertical gas permeability through the refuse. Thus, the increase in the final biocover thickness enhances resistance to the vertical gas flow. The benefit of a thicker biocover is enhanced when the tire layer is not installed because without the tire layer here is uneven flow distribution. In this case, the thicker biocover tends to even out the vertical flow in the system more. On the other hand, the use of the tire layer minimizes the influence of the biocover thickness and allows one to use a thinner biocover to achieve a similar efficiency of methane capture.

The depth of oxygen intrusion is also affected by the thickness of the biocover. The maximum depth of the 4 percent oxygen contour is shown in Figure 2-20. As the biocover thickness increases, the penetration of oxygen into the waste decreases. The influence of biocover thickness on oxygen penetration is reduced when the tire layer is installed.

It is important to note that this analysis did not take into account methane oxidation within the biocover. Future simulations will include this process, using data generated from laboratory and field measurements.
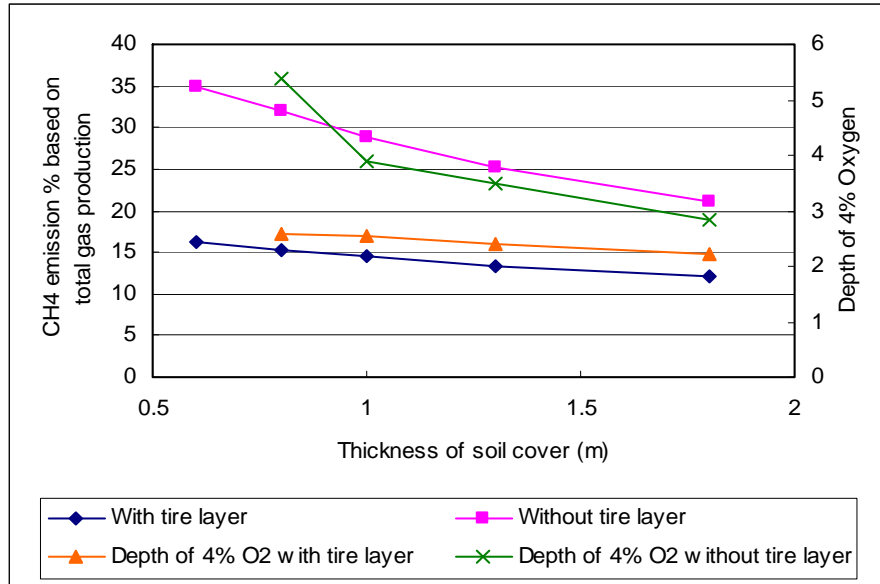
Figure 2-20. Percent change in methane emissions and depth of 4% oxygen contour (m) as a function of thickness of biocover (soil cover).

Photo Credit: Yolo County Planning & Public Works Department

2.5   Conclusions

This simulation study examined the peaking power operation of a hypothetical landfill. This analysis concludes the following:

- If a horizontal tire layer is installed at the top of the landfill, the variation of horizontal to vertical gas permeability in the waste has a minimal effect on methane collection efficiency.

- The construction of a horizontal tire layer can *increase* the methane collection efficiency by 50 percent for standard (constant) pumping conditions.

- If the landfill is operated in peaking power mode, the increase in methane emissions is *minor* (from 13.7 to 14.5 percent of the methane generated) if a horizontal tire layer is installed.

- A horizontal tire layer also significantly *decreases* the intrusion of oxygen into the landfill (see Figures 2-14 and 2-15).

- Methane collection and peaking power performance is improved if the horizontal tire layer is placed deeper in the landfill. However, greater oxygen is drawn into the landfill as the tire layer is placed deeper.

- The depth of the pancake well has a minor influence on peaking power operations, as long as a horizontal tire layer is installed.

- The thicker the biocover layer the better the efficiency of methane collection.

47

From this analysis it is clear that peaking power operation with a horizontal tire layer should result in both increased methane collection efficiencies and reduced methane emissions, when compared to cases with standard vertical gas collection wells without horizontal tire layers. While these results must be supported by field tests, they do suggest that the operation of a landfill in peaking power mode (with a horizontal tire layer) could be both environmentally and economically beneficial. Future simulations will examine the potential increase in income associated with improved methane capture under peaking power operations.

2.5.1 Preliminary Assessment of Biocover Materials

2.5.1.2 Objectives

Biocover materials can support the growth of microbial populations and enhance the oxidation of fugitive methane from landfills. The purpose of this study was to evaluate the addition of biocover materials to the top of traditionally clay-covered landfills. Providing the appropriate conditions, the growth of methane-consuming bacteria can be accelerated, which in turn can reduce the release of fugitive methane to the atmosphere. In order to understand the movement of water and landfill gases in biocover materials, pneumatic and hydraulic parameters of these materials must be measured in the laboratory under controlled conditions.

In this work three different types of tests were conducted: (a) compaction tests, (b) air permeability tests, and (c) moisture content measurements. Compaction tests were conducted to determine the effect of an applied external load on the bulk density of biocover materials, particularly mixtures of compost and woodchips. The applied load was selected to mimic typical compaction practices for the construction of landfill covers. Knowing the bulk density of various mixtures of woodchips and compost, the required mass of these materials to cover particular landfill areas with a specified thickness can be computed. In addition to the compaction tests, air permeability measurements were performed in a volume-adjustable cell designed specifically for these tests. Air permeabilities were measured for three different mixtures that will be tested as biocover materials at Yolo County: compost, greenwaste, and a mixture of 70 percent compost and 30 percent woodchips. Moisture content analyses were conducted on representative samples of these three biocover materials. The results of these laboratory tests are presented below.

2.5.2 Materials and Methods

2.5.2.1 Materials

Any medium that can support the growth of microbial population can potentially be used as a biocover material. However economic considerations usually decrease the range of appropriate materials. Three types of biocover materials were evaluated in these tests: compost, mixtures of compost and woodchips, and greenwaste. These materials were supplied by Yolo County Central Landfill and were intended for use as the biocover installed on a new anaerobic landfill cell for peaking power operation.

Due to lack of knowledge about the effect of addition of woodchips to pure compost, a compaction test was conducted to evaluate the compressibility of different mixtures. Four compositions of woodchips and compost material were prepared for this test. The unpacked, loose materials were used to prepare specific volume percentage mixtures, and then these

mixtures were compacted in test cells to determine the change in bulk density of the sample with compaction. The characteristics of the four samples tested are presented in Table 5.3-1. Knowing the bulk density of these mixtures can determine the required amount of the mixtures to cover particular landfill areas with prescribed thicknesses of biocover materials.

Table 2-3. Properties of sample mixtures

Sample No.	Volume % of compost	Volume % of woodchips	Weight of compost (g)	Weight of woodchips (g)
1	100	0	8862.4	0
2	90	10	7922.7	372.6
3	70	30	6171.6	801.8
4	50	50	4281.1	1353.6

For the air permeability and moisture content tests, three different types of biocover materials were studied: pure compost, a mixture of 70 percent compost and 30 percent woodchips (volume percentage) and greenwaste, which is composed of plant residues. These materials were used as biocover materials on the top cover of the new anaerobic test cell constructed at Yolo County Central Landfill. The biocover materials were shipped from this Yolo County to the University of Delaware for the laboratory tests.

2.5.2.2 Compaction Tests

Compaction tests were performed in order to understand the effect of woodchips addition on the bulk density of compost/woodchip mixtures. This information was needed to help select the composition of compost/woodchips to use in the construction of the biocover for the new test cell at Yolo County Central Landfill. These measurements would also help in purchasing appropriate amounts of compost and woodchips to construct biocovers of specified thickness.

Due to the relatively large size of woodchips, Proctor Tests (falling hammer), which are usually used for soil, could not be used to determine the compaction of these mixtures. The cylindrical compaction chamber used in the experiments has an inside diameter of 20.3 centimeters (cm) and a height of 39.0 cm. The woodchips and compost materials were mixed manually in large trash bags in order to reach homogenous mixtures. The Tinius Olsen, Super "L" Universal Testing Machine 200K, was used to compress the mixtures. The samples were compressed to 48.263 kP and the height reduction was read from the compaction device. After an initial compaction step, the load was removed from the chamber and then the height of mixture was re-measured. The load was then applied three more times in order to study the effect of further compaction on mixture compressibility. The pictures of a prepared samples and the compaction machine are presented in Figures 2-21 and 2-22, respectively.

Figure 2-21. View of compaction chamber filled with mixture

Photo Credit: University of Delaware

Figure 2-22. View of Tinius Olsen, Super "L" Universal Testing Machine 200K

Photo Credit: University of Delaware

2.5.2.3 Air Permeability Tests

A volume adjustable, cylindrical cell was built at the University of Delaware for measuring the gas permeability and bulk density of biocover materials. The different sections of the cell are illustrated in Figures 2-23 and 2-24. The main body is made of PVC pipe. Twenty metallic ports were positioned on sides of the main body for pressure measurements. A rubber inner tube was used on the movable upper plate to provide a gas-tight seal at the top of the chamber. Two circular aluminum plates served as upper and lower caps to the cell. The gas-tight seal at the bottom of the chamber was maintained by a bolted flange compressing a rubber gasket.

Samples of each biocover material were compacted in the chamber using an aluminum rod. Each sample was packed in several batches. Each batch was approximately 2-inch thick of loose porous material and was rodded throughout until no recognizable height reduction occurred. The pressure gauges (Ashcroft, c-68930-02, ±0.05 in H_2O) were used to measure the pressure at the bottom of the chamber and immediately after the rotameter (Cole-Parmer, c-32457-44, ± 0.5 liter per minute), which was used to record the air flow rates for the tests. By measuring these pressures, the volumetric air flows could be corrected to standard temperature and pressure (STP). The tests were performed at air flow rates of 0.4, 1, 2, 3, 4, and 5 liter/min (STP). The air pressures at five ports spaced 10.2 cm along the chamber were measured for each flow rate. Using these data the air permeability can be measured for each material [1].

The three porous media that were used as biocover materials in the new anaerobic test cell at the Yolo County Central Landfill were chosen in this study. They were compost, greenwaste, and a mixture of 70 percent compost and 30 percent woodchips (volume percent). The dry weight percent of the compost/woodchip mixture was 82 percent compost and 18 percent woodchips.
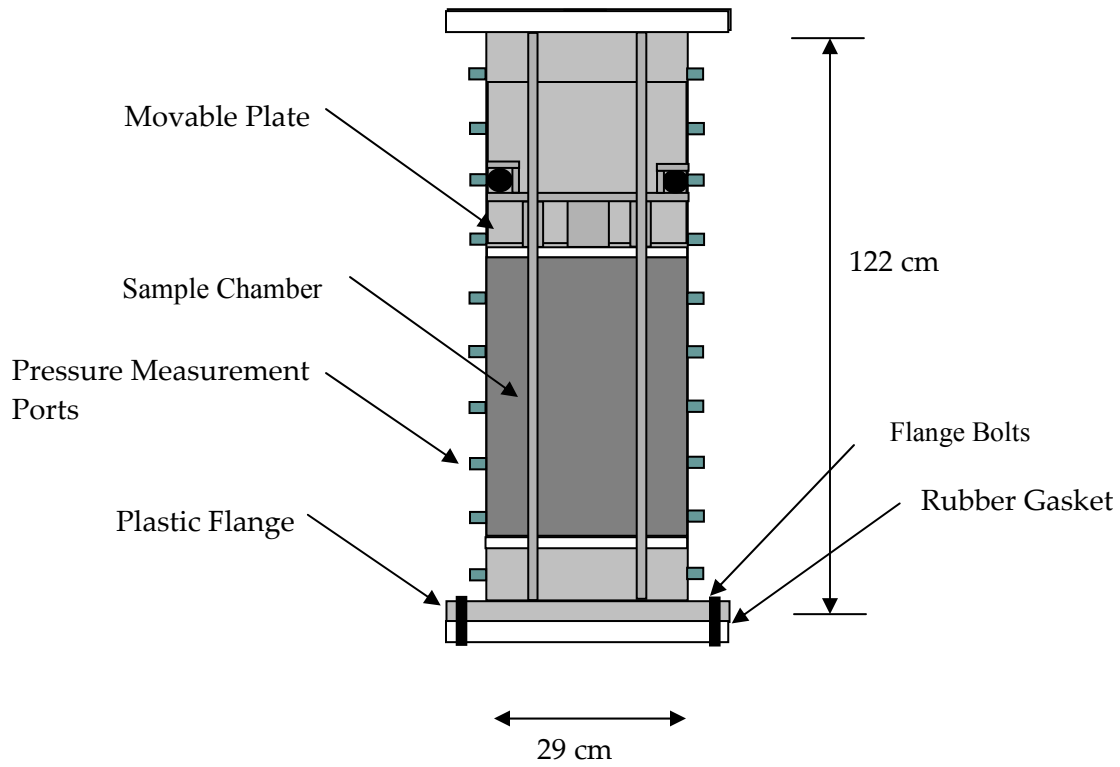
Figure 2-23. Side view of experimental unit used for air permeability tests of biocover materials

Figure 2-24. Photograph of experimental cell used for air permeability tests of biocover materials

2.5.2.4 Moisture Content Measurements

In order to determine the moisture content of the biocover materials used in the air permeability tests, three large representative samples for each biocover type were analyzed. The masses of these samples were 35.6 ± 36.8SD g (Mean ± 2 SD; SD = Standard Deviation), 282.8 ± 95.2SD g and 505 ± 33SD g for pure compost, 70 percent compost and 30 percent woodchips mixture, and greenwaste. The samples were weighed, placed in an oven at 104° Celsius (C), and weighed daily to ensure complete drying for three days. No additional mass reduction was observed after three days for all samples.

2.6   Results

2.6.1   Compressibility Tests

The initial heights of samples for the compaction test were different. This was due to uncertainty in the required amount of each mixture for the compaction tests. The initial heights of samples (H_0) were 35.2 cm, 39.1 cm, 36.8 cm, and 39.1cm for sample Nos.1 to 4, respectively.

Because of this variation, the dimensionless degree of compaction was used to compare between samples. The results from the compaction tests of these four samples are presented in Tables 2-4, 2-5, 2-6, and 2-7. Bulk densities were corrected to represent mass of dry solid per sample volume.

Table 2-4. Compaction results for sample No. 1–100% compost

Compaction step	Height reduction, cm	Cumulative height reduction, cm	Height of sample, cm, (H)	Dimensionless compacted height, (H/H_0)	Bulk Density, gr/cm^3
1st	9.6	9.6	25.7	0.728	0.63
2nd	0.4	10.0	25.3	0.717	0.63
3rd	0.3	10.3	25.0	0.708	0.63
4th	0.3	10.6	24.7	0.700	0.66

Source: University of Delaware

Table 2-5. Compaction results for sample No. 2–90% compost 10% woodchips

Compaction step	Height reduction, cm	Cumulative height reduction, cm	Height of sample, cm, (H)	Dimensionless compacted height, (H/H_0)	Bulk Density, gr/cm^3
1st	6.8	6.8	32.3	0.827	0.55
2nd	0.7	7.5	31.6	0.810	0.55
3rd	0.5	8.0	31.1	0.795	0.55
4th	0.5	8.5	30.6	0.784	0.58

Source: University of Delaware

Table 2-6. Compaction results for sample No. 3–70% compost 30% woodchips

Compaction step	Height reduction, cm	Cumulative height reduction, cm	Height of sample, cm, (H)	Dimensionless compacted height, (H/H_0)	Bulk Density, gr/cm^3
1st	7.3	7.3	29.6	0.803	0.55
2nd	0.5	7.8	29.0	0.787	0.55
3rd	0.5	8.3	28.6	0.776	0.58
4th	0.4	8.7	28.2	0.765	0.58

Source: University of Delaware

Table 2-7. Compaction results for sample No. 4–50% compost 50% woodchips

Compaction step	Height reduction, cm	Cumulative height reduction, cm	Height of sample, cm, (H)	Dimensionless compacted height, (H/H$_0$)	Bulk Density, gr/ cm^3
1st	5.0	5.0	34.1	0.873	0.42
2nd	0.5	5.5	33.5	0.858	0.42
3rd	0.5	6.0	33.1	0.847	0.42
4th	0.5	6.5	32.6	0.835	0.42

Source: University of Delaware

The bulk density changes considerably due to different amounts of woodchips. Generally it can be concluded that the higher the percentage of woodchips the less the bulk density. Also, the most significant compaction occurs in the first compaction step. No appreciable height reduction was observed after subsequent compaction steps (less than 2 percent of height reduction after each step).

2.6.2 Air Permeability Tests

The air permeability tests were performed on three types of biocover material, all described in the Materials and Methods section. For each material, a constant air flow rate was established through the experimental column. The air pressures at different ports along the sample chamber were measured. Knowing the flow rate and cross sectional area of the chamber, the Darcy's velocity was computed. A new flow rate was established in the column and the measurements repeated. Each pressure gradient measured along the chamber was divided by air viscosity and distance between sample ports and plotted versus the superficial (Darcy's) velocity. Examples of these plots are shown in Figures 2-25 and 2-26 for the mixture containing 70 percent compost and 30 percent woodchips for one set of pressure ports. Because the data support a linear model (R-squared values are near 1), Darcy's law applies for gas flow to these media and the slope of the fitted line is the air permeability in m².

In order ensure that the air permeability was homogeneous throughout the chamber, air permeabilities were measured for four separate sections of each column, each section 10.2 cm in length. There was no systematic variation in the measured air permeability with location, which indicated that each of the biocover materials was packed homogeneously in the column. Because of this finding, the data were averaged to determine a best estimate of the air permeability for each biocover material. The mean and the 95 percent confidence interval of the mean are reported in Table 2-8 for the materials tested.

$y = 8.0766E-12x + 5.5222E-07$

$R^2 = 9.9517E-01$
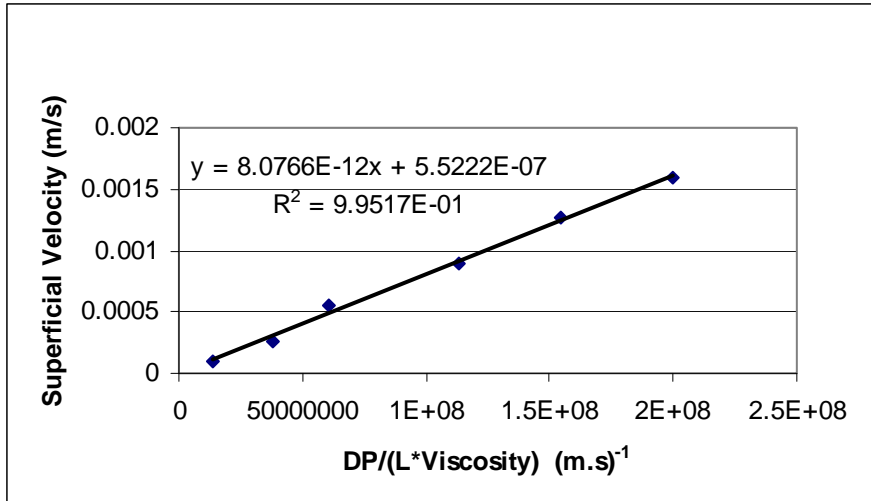
Figure 2-25. Plot of air permeability calculation for one set of pressure ports

Photo Credit: University of Delaware ; Photo Credit: Yolo County Planning & Public Works Department

$y = 7.5340E-12x - 2.9971E-05$

$R^2 = 9.9883E-01$
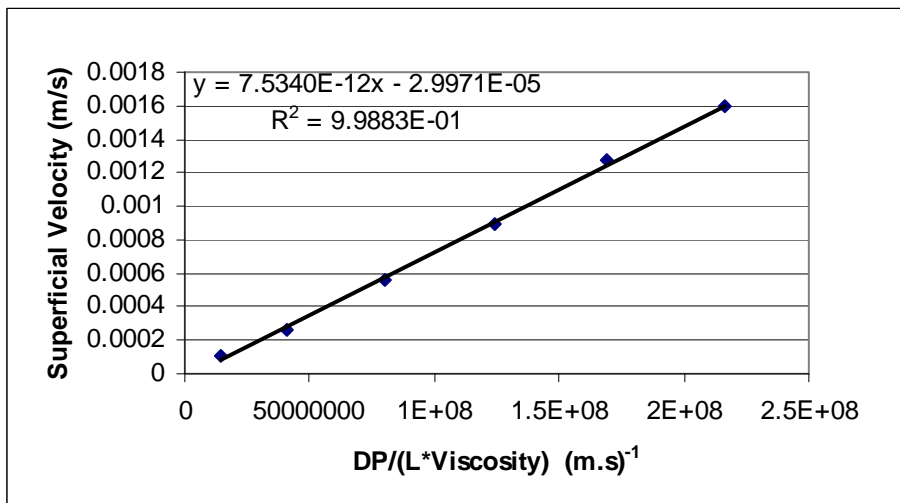
Figure 2-26. Plot of air permeability calculation for one set of pressure ports

Photo Credit: University of Delaware ; Photo Credit: Yolo County Planning & Public Works Department

Table 2-8: Air permeability of various biocover materials

Biocover Type	Mean Air Permeability (m^2)	Standard Deviation	95% Confidence Interval	Bulk Density (gr/cm^3)
Compost	9.95E-12	2.45E-12	6.21E-13	0.71
Compost (70%) - Woodchips (30%)	7.86E-12	1.55E-12	3.91E-13	0.61
Greenwaste	8.66E-11	9.69E-11	2.45E-11	0.69

Source: University of Delaware

The greenwaste shows the highest gas permeability of the materials tested, probably because the particle sizes appeared larger for this medium. Comparing the compost to the mixture of 70 percent compost and 30 percent woodchips, it is apparent that the addition of woodchips had a negligible effect on the gas permeability.

2.6.3 Moisture Content Measurements

The results of the moisture content measurements for the materials tested in the air permeability experiments are presented in Table 2-9, following the procedures outlined above. The weight of samples was measured daily for three days, after which no significant mass loss (less than 1 percent change in mass during a 24-hour period) was observed.

Table 2-9. Measured moisture content of various biocover materials

Biocover Type	Mean Moisture Content (%)	Standard Deviation	95% Confidence Interval
Compost	30.64	1.95	4.85
Compost 70%- Woodchips 30%	30.95	0.64	1.60
Greenwaste	6.22	0.11	0.28

Source: University of Delaware

These data suggest that the addition of woodchips had little effect on the initial moisture content of the mixture. The greenwaste had low water content and may not support significant microbial growth without the addition of water to this material in the field.

2.6.4 Conclusions

After performing the compaction, air permeability, and moisture content analyses, the following conclusions can be drawn from the data.

Samples with higher amount of woodchips are compacted to smaller densities than those with lower amount of woodchips. The bulk density was 0.64 gr/cm³ and 0.42 gr/cm³ for pure compost and 50 percent compost-50 percent woodchips, respectively. This shows more than a 35 percent decrease.

The most significant degree of compaction is achieved after the first compaction step. Only minor amounts of additional compaction occur with subsequent compaction steps. Almost 90 percent of compaction happened during the first compaction step for all samples.

To reach a final biocover thickness of either 1 foot (ft) or 3 ft, the approximate amount of each mixture needed is presented in Table 2-10, based on the compaction densities reported in Tables 4 through 7. The information in this table can be used to help estimate the required amount of biocover materials needed in the field.

Table 2-10. Approximate initial thickness of material required for achieving the final desired height

Sample No.	Dimensionless compacted height, (H/H_0)	Initial height, ft (Final height = 30.5 cm)	Initial height, ft (Final height = 91.4 cm)
1	0.700	43.6	130.7
2	0.784	38.9	116.6
3	0.765	39.9	119.6
4	0.835	36.5	109.5

Source: University of Delaware

The greenwaste showed the highest air permeability, which may result in higher gas flows through greenwaste biocovers as compared to biocovers constructed of pure compost or the compost-woodchips mixture. This must be considered when interpreting the methane flux-chamber tests conducted in the field.

The optimum condition for microbial growth is highly dependent on water availability inside the medium. The low moisture content of greenwaste may not support microbial growth, without the addition of water. By measuring the water retention curve for these materials, the air permeability at different moisture contents can be predicted. Consequently, a better understanding of water flows inside the biocover material will be achieved with these additional measurements.

The addition of woodchips to compost has a minor effect on the air permeability and moisture content. However, it probably significantly affects porosity, which was not part of this study. The woodchips may enhance the structure of the biocover and delay the collapse of biocover material.

Based on the results of the tests reported above, a single step compaction test to estimate compaction of biocover materials seems reasonable. A tight biocover layer, one with low gas permeability, may be achieved using only pure compost. However, addition of woodchips

increases the physical strength and as a result may delay the replacement time of biocover materials, without reduction in gas permeability.

To determine the best medium for biocover operations, additional tests are needed. These tests include ongoing experiments by Dr. Mort Barlaz at North Carolina State University to assess methane oxidation in greenwaste, and measurements of methane flux through various thicknesses of different biocover materials installed on top of the peaking power test cell at the Yolo County Central Landfill, as discussed in Section 4.1.

In addition to these laboratory experiments and field tests, though, it is important to understand the flow of methane gas and water through the biocover materials. Other research indicates that the porous medium properties affecting gas and liquid flow will dramatically influence the utility of the biocover material for methane oxidation, particularly under different climatic conditions. In this work the authors have measured some of these properties. Additional tests are needed to determine the water retention curve and total porosity of these biocover materials. With these data coupled with the laboratory and field results, it should be possible to predict the efficiency of the biocover materials under a wide range of rainfall and temperature conditions.

Chapter 3:
Project Construction

3.1 Overview

Construction of a Peaking Power cell was carried out between January 2003 and August 2005. A schematic cross sectional view of the Peaking Power Project area is illustrated in Figure 3-1.
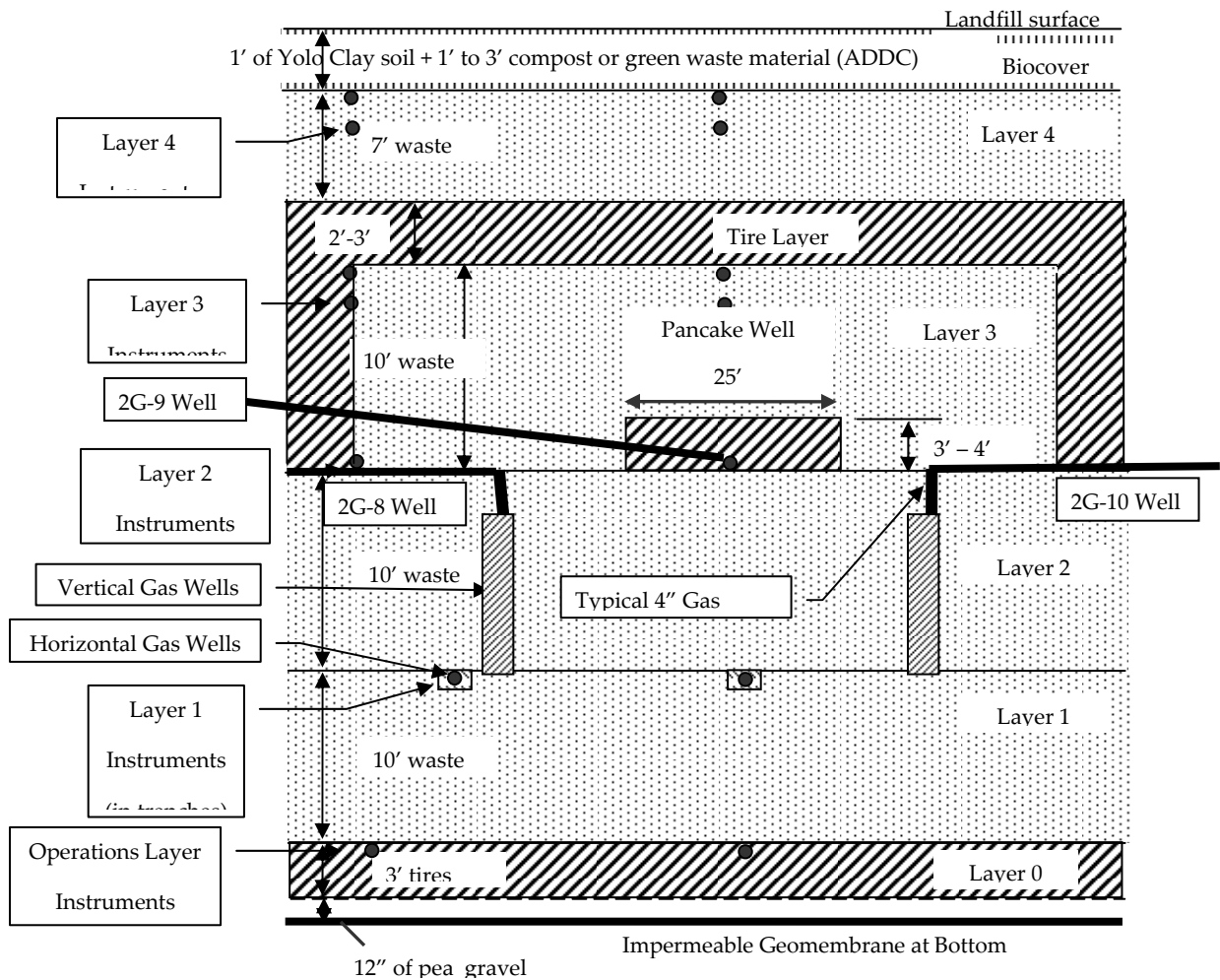
Figure 3-1. Cross-section of peaking power area

Source: Yolo County Planning & Public Works Department

3.1.1. Construction of Waste Filling and Operations Layer

Construction of waste filling consisted of placement of waste over the impermeable geomembrane protected by 12 inches of pea gravel and three feet of operations tire layer. The

tire operations layer was spread across the impermeable geomembrane lining the floor of the peaking power area between January and February of 2003.

Waste placement in the Peaking Power area was in four separate layers, where the first three were of an approximate thickness of 10 feet, and the fourth of approximately 7 feet (Figure 3-1). Between the third and fourth lifts was an un-compacted, permeable layer 3 feet thick, comprised of shredded tires. This layer was extended on the side slopes, ending near the top of Layer 2. Waste placement in Layer 1 was carried out between March and April of 2004, while the second lift was placed between November and December of 2004; finally, the third lift was placed in August 2005. The permeable tire layer was also placed in August of 2005. The fourth and final waste layer was placed in September 2005, and covered with one foot of cover soil, followed by the biocover, as described later in Section 0.

3.1.2 Construction of Pressure Sensing Tubes and Other Instrumentation

Instrumentation was included in the cell to allow for monitoring of the waste after the completion of construction. This instrumentation included PVC moisture sensors, thermisters, and High Density Polyethylene (HDPE) tubes to remotely measure gas composition and pressure. The tubes and wires for the sensors were run from the point of insertion out of the cell through 1 ¼-inch HDPE SDR 11 conduit. Layer 1 sensors were laid in a bedding of green waste and covered with another layer of greenwaste, and the conduit covered with shredded tires. In Layer 2, sensors were covered with shredded tires and the conduits covered with contaminated soil. In Layer 3, the conduits were run in trenches approximately 2 feet deep dug into waste. These trenches were later back-filled with waste and then covered with shredded tires. Layer 4 sensor lines were installed in trenches through the cover layer so they lay on top of the Layer 4 waste. In Layers 3 and 4, the tubes were connected via a barbed fitting to a ¾-inch galvanized pipe that was then inserted 3 feet deep into a vertical hole made in the waste. As-built drawings showing the location of sensors and tubes are provided in Appendix A.

3.1.3 Construction of Vertical and Horizontal Gas Collection System

Two vertical wells were constructed in the Peaking Power area, a well to the north (2-G8-P2W) of the pancake collection well, and a well to the south (2-G10-P2W) of the pancake well (see Figure 3-1). Gas collection is through a 15-foot length, 4-inch diameter, schedule 40 PVC pipe, perforated and installed in wire cages filled around with shredded tire. These wells began at the top surface of the first layer of waste, and terminated at the top of the second layer (see Figure 3-1).These wells both connect to separate 4-inch HDPE lines that exit the west face of the cell.

3.1.4 Construction of Pancake Well and Permeable Layer
3.1.4.1 Construction of the Pancake Well

The pancake well was constructed at the top of Layer 2, over a 4 foot bedding of greenwaste. The well is 4 feet deep, with a diameter of approximately 25 feet, and is comprised of single pass shredded tires. Gas collection occurs through a 25 foot long, four foot diameter HDPE SDR 11 pipe perforated with three 1-inch holes every 12 inches that runs east to west under the ring of shredded tires. The capped end of the collection pipe terminates at the far eastern periphery of the well.

3.1.5 Construction of the Permeable Layer

The permeable tire layer was constructed directly on top of Layer 3. This layer is comprised of 4 feet of uncompressed shredded tires. A trench of 4 feet deep by 4 feet wide was constructed around the perimeter of Layer 3 and back-filled with shredded tires to serve as a trench drain and divert possible leachate seeps.

3.1.6 Construction of Automatic Gas Sampling System

3.1.6.1 Physical Description

An automatic gas sampling system was constructed to automatically sample and log gas composition from various tubes throughout the cell. This system is installed in the instrumentation shed remotely located to the south-west of the peaking power area. The system consists of a KNF Neuberger single head vacuum pump, a Valco Instruments Co., Inc. (VICI) multiposition electronic actuator and rotary valve, a LandTec Landfill Gas Extraction Monitor 2000 (GEM 2000), a ChronTrol programmable timer, and a series of filters to remove moisture from the landfill gas prior to contact with the instrumentation.

Tubes from the Peaking Power cell enter the instrumentation shed and are organized in an array similar to that seen in Figure 3-2. From this array, the selected tubes are connected to the multiposition valve by removable tubes (not shown); output from this valve continues to the vacuum pump. Output from the pump runs to an external vent, and has a sampling port for the GEM 2000. In order to protect instrumentation, moisture is removed by cartridge filters located outside the shed.

The rotary valve and actuator are shown in Figure 3-3, with tube input and output streams also labeled.
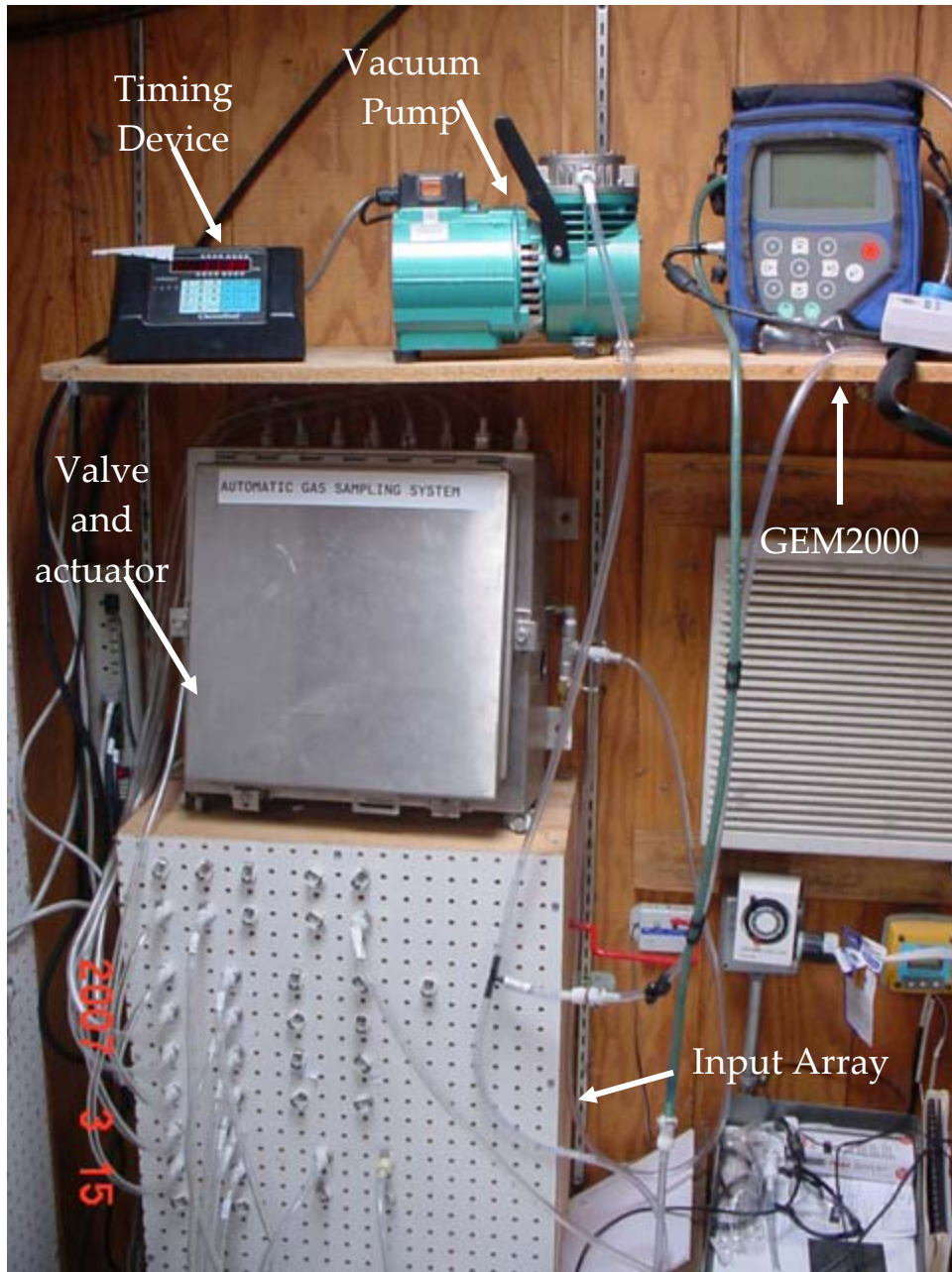
Figure 3-2. Automatic gas sampling system set-up

Source: Yolo County Planning & Public Works Department
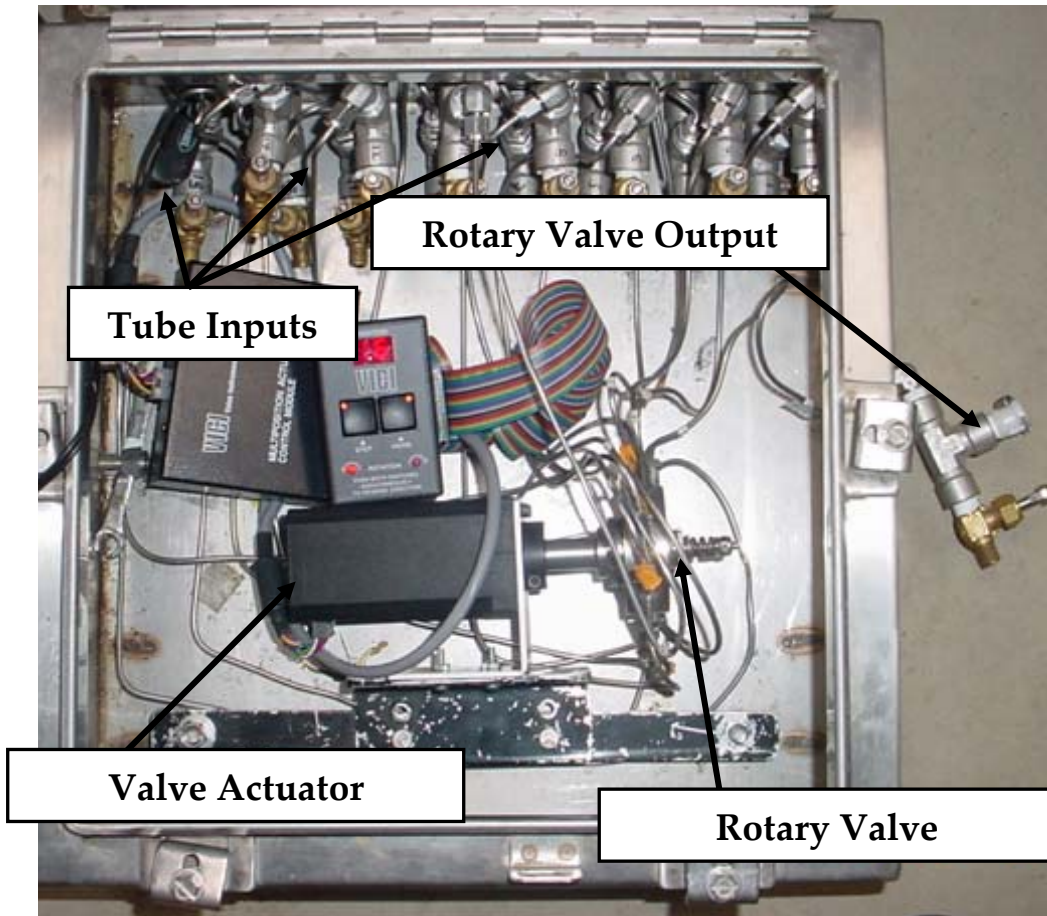
Figure 3-3. Rotary valve and valve actuator

Source: Yolo County Planning & Public Works Department

3.1.7 Operation

During operation, the pump is left on continually, the valve actuator switches through tubes, and the GEM 2000 turns on at specified intervals. The valve will remain at a particular setting for 15 minutes, ensuring the sampling tube between the shed and the Peaking Power area has purged sufficiently. After 13.5 minutes, the GEM 2000 turns on and begins sampling (30 second warm-up time, one minute sampling time). As the GEM 2000 finishes sampling and logs the data, the ChronTrol timer signals the actuator which switches the rotary valve to a new stream, and the process repeats (15 minutes total elapsed time per reading).

Gas enters the shed through a bank of filters located outside and through an array of quick-connect tubes. Up to 15 tubes can be sampled at a given time (with one designated for atmospheric), for a total of 16 tube readings. The selected tubes are connected to the automatic valve actuator by extension tubing which runs from the array in the instrumentation shed to the valve control box.

3.1.8 Construction of Landfill Gas Removal System

3.1.8.1 Gas Collection Summary

The Peaking Power LFG removal system was made continuous with the existing collection system, connecting at the north-west corner of the peaking power area. From here, gas is conveyed a short distance to the power generating facility. Gas is collected through the horizontal and vertical gas collection system and through the north well (2-G8-P2W), the pancake well (2-G9-P2W), and the south well (2-G10-P2W) through the 4-inch HDPE pipes exiting the cell on the west face, and along into a 8-inch HDPE header that runs around the perimeter of the peaking power cell; this pipe can be seen in Figure 3-4.
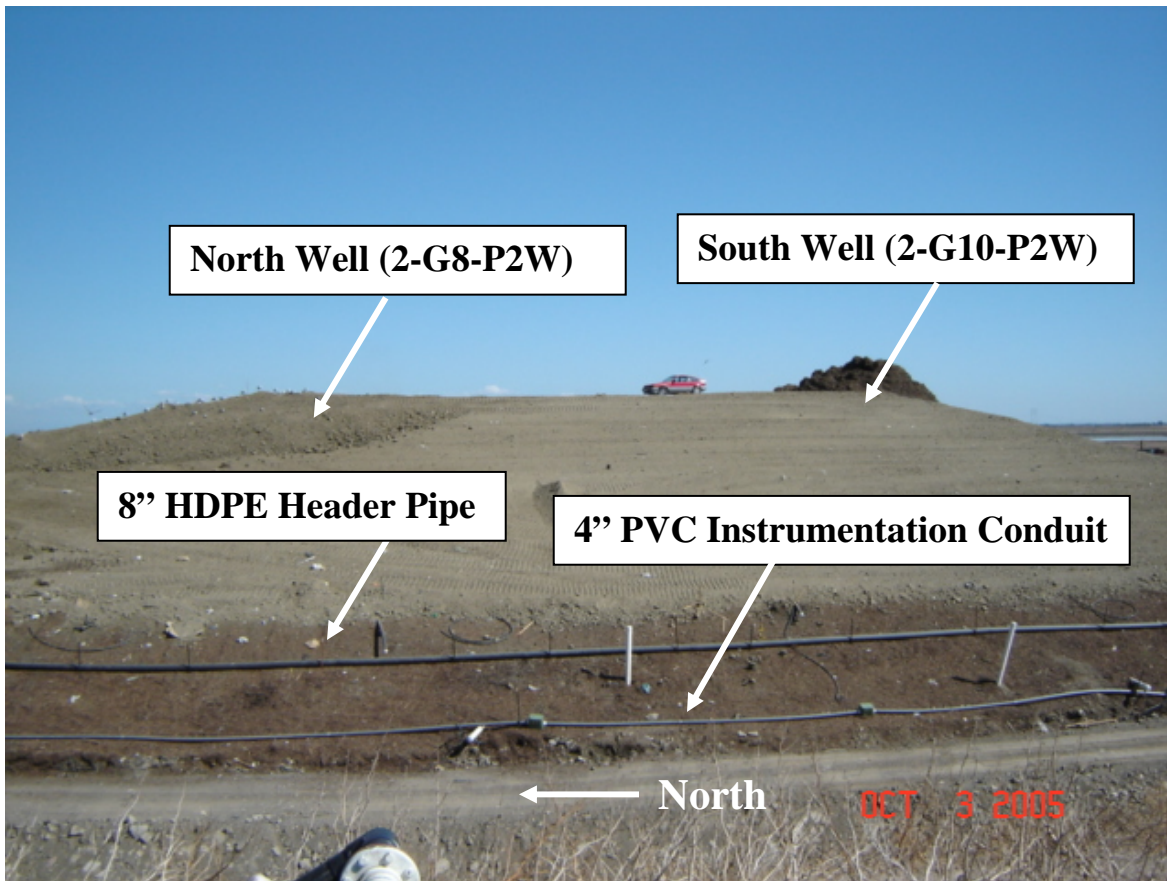
Figure 3-4. Horizontal main header on west aspect of peaking power cell

Source: Yolo County Planning & Public Works Department

3.1.9 Construction of Pancake Well Flow Measurement and Control System

Peaking flow rate was controlled from the pancake well (2-G9-P2W) by four valves connected in a combination of serial and parallel configuration; this setup is depicted in Figure 3-5. The most southern pipeline consists of two valves in series; the first valve, an electronically actuated on/off valve, controlled by a timer in the blue instrumentation shed, switches between "on-peak" flow rate (valve open), and "off-peak" flow rate (valve closed). The two northern-most extensions comprise the "off-peak" flow, and the two valves allow for coarse and fine adjustment of LFG flow-rate.

Because the two vertical wells were used to collect gas under peaking conditions for a transient period of time, a single valve was used to adjust flow manually and switch between on- and off-peak conditions.
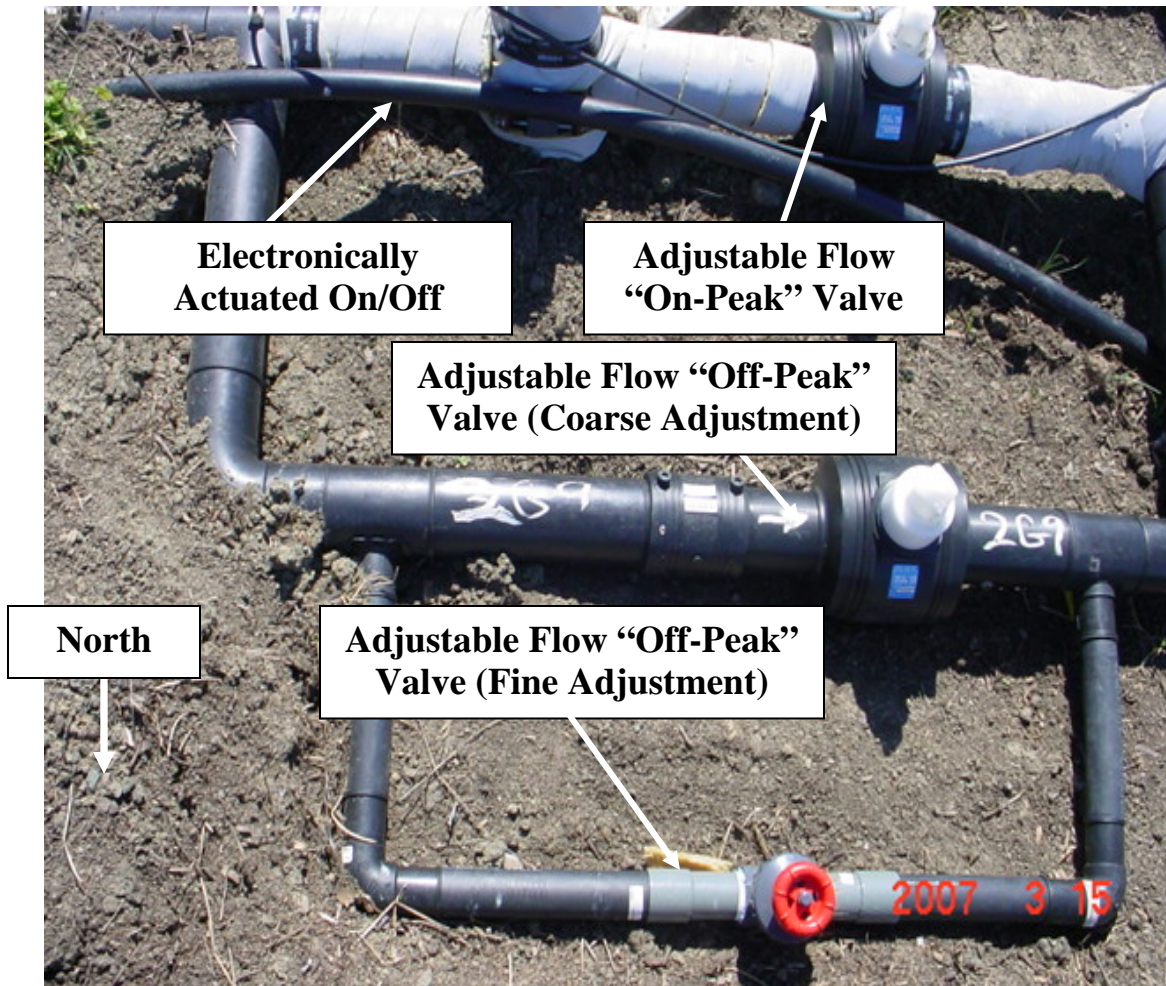
Figure 3-5. Peaking power valve setup

Source: Yolo County Planning & Public Works Department

3.1.10 Construction of Final Cover and Biocover

3.1.10.1   General Construction

After placement of the final layer (Layer 4, see Figure 4-1), 1 foot of cover soil was placed and compacted on the top and side slopes of the cell. Directly on top of the soil cover layer, a biocover layer was constructed; the side slopes were covered with one foot of compacted greenwaste.

In order to test the performance of various types of biocover material, the top of the Peaking Power area was subdivided into nine areas, described in Table 3-1. A drawing of these areas, along with more detailed descriptions, can be found in Section 4.1, as well as Appendix A.

Table 3-1. Biocover area description

Area #	Thickness (Feet)	Biocover Material
1	3	Compost/Wood Chip Mixture
2	1	Compost/Wood Chip Mixture
3	3	Compost
4	3	Greenwaste
5	1	Compost
6	1	Greenwaste
7	1	Greenwaste
8	2	Greenwaste
9	No biocover placed, 1' of soil only (Control Area)	

3.1.11 Method of Construction of Compost and Wood Chip Mixture

The compost to wood mixture was four parts compost to one part wood, by volume. A loader bucket was used to measure the volume of compost as well as wood chips. An appropriate layer of woodchips was placed on a measured layer of compost; these layers were then picked up and mixed using a paddle scraper, and then dumped on top of the Peaking Power cell with the scraper. The material was subsequently spread and further mixed and compacted using a track loader until the appropriate depths were achieved.

Chapter 4:
Project Outcomes

4.1 Biocover and Flux Chamber Measurements

4.1.1 Experimental Design and Methods

4.1.1.1 Field and Laboratory Experimental Design

CH_4 emissions were measured in the field in January and November 2006 using 1 m^2 static chambers. These two sampling events correspond to the rainy and dry seasons, respectively. Each sampling campaign lasted about two weeks during which time four to five emissions measurements were made with the LFG collection system at high vacuum, followed by a similar number of measurements with the system at low vacuum. No tests were conducted for at least 24 hours after adjustment of the LFG system to allow for equilibration of pressure. Tests were conducted on eight cover types including a soil control as described in Table 4-1. The variation in CH_4 concentration with depth was measured for most of the cover types with the LFG system at high and low vacuum. A layout of the test area is presented in Figures 4-1 and 4-2.

Table 4-1. Description of covers tested for CH4 emissions

Cover Types	Thicknesses (m)
Compost + Wood Chips	0.91, 0.31
Compost	0.91, 0.31
Green waste	0.91, 0.61, 0.31
Soil	0.31
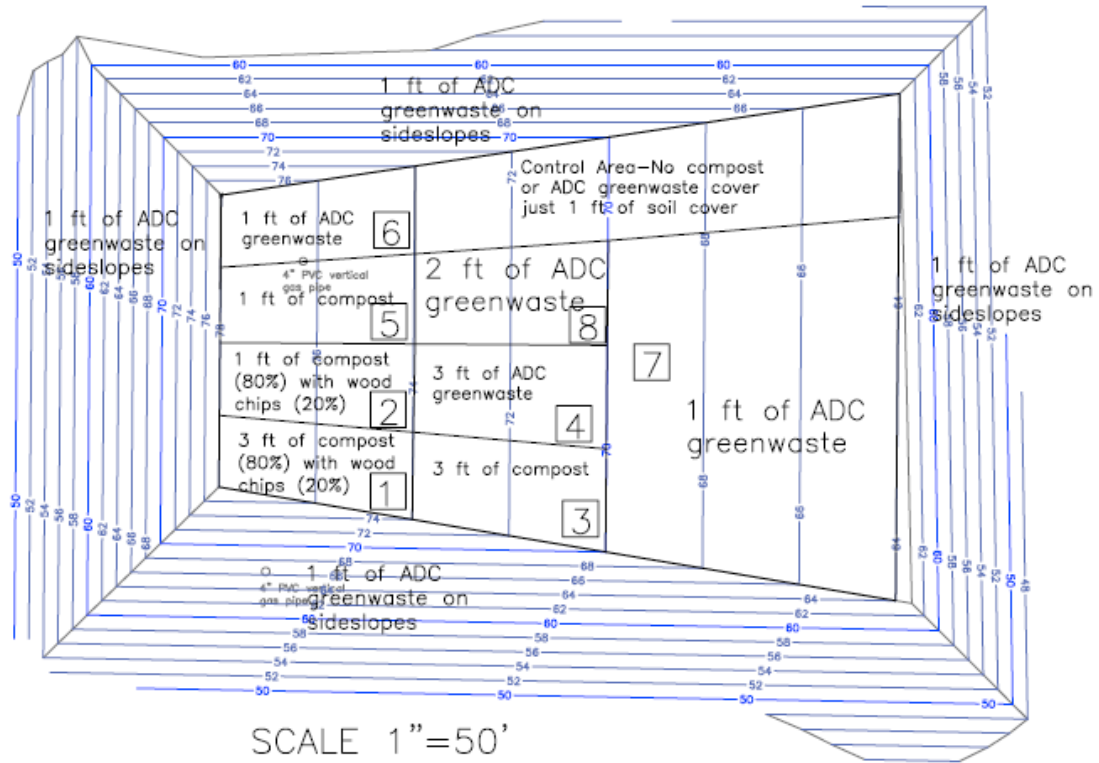
Figure 4-1. Landfill plan showing different landfill covers in place

Photo Credit: Yolo County Planning & Public Works Department
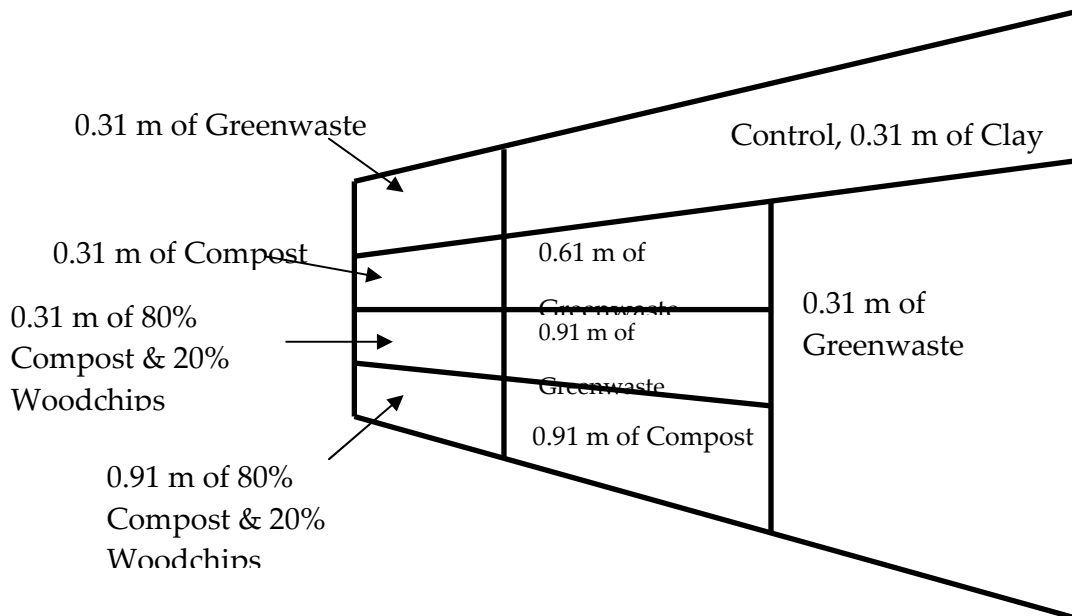
Figure 4-2. Schematic diagram showing different landfill covers

Photo Credit: Yolo County Planning & Public Works Department

69

Laboratory tests were conducted in columns to evaluate several factors thought to influence CH_4 oxidation at the landfill. Eight columns were used to assess the effects of moisture addition and pulsed vs. continuous flow. For each phase of the experiment, four columns were operated with a continuous flow of CH_4, and four columns were operated in a pulsed mode, receiving CH_4 for eight days followed by eight days with no CH_4 flow. Within each set of four columns, two were operated with moisture addition and two were operated without moisture addition to simulate the rainy and dry seasons, respectively. The assessment of the pulsed flow was intended to simulate the high and low vacuum of the LFG collection system. While a time interval of 24 to 48 hrs would have been a more appropriate simulation of field operation, this time interval was too short to allow for the column to reach steady state for purposes of measuring CH_4 oxidation. Rainfall and evaporation data for Yolo County, California, were obtained from the California Irrigation Management Information System (CIMIS), California Department of Water Resources (DWR) to simulate the net infiltration and were used to determine the amount of water to be added to the columns (http://wwwcimis.water.ca.gov/cimis/data.jsp). Water addition was calculated as rainfall minus evaporation and surface run-off was assumed to be negligible; 59 mililiters (mL)/week of water was added to the moisture addition columns. All treatments were conducted in duplicate. Columns were operated for 31 to 55 days at a series of increasing pressure gradients that were designed to represent the pressure gradients expected in the landfill. The pressure gradient in the field was estimated in work that was conducted at the University of Delaware. The maximum expected pressure gradient for the 0.61 m cover comprised of one year old shredded green waste was estimated and converted to a superficial velocity (Darcy velocity) that ranged from 10^{-5} to 10^{-6} m/s. A velocity of 10^{-5} m/s translated to a LFG flow rate of 5 mL/min (294.3 gm/m^2-day of CH_4) for the 10.2 cm diameter column used in this study. The LFG feed rate of 5 mL/min was increased to 10 mL/min and 15 mL/min in phases two and three of the experiment. As explained in the results, limited testing was also conducted at 2.5 mL/min.

4.1.2 Static Design

The static chamber consisted of a $1m^2$ stainless steel collar and a lid (Figure 4-3). The lid included a battery powered fan to mix the chamber headspace and an outlet fitted with a luer connection (Cole-Parmer EW-34507-34) so that a syringe could be used to collect samples for gas analysis. The luer adapter was held in place with a nut and washer. A three-way male lock stopcock (Cole-Parmer EW-30600-25) was placed in the luer adapter to contain gas in the static chamber except during sampling. A 0.4 cm hole was drilled at the top of the chamber for the luer adapter. Weather stripping was used to form a gasket between the chamber and the top and the top and collar were connected with binder clips. The capacity of the fan to mix the chamber contents completely in less than 30 seconds was verified in preliminary work. This was appropriate given the five minute sampling frequency.
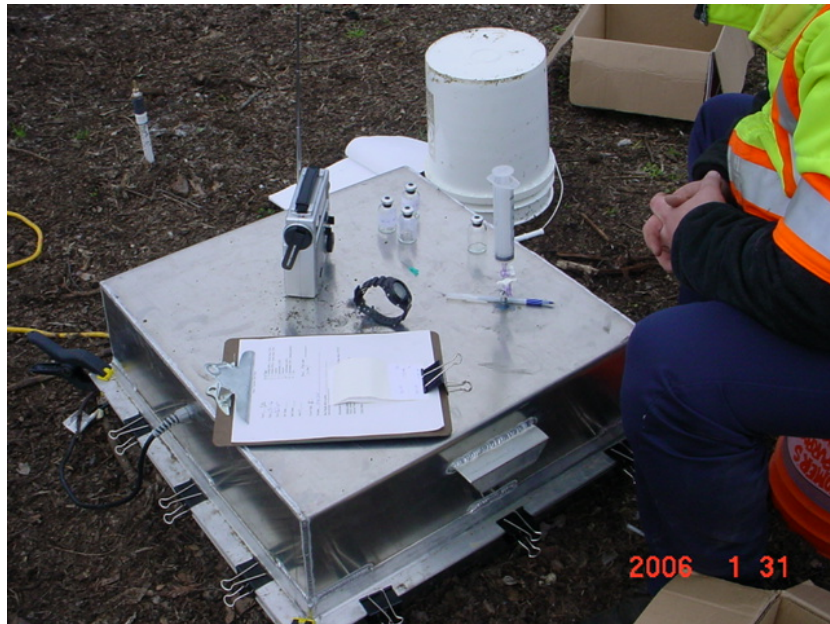
Figure 4-3. Static chamber used for emissions measurements

Photo Credit: Yolo County Planning & Public Works Department

4.1.3 Chamber Tests

Chamber collars were left in place over the entire test program and the lids were moved between collars for each test. Prior to each field test program, vegetation inside each collar was trimmed to eliminate interference with the fan. In addition, the exact collar depth was measured on four sides and the average depth was used to calculate the chamber volume that is required to calculate the methane flux. To begin a test, the lid was placed over the collar with the valve open to preclude a pressure increase. Once ready, the valve was closed which represents time zero. The first sample was collected after approximately two minutes to allow for complete mixing in the chamber. Samples were collected with a 60 mL plastic syringe inserted into the locking stopcock. The syringe was flushed with sample by withdrawing gas and injecting it back into the chamber, after which a 60 mL sample was collected and injected into evacuated 20 mL serum bottles sealed with butyl rubber stoppers and aluminum crimps. Samples were collected at approximately five minute intervals for 25 minutes.

4.1.3.1 Soil Column Construction and Assembly

Laboratory-scale column experiments were conducted with aged green waste that is being used as a daily cover at the Yolo County Landfill. The green waste was about two years old at the time that it was used to fill the columns. Each PVC column was 10.2 cm in diameter and 0.91 m long. The bottom 0.15 m was filled with gravel, followed by 0.61 m of aged green waste and a 0.15 m headspace (Figure 4-4). Columns were sealed at both ends with PVC caps. The (CH_4+CO_2) gas inlet was in the middle of the gravel layer, 0.075 m from the bottom of the column. Sample ports in the green waste were made from a compression fitting that was used to penetrate the column and a male hose barb that was used to connect tubing on the inside of

71

the column. The tygon tube was terminated in the center of the column to facilitate even gas distribution. Gas sampling ports were located 0.05, 0.2, 0.36, and 0.51 m below the top of the compost. The air inlet was located 0.13 m below the top of column, about 0.025 m above the compost. Here too, a compression fitting and male hose barb were used to connect Tygon tube inside the column. The inlet had a 0.05 m extension inside the column for proper distribution of air. The objective was to provide atmospheric conditions above the green waste surface. Water was added using a compression fitting and male hose barb from the top of the PVC cap. A perforated tygon tube was connected to the fitting for distribution of water at the top of compost.

The synthetic LFG flow to the columns was supplied from a premixed gas cylinder containing 50 percent CH_4 and 50 percent CO_2. The gas flow was regulated at 5, 10, and 15 mL/min in Phases 1, 2 and 3, respectively, using AALBORG gas mass flow controllers (Model GFC17, NY, USA). Air was supplied a rate of 50 mL/min in Phase 1 and 85 mL/min in Phases 2 and 3 to provide oxygen in excess of the stoichiometric requirement. The air flow rate was controlled by Cole-Parmer flow meters (Model C-32003-04).
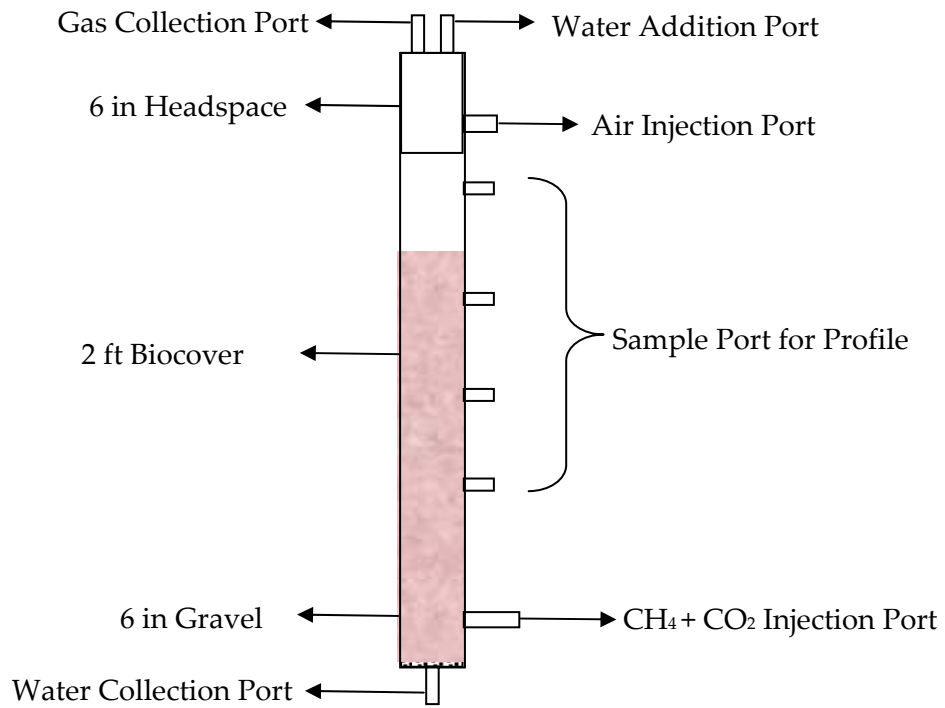
Figure 4-4. Picture (a) and Schematic (b) of the column system to study the effect of pressure gradient, moisture addition, and pulsed flow on methane oxidation

Photo Credit: Yolo County Planning & Public Works Department

4.1.3.2 Column Filling

The target dry density of 0.7 gm/cm^3 was determined at the University of Delaware based on dry bulk density values of the samples obtained from Yolo County. This translates to a wet density of 1.01 gm/cm^3 based on the compost moisture content. Gravel was used to fill the lower 0.15 m of the columns. After covering the gravel with a layer of cheese cloth, compost was added in 0.08 m thick layers. Each layer was compacted with a rod (1.22 m long by 1.4 cm diameter) to ensure uniform packing and gas flow. A uniform load was applied by dropping the rod 30 to 40 times from approximately 7.6 cm above of the compost.

4.1.3.3 Column Operation and Monitoring

All columns trials were conducted at 22° +/- 2°C. The first phase was conducted for 55 days to determine the effect of pulsed flow. The following two phases were shorter (36 days and 31 days) as explained in the results.

The extent of CH_4 oxidation was calculated from measurement of the CH_4 volume entering and leaving a column. CH_4 entering a column was recorded on the mass flow controllers that were calibrated for the LFG mixture. All of the gas exiting the column could not be collected so it was necessary to sample the exit gas and analyze composite samples. The exit gas flow rate was measured three times a day using a bubble meter. At each measurement time, the flow was measured twice and the measurements were repeated if the readings deviated by more than 2 percent. A gas sample was collected each time that the gas flow was measured and stored in a Tedlar® gas bag. In all cases, gas samples were collected at least two hours apart. To collect a gas sample, the column effluent line was connected to a gas bag for 10 minutes. Gas samples from two days were combined in one bag for composition analysis. Gas samples were transferred from the Tedlar® bags to 20 mL evacuated serum bottles using a 60 mL syringe. The gas composition and average flow rate over this two day period were used to calculate the volume of CH_4 in the effluent. For the columns receiving water, 59 mL water was added weekly and samples were always collected at least 24 hours after a water addition. For the pulsed flow columns, samples were not collected in the first 40 hours after the introduction of CH_4 to allow for flushing of the column with at least six pore volumes of gas. Periodically, samples were also collected from the samples ports to determine the depth of O_2 diffusion in the compost. Gas profile samples were always collected at least 18 hours before collection of an effluent gas sample.

4.1.4   Analytical Methods

Gas concentrations were determined on an SRI gas chromatograph (GC) equipped with a CTR1 column, a thermal conductivity detector (TCD) and a flame ionization detector (FID). The temperature of the column oven, TCD, and FID were 75, 102, and 144°C, respectively. Helium (He) was used a carrier gas together with H_2 and air. The pressures were 0.207 N/mm^2 for the carrier gas, 0.131 N/mm^2 for H_2, and 0.048 N/mm^2 for air during the analysis. The carrier gas flow rate (He) was 100 mL/min. Each gas sample was routed through the TCD followed by the FID. Thus, if a sample was too dilute to be detected by TCD, then it was detected by FID.

4.1.4.1 Moisture and Solids Analysis

The moisture content of the compost was measured based on the moisture loss at 75°C. Cellulose and hemicellulose were measured as described by Davis (1998). Briefly, a ground sample was subjected to a 72 percent (w/v) H_2SO_4 hydrolysis, followed by a secondary hydrolysis in 3 percent (w/v) H_2SO_4. The hydrolyses converted cellulose and hemicellulose to their respective monomeric sugars, glucose, xylose, mannose, arabinose, and galactose, that were quantified by HPLC-equipped with a pulsed electrochemical detector. The glucose originated from cellulose and the other sugars from hemicellulose. The solids that remain after the hydrolyses contained acid-insoluble lignin, other organics and inorganics. The lignin concentration is calculated based on the loss on ignition at 550°C.

4.1.4.2 Stable Carbon Isotope Analysis

The technique for the in-situ determination of CH_4 oxidation is based upon measuring the difference in $\delta^{13}C$ between produced or anoxic zone CH_4, which is not affected by oxidation, and that emitted from the landfill cover soil that has been subjected to oxidation (Chanton et al. 1999). Combined with estimates of the preference of the bacteria for $^{12}CH_4$ relative to $^{13}CH_4$, α, the fraction of CH_4 oxidized as it passes through a landfill cover soil can be estimated.

For chamber incubations in which the CH_4 concentration increased over time, the fraction oxidized was determined by equation 1 (Chanton et al. 1999), which describes isotopic fractionation in an open system:

$$f_o = [(\delta E - \delta A)/(\alpha_{ox} - \alpha_{trans})]*1000*100 \tag{1}$$

where, f_o is the percent of CH_4 oxidized in transit through the cover, $\delta E = \delta^{13}C$ value of emitted CH_4, $\delta A = \delta^{13}C$ value of anoxic zone CH_4, α_{ox} is the isotopic fractionation factor for bacterial oxidation and α_{trans} is the isotopic fractionation factor associated with gas transport. Some have argued that gas transport across the cover is dominated by advection (Liptay et al. 1998; Bergamaschi et al. 1998). Therefore, α_{trans} was assumed to be 1. If diffusion is important in CH_4 transport, then α_{trans} will be >1, and equation 1 defines the lower limit of CH_4 oxidation. The term α is defined as k_l/k_h where k_l and k_h refer to the rate constants of the light and heavy isotope, respectively. The bacterial fractionation factor associated with methanotrophic metabolism was determined from incubations of landfill cover samples at different temperatures (Chanton and Liptay 2000).

Anoxic zone CH_4 (δA) was collected from the gas collection header. Gas collected from a header is representative of anoxic zone CH_4 as there is very little spatial and almost no temporal variability in the isotopic composition of landfill CH_4 (Chanton and Liptay 2000; Chanton et al. 1999). Emitted CH_4 was collected from the headspace of the static chambers. The measured CH_4 $\delta^{13}C$ at the end of a chamber test was corrected for the presence of initial CH_4 through a mass balance to obtain the $\delta^{13}C$ of accumulated CH_4 ($[CH_4]_{xs}$). This term defines the $\delta^{13}C$ of CH_4 added to (or removed from) the CH_4 in the chamber at the start of the flux measurement (eqn. 2):

$$[\delta CH_4]_{xs} = (([CH_4]_{(meas)} *[\delta CH_4]_{(meas)}) - ([CH_4]_i*[\delta CH_4]_i))/([CH_4]_{(meas)} - [CH_4]_i) \tag{2}$$

where $[CH_4]_{(meas)}$ and $[\delta CH_4]_{(meas)}$ represent the concentration and $\delta^{13}C$ value of CH_4 in the chamber at the final time, $[CH_4]_i$ and $[\delta CH_4]_i$ represent the concentration and $\delta^{13}C$ value of chamber CH_4 at the initiation of the experiment, and $[CH_4]_{xs}$ and $[\delta CH_4]_{xs}$ represent the "excess" CH_4 or CH_4 added (or removed) from the chamber over the incubation time and its isotopic value.

4.1.4.3 Data Analysis

The percent CH_4 oxidized in the laboratory columns were calculated as:

$$\text{percent } CH_4 \text{ oxidized} = (CH_4 \text{ in} - CH_4 \text{ out}) / (CH_4 \text{ in}) \tag{3}$$

The CH_4 flux from a soil cover, as measured by the static chamber test, was calculated using the flowing equation:

$$\text{Flux} = V/A * \Delta c / \Delta t \tag{4}$$

where V is the static chamber volume (m^3), A is the surface area enclosed by the chamber (m^2) and $\Delta c / \Delta t$ is the slope of a plot of CH_4 concentration (ppmv) versus time (min). Flux data were then converted to a mass emission rate by using the ideal gas law. A non-zero CH_4 flux was only reported if the slope ($\Delta c / \Delta t$) was statistically different from zero ($p < 0.05$). Otherwise, a flux of zero was reported. The Regression Analysis add-in of MS Excel was used to calculate the probabilities. The correlation coefficients (r^2) for static chamber tests were generally above 0.95.

4.1.5 Results

The laboratory columns were operated for about 140 days to evaluate the CH_4 oxidation potential of the two year old green waste. The results of these tests are presented first, followed by results of the landfill cover emissions testing program.

The CH_4 oxidation rates for each column are presented in Tables 4-2 to 4-5 for each LFG feed rate. The data are plotted in Figures 4-5 and 4-6 for the continuous and pulsed flow columns, respectively. Average CH_4 uptake for each phase of the experiment is presented in Table 4-6, as the percentage of the inlet CH_4 that was oxidized, and in Table 4-7 as the gm CH_4 oxidized/m^2-day. Data for Column 4 have been excluded due to evidence of leakage. In some cases, negative values are reported which implies CH_4 production. The negative values are in general low and random and likely reflect a combination of experimental errors in measuring zero oxidation. In general, there was high variability between columns and limited reproducibility. As such, more general observations are presented with the use of statistical tests only where judged appropriate. All columns were operated in continuous flow mode after 55 days because pulsed mode did not appear to have any effect on CH_4 oxidation at the 5 mL/min flow rate. The final phase of testing, at a feed rate of 2.5 mL/min was added at the end of the experiment based on the results.

4.1.5.1 Effect of Gradient

The effects of pressure gradient on CH_4 oxidation were assessed by measuring CH_4 oxidation at flow rates of 5, 10, and 15 mL LFG/min. These flow rates correspond to CH_4 fluxes of 294.3, 588.7 and 883.01 gm/m^2-day. As presented in Table 4-6 and Figures 4-5 and 4-6, the fraction of the feed CH_4 that was oxidized decreased in each column as the CH_4 flow rate increased. While

the average percentage CH_4 oxidation ranged from 27 to 69 percent at the lowest flow rate, this decreased substantially at the highest flow rate when only column 2 exhibited CH_4 oxidation above 67 percent. Although Columns 1 and 2 were replicates, almost no CH_4 oxidation was measured in Column 1 at 10 or 15 mL/min.

CH_4 uptake was also expressed as the gm of CH_4 uptake per m^2-day which is consistent with the manner in which CH_4 emissions data are typically expressed. With the possible exception of Columns 2 and 6, average CH_4 uptake also decreased as the pressure gradient increased. The decrease in percent CH_4 oxidation suggests that the amount of CH_4 fed exceeded the oxidation capacity of the system, presumably because there was insufficient retention time in regions where CH_4 and O_2 mixed. Column 2 exhibited the most CH_4 uptake and uptake actually increased with gas feed rate while it was more variable in Column 6. Unfortunately, Columns 1 and 5, which were replicates of 2 and 6, exhibited decreased CH_4 uptake with increasing gas flow rate.

Based on the results of the 5, 10, and 15 mL/min flow rates, limited work was also conducted at 2.5 mL/min. After decreasing the flow rate from 15 mL/min to 2.5 mL/min, the fraction of CH_4 oxidized increased in the no water addition columns (1, 2, 5, 6), suggesting: (1) that the lower pressure gradient increased oxidation, and (2) some inhibition due to moisture addition. The effect of moisture addition is discussed below. The behavior of Column 2 is surprising as the mass of CH_4 oxidized decreased substantially at the lowest gas feed rate. One explanation for this would be preferential flow of some fraction of the gas.

The effect of the pressure gradient on the gas profile is each column is presented in Figure 4-7 and the complete data set is presented in Appendix B. The profile data do not suggest an effect attributable to pressure gradient, suggesting that oxygen penetration was controlled by diffusion.

Table 4-2. Methane oxidation (%) for 5 mL/min of (CH_4+CO_2) and 50 mL/min air in laboratory columns

	Pulsed CH_4 Flow			Continuous CH_4 Flow			
	- Water Addition		+ Water Addition	- Water Addition		+ Water Addition	
Column	1	2	3	5	6	7	8
Day							
4.11	33.8	95.8	22.6	15.4	ND*	-3.5	87.7
6.26	23.9	98.9	53.8	35.6	ND	15.4	94.5
8.53	47.2	91.1	43.4	90.2	ND	13.2	90.5
10.5				36.1	ND	9.3	96.0
12.11				33.0	ND	34.3	66.5
14.5				74.5	60.0	77.8	91.9

	Pulsed CH_4 Flow			Continuous CH_4 Flow			
	- Water Addition		+ Water Addition	- Water Addition		+ Water Addition	
Column	1	2	3	5	6	7	8
Day							
16.5				24.6	73.1	13.9	79.0
18.2	71.8	96.5	49.7	20.6	81.8	5.4	93.5
20.2	32.4	94.9	51.4	62.4	51.2	52.7	100.0
22.5	29.5	91.1	13.5	23.1	63.3	61.5	81.9
24.3	33.9	92.0	11.5	34.1	72.5	51.9	79.5
26.3				23.0	55.0	45.8	52.9
28.4				17.5	44.8	25.7	66.6
30.4				26.6	57.0	61.5	73.8
32.2				18.9	50.6	53.5	38.5
34.24				100.0	30.5	100.0	71.1
36.06				32.3	43.4	57.1	66.7
38.27	56.4	93.9	-13.0	15.2	43.4	57.1	66.7
40.18	26.5	90.3	-0.1	-10.9	43.7	55.2	68.3
42.31				9.3	40.3	56.7	62.7
44.27				16.9	38.3	54.7	61.9
46.27				17.3	37.2	54.4	61.5
48.32				13.9	47.6	49.3	76.4
50.26	63.8	90.9	35.1	20.9	50.1	25.0	17.5
52.29	34.6	87.3	22.3	25.6	62.9	40.2	29.6
54.29	14.5	83.5	31.2	14.1	54.4	34.6	-7.1

*ND = No column 6 data due to problems with mass flow controller

Data collected by Yolo County project team

Table 4-3. Methane oxidation (%) for 10mL/min of (CH$_4$ + CO$_2$) as well as 50 mL/min and 85 mL/min air in laboratory columns

	Continuous CH$_4$ Flow						
	- Water Addition		+ Water Addition	- Water Addition		+ Water Addition	
Column	1	2	3	5	6	7	8
Day							
4.35	8.3	74.2	18.6	-1.5	47.4	10.3	-6.0
6.34	15.8	75.7	0.2	8.8	50.8	12.8	-4.1
8.61	-3.4	70.6	5.5	-0.4	41.1	7.6	-8.4
12.61	21.2	76.5	24.6	2.4	32.0	12.2	18.3
14.64	17.7	72.2	2.4	1.3	37.3	6.6	0.5
16.7	4.0	71.3	21.6	19.8	31.1	11.4	0.6
18.6	11.4	75.4	19.7	18.6	34.5	14.6	11.6
22.6	-2.6	67.7	-2.7	23.7	20.5	5.2	-6.8
24.6	-2.2	71.8	25.9	16.2	24.2	20.4	19.3
26.7*	-13.8	70.1	-1.0	-11.6	25.2	3.5	-16.7
28.6	-8.3	72.0	22.3	-10.0	33.9	-1.5	-6.5
30.7	-15.0	67.1	-8.7	-9.2	19.1	-4.9	-8.0
32.6	0.2	70.0	11.9	7.2	20.5	-5.1	-18.4
34.6	0.6	74.4	4.0	-2.8	26.0	14.7	-6.8
36.4	-7.9	71.7	-3.2	-6.9	27.1	-2.0	-8.2

* Air flow rate was changed from 50 mL/min to 85 mL/min on this day

Data collected by Yolo County project team

Table 4-4. Methane oxidation (%) for 15 mL/min of (CH_4+CO_2) and 85 mL/min air in laboratory columns

	Continuous CH_4 Flow						
	- Water Addition		+ Water Addition	- Water Addition		+ Water Addition	
Column	1	2	3	5	6	7	8
Day							
3.42	5.59	69.34	17.26	4.0	21.1	10.0	63.8
5.33	-7.59	68.1	4.6	-4.7	14.5	0.6	58.0
7.4	0.8	75.2	1.2	15.0	25.1	-4.9	23.8
9.35	2.4	66.5	-2.8	-6.0	22.3	-4.5	-9.2
11.37	2.8	65.4	12.0	9.1	14.2	-1.8	-17.0
13.3	-11.3	63.4	-5.7	-13.8	6.9	-11.1	-17.1
15.3	6.3	68.6	-2.1	0.9	29.2	-8.6	-13.9
17.3	4.0	64.4	3.1	-1.9	8.4	-3.7	-13.0
19.4	-8.5	65.2	-8.4	-11.4	7.7	-9.7	-17.1
21.38	-5.8	67.3	4.6	-7.4	10.5	-6.7	-2.8
25.34	18.9	64.7	22.3	-7.5	6.0	2.4	0.5
27.36	-18.4	62.9	-16.6	-17.5	6.3	-14.9	-21.3
29.3	-1.4	70.5	15.3	-13.6	11.9	3.0	8.8
31.3	1.6	65.7	13.3	-6.2	19.6	11.8	6.2

Data collected by Yolo County project team

Table 4-5. Methane odixation (%) for 2.5 mL/min of (CH_4 + CO_2) and 50 mL/min air in laboratory columns

	Continuous CH_4 Flow						
	- Water Addition		**+ Water Addition**	**- Water Addition**		**+ Water Addition**	
Column	**1**	**2**	**3**	**5**	**6**	**7**	**8**
Day							
4.5	17.2	74.8	13.4	22.4	63.6	2.7	-22.7
6.4	46.2	83.4	37.7	47.6	77.8	35.8	7.6
8.2	27.3	80.0	16.3	32.5	66.8	13.4	-13.2
10.4	26.5	78.1	10.4	28.9	68.6	20.7	3.2
12.4	40.6	75.2	28.9	37.3	52.6	-12.8	-17.3
16.4	33.7	77.4	ND*	ND	ND	-6.6	-21.2
18.4	33.1	76.4	ND	ND	ND	2.9	-13.7

*Columns were taken apart for moisture analysis

Data collected by Yolo County project team
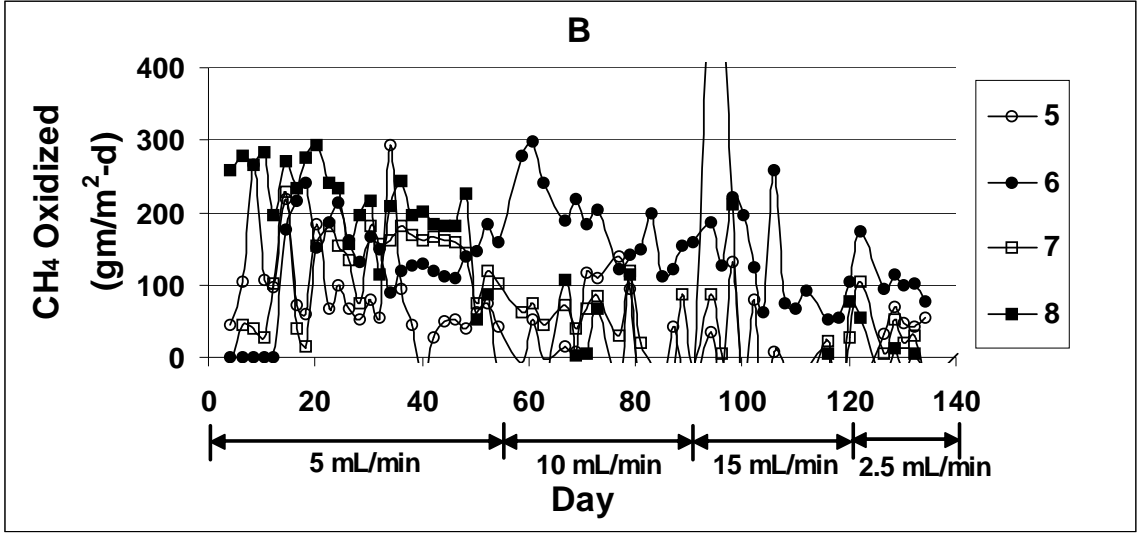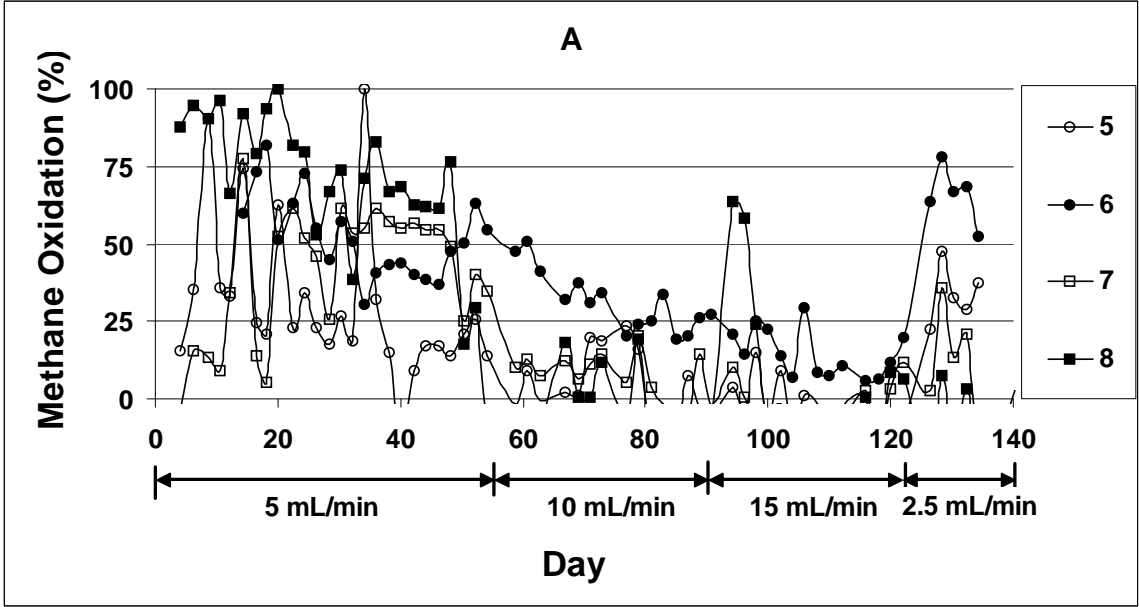
Figure 4-5. Methane oxidation in continuous flow laboratory columns; (A) expressed as percent oxidation and (B) expressed as methane uptake rate. Columns 5 and 6–No Water Addition; Columns 7 and 8–Water Addition

Photo Credit: Yolo County Planning & Public Works Department

82
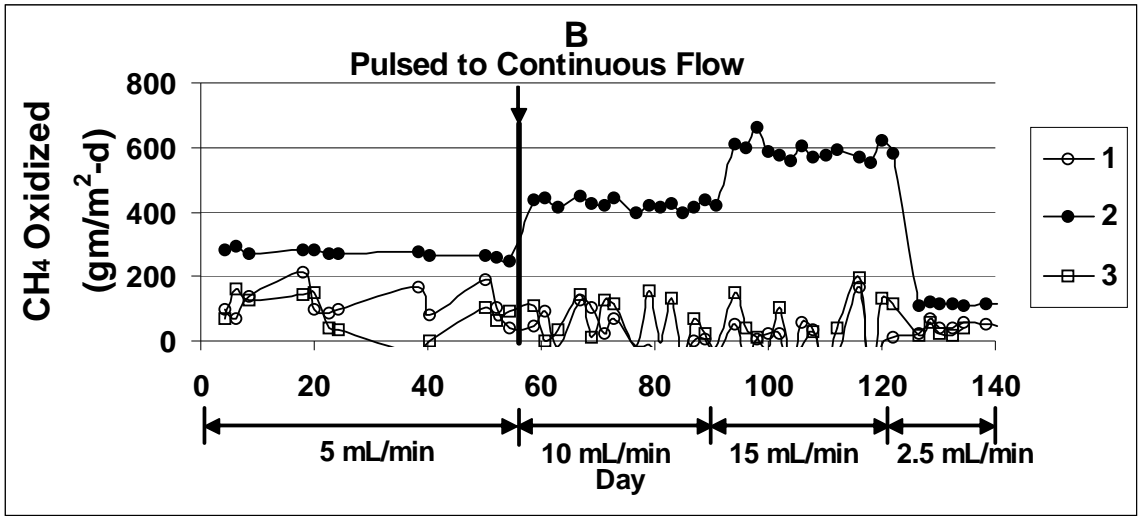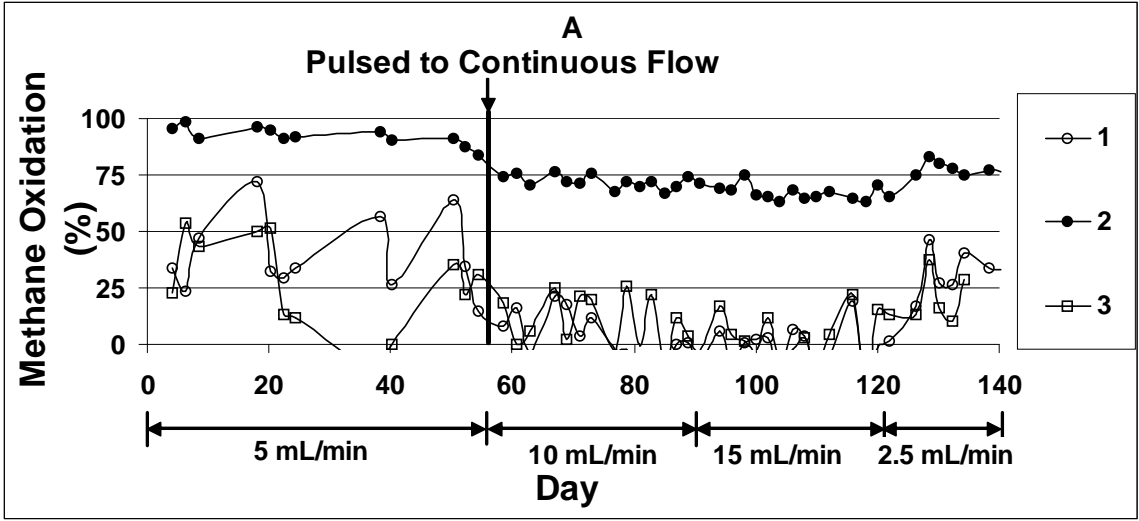
Figure 4-6. Methane oxidation in pulsed flow columns; (A) Expressed as percent oxidation and (B) expressed as methane uptake rate. Columns 1 and 2–No Water Addition; Column 3–Water Addition

Photo Credit: Yolo County Planning & Public Works Department

Table 4-6. Average CH$_4$ oxidation at each feed gas flow rate (%)

Gas Flow (mL/min)		% CH$_4$ Oxidized						
		*Pulsed Methane Flow			Continuous Methane Flow			
		- Water Addition		+ Water Addition	- Water Addition		+ Water Addition	
		1	2	3	5	6	7	8
5	Average	39.0	92.2	26.8	30.4	52.3	40.9	68.6
	s.d.	17.2	4.2	21.3	25.0	13.1	21.3	25.5
10	Average	1.7	72.0	9.4	3.7	31.4	7.1	-2.7
	S.d.	11.2	2.8	11.8	11.5	9.7	7.8	11.2
15	Average	-0.6	67.4	2.1	-1.0	16.6	-3.8	6.5
	S.d.	6.7	3.6	8.3	9.3	8.2	6.4	33.4
2.5	Average	32.1	77.9	21.3	33.7	65.9	8.0	-11.1
	S.d.	9.6	3.0	11.6	9.4	9.1	16.7	11.8

*Columns were operated in pulsed mode at 5 mL/min. At other phases columns 1, 2, and 3 were operated in continuous mode.

Data collected by Yolo County project team

Table 4-7. Average CH$_4$ oxidized at each feed gas flow rate [gm-CH$_4$/(m^2-d)]

Gas Flow (mL/min)		gm CH$_4$/(m^2-d) Oxidized						
		*Pulsed Methane Flow			Continuous Methane Flow			
		- Water Addition		+ Water Addition	- Water Addition		+ Water Addition	
		1	2	3	5	6	7	8
5	Average	114.9	271.4	78.8	89.5	124.3	120.3	202.0
	S.d.	50.6	12.4	62.6	73.6	70.9	62.8	75.1
10	Average	10.3	424.1	55.4	21.8	184.8	41.6	-15.6
	S.d.	65.9	16.4	69.3	68.0	56.9	45.7	65.8
15	Average	-6.7	591.2	36.6	-38.4	128.4	-24.0	31.4
	S.d.	80.6	28.9	96.4	80.6	67.6	67.9	241.5
2.5	Average	47.2	114.6	31.39	49.65	96.9	11.8	-16.3
	S.d.	14.14	33.2	4.42	13.9	13.4	24.5	17.4

*Columns were operated in pulsed mode at 5 mL/min. At other phases columns 1, 2, and 3 were operated in continuous mode.

Data collected by Yolo County project team

4.1.5.2 Effect of Infiltration

Columns 3, 7, and 8 received weekly moisture additions while the remaining columns did not. As CH_4 oxidation was observed in many columns, the initial compost moisture content was clearly sufficient to support CH_4 oxidation.

The profile data are presented in Figure 4-7 and are divided by columns that did and did not receive a moisture addition in Table 4-8. These data show that the O_2 concentration in all columns was comparable after four days. Thereafter, the O_2 concentration at each level was lower in the columns that received moisture addition. Similarly the methane concentration was higher at each level. Apparently, the addition of moisture filled some of the compost pore space, thus decreasing the potential for gaseous diffusion. The added moisture may also have stimulated decomposition of the compost which would increase O_2 uptake by the compost. The decrease in O_2 concentration would suggest inhibition of CH_4 oxidation based on limited O_2 availability although for the 5, 10, and 15 mL/min tests, there is too much variability in the CH_4 uptake data to make a definitive statement. The effect appears more clearly at the 2.5 mL/min test where methane oxidation was consistently lower in the columns that received moisture.

Table 4-8. Average O^2 and CH_4 concentration profiles in moisture addition and no moisture addition columns

Depth Below Top of the Compost (cm)	O_2			CH_4		
	Avg. in Moisture Addition Columns (SD)	Avg. in No Moisture Addition Columns (SD)	p^*	Avg. in Moisture Addition Columns (SD)	Avg. in No Moisture Addition Columns (SD)	p^*
Day 4: 50 ml/min Air + 5 ml/min LFG						
5.1	9.8 (3.2)	11.5 (1.0)	0.46	18.8 (9.6)	13.6 (7.0)	0.49
20.3	2.5 (1.4)	2.2 (0.7)	0.74	39.1(9.5)	38.9 (6.5)	0.97
35.6	1.5 (0.3)	1.6 (0.5)	0.67	45.9 (2.6)	46.4 (0.2)	0.77
50.8	1.2 (0.3)	1.2 (0.1)	0.87	48.4 (2.0)	48.8 (0.8)	0.77
Day 55: 50 ml/min Air + 5 ml/min LFG						
5.1	0.7 (0.1)	8.2 (2.4)	0.009	50.3 (0.1)	11.8 (4.6)	0.00
20.3	0.6 (0.03)	3.7 (2.9)	0.21	50.2(0.3)	33.7 (13.3)	0.16
35.6	0.7 (0.2)	1.7 (1.4)	0.27	49.8 (0.3)	44.1 (6.1)	0.15
50.8	0.6 (0.1)	1.9 (2.3)	0.33	50.1 (0.3)	45.5 (6.9)	0.28
Day 90: 85 ml/min Air + 10 ml/min LFG						
5.1	0.8 (0.1)	7.9 (2.3)	0.009	48.4 (0.2)	22.8 (3.5)	0.001
20.3	0.7 (0.02)	3.5 (0.5)	0.01	48.7 (0.2)	41.5 (1.4)	0.01

Depth Below Top of the Compost (cm)	O$_2$			CH$_4$		
	Avg. in Moisture Addition Columns (SD)	Avg. in No Moisture Addition Columns (SD)	p*	Avg. in Moisture Addition Columns (SD)	Avg. in No Moisture Addition Columns (SD)	p*
35.6	0.7 (0.02)	1.2 (1.1)	0.42	48.1 (0.04)	46.5(2.6)	0.31
50.8	0.7 (0.1)	0.7 (0.03)	0.73	48.3 (0.4)	48.1 (0.2)	0.41
Day 121: 85 ml/min Air + 15 ml/min LFG						
5.1	0.6 (0.2)	6.9 (2.1)	0.01	49.2 (0.3)	26.1 (4.5)	0.002
20.3	0.6 (0.02)	5.0 (3.7)	0.33	49.1 (0.2)	40.6 (4.7)	0.24
35.6	0.6 (0.1)	1.9 (1.7)	0.22	48.8 (0.2)	45.6 (4.1)	0.22
50.8	0.6 (0.2)	3.3 (5.4)	0.39	48.3 (0.4)	41.6 (13.2)	0.38

* The probability that the mean O$_2$ or CH$_4$ concentration is statistically similar between columns that did and did not receive a water addition.

Data collected by Yolo County project team

(a)
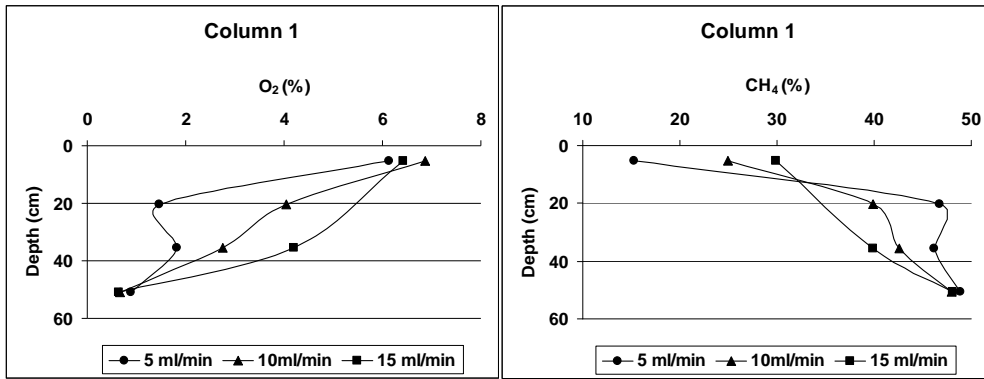
(b)
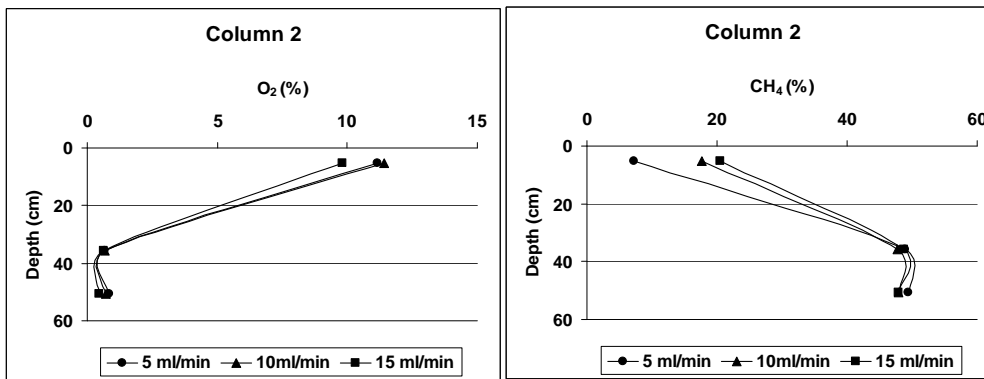
(c)
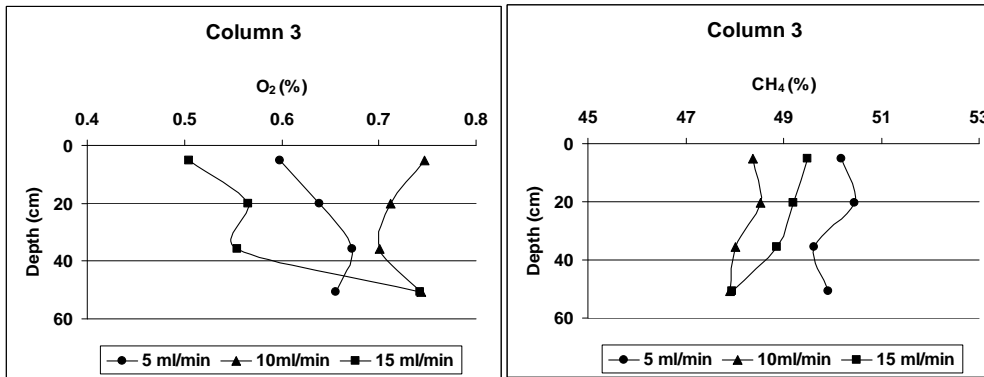
(d)
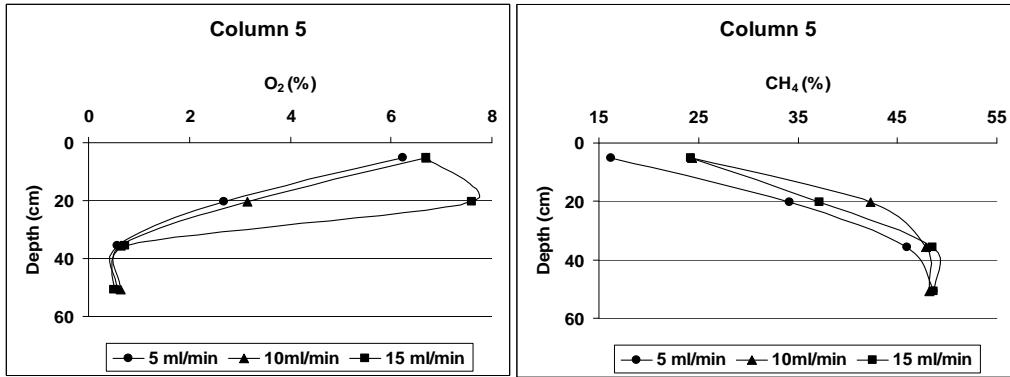
(e)
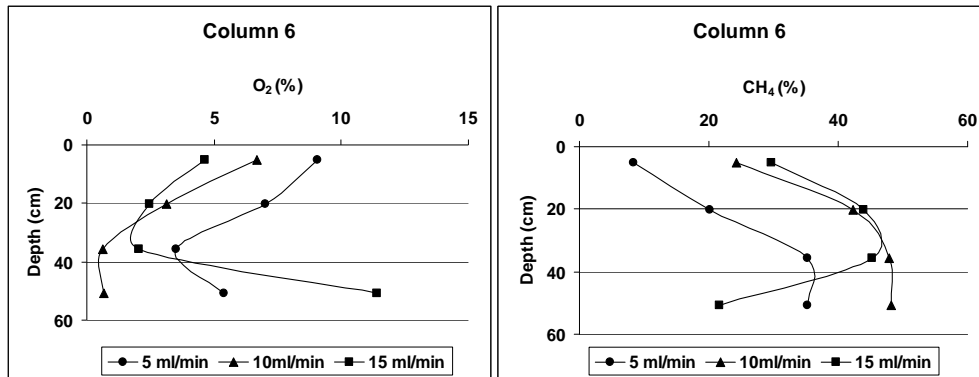
(f)

)
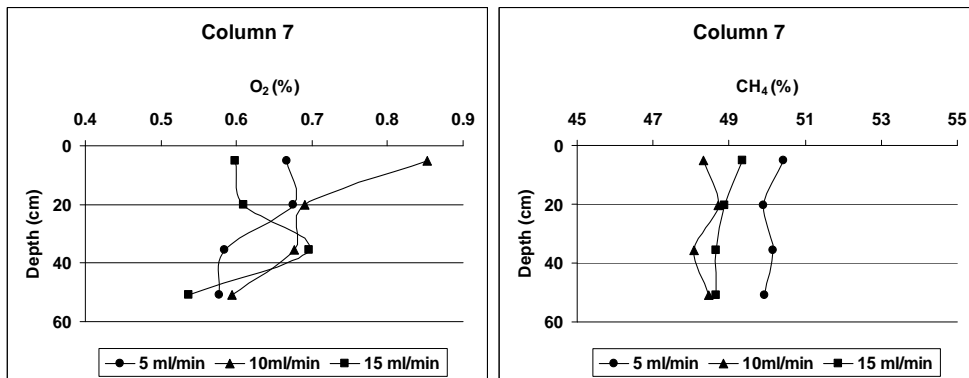
(g)
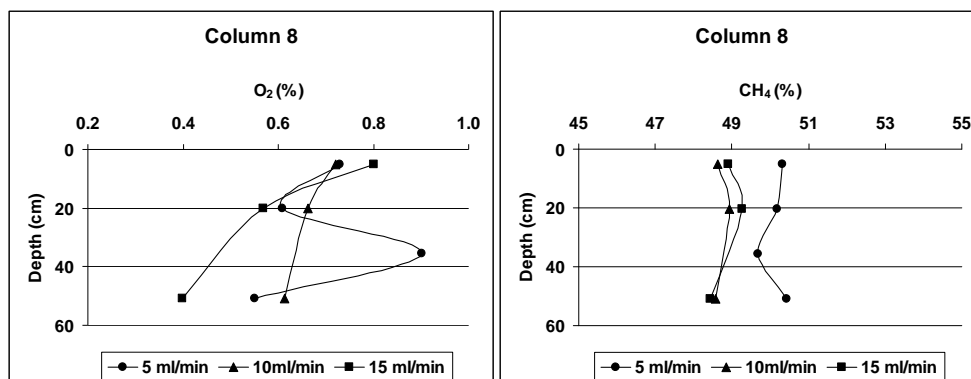
Figure 4-7. O$_2$ and CH$_4$ profiles. Profiles were collected on Days 55, 90, and 121 for 5, 10, and 15 ml/min flow rates, respectively. Note that the X-axis scale varies between plots.

Photo Credit: Yolo County Planning & Public Works Department

The moisture contents of the columns at the end of the experiment are summarized in Tables 4-9 and 4-10 and profiles with depth are presented in Figure 4-8. The total volume of water added to Columns 3, 7, and 8 over the experimental period was 1.18 L per column. Assuming initial compost moisture content of 31.2 percent, this volume of water would have increased the compost moisture content to 44.35 percent if the moisture was spread evenly throughout the column, or to 64.6 percent if the moisture wetted the top 25 percent of the compost only. These values do not include evaporative losses or the production of water as an end product of CH$_4$ oxidation. The volume of water produced from the cumulative methane oxidized in each column ranged from 172 mL to 960 mL (Table 4-9). As evidenced by the moisture content at the end of the experiments, moisture addition resulted in increased compost moisture content. In addition, standing water was measured above the compost in the water addition columns at takedown (Table 4-9). This pattern is also illustrated by the profile data. In the columns that did not receive moisture addition, an increase in the moisture content was measured at the mid-depths (20 to 40 cm). The likely explanation for this is that the mid-depths are where there was maximum overlap of CH$_4$ and O$_2$ and subsequent methane oxidation. The higher moisture is consistent with water as an end product of methane oxidation. This same observation was reported by Hilger et al. (2000).

Table 4-9. Moisture contents, water produced and water added in columns

Column	Depth Below Top of the Compost (cm)	Moisture Contents (%)	Water Accumulated Above Compost (mL)	Water Produced from Oxidation (mL)	Water Added (mL)
1	5.1	35.2		210	
	20.3	40.5			
	35.6	39.3			
	50.8	38.2			
2	5.1	34.7		960	
	20.3	39.1			
	35.6	40.1			
	50.8	39.5			
3	5.1	44.5	100	170	1180
	20.3	40.0			
	35.6	40.8			
	50.8	31.8			
5	5.1	29.8		140	
	20.3	31.3			
	35.6	32.3			
	50.8	29.5			
6	5.1	31.0		340	
	20.3	32.6			
	35.6	32.0			
	50.8	30.7			
7	5.1	51.6	350	172	1180
	20.3	43.3			
	35.6	39.2			
	50.8	38.3			

Column	Depth Below Top of the Compost (cm)	Moisture Contents (%)	Water Accumulated Above Compost (mL)	Water Produced from Oxidation (mL)	Water Added (mL)
8	5.1	53.9	270	240	1180
	20.3	45.8			
	35.6	40.8			
	50.8	39.7			

Data collected by Yolo County project team

Table 4-10. Average moisture contents in moisture addition and no moisture addition columns

Depth Below Top of the Compost (cm)	Avg. Moisture Content in No Water Addition Columns (SD)	Avg. Moisture Content in Water Addition Columns (SD)	p*
5.1	32.7 (2.7)	50.0 (4.9)	0.013
20.3	35.8 (4.6)	43.1 (2.9)	0.054
35.6	35.9 (4.4)	40.3 (0.9)	0.137
50.8	34.5 (5.1)	36.6 (4.2)	0.574

*The probability that the mean moisture content is statistically similar between columns that did and did not receive a water addition

Data collected by Yolo County project team
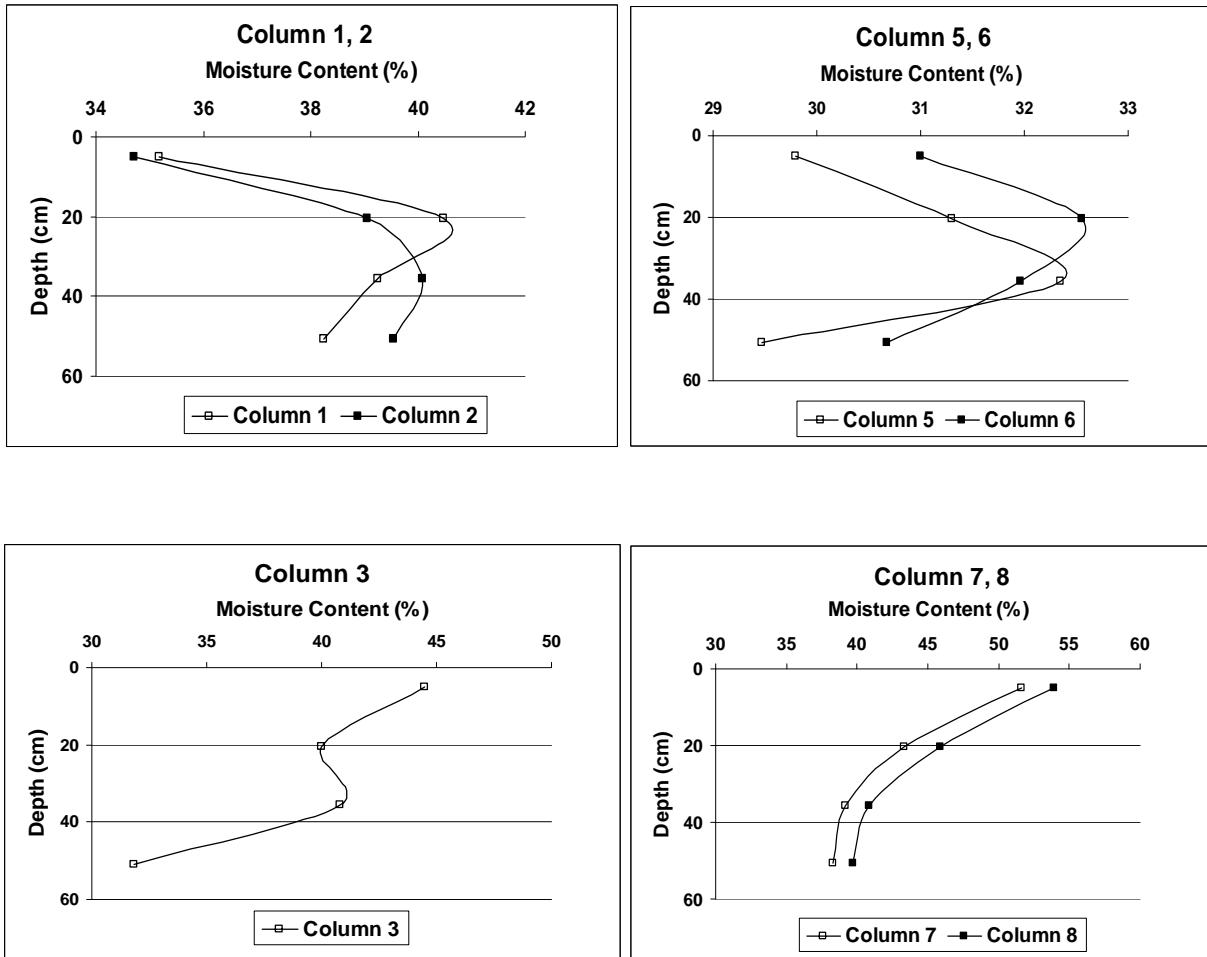
Figure 4-8. Moisture content profiles in the columns at the end of the experiment. Columns 3, 7, and 8 received moisture addition.

4.1.5.3 Effect of Pulsed Flow

Pulsed flow was evaluated to simulate the field operation in which the cover would be exposed to little or no CH_4 while the gas collection system was operated at full vacuum and increased CH_4 when the system was operated at low vacuum. The effect of pulsed flow was discontinued after the first phase of the experiment at a gas flow rate of 5 mL/min. Thereafter, Columns 3, 7, and 8 were all replicates as were Columns 1, 2, 5, and 6.

The average CH_4 uptake data do not suggest any effect associated with pulsed flow (Table 4-2, Figures 4-5, 4-6). Even when the methanotrophic bacteria are deprived of CH_4 for eight days, their overall CH_4 uptake was comparable to that in the columns with a continuous feed of CH_4. Interestingly, pulsed flow Column 2 had the highest CH_4 uptake of any column.

4.1.5.4 Compost Quality

The covers were characterized to evaluate whether there was evidence of decomposition over about a year. Covers were sampled about two weeks apart in late January and February 2006 and again in April 2007. Solids composition data as well as biological indicators of cover stability are presented in Tables 4-11 and 4-12. For the initial sampling in 2006, samples collected from covers of the same type but varying thickness should be replicates.

Based on the initial sampling, there was considerable variability in several parameters, which serves to emphasize the heterogeneity of the cover materials. For example, the organic content and C:N ratio varied between the 0.31 and 0.91 m green waste covers. According to the Woods End Laboratory, materials with percent C losses per day of 0.2 to 0.8 and 0.8 to 1.5 are classified as "medium to high stable" and "medium stable," respectively. The higher CO_2 production in the green waste was expected as it is a fresher material. However, the Woods End Laboratory also suggests that finished compost has a C:N of <17, suggesting that the 0.31 m green waste sample was more decomposed than both the compost and 0.91 m green waste samples (Table 4-11).

The solids composition should not differ as function of cover thickness as is the case for the compost + wood chips cover. However, results are more variable for both the compost only and green waste materials. For example, the organic solids varied between 20.5 and 38.1 percent in the two compost samples and between 31 and 45 percent for three green waste samples in 2006. In both cases, the samples from the shallowest cover (0.31m) had the lowest organic content suggesting that dilution with soil may be have an effect on the measured organic content. If this explanation were correct, then the cellulose + hemicellulose to lignin ratio (CH:L) would be consistent among all samples. While the CH:L is not perfectly consistent, it does exhibit less variability which suggests that soil may have resulted in some dilution in the 0.31 m covers. However, in the 2007 samples, the organic solids content was lowest in the thickest covers.

Table 4-11. Characterization of biocovers[a]

	0.31 m Compost	0.91 m Compost	0.31 m Green waste	0.91 m Green waste
Solids (%)	69.1	60	53.5	35.4
Moisture (%)	30.9	40	46.5	64.6
Organic Content (% dry wt)	20.3	32.3	21.4	64.0
C:N	13.5	11.9	9.6	23
Carbon Loss/day (% of total C per day)	0.33	0.3	0.81	1.11
mg CO_2-C/(g VS-day)	1.8	1.60	4.4	6.0
Total N	0.815	1.47	1.21	1.51
Total C	11.0	17.4	11.6	34.6

[a]Tests were conducted by Woods End Research Laboratory in Mount Vernon, Maine. Samples were collected in early February, 2006.

Source: Woods End Research Laboratory

The composition of the solids in the various covers is summarized in Table 4-12. There was a consistent decrease in the moisture content of each cover between January 2006 and April 2007. This is consistent with the higher rainfall (2.37 in) and low evapotranspiration (1.4 in) in January 2006 relative to low rainfall (1.61) and high evapotranspiration (5.14 in) in April 2007 in Yolo County, California, (http://wwwcimis.water.ca.gov/cimis/monthlyReport.do).

Cellulose, hemicelluloses, and lignin represent the major biodegradable organics in vegetative matter. Over time, the cellulose and hemicellulose are expected to biodegrade more rapidly than the lignin. Thus, the cellulose plus hemicellulose to lignin ratio (CH:L) can be used as an indicator of biodegradation. The advantage of this ratio is that it eliminates any dilution with soil that would decrease the absolute concentrations of each compound.

The CH:L consistently decreased with time in the green waste but not in compost and compost + wood chips covers (Figure 4-9). The most dramatic decrease occurred in the thinnest cover (0.31 m) which may be due to the increased availability of oxygen in this cover. There was essentially no change in the CH:L of the compost covers which is consistent with the fact that the compost was the most decomposed material (lowest CH:L) initially. There was also a larger decrease in the CH:L in the 0.31 m compost + wood chips cover relative to the 0.91 m cover of the same materials. This too is consistent with the possibility that the additional availability of oxygen in the shallower cover enhanced biodegradation.

The organic solids content would also be expected to decrease over time but there is not a consistent trend (Figure 4-9). The organic solids measure is less sensitive that the CH:L and would be affected by dilution with soil. The last column in Table 4-12, the fraction of the total organic solids that can be accounted for as cellulose, hemicellulose, and lignin, is an internal check on the analyses. The range of values, 69.5 to 81.9 percent in 2006 and 61.4 to 82.4 percent

in 2007 are typical of this type of analysis. The remaining organic matter includes small quantities of other compounds present in vegetative material.

It is also interesting that no cover material had an organic solids content above 44.6 percent in 2006 and 45.2 percent in 2007. This suggests that all materials, as applied to the landfill, contained significant quantities of soil. For purposes of comparison, the composition of fresh leaves, grass and branches, as measured in previous research, are also reported in Table 4-13. In all cases, the cellulose, hemicellulose, and organic solids are considerably higher than the samples collected from the biocovers. This suggests that biodegradation has occurred in the biocover materials used, and that they have been diluted with soil.

In summary, there was measurable biodegradation of the green waste during a 15-month period. In practice, a thicker cover will mitigate this issue to some extent. It may be necessary to supplement green waste covers with fresh material at some interval. However, the field emissions data discussed next suggest that the 0.61 and 0.91 m green waste covers performed quite well. Additional monitoring of these covers would be desirable.

Table 4-12. Composition of solids in the test covers in January-February 2006 and April 2007

Sample ID		H$_2$0 (%)	Cellulose (%)		Hemicellulose (%)		Lignin (%)		(Cell + Hemi) /Lignin	Organic solids (OS) (%)		(Cell+Hemi+Lig) / OS[a]
			Avg.	RPD[b]	Avg.	RPD[b]	Avg.	RPD[b]	From avg.	Avg.	RPD[b]	%
0.91 m Compost (80%) + Wood Chips (20%)	2006	42.0	4.4	15.3	2.0	14.4	20.0	4.8	0.30	34.0	3.5	77.4
	2007	22.4	4.4	0.1	2.0	0.0	19.1	0.0	0.33	31.8	0.0	80.1
0.31 m Compost (80%) + Wood Chips (20%)	2006	43.4	4.8	1.0	2.1	2.7	19.1	0.4	0.40	32.0	5.1	81.4
	2007	20.3	4.4	0.0	1.8	0.0	20.3	0.0	0.30	35.7	0.0	74.2
0.31 m Compost	2006	30.7	1.4	9.0	0.8	11.2	12.1	4.0	0.20	20.5	1.4	69.5
	2007	20.6	3.5	0.1	1.8	0.1	21.7	0.0	0.24	37.0	0.0	73.2
0.91 m Compost	2006	44.7	4.1	16.4	1.8	10.3	25.0	6.2	0.20	38.1	0.6	81.3
	2007	22.9	2.5	0.0	1.4	0.0	19.2	0.0	0.20	32.5	0.0	70.8
0.91 m Green waste	2006	55.3	5.9	6.4	3.9	4.9	24.4	8.8	0.40	44.6	3.7	76.7
	2007	37.5	5.5	0.0	3.4	0.0	28.3	0.0	0.32	45.2	0.0	82.4
0.61 m Green waste	2006	54.8	3.6	2.0	2.8	2.3	22.3	9.9	0.30	35.1	0.6	81.9
	2007	22.9	3.4	0.0	2.6	0.0	23.2	0.0	0.26	43.4	0.0	67.3
0.31 m Green waste	2006	49.7	4.1	22.7	3.3	12.5	17.6	14.3	0.40	31.4	2.9	80.0
	2007 (a)	16.4	2.6	0.0	2.0	0.0	19.8	0.0	0.23	31.0	0.0	78.5
	2007 (b)	23.5	3.4	0.0	2.6	0.1	24.5	0.1	0.25	37.6	0.0	81.2
0.31 m Soil	2006	22.9	na		na		na		na	7.0	1.0	

Sample ID		H$_2$0 (%)	Cellulose (%)		Hemicellulose (%)		Lignin (%)		(Cell + Hemi) /Lignin	Organic solids (OS) (%)		(Cell+Hemi+Lig) / OS[a]
			Avg.	RPD[b]	Avg.	RPD[b]	Avg.	RPD[b]	From avg.	Avg.	RPD[b]	%
	2007	13.3	0.1	0.1	0.1	0.0	3.1	0.1	0.07	6.1	0.0	54.4
0.31 m Green waste on side slopes	2007	18.4	3.4	0.0	2.5	0.0	23.1	0.0	0.25	36.9	0.0	78.4
0.31 m Green waste on side slopes	2007	11.9	0.4	0.0	0.4	0.0	5.0	0.0	0.17	9.6	0.1	61.4

a. The fraction of the cellulose, hemicellulose and lignin that is accounted for in the organic solids analysis.

b. The relative percent deviation. This is the standard deviation of duplicate analyses divided by the mean.

Data collected by Yolo County project team

Table 4-13. Typical solid composition for leaves and grass published in literature

	Cellulose (%)	Hemi-cellulose (%)	Lignin (%)	(Cell + Hemi) /Lignin	Organic Solids (%)	(Cell+Hemi +Lig)/ OS
Leaves (Unpublished)	13.1	9	36.8	0.6		
Leaves (Eleazer et al., 1997)	15.3	10.5	43.8	0.6	90.2	77
Branches (Eleazer et al., 1997)	35.4	18.4	32.6	1.7	96.3	89
Grass (Eleazer et al., 1997)	26.5 & 25.6	10.2 & 14.8	28.4 & 21.6	1.3 & 1.9	85.0 & 87.8	77 & 71

Data collected by Yolo County project team
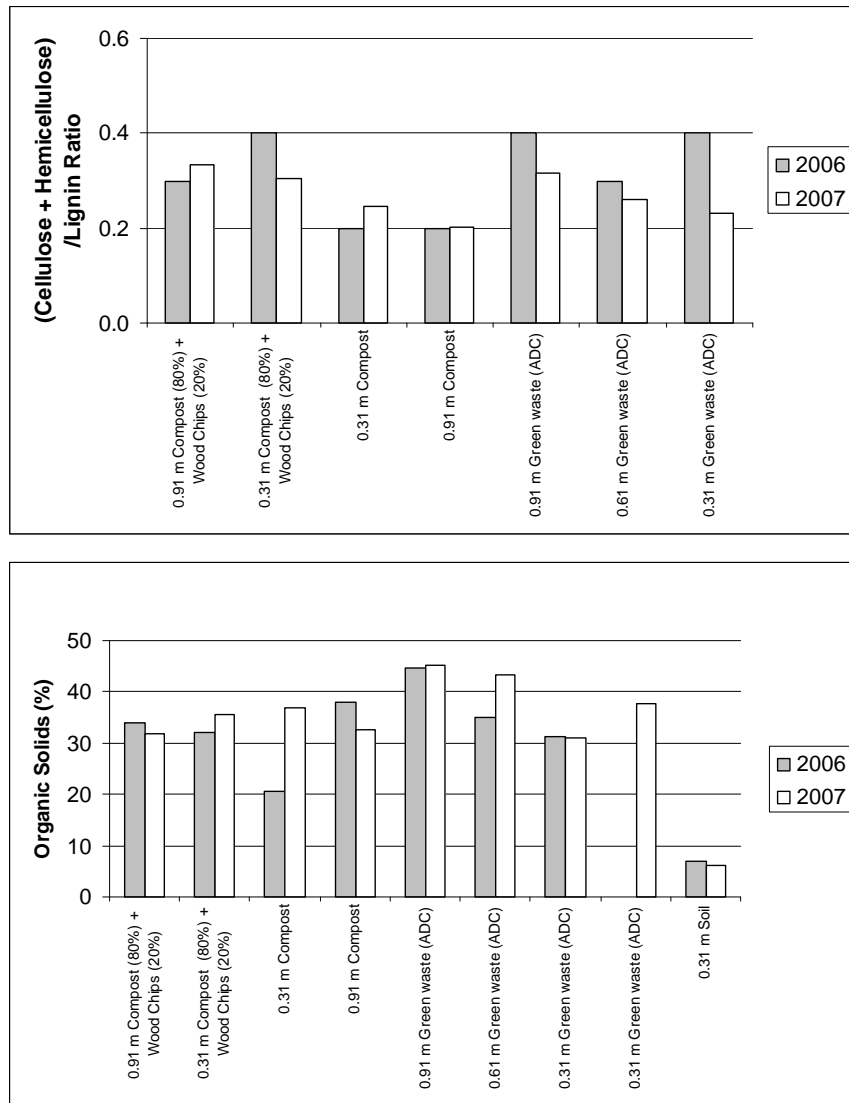
Figure 4-9. CH:L ratio and organic solids of different types of covers in 2006 and 2007

Photo Credit: Yolo County Planning & Public Works Department

4.1.5.5 Methane Emissions Tests

CH_4 emissions from the alternate covers during both the rainy season and dry season field tests are summarized in Table 4-14. Emissions were measured with the gas collection system at both a high setting, to simulate gas collection during peak power demand, and a low setting to simulate a time period when the objective was to store gas in the landfill.

In the rainy season tests, there was a statistically significant decrease in CH_4 emissions when the gas system vacuum was increased for the covers with the highest emissions (0.91 m compost + wood chips, 0.31 m compost, soil). The elevated emissions in the 0.91 m compost + wood chips, and in the 0.31 m compost are surprising as the compost was expected to promote the most CH_4 oxidation. All covers were noticeably wet, which could result in two factors that would promote CH_4 emissions. First, the moisture would fill up pore space that would otherwise be occupied by air. As the oxidation of CH_4 is dependent on the presence of O_2, pore space filled with water would hinder CH_4 oxidation. In addition, the saturated nature of the cover materials could also promote anaerobic biodegradation and CH_4 production within the compost. To evaluate this possibility, a sample of each cover was put in a serum bottle on arrival at NC State University as a qualitative measure as to whether the samples were producing CH_4. The only sample that did not produce CH_4 was the 0.91 m green waste. In fact, even the soil produced CH_4. These results suggest that the wet nature of the biocovers precluded optimum CH_4 oxidation with the gas system in the low vacuum position.

In no case was there an increase in CH_4 emissions associated with reduced gas collection system vacuum during the dry season tests (Table 4-14). The seemingly high average flux for the soil cover is heavily influenced by one outlier (22.97 gm CH_4/m^2-day). This is also the case for the 0.31 m green waste cover which had the second highest average CH_4 emission. While limited, the data in Table 4-14 do not indicate increased emissions associated with the side slope. Individual flux measurements are presented in Tables A6 and A7 in Appendix A.

CH_4 emissions during the rainy and dry seasons are also compared in Table 4-14. While the gas collection system was not operating at exactly the same level during the two different seasons (normally landfill gas generation declines as the organic fraction of waste is decomposed), the comparison can provide some indication of the extent to which climate influences CH_4 oxidation at both high and low vacuum. At low vacuum, CH_4 emissions were statistically higher during the rainy season in the 0.91 m compost + wood chips cover but not in the 0.31 m compost + wood chips cover. Similarly, CH_4 emissions were statistically higher in the 0.91 m compost cover but not in the 0.31 m compost cover. In the case of green waste, emissions were statistically higher during the rainy season at all thicknesses. Comparing CH_4 emissions between the rainy and dry seasons at high gas collection system vacuum, rainy season emissions were higher in the 0.31 m compost and 0.91 m green waste covers but lower in the 0.31 m green waste cover. While there are many confounding issues, the data suggest that emissions at low vacuum during the rainy season are the highest.

4.1.5.6 Quantification of Methane Oxidation by Stable Isotope Analysis[1]

Selected samples were analyzed to quantity the percent oxidation in the covers by using the stable isotope method. Rainy season CH_4 oxidation results are summarized in Table 4-15. It is important to note that a percent CH_4 oxidation can only be calculated in static chambers for which there was a positive emission. Thus, the absence of CH_4 oxidation in the 0.31 m compost + wood chips cover should not be considered as a poorly performing cover as the average CH_4 flux was zero (Table 4-14). With the exception of the 0.91 m and 0.61 m green waste cover, CH_4 oxidation was relatively low. The most likely explanation for this is that the covers were so wet as to limit CH_4 oxidation. The high CH_4 oxidation in the 0.91 m green waste cover is interesting as this cover also had the highest emission level during the rainy season. This suggests that relatively high amounts of CH_4 passed through this cover and that some was oxidized. As noted above, despite the wet nature of the cover, there was no indication that the cover was producing CH_4.

Dry season CH_4 oxidation data are presented in Table 4-16. When observed, CH_4 oxidation varied from 5 to more than 99 percent. The large number of measurements exhibiting negative values is quite unusual. In every case, these anomalous values were associated with the one foot soil cover. It may be that the gas extraction system was particularly effective during this test in this particular area and caused air flow downward into the soil. In systems where CH_4 diffuses upwards against a flow of downward air, negative isotopic values of emitted CH_4 have been observed. However, there were an equal number of observations of negative values at both low and high vacuum which is somewhat surprising. More negative values under high flow would have been expected if this explanation is correct.

---

1. This section was written by Dr. Jeff Chanton at Florida State University.

Table 4-14. CH$_4$ emissions for alternate covers during the rainy and dry seasons (gm CH$_4$/m^2-day)

	Area	0.91 m compost + wood chips	0.31 m compost + wood chips	0.91 m compost	0.31 m compost	0.91 m green waste	0.61 m green waste	0.31 m green waste	0.31 m soil	0.31 m side slope green waste and shredded tires	0.31 m side slope close to bottom, green waste only
Rainy Season	*Gas System at Low Vacuum (47-63 cfm)*										
	Average	20.85 (a, b)	0.00	0.20 (b)	20.41 (a, b)	5.37 (b)	0.89 (b)	0.17 (b)	13.37 (a)	NM*	NM
	Std. Dev.	5.7	0.0	0.1	3.7	2.4	1.0	0.2	8.7	NM	NM
	Gas System at High Vacuum (117 cfm)										
	Average	3.28 (a)	0.00	0.14	2.28 (a,d)	3.34 (d)	0.21	0 (d)	1.68 (a)	NM	NM
	Std. Dev.	3.20	0.00	0.12	1.43	2.06	0.35	0.00	0.55	NM	NM
Dry Season	*Gas System at Low Vacuum (30 cfm)*										
	Average	0 (b)	0.005	0.0002 (b)	-0.003 (b)	0.015 (b)	0.002 (b)	1.998 (b)	5.255	NM	NM
	Std. Dev.	0	0.007	0.009	0.008	0.021	0.009	1.257	9.918	NM	NM
	Gas System at High Vacuum (60 cfm)										
	Average	0.002	-0.0004	0.000	-0.002(d)	0.021 (d)	0.002	1.65 (d)	1.123	-0.049	1.280
	Std. Dev.	0.004	0.001	0.000	0.004	0.018	0.004	1.027	1.426	0.149	1.036

*NM = Not Measured

a. Averages denoted with an "a" indicate a significant difference between the high and low vacuum tests during the rainy season (p<0.05).

b. Averages denoted with a "b" indicate a significant difference between the rainy and dry season tests at low vacuum (p<0.05).

c. Averages denoted with a "d" indicate a significant difference between the rainy and dry season tests at high vacuum (p<0.05).

Data collected by Dr. Jeff Chanton

Table 4-15. CH_4 oxidation in selected samples during rainy season tests (%)[a]

Area	0.91 m compost + wood chips	0.31 m compost + wood chips	0.91 m compost	0.31 m compost	0.91 m green waste	0.61 m green waste	0.31 m green waste	0.31 m soil
	Gas System at Low Vacuum (47-63 cfm)							
1/23/2006	0		14.8	5.1	62.6			12.7
1/24/2006			13.2					
1/25/2006				6.7		74.5		
1/25/2006							0.5	16.9
1/25/2006	10.1				79.6		0.4	
	Gas System at High Vacuum (117 cfm)							
1/30/2006	16					85.7		25.5
1/30/2006				8.8	98.1			23.5
1/31/2006	0		20.8					
1/31/2006				10.9	83.3			

a. For selected samples, the fraction of CH_4 passing through the cover that was oxidized was estimated from changes in the $^{13}C/^{12}C$ ratio between landfill gas and emitted CH_4. Data are presented as a % of CH_4 biologically oxidized while passing through a cover. Data collected by Dr. Jeff Chanton

Table 4-16. CH$_4$ oxidation in selected samples during dry season tests (%)[a]

Area	0.91 m compost + wood chips	0.31 m compost + wood chips	0.91 m compost	0.31 m compost	0.91 m green waste	0.61 m green waste	0.31 m green waste	0.31 m soil	Side Slope green waste and shredded tires	Side Slope close to bottom, green waste only
	Gas System at Low Vacuum (30 cfm)									
11/15/2006							16.3	-4.2		
11/16/2006							16.5	-25.9		
11/16/2006							26	-20.9		
11/16/2006							12.6	-32.5		
11/16/2006							14.1	-15.3		
	Gas System at High Vacuum (60 cfm)									
11/29/2006					4.93		22.9	-14.7		64.9
11/30/2006					12.1		24.2	-17.4		86.5
11/30/2006							25.6	-12		25.6
11/30/2006							15.9	-6		99.8

Data collected by Dr. Jeff Chanton

4.1.5.7 Gas Profiles During Field Testing

Gas profile data of the alternate covers are summarized in Tables 4-17 and 4-18 for the rainy and dry season, respectively. Selected data are also presented in Figure 4-10. Similar to the emission tests, the profiles were measured with the gas collection system at both high and low vacuum. The clearest measure of the effect of climate is that CH_4 concentrations for the dry season were in the ppmv range while the corresponding concentrations were in the percent range for the rainy season tests.

To evaluate the effect of the vacuum level, the CH_4 concentration closest to the surface was compared for each cover. During the rainy season, the elevated vacuum resulted in a decrease in the CH_4 concentration in the following covers: (1) 0.91 m compost + wood chips, (2) 0.31 m compost, (3) 0.61 m green waste and (4) 0.31 m soil. However, there was no effect in the 0.31 m compost + wood chips, and the 0.91 m compost, and the opposite trend was measured in the 0.91 and 0.61 m green waste. Thus, general statements on cover performance based on the CH_4 profile data are not possible. It seems likely that the high moisture levels in the covers dominated their performance. During the dry season tests, the CH_4 concentration closest to the surface was consistently lower during high vacuum. CH_4 concentrations were all below 150 ppmv, which is well below the 500 ppmv regulatory requirement at 15 cm above the cover.

In the 0.91 m compost + wood chips cover, the CH_4 concentration exhibited a maximum and the O_2 concentration a minimum at the middle depth during both the high and low vacuum samplings during the rainy season. The most logical explanation for this is that there was methane generation in microniches in this cover. However, there are not sufficient data to be conclusive.

The O_2 profile data for selected covers are illustrated in Figure 4-10 although there are only limited data available. In the 0.91 m compost + wood chips, the 0.91 m compost and 0.91 m green waste, there appears to be a slight increase in O_2 at the deepest depth at high vacuum relative to low vacuum during the rainy season. This is consistent with the fact that there was less methane in the cover at high vacuum and also an increased gradient for O_2 infiltration. In addition, there was greater O_2 penetration in these covers during the dry season relative to the rainy season (Figure 4-10) though there are insufficient data to assess the effect of vacuum during the dry season.

Table 4-17. Gas composition versus cover depth during the rainy season

							Gas Collection System Vacuum[a]
Rainy Season							
Cover Type	**Depth (cm)**	**Date**	**CH₄ (%)**	**CO₂ (%)**	**O₂ (%)**	**N₂ (%)**	**Gas Collection System Vacuum[a]**
0.91 m compost + wood chips	15.2	1/23/06	21.0	19.6	11.7	47.8	Low
	35.6	1/23/06	43.6	43.5	1.6	11.3	
	53.3	1/23/06	36.4	38.1	5.1	20.4	
	15.2	1/26/06	3.6	6.1	21.6	68.8	High
	35.6	1/26/06	37.7	44.6	2.3	15.4	
	53.3	1/26/06	26.9	28.8	9.9	34.4	
	15.2	1/31/2006	2.3	5.1	22.3[b]	70.2	High
	35.6	1/31/2006	28.8	41.4	2.0	27.8	
	53.3	1/31/2006	26.4	33.8	6.6	33.6	
0.31 m compost + wood chips	15.2	1/23/06	0.0	1.7	21.4	76.9	Low
	15.2	1/26/06	0.3	9.2	15.9	74.5	High
	15.2	1/31/06	0.0	9.5	13.2	77.5	High
0.91 m compost	15.2	1/23/06	0.43	0.30	24.5[b]	74.8	Low
	34.3	1/23/06	28.5	22.5	2.5	46.4	
	59.7	1/23/06	36.0	19.5	3.1	41.4	
	15.2	1/26/06	0.0	0.3	24.7[b]	75.0	High
	34.3	1/26/06	32.0	24.4	3.5	40.1	
	59.7	1/26/06	40.8	23.5	2.2	33.5	
	15.2	1/31/2006	0.3	0.3	26.5[b]	73.0	High
	34.3	1/31/2006	27.6	26.5	2.9	43.0	
	59.7	1/31/2006	26.5	20.7	7.5	45.1	
0.91 m green waste	15.2	1/23/06	0.4	14.5	12.0	73.0	Low
	30.5	1/23/06	5.6	28.7	2.9	62.7	

Rainy Season							
Cover Type	**Depth (cm)**	**Date**	**CH₄ (%)**	**CO₂ (%)**	**O₂ (%)**	**N₂ (%)**	**Gas Collection System Vacuum[a]**
	15.2	1/26/06	0.7	6.3	19.8	73.2	**High**
	30.5	1/26/06	12.2	29.7	5.0	53.1	
	15.2	1/31/2006	12.2	27.5	4.2	56.1	**High**
	30.5	1/31/2006	1.3	12.3	14.8	71.5	

[a]Low vacuum: 47-63 cfm and high vacuum: 117 cfm

Data collected by Yolo County project team

Table 4-17. Gas composition versus cover depth during the rainy season (Continued)

Rainy Season							
Cover Type	**Depth (cm)**	**Date**	**CH₄ (%)**	**CO₂ (%)**	**O₂ (%)**	**N₂ (%)**	**Gas Collection System Vacuum[a]**
0.31 m compost	15.2	1/23/06	23.4	24.6	12.2	39.7	**Low**
	15.2	1/26/06	5.6	5.6	21.6	67.2	**High**
	15.2	1/31/2006	4.2	6.0	22.6[b]	67.1	**High**
0.31 m green waste	15.2	1/23/06	0.2	1.4	22.7[b]	75.8	**Low**
	15.2	1/26/06	0.0	1.6	25.1[b]	73.3	**High**
	15.2	1/31/2006	0.0	2.2	23.8[b]	74.2	**High**
0.31 m green waste	15.2	1/26/06	0.4	0.7	25.8[b]	72.9	**High**
	15.2	1/31/2006	14.0	12.5	13.6	57.7	**High**
0.61 m green waste	15.2	1/23/06	17.5	16.1	7.5	58.9	**Low**
	15.2	1/26/06	3.6	7.0	18.2	71.2	**High**

Rainy Season							
Cover Type	**Depth (cm)**	**Date**	**CH$_4$ (%)**	**CO$_2$ (%)**	**O$_2$ (%)**	**N$_2$ (%)**	**Gas Collection System Vacuum[a]**
	15.2	1/31/2006	5.7	15.3	10.8	68.1	**High**
	15.2	1/23/06	6.6	3.4	21.9[b]	68.0	**Low**
0.31 m soil							
	15.2	1/26/06	0.3	0.0	26.7[b]	73.0	**High**
	15.2	1/31/2006	0.2	0.0	26.7[b]	73.1	**High**

[a]Low vacuum: 47-63 cfm and high vacuum: 117 cfm

[b]O$_2$ concentrations greater than 21% reflect analytical error.

Data collected by Yolo County project team

Table 4-18. Gas composition versus cover depth during the dry season

Dry Season							
Cover Type	**Depth (cm)**	**Date**	**CH$_4$ (ppm)**	**CO$_2$ (%)**	**O$_2$ (%)**	**N$_2$ (%)**	**Gas Collection System Vacuum[a]**
	17.8	11/15/2006	19	4.5	17.0	78.5	
	33.0	11/15/2006	12	4.2	17.2	78.6	**Low**
	50.8	11/15/2006	14	7.8	13.3	78.9	
0.91 m compost + wood chips							
	17.8	11/30/2006	11	2.5	18.6	78.9	
	33.0	11/30/2006	8	2.8	18.2	79.0	**High**
	50.8	11/30/2006	73	4.4	16.4	79.2	
0.31 m compost + wood chips	16.5	11/15/2006	34	4.6	17.0	78.3	**Low**
	16.5	11/30/2006	13	1.8	19.8	78.4	**High**
	17.8	11/15/2006	22	7.0	14.6	78.4	
	31.8	11/15/2006	26	9.3	11.3	79.4	**Low**
0.91 m compost	57.2	11/15/2006	138	13.2	6.6	80.2	
	17.8	11/30/2006	8	4.0	17.2	78.8	**High**

							Gas Collection System Vacuum[a]
Dry Season							
Cover Type	**Depth (cm)**	**Date**	**CH$_4$ (ppm)**	**CO$_2$ (%)**	**O$_2$ (%)**	**N$_2$ (%)**	**Gas Collection System Vacuum[a]**
	31.8	11/30/2006	11	6.9	13.7	79.4	
	57.2	11/30/2006	73	12.0	7.8	80.1	
0.91 m green waste	25.4	11/15/2006	55	4.7	16.3	79.0	**Low**
	30.5	11/15/2006	40	4.6	16.8	78.6	
	0.0						
	17.8	11/30/2006	31	4.7	16.3	79.0	**High**
	25.4	11/30/2006	11	4.7	15.9	79.3	
0.31 m compost	20.3	11/15/2006	8	1.8	20.2	78.0	**Low**
	20.3	11/30/2006	18	0.0	21.0	79.0	**High**
0.31 m green waste	17.8	11/15/2006	90	3.0	18.4	78.6	**Low**
	17.8	11/30/2006	54	2.0	19.3	78.6	**High**

[a]Low vacuum: 30 cfm and high vacuum: 60 cfm

Data collected by Yolo County project team
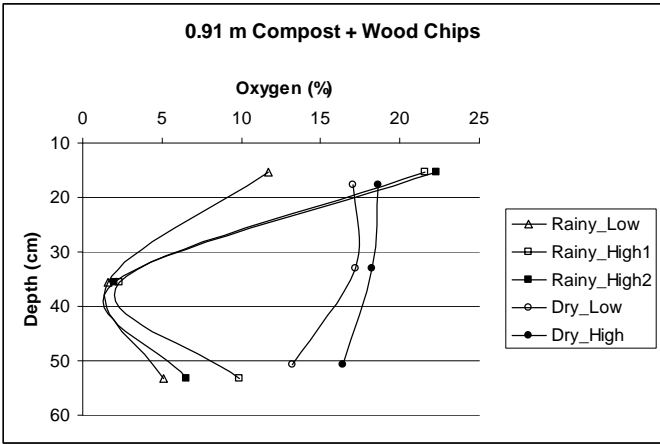
(a)
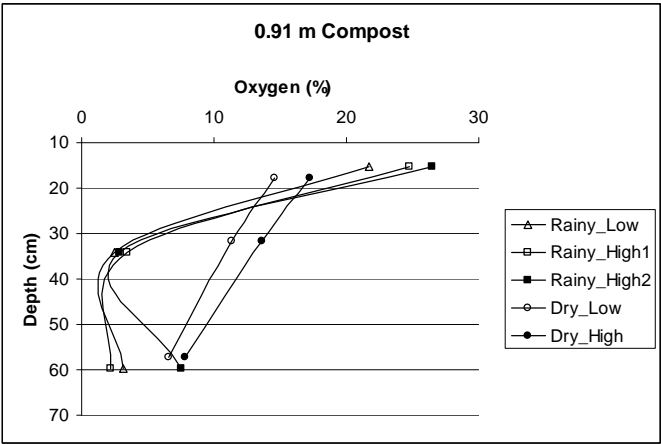
(b)
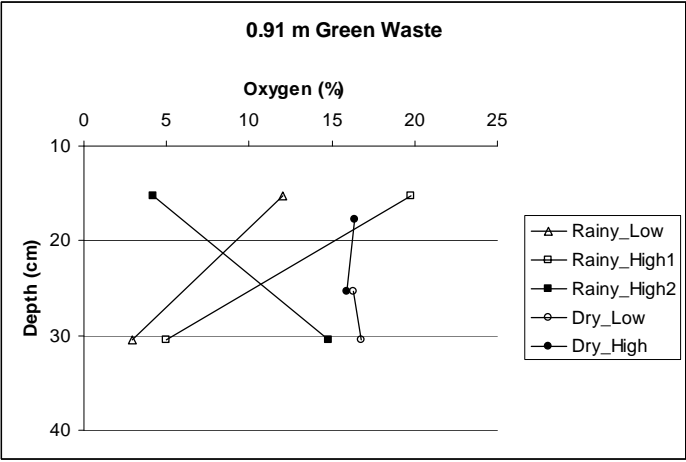
(c)

Figure 4-10. O$_2$ profiles in (a) 0.91 m compost + wood chips; (b) 0.91 m compost; and (c) 0.91 m green waste

Photo Credit: Yolo County Planning & Public Works Department

4.1.5.8 Discussion of Field Methane Emissions Data

The measured methane fluxes, selected profile data and methane oxidation data are summarized in Tables 4-19 and 4-20. In general, there is consistency between these three measures. During the rainy season at low vacuum, the covers with the highest measured fluxes were the 0.91 m compost + wood chips, the 0.31 m compost and the soil. These three covers had the most CH$_4$ at the top of the cover and among the lowest methane oxidation fractions. This

later measure must be used with some caution for several reasons. First, methane oxidation was not measured on every sample. Second, methane oxidation is only measured in samples with a positive flux. Third, 20 percent oxidation in a cover with a flux of 100 CH_4/(m²-day) is more significant than 50 percent oxidation in a cover with a flux of 10 gm CH_4/(m²-day). Fluxes at high vacuum were sufficiently low that a relationship between methane flux, profile and methane oxidation is less clear. However, even here two of the three covers with the highest fluxes (0.91 m compost + wood chips, 0.31 m compost) have the highest methane at the top of the cover and the lowest percent methane oxidation. During the dry season, fluxes were so low and profile data sufficiently sparse that no discussion of relationships between flux, profiles, and methane oxidation is warranted.

Table 4-19. CH$_4$ Flux, CH$_4$, and O$_2$ cover concentration and CH$_4$ oxidation during the rainy season

Cover Type	Depth (m)	CH$_4$ Flux (gm/m^2-d)	CH$_4$ Concentration[a] (%)	O$_2$ Concentration[a] (%)	Oxidation[b] (%)
Low Vacuum (47-63 cfm)					
compost + wood chips	0.91	20.85 ± 5.7	21, 43.6, 36.4	11.7, 1.6, 5.1	0, 10.1
compost + wood chips	0.31	0.0	0.0	21.4	
compost	0.91	0.2 ± 0.1	0.12, 28.5, 36	23.1, 2.5, 3.1	14.8, 13.2
compost	0.31	20.41 ± 3.7	23.4	12.2	5.1, 6.7
green waste	0.91	5.37 ± 2.4	0.4, 5.6	12.0, 2.9	62.6, 79.6
green waste	0.61	0.89 ± 1.0	17.5	7.5	74.5
green waste	0.31	0.17 ± 0.2	0.2	22.7	0.5, 0.4
soil	0.31	13.37 ± 8.7	6.6	21.9	12.7, 16.9
High vacuum (117 cfm)					
compost + wood chips	0.91	3.28 ± 3.2	i. 3.6, 37.7, 26.9 ii. 2.3, 28.8, 26.4	i. 21.6, 2.3, 9.9 ii. 22.3, 2.0, 6.6	16, 0
compost + wood chips	0.31	0.0	i. 0.3 ii. 0.0	i. 15.9, 13.2	
compost	0.91	0.14 ± 0.12	i. 0.0, 32.0, 40.8 ii. 0.3, 27.6, 26.5	i. 24.7, 3.5, 2.2 ii. 26.5, 2.9, 7.5	20.8
compost	0.31	2.28 ± 1.43	i. 5.6 ii. 4.2	i. 21.6 ii. 22.6	8.8, 10.9
green waste	0.91	3.34 ± 2.06	i. 0.7, 12.2 ii. 12.2, 1.3	i. 19.8, 5.0 ii. 4.2, 14.8	98.1, 83.3
green waste	0.61	0.21 ± 0.35	i. 3.6 ii. 5.7	i. 18.2 ii. 10.8	85.70
green waste	0.31	0.0	i. 0.0 ii. 0.4 iii. 14.0	i. 24.45 ii. 25.8, iii. 13.6	
soil	0.31	1.68 ± 0.55	i. 0.3 ii. 0.2	i. 26.7 ii. 26.7	25.5, 23.5

a. CH$_4$, O$_2$, CO$_2$, and N$_2$ concentrations at specific depths are documented in Table 4-12. The CH$_4$ and O$_2$ concentrations measured in shallow (15.2 cm), medium (30.5-35.6 cm) and deep (53.3-59.7 cm) depth of each cover are entered in order in each cell. A single entry represents the shallowest depth and a double entry represents shallow and medium depth where applicable. The notation (i), (ii) and (iii) in single cell represents multiple samplings.
b. For selected samples, the fraction of CH$_4$ passing through the cover that was oxidized was estimated from changes in the ^{13}C/^{12}C ratio between landfill gas and emitted CH$_4$. Data are presented as a % of methane biologically oxidized while passing through a cover. Percent CH$_4$ oxidation was only calculated in static chambers for which there was a positive emission.

Data collected by Yolo County project team

Table 4-20. CH$_4$ Flux, CH$_4$, and O$_2$ cover concentration and CH$_4$ oxidation during the dry season

Cover Type	Depth (m)	CH$_4$ Flux (gm/m^2-d)	CH$_4$ Concentration[a] (ppm)	O$_2$ Concentration[a] (%)	Oxidation[b] (%)
Low Vacuum (30 cfm)					
compost + wood chips	0.91	0.0	19, 12, 14	17, 17.2, 13.3	
compost + wood chips	0.31	0.005 ± 0.007	34	17	
compost	0.91	0.0002 ± 0.009	22, 26, 138	14.6, 11.3, 6.6	
compost	0.31	-0.003 ± 0.008	8	20.2	
green waste	0.91	0.015 ± 0.021	NR, 55, 30.5	NR, 16.3, 16.8	16.3, 16.5, 26, 12.6, 14.1
green waste	0.61	0.002 ± 0.009			
green waste	0.31	1.998 ± 1.257	90	18.4	
soil	0.31	5.255 ± 9.918			
High Vacuum(60 cfm)					
compost + wood chips	0.91	0.002 ±	11, 8, 73	18.6, 18.2, 16.4	
compost + wood chips	0.31	-0.0004 ± 0.001	13	19.8	
compost	0.91	0	8, 11, 73	17.2, 13.7, 7.8	
compost	0.31	-0.002 ± 0.004	18.0	21.0	
green waste	0.91	0.021 ± 0.018	31, 11	16.3, 15.9	4.93, 12.1
green waste	0.61	0.002 ± 0.004			
green waste	0.31	1.65 ± 1.027	54	19.3	22.9, 24.2, 25.6, 15.9
soil	0.31	1.123 ± 1.426			-14.7, -17.4, -12, -6
green waste + shredded tires		-0.049 ± 0.149			
green waste		1.28 ± 1.036			64.9, 86.5, 25.6, 99.8

a. CH$_4$, O$_2$, CO$_2$, and N$_2$ concentrations at specific depths are documented in Table 4-13. The CH$_4$ and O$_2$ concentrations measured in shallow (15.2 cm), medium (30.5-35.6 cm) and deep (53.3-59.7 cm) depth of each cover are entered in order in each cell. A single entry represents the shallowest depth and a double entry represents shallow and medium depth where applicable. The notation (i), (ii) and (iii) in single cell represents multiple samplings.

113

b. For selected samples, the fraction of CH_4 passing through the cover that was oxidized was estimated from changes in the $^{13}C/^{12}C$ ratio between landfill gas and emitted CH_4. Data are presented as a % of methane biologically oxidized while passing through a cover. Percent CH_4 oxidation was only calculated in static chambers for which there was a positive emission.

Data collected by Yolo County project team

4.1.6 Conclusions

The column experiments were conducted to evaluate the performance of a biologically active cover material and the effects of pressure gradient, moisture infiltration, and CH_4 flow regime on CH_4 oxidation. The initial flux of 5 mL/min or 294.4 gm CH_4/m^2-d is in the midrange of reported landfill CH_4 fluxes (Kunz and Lu 1980; Jones and Nedwell 1990; Jones and Nedwell 1993; Bogner and Spokas 1993). The higher flux rates of 588.6 and 883.01 gm CH_4/m^2-d later were at the upper range of reported values although fluxes above 1000 have been reported (Abichou et al. 2006a). As summarized in Figures 4-5 and 4-6 and Table 4-6, methane oxidation decreased as the flux or pressure gradient increased. The CH_4 flux exceeded the oxidation capacity of the system, presumably because there was insufficient retention time in regions where CH_4 and O_2 mixed. This observation is reinforced in the columns that did not receive a water addition by the considerable increase in CH_4 oxidation when the CH_4 feeding rate was decreased from 883.01 to 147.2 gm/m^2-day. This result is consistent with the decrease in CH_4 oxidation with increasing flow in the range of 160 to 319 gm CH_4/m^2-d reported previously (Stein and Hettiaratchi 2000).

The addition of moisture was inhibitory for O_2 diffusion in the compost as evidenced by the reduced O_2 concentrations at depth in the water addition columns (Tables 4-8 and 4-9 and Figure 4-7). This is consistent with the observation of standing water in the columns when they were destructively sampled. The excess moisture hindered oxygen diffusion which is required for CH_4 oxidation. The inhibitory effect of water addition on methane oxidation was most apparent at the end of the experiment at the 147.2 gm/m^2-day flux. The inhibitory effect would be expected to increase over time as moisture was added weekly. Thus, it is logical that the effect was clearest near the end of the experimental work.

The highest oxidation rate reported previously, 410.1 gm CH_4/m^2-d, represents 100 percent oxidation in columns filled with municipal solid waste compost (Humer and Lechner 1999). Other laboratory-scale CH_4 oxidation rates include 166g CH_4 m^{-2} d^{-1} (Kightley et al. 1995), 100 g CH_4 m^{-2} d^{-1} (Visvanathan et al. 1999), and 144g CH_4 m^{-2} d^{-1} (Stein and Hettiaratchi 2000). The maximum oxidation rate measured in this study was 664.2 gm CH_4/m^2-d observed in Column 2. The average CH_4 oxidation rates observed in this study are comparable with reported oxidation rates for biocovers and higher than oxidation rates reported for soil covers (Humer and Lechner 1999; Berger et al. 2005; Hilger et al 2000; Kightley et al. 1995; Visvanathan et al. 1999; Stein and Hettiaratchi 2000).

Field-scale experiments were conducted to assess the performance of several different cover materials under varying climatic conditions and LFG collection vacuum. The effect of climate was significant. In the rainy season tests, there was a statistically significant decrease in CH_4 emissions when the gas system vacuum was increased for the covers with the highest emissions (0.91 m compost + wood chips, 0.31 m compost, soil). In contrast, there was not an increase in

CH$_4$ emissions associated with reduced gas collection system vacuum during the dry season tests (Table 4-14). While there were many confounding issues, the data suggest that emissions at low vacuum during the rainy season are the highest (Table 4-14) but that overall, the covers were effective in controlling gas release. The emissions data are consistent with the gas profile data where CH$_4$ concentrations for the dry season were in the ppm range while the corresponding concentrations were in the percent range for the rainy season tests.

In the field, the highest CH$_4$ emission was 20.85 gm CH$_4$/m^2-d in 0.91 m compost + wood chips and 5.255 gm CH$_4$/m^2-d in 0.31 m soil during the rainy and dry season, respectively. When CH$_4$ oxidation was measured, it varied from 5 to more than 99 percent in the field. These values are consistent with the previously reported field scale studies though some extreme values are also available (Abichou et al. 2006a; Abichou et al. 2006b; Borjesson et al. 2001; Barlaz et al. 2004; Schuetz et al. 2003; Humer and Lechner 2001; Borjesson et al. 2001; Jones and Nedwell 1993). Emissions of 9 to 130 g CH$_4$ m^{-2}d^{-1} have been reported at landfill sites in the northeastern United States (Chanton et al. 1999). The highest reported field-scale CH$_4$ oxidation rates are 214.4 g CH$_4$ m^{-2} d^{-1} (Humer and Lechner 2001) and 149.8 g CH$_4$ m^{-2} d^{-1} (Borjesson et al. 1997) although these values may be an underestimate since methane oxidation could only be measured when it was positive.

Both the field and lab results indicate that high moisture can inhibit methane oxidation. As the overall objective of this project was to assess the efficacy of the peak power concept, it is encouraging to note that during the dry season, there was no increase in emissions during periods when the gas collection system vacuum was reduced.

There was an increase in CH$_4$ emissions at low vacuum during the rainy season. However, this may not be critical as the hottest temperatures and associated highest demand for electricity are likely to occur during the dry season. The results suggest that it would be prudent to operate the gas system to maximize methane collection during periods when then cover soils are saturated with moisture as during this state, CH$_4$ oxidation will likely be reduced. Further field tests would be required to more precisely determine the extent to which slight reductions in gas collection vacuum may be possible when the cover is saturated. Except the soil and 0.31 m green waste, all covers of different thicknesses performed well. So the cover type to be used in the field should be based on availability of the material and cost.

4.1.7 Modeling and Comparison with Spring 2007 Data
4.1.7.1 Objectives
The overall objective of peaking power project is to evaluate the feasibility of operating landfills in a peaking-power mode. In the earlier preliminary modeling, the results showed that (1) peaking power operations should result in minor increases in methane emissions (not accounting for biocover methane oxidation) if a horizontal tire layer is installed, and that (2) the construction of a horizontal tire layer can *increase* the methane collection efficiency by 50 percent over conventional (constant) pumping conditions without a tire layer. A horizontal tire layer also significantly *decreases* the intrusion of oxygen into the landfill. The modeling helped to guide the design of the peaking power landfill test cell constructed at the Yolo County Central Landfill by estimating the influence of different operational parameters.

In this report the feasibility of peaking power operations is further evaluated in terms of its influence on methane emission and oxygen intrusion. The model used is an improved version over prior models employed in earlier work to describe LFG transport. For this reason, a few important simulation cases are re-evaluated and analyzed using the improved model. This report summarizes the results from six different modeling situations or cases:

Case 1: evaluate the influence of biocover permeability on methane emission and oxygen intrusion.

Case 2: evaluate the influence of anisotropy in gas permeability of the refuse on methane emissions.

Case 3: estimate the effect of transient atmospheric pressure changes on methane emissions and peaking power operation.

Case 4: evaluate the effect of the pumping rate on methane emissions and oxygen intrusion into the landfill.

Case 5: evaluate the effect of the permeable layer near the landfill surface, specifically the depth of tire layer on methane emissions and peaking power operation, and the width of tire layer on methane emissions and peaking power operation.

Case 6: compare simulation results with field data collected from the Yolo County peaking-power landfill cell to validate the modeling approach.

4.1.8 Methodology

4.1.8.1 Numerical simulator

To simulate landfill gas migration, a multiphase and multi-component simulator was used, TMVOC (Pruess and Battistelli 2002). TMVOC is an extended version of the TOUGH2 computer code (Pruess et al. 1999) that has been widely used to simulate geothermal reservoirs, contamination of nuclear waste disposal sites, environmental pollution assessment and remediation, and hydrology of unsaturated and saturated zones. TOUGH2 and TMVOC belong to the MULKOM family of codes, developed in the Earth Sciences Division of Lawrence Berkeley National Laboratory (LBNL). The main distinguishing feature of TMVOC is its capability to simulate multiphase contamination and remediation processes involving non-aqueous phase liquids (NAPLs). TMVOC uses a general integral finite difference formulation, and it consists of multiphase, multi-component mass and energy balance equations. A brief description of the governing equations used in TMVOC is presented in this section.

The mass balance equations for component κ for an arbitrary flow region V_n with surface area Γ_n is given by

$$\frac{d}{dt}\int_{V_n} M^{\kappa} dV_n = \int_{\Gamma_n} (\mathbf{F}^{\kappa} \bullet \mathbf{n}) d\Gamma_n + \int_{V_n} q^{\kappa} dV_n \qquad (1)$$

where M^{κ} is the mass of component κ per unit porous medium volume, $\mathbf{F}^{\kappa}$ is the mass flux of component κ into V_n, $\mathbf{n}$ is inward unit normal vector, and q^{κ} is the rate of mass generation of

component κ per unit volume. The left-hand side of equation (1) represents the change of mass in the volume V_n per unit time, and the right-hand side describes the fluxes through the boundaries of the region and the sinks or sources in the volume.

The phase fluxes follow a multiphase extension of Darcy's law and are given by

$$\mathbf{F}_\beta^\kappa = -k\frac{k_{r\beta}\rho_\beta}{\mu_\beta}x_\beta^\kappa(\nabla P_\beta - \rho_\beta\mathbf{g}) + \mathbf{f}_\beta^\kappa \tag{2}$$

where k is the absolute permeability and is equal to the single-phase liquid permeability, $k_{r\beta}$ is relative permeability to phase β, μ_β is viscosity, and ρ_β is molar density. x_β^κ is the mole fraction of component κ in phase β. $\mathbf{g}$ is the vector of gravitational acceleration, and

$$P_\beta = P + P_{c\beta} \tag{3}$$

is the fluid pressure in phase β, which is the sum of the pressure P of a reference phase (usually taken to be the gas phase), and the capillary pressure $P_{c\beta}$. Absolute permeability of the gas phase increases at low pressures according to the relation given by Klinkenberg (1941)

$$k = k_\infty\left(1 + \frac{b}{P}\right) \tag{4}$$

where k_∞ is the permeability at "infinite" pressure, and b is the Klinkenberg b-factor, which describes gas slippage that effectively increases gas permeability at low pressures. $\mathbf{f}_\beta^\kappa$ is the diffusive mass flux of component κ in phase β. In TMVOC a diffusive flux of component κ in phase β is written as

$$\mathbf{f}_\beta^\kappa = -\phi\tau_0\tau_\beta\rho_\beta d_\beta^\kappa\nabla x_\beta^\kappa \tag{5}$$

where ϕ is the porosity; $\tau_0\tau_\beta$ is the tortuosity which includes the medium tortuosity, τ_0, and the saturation-dependent tortuosity, $\tau_\beta = \tau_\beta(S_\beta)$; ρ_β is molar density; and d_β^κ is the diffusion coefficient of component κ in phase β, which is calculated from the binary diffusivities by the Wilke method (API 1977). The definition of a single effective multiphase diffusion coefficient is as follows:

$$\sum_\beta^\kappa \equiv \phi\tau_o\tau_\beta\rho_\beta d_\beta^\kappa \tag{6}$$

For general three fluid phase conditions, the total diffusive flux through all fluid phases is then given by

$$\mathbf{f}^\kappa = -\sum_g^\kappa\nabla x_g^\kappa - \sum_w^\kappa\nabla x_w^\kappa - \sum_o^\kappa\nabla x_o^\kappa \tag{7}$$

where the subscripts "g", "w", and "o" represent the gas, water, and NAPL phases, respectively.

The multiphase extension of Darcy's law also includes the effects of relative permeabilities and capillary pressures between phases. Several multiphase relative permeability and capillary pressure models are available in TMVOC. In this study the van Genuchten –Mualem model (Mualem 1976; van Genuchten 1980) was used, and it is given by

$$k_{rl} = \sqrt{S^*}\{1 - (1 - [S^*]^{1/\lambda})^{\lambda}\}^2 \tag{8}$$

$$k_{rg} = \begin{cases} 1 - k_{rl} & if \ S_{gr} = 0 \\ (1 - \hat{S})^2(1 - \hat{S}^2) & if \ S_{gr} > 0 \end{cases} \tag{9}$$

$$P_{cap} = -P_0([S^*]^{-1/\lambda} - 1)^{1-\lambda} \tag{10}$$

with

$$S^* = (S_l - S_{lr})/(S_{ls} - S_{lr}), \ \ \hat{S} = (S_l - S_{lr})/(1 - S_{lr} - S_{gr}) \tag{11}$$

$$P_0 = \rho_w g / \alpha \tag{12}$$

where S_{lr} is the irreducible water saturation, S_{ls} is the satiated water saturation, and S_{rg} is the irreducible gas saturation. The parameter λ is a pore-size distribution index that determines the shape of the functions, and α is a capillary strength parameter. Equation (9) for gas relative permeabilities is taken from Corey (1954).

4.1.9 Improvements in TMVOC

The advantages of using TMVOC instead of T2VOC, which was also developed by LBNL (Falta et al. 1995) and used in earlier work, are: (1) TMVOC is capable of modeling multiple gaseous components, and (2) all transport equations used in TMVOC are solved using molar-based concentrations. In T2VOC, only one gaseous component can be modeled other than air and water vapor. So, air had to be substituted for CO_2, which is one of the major LFG components. Using TMVOC, this unnecessary assumption was discarded, and the simultaneous transport of CH_4, CO_2, and air was fully simulated. Oxygen concentrations were computed from the air concentration multiplied by 0.21, assuming a constant ratio of oxygen to nitrogen and no consumption oxygen in landfills. Better predictions of multi-component diffusion are achieved using the molar-based mass flux equations as well (Fen and Abriola 2004).

In this study, two important modifications were incorporated in the code. First, to incorporate temporal atmospheric pressure changes, an optional function was added so that a time-dependent Dirichlet condition (i.e. gas pressure) was established at the landfill surface. Second, the mathematical model for air diffusion was modified and conforms to a criterion established by Bird et al. (1960). These authors showed that the sum of all molecular diffusive fluxes in the gas phase must be zero, a requirement that is now met in the modified version of TMVOC. The diffusion of CH_4 and CO_2 are calculated from the concentration gradients of each component, but the diffusion of air is calculated as the negative sum of diffusive fluxes of CH_4 and CO_2. The details of the modifications were discussed at length in Jung and Imhoff (2007). Because of these

improvements and modification in the model, the current modeling results are different and more accurate than the results reported in the two earlier interim reports.

4.1.10 Description of Model Domain and Initial and Boundary Conditions

4.1.10.1 Description of base case simulations

At the Yolo County Central Landfill a new anaerobic test cell was constructed with a horizontal tire layer beneath the top cover, and with a single well, referred to as a "pancake" well or pancake layer, installed in the center (approximately) of the cell. In this study the authors simplified and idealized this complicated three-dimensional landfill system by evaluating peaking power operations for a hypothetical landfill. Considering the characteristics of gas flows at Yolo County, a two-dimensional axisymmetric, radial domain was selected. Figure 4-11 shows a schematic of the model domain: 46.0 m in radius and 12.4 m in depth. The domain includes three major material types: refuse, tire layers, and the biocover, which serves as an intermediate landfill cover. One of the tire layers is installed between the biocover and the pumping well and acts as a permeable layer to distribute the gas pressure evenly near the top of the landfill. The remaining tire layer, a pancake well, serves as the pumping well to allow uniform flow into the extraction piping. Both tire layers are 0.6 m thick, and the pancake tire layer has a radius of 3.8 m. The permeability of tire layers was specified based on measurement by Warith et al. (2004). The biocover has a thickness of 1.0 m. The refuse represents general municipal solid waste (MSW) in landfills. Considering that waste dumped in landfills has been packed over time and by the weight of overlying waste, the domain for the refuse was divided into five layers having different permeabilities and porosities. As the depth of the layer increases, the layer has smaller permeability and porosity. The permeability of each layer was specified based on the recent field measurements by Jain et al. (2005), assuming that the permeability of waste decreases exponentially decreases depth. The variation of refuse permeability with depth was based upon the empirical relationship between vertical stress and hydraulic conductivity in landfills (Yildiz et al. 2004). In this case, the horizontal intrinsic permeability was calculated using the following equation.

$$k_h = ae^{-bD}$$

(13)

where a and b are empirical constants. The constants estimated from a nonlinear regression analysis were 2.5×10^{-11} m² and 0.12 m⁻¹, respectively. The vertical permeability k_v was specified as 10 times smaller than the horizontal permeability based on the same reasoning that waste may undergo vertical stress by weight of overloaded waste. Thus, the anisotropy ratio was specified as $k_h / k_v = 10$. The porosity of each layer was also modified using the empirical relationship by Kozeny-Carmen Bear (1972):

$$k_h \propto \frac{\phi^3}{(1-\phi)^2}$$

(14)

The general properties of each layer utilized in the base case simulations are given in Table 7.2-1. For capillary pressure and relative permeability relationships, the van Genuchten–Mualem model (Mualem 1976; van Genuchten 1980) was used, and the model parameters are also

119

presented in Table 4-21. The discretization used in the simulations is shown in Figure 4-12. The horizontal or vertical length of a grid decreases the closer the grid is to a layer interface.
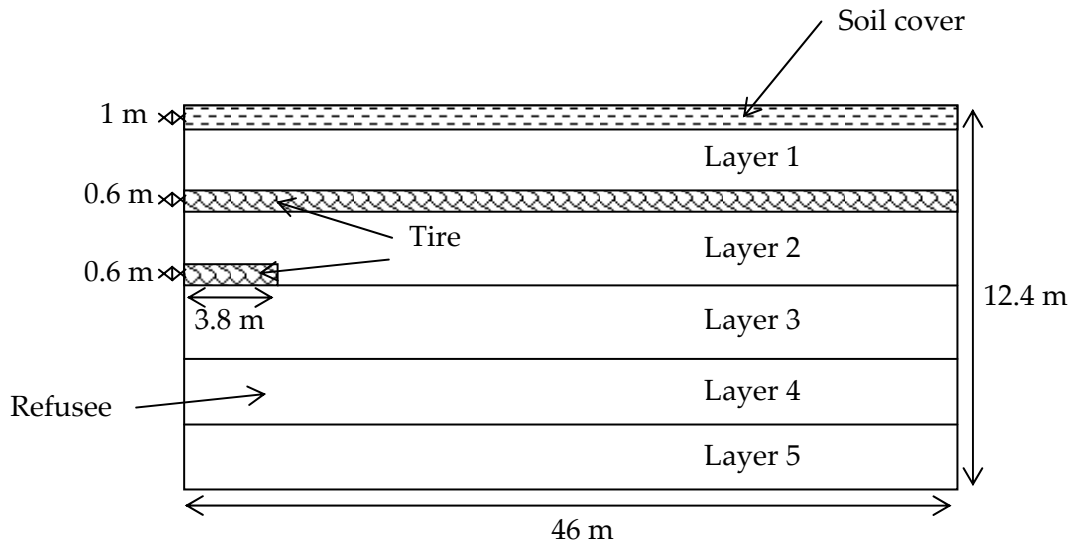
Figure 4-11. Schematic profile of one half of the model domain. A radially symmetric domain is used for all simulations. The thickness of layer 1 to 5 is 2.1, 2.4, 2.3, 2.0, and 2.0 m, respectively.

Photo Credit: Yolo County Planning & Public Works Department

Table 4-21. General properties of model domain for base simulations

		Trash					Tire	Biocover
Density (kg/ m^3)		710					480	1,700
Porosity		Layer					0.50	0.35
		1	2	3	4	5		
		0.51	0.48	0.45	0.425	0.4		
Aqueous phase saturation		0.21					0.21	0.15
Intrinsic Horizontal Permeability (m^2)		Layer					3.0e-8	1.0e-12
		1	2	3	4	5		
		1.95e-11	1.39e-11	1.05e-11	8.1e-12	6.4e-12		
Intrinsic Vertical Permeability (m^2)		Layer					3.0e-9	1.0e-13
		1	2	3	4	5		
		1.95e-11	1.39e-11	1.05e-11	8.1e-12	6.4e-12		
van Genuchten –Mualem parameters	λ	0.59					0.59	0.457
	S_{lr}[†]	0.21					0.21	0.15
	S_{ls}	1.00					1.00	1.00
	S_{rg}	0.005					0.005	0.10
	$1/P_0$	8.4e-4					8.4e-4	5.11e-4
	P_{max}	1.0e5					1.0e5	1.0e7

[†] For capillary pressure function, S_{lr} was 0.20, 0.20, and 0.14 for trash, tire, and biocover, respectively.

Data collected by Yolo County project team

4.1.10.2   Initial and boundary conditions

The pumping rate, Q, in the system was varied in the simulations to reflect peaking power operations and calculated based on the landfill gas generation rate (25 m³/ton/year), which was assumed to consist of 55 percent methane and 45 percent carbon dioxide. The diffusion coefficients of the landfill gases are listed in Table 4-22. For base-case simulations, the pumping rate was set equal to 1.5 times the landfill gas generation rate to represent "overpull" conditions during peak energy demand periods, and set to 0.5 times the landfill gas generation rate to represent "underpull" when energy demands are less. During the daytime the pump was operated for 12 hours in the overpull condition, and during the night it was operated for 12

hours in the underpull condition. All simulations in this study were based on this pumping sequence.

Table 4-22. Parameters for diffusion coefficients

$D^R_{CH_4-air}$ $(m^2/s)^a$	2.096e-5
$D^R_{CO_2-air}$ $(m^2/s)^a$	1.573e-5
$D^R_{water-air}$ $(m^2/s)^a$	2.130e-5
T_R $(K)^b$	293.2
P_R $(Pa)^c$	1.013e5
θ^d	1.6

[a] Experimentally determined binary diffusivities at a temperature of T_R and a pressure of P_R

where $D_{ij} = D^R_{ij} \dfrac{P_R}{P} \left(\dfrac{T}{T_R} \right)^{\theta}$

[b, c] Standard temperature and pressure.
[d] Experimentally determined constant.
Data collected by Yolo County project team
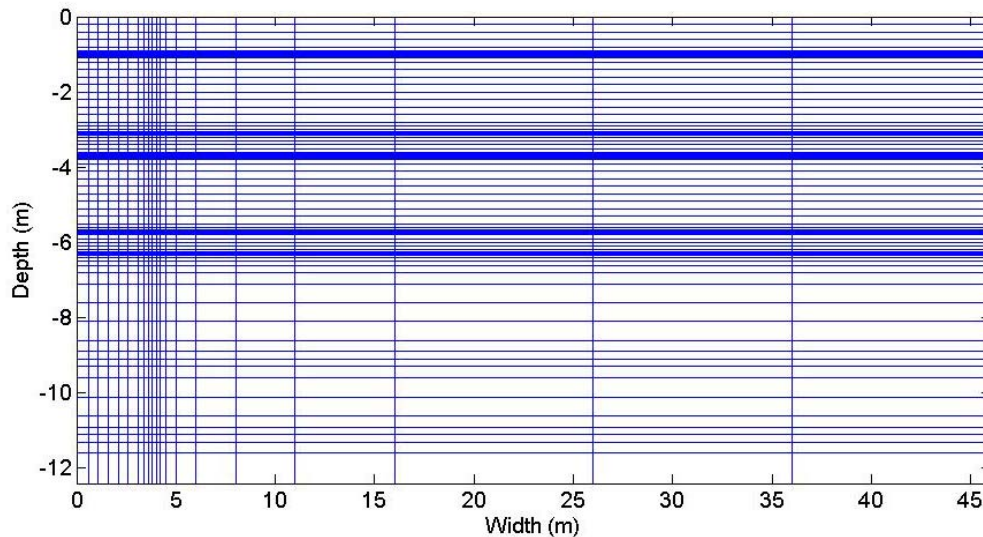
Figure 4-12. Domain discretization of one half of the model domain

Photo Credit: Yolo County Planning & Public Works Department

To describe fluid flow across the boundaries of the domain, two conditions were applied. The first is for the top grid blocks, designated as the atmosphere. The top surface was a Dirichlet boundary condition of constant temperature (25°C) and pressure (1.013 × 10⁵ Pa). The second

boundary condition was a no flux boundary condition for the lateral and bottom borders of the simulation domain. The lateral condition represents the imaginary boundary between neighboring extraction wells, which are equidistant from each other.

Various cases were simulated to explore different setup conditions and the sensitivity of important model parameters. Each case required changes in the grid size, permeability, or formation properties; however, most of the initial and boundary conditions were fixed as shown in Table 4-23. In addition, several assumptions were made to complement the lack of field data and to simplify the simulations. First, the project team assumed isothermal conditions within the landfill. Second, the generation rate of landfill gas was steady since the simulation period was too short to account for the decrease in the rate of landfill gas generation associated with waste stabilization. Third, the thermodynamic properties of all solid materials and the gas generation rate were uniform throughout the domain. Fourth, no chemical and biological degradation processes were explicitly considered: instead, a constant landfill gas generation rate was specified for each grid block in the domain.

Table 4-23. Initial and boundary conditions used in base-case simulations

Landfill depth (m)	12.4
Landfill diameter (m)	46
Tire layer depth (m)	3.1
Pancake depth (m)	5.5
Biocover thickness (m)	1.0
Atmosphere temperature (℃)	25
Atmosphere pressure (Pa)	1.013e5
Landfill gas generation (m^3/ton/year) (55 % of methane and 45 % of carbon dioxide)	25

The modeling process was divided into three parts. It began with generating a grid that was pre-determined to effectively describe the system. Next, a natural state that corresponds to the condition prior to pumping well operation was calculated. In this natural state the system is in steady-state, meaning thermodynamic conditions and the mass fraction of each component are time-independent for the whole domain. Using these steady-state conditions as the initial conditions of the subsequent simulation, one important parameter was changed: constant or time-dependent pumping rates in the pancake well were specified. After this change, the simulation was run until quasi-steady states in the system were achieved.

4.1.11 Results

4.1.11.1 Determination of steady-state conditions

Figure 4-13 shows the methane emission rate from the landfill versus simulation time once time-dependent pumping within the pancake well was initiated at the end of Day 1. Based on

the output of this simulation, the system satisfies steady-state conditions at the end of Day 14. Thus, all simulation results presented below are for the 24-hour period beginning on Day 15.
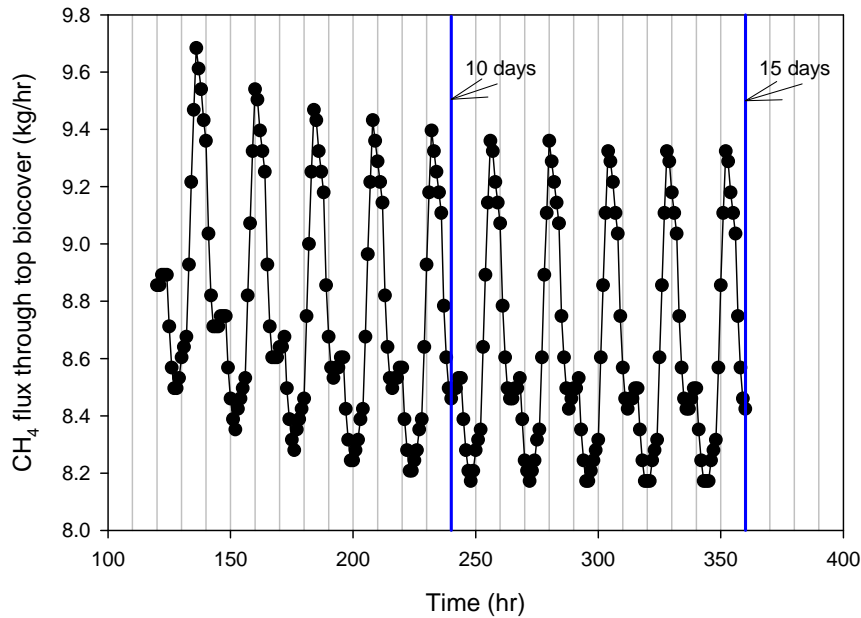
Figure 4-13. Variation of methane emission with elapsed simulation time for base case simulation

Photo Credit: Yolo County Planning & Public Works Department

Figure 4-14 shows the influence of peaking-power operation on fugitive methane emissions. It is important to note that operating the pumping well in peaking power mode (with the tire layer at the top of the landfill) does NOT result in significant increases in methane emissions from the landfill. When the landfill was operated at a constant pumping rate equal to the landfill gas generation rate, 15.5 percent of the methane generated escaped from the landfill. During peaking power operations, when the pumping well was operated for 12 hours in overpull (pumping rate = 1.5 × landfill gas generation rate) followed by 12 hours in underpull (pumping rate = 0.5 × landfill gas generation rate), only 16.1 percent of the methane generated escaped from the landfill. If the effect of methane oxidation in the biocover were included in the analysis, significantly smaller amounts of methane would be predicted to escape into the atmosphere.
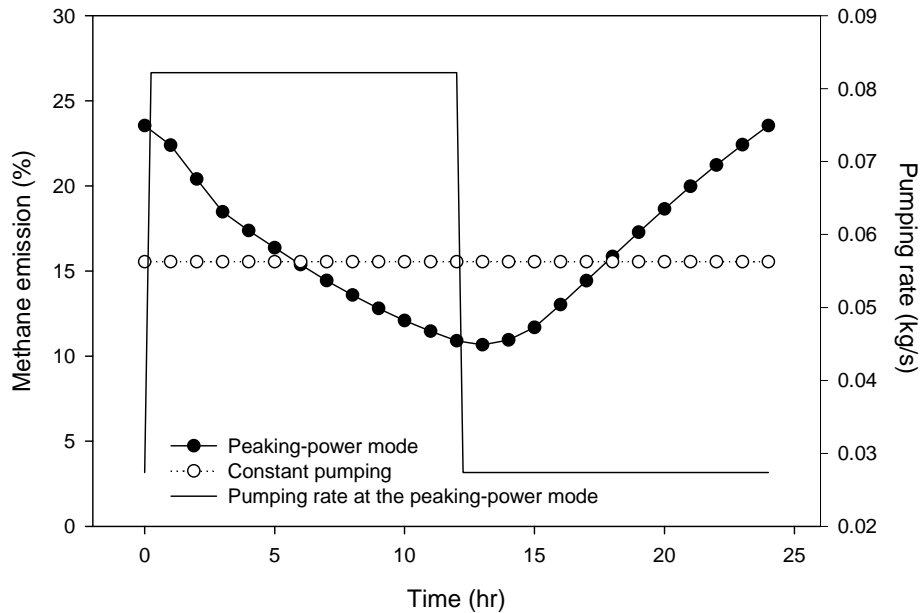
Figure 4-14. Comparison of methane emissions at different pumping modes: (1) peaking-power and (2) constant.

Photo Credit: Yolo County Planning & Public Works Department

Case 1: Effect of biocover permeability

Methane emissions from landfills are in part controlled by the rate of oxidation as CH_4 is transported through the cover material on top of the landfill. Biocovers have been used to minimize methane emissions by optimizing microbial oxidation in intermediate landfill covers. Several factors, including moisture content, temperature, and soil nutrient content control methane oxidation by aerobic methanotrophic microorganisms. Apart from the microbial aspect, biocovers also serve as a physical barrier that mitigates methane emissions. The structure of biocovers is easily changed by environmental conditions such as precipitation, which decreases the air permeability, and these changes may directly affect peaking-power operation. In this section, the influence of physical factors of the biocover, i.e. permeability and porosity, are evaluated for their influence on methane emissions and air intrusion.

A range of gas permeabilities for biocovers were evaluated, which accounts for the effect of rainfall events, which reduce gas permeabilities. The smallest permeability tested was 100 times smaller than that of the base case. The porosity of biocovers, related to the permeability through equation (14), was also modified. Table 4-24 shows the permeability and porosity used in these simulations. Figures 4-5a and 4-5b show methane and oxygen fluxes at the landfill surface over 24 hours. The negative values in Figure 4-5b indicate the intrusion of O_2 into the landfill. The influence of peaking-power operation on the fluxes was diminished with the decrease of the permeability and porosity of the biocover. When the permeability was reduced to 10 times

125

smaller than the permeability of the base case, the ratio of the maximum to minimum CH_4 fluxes over 24 hours was also reduced from 2.2 to 1.34. The ratio was further decreased to 1.09 when the permeability was 100 times smaller than the permeability of the base case.

Table 4-24. Permeability and porosity ranges of biocover evaluated in Case 1

	Intrinsic horizontal permeability (m^2)	Intrinsic vertical permeability (m^2)	Porosity
k_{bc}	1.0e-12	1.0e-13	0.35
0.5 k_{bc}	5.0e-13	5.0e-14	0.294
0.1 k_{bc}	1.0e-13	1.0e-14	0.188
0.05 k_{bc}	5.0e-14	5.0e-15	0.154
0.01 k_{bc}	1.0e-14	1.0e-15	0.094

Data collected by Yolo County project team
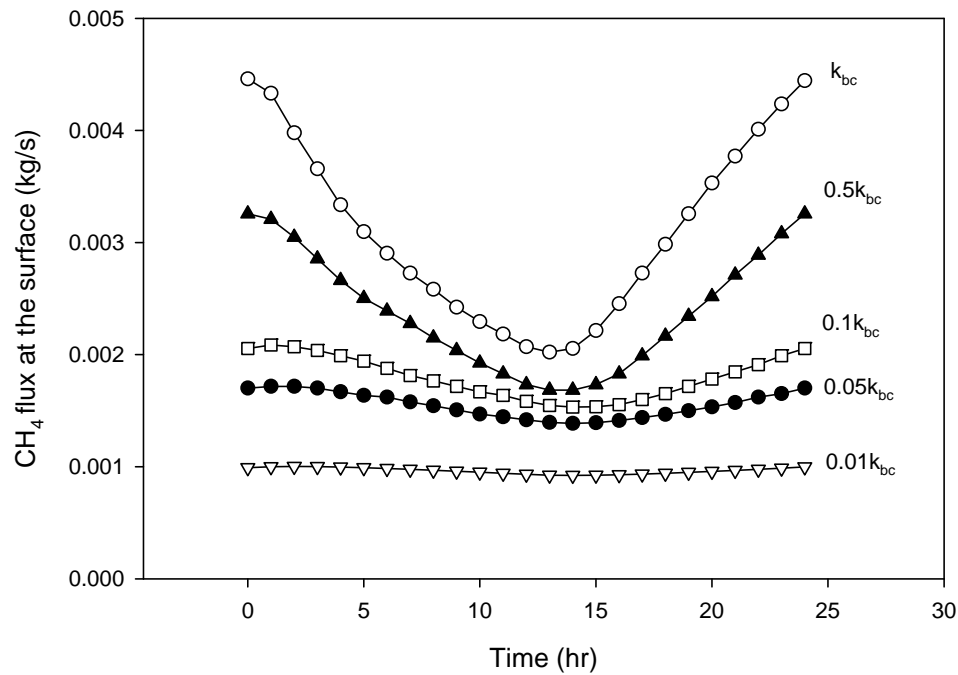
Figure 4-15a. Methane fluxes at the top landfill surface as a function of the permeability of biocover for a 24-hour period

Photo Credit: Yolo County Planning & Public Works Department
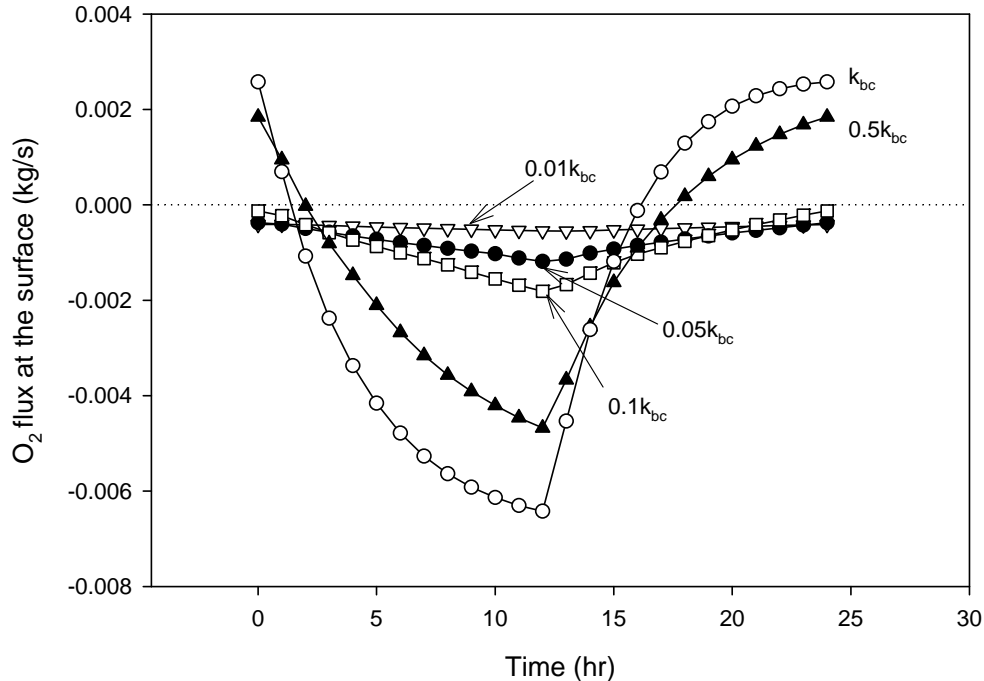
Figure 4-15b. Oxygen fluxes at the top landfill surface as a function of the permeability of biocover for a 24-hour period. The negative values mean the intrusion of oxygen into the landfill.

Photo Credit: Yolo County Planning & Public Works Department

The average CH_4 emission rate based on the total CH_4 generation rate is shown in Table 4-25. The waste volume percent having over 3 percent O_2 concentration above the pancake well was calculated at the maximum O_2 intrusion point over 24 hours. This value was used to approximate the area that does not have favorable conditions for CH_4 generation by anaerobic methanogenic microorganisms. Methane emissions were reduced from 16.1 to 6.0 percent, and the volume percent having over 3 percent O_2 was also reduced from 61.4 to 30.6 percent when the gas permeability in the biocover was reduced by a factor of 10 from base case simulations. This result shows that the environmental conditions that determine the permeability and porosity of biocovers solely affect the methane emission and oxygen intrusion independent of biological activity in biocovers. When the permeability and porosity were reduced, methane emissions were reduced because the escaping CH_4 experienced more resistance to transport. But, at the same time, the oxidation of CH_4 may be decreased because the diffusion of O_2 to the biocover is also reduced, which is necessary for methanotrophs. Also, when it rains and overall gas permeability drops, preferential wetting fronts will form in biocovers and much more preferential flow of gas will be developed in the biocover. This will limit methane oxidation. Thus, the combined effect of these factors should be evaluated in future work.

Table 4-25. Fugitive methane emissions and oxygen intrusions as a function of the permeability of biocover

Biocover permeability	CH$_4$ emission (%)[§]	Waste volume over 3 % O$_2$ concentration (%) [†]
k_{bc} [††]	16.1	61.4
0.5 k_{bc}	14.7	58.3
0.1 k_{bc}	11.2	50.2
0.05 k_{bc}	9.7	46.1
0.01 k_{bc}	6.0	30.6

[§]The methane emission is averaged for a 24-hour period.

[†] The volume percent is calculated based on the waste volume above the pancake well.

[††] k_{bc} represents the biocover permeability of the base case.

Data collected by Yolo County project team

Case 2: Effect of permeability and anisotropy of waste

Permeability and anisotropy of refuse are important factors that may affect the efficiency of collecting LFG. Despite the significance, very few data are available. The difficulty of estimating the influence and collecting data also arises from the variation of those waste properties over time due to compaction of refuse and leachate recirculation. Thus, in this section, the effect of permeability and anisotropy of waste on methane emissions was estimated in peaking-power mode.

The modeling results are shown in Figure 4-16. Methane emissions varied according to the change of pumping mode, as shown in Figure 4-14. However, no matter how big the permeability was and how different the anisotropy ratio was, the methane emission rate was essentially constant when the tire layer was installed. The difference among three anisotropic ratios was within 1 percent, so the averaged data is illustrated in Figure 4-16. On the other hand, when the tire layer beneath the biocover was not present, methane emissions increased dramatically with the decrease of permeability. This variation was more pronounced at lower anisotropy ratios. The methane emission rate increased from 16.6 to 30.5 percent when the ratio of horizontal to vertical permeability was 3 versus 10. This means that the permeable tire layer minimizes the undesirable decrease in the methane collection rate by variable waste conditions and also reduces methane emission itself. This fact is very useful in terms of operating bioreactor landfills because important parameters such as moisture content and porosity vary with time and they greatly affect air permeability of waste. When liquid is added, the moisture content is increased, which blocks pores for gas flow. And with waste stabilization and settlement, the porosity is decreased. Both of these factors reduce the gas permeability and the efficiency of methane collection. So at this point, it can be said that the new landfill design that includes the permeable layer enhances methane collection efficiency. With this permeable layer installed, the impact of peaking-power operation on methane emissions is minor, even when significant changes in gas permeability in the waste occur.
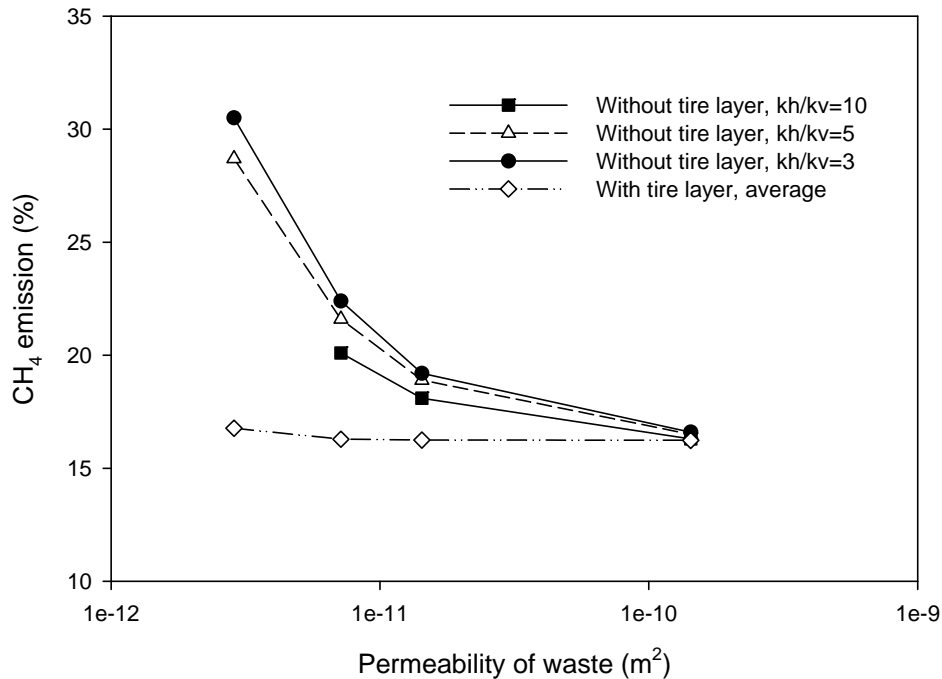
Figure 4-16. Variation of methane emission depending on the gas permeability and waste anisotropy ratio (k_h/k_v). When the horizontal tire layer is installed, the averaged result is shown because the variation among different cases is negligible.

Case 3: Effect of atmospheric pressure change

Atmospheric pressure is one of the major environmental factors that influences methane emissions. For this simulation, specific barometric pressure data near the project site (Sacramento, California) were obtained from the National Climatic Data Center of the National Oceanic and Atmospheric Administration (NOAA). The 24-hour pressure data were averaged for a one-month period, and then input as the top boundary condition in the numerical simulation. Atmospheric pressures increase with sunrise, decrease from noon till sunset, and during night time remain essentially constant. Figures 4-17a and 4-17b show the barometric pressure change and the pumping rate change used in this section, respectively.

To separate the influence of peaking-power operation and atmospheric pressure changes, methane emissions were compared for three conditions: (1) peaking-power mode with variation of atmospheric pressure, (2) peaking-power mode with constant atmospheric pressure, and (3) constant pumping mode with variation of atmospheric pressure. As shown in Figure 4-17c, the change resulting from the barometric pressure variation was minor compared to the impact of peaking-power operation. In addition, the variation of methane emissions associated with atmospheric pressure changes was more related to the rate of the pressure change rather than the pressure itself. In peaking power mode, the variation of the CH_4 emissions was much larger than in constant pumping mode. In overpull, the methane emission was consistently reduced

from 21.9 to 10.6 percent, whereas it increased again after the pumping mode was changed to underpull. However, the averaged CH_4 emission over 24 hours was almost the same, and it differed only within 1 percent from the constant pumping case. That is, peaking-power operation had a negligible influence on methane emissions even when coupled with atmospheric pressure changes.
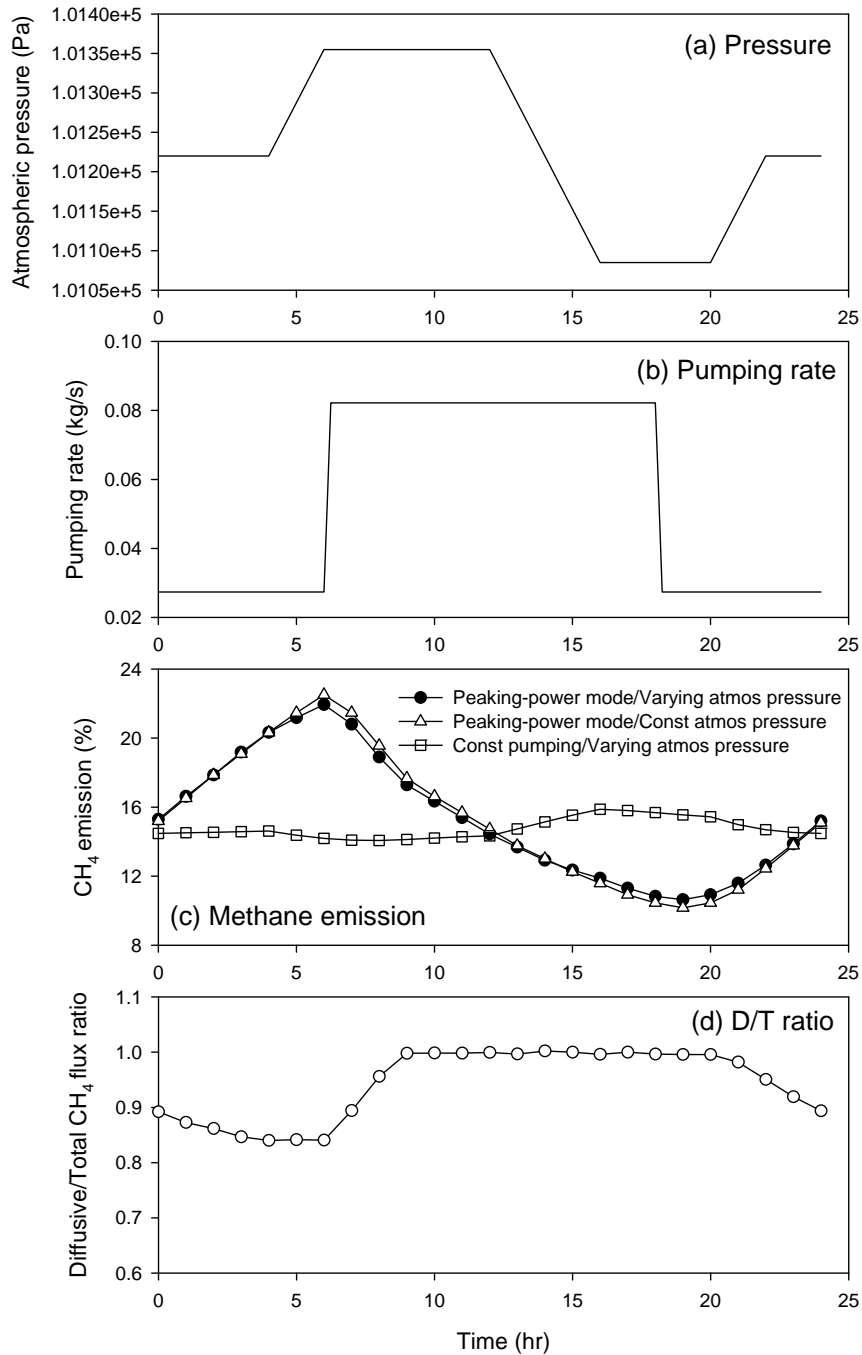
Figure 4-17. (a) Variation of atmospheric pressure, (b) variation of pumping rate, (c) variations in methane emissions associated with pumping rate and atmospheric pressure changes over a 24-hour period, and (d) variation of diffusive methane emissions associated with pumping rate and atmospheric pressure changes over a 24-hour period. The relative diffusive flux is calculated based on the total methane flux.

Photo Credit: Yolo County Planning & Public Works Department

131

In Figure 4-17d the relative contribution of diffusive and advective fluxes on the total CH_4 emission at the landfill surface is indicated. In overpull, the diffusive flux was comprised mostly of CH_4 emissions. The ratio of the diffusive to total flux started to decrease after the pumping mode was changed to underpull, and it continued to the end of the underpulling period. The decrease of the methane emission in overpull results from dilution by air intrusion, and the increase of the methane emission in underpull is caused by the temporal upward advective flux, which is related to the pressure build-up during underpulling. Surprisingly, the advective flux contributed only up to 15 percent of the total CH_4 emissions, implying that molecular diffusion is the dominant transport mechanism. This result is somewhat different from other studies where a more remarkable difference in methane emissions occurred due to changes in barometric pressures (Czepiel et al. 2003; Poulsen et al. 2003). The project team hypothesizes that cracks/fissures formed in the soil cover at these field sites that significantly increased advective fluxes over diffusive fluxes and also caused more dramatic variations of methane emissions with atmospheric pressure changes. If there is a crack in the packed soil or biocover, most of the gas transport will occur through this opening, since the resistance of gas flow is smaller at this weak point. But in these simulations, it is assumed that the biocover is not cracked, so possible preferential gas flux is not considered. Future work should examine the influence of cracks in biocovers on methane emissions during peaking power operations.

Case 4: Effect of pumping ratio

Controlled landfills include facilities to collect landfill gases. A pumping well is the most commonly used gas-collecting system. The pumping rate for the gas collection well is typically calculated based on the estimated gas production rate of the landfill. Typically, landfill gas collection wells are operated at constant pumping rates. In this study the effect of peaking power operation on methane collection efficiency was studied. With peaking power operation, the pump is operated in the overpull condition during the day, gas extraction rate exceeds the rate of gas generation, and at nighttime it is operated in the underpull condition, gas extraction rate is below the rate of gas generation. For Case 4 simulations, the time-averaged gas extraction rate was kept constant and equal to the landfill gas generation rate. The ratio of overpull to underpull was varied, though, to determine its influence on methane collection. Figure 4-18 shows the variation of methane emissions versus pumping ratio. When the pumping ratio is increased, greater landfill gas is extracted during the day and less at night; the variation of methane emissions with time is also increased. The total methane emissions summed up for 24 hours show little increase as the pumping rate is increased from two to five: the increase in methane emissions is less than one percent as shown in Figure 4-19. The ratio of oxygen to methane flux at the pumping well is also almost the same. Thus, elevated methane emissions and reduced methane capture in the underpull period is canceled out by improved methane capture during the overpull period. Thus, it may be possible to significantly increase pumping during the overpull period (and reduce the pumping during the underpull at night) to collect more methane and generate more electricity during the daytime, while having minimal effect on fugitive methane emissions and air intrusion into the landfill. If this result is substantiated in future field tests, it suggests that even more LFG may be collected in the day for peak power

needs than was assumed in the base-case simulations (50 percent higher gas extraction for overpull, and 50 percent lower gas extraction during underpull).
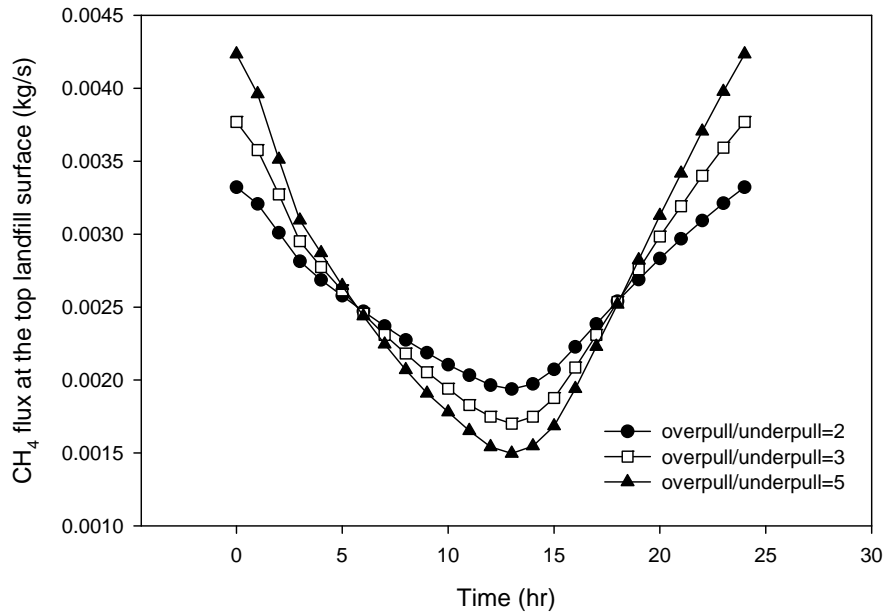
Figure 4-18. Fugitive methane emissions as a function of the pumping ratio (Q overpull/Q underpull) for a 24-hour period. The time-averaged pumping rate is kept constant and equal to the landfill gas generation rate.

Photo Credit: Yolo County Planning & Public Works Department
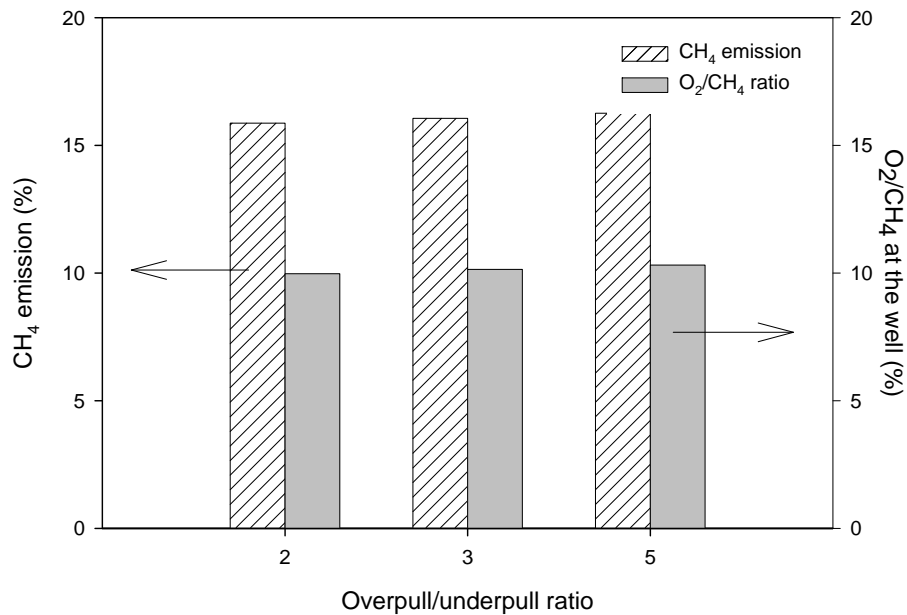
Figure 4-19. Fugitive methane emissions and ratios of oxygen to methane at the pumping well as a function of the pumping ratio (Q overpull/Q underpull). The methane emission is averaged over a 24-hour period.

Case 5: Effect of permeable layer

An innovative design feature tested in this study is the tire layer installed between the biocover and the pumping well. This permeable layer acts to distribute the gas pressure evenly near the top of the landfill. The modeling results discussed above showed that the tire layer played an important role in obtaining stable methane collection and LFG emissions. In this section the influence of the relative configuration of the tire layer is discussed.

4.1.12 Effect of depth of tire layer

The influence of depth of permeable layer on methane emissions and oxygen intrusions was estimated, and the results are shown in Figure 4-20. When the depth was varied from 0 (right under the landfill cover) to 2.9 m, methane emissions were decreased, but oxygen intrusion increased. The extent of oxygen intrusion is determined as before, by calculating the percent of the waste volume having oxygen concentrations over 3 percent in the region above the pumping well. While the decrease of the methane emission was about 6 percent in the testing range, the increase of the oxygen intrusion rate was about 23 percent. The results emphasize the role of a tire layer as a barrier to methane emission and air intrusion. These results also point to the conflicting benefits of the tire layer emplacement: near-surface emplacement decreases oxygen intrusion but increases methane emissions.
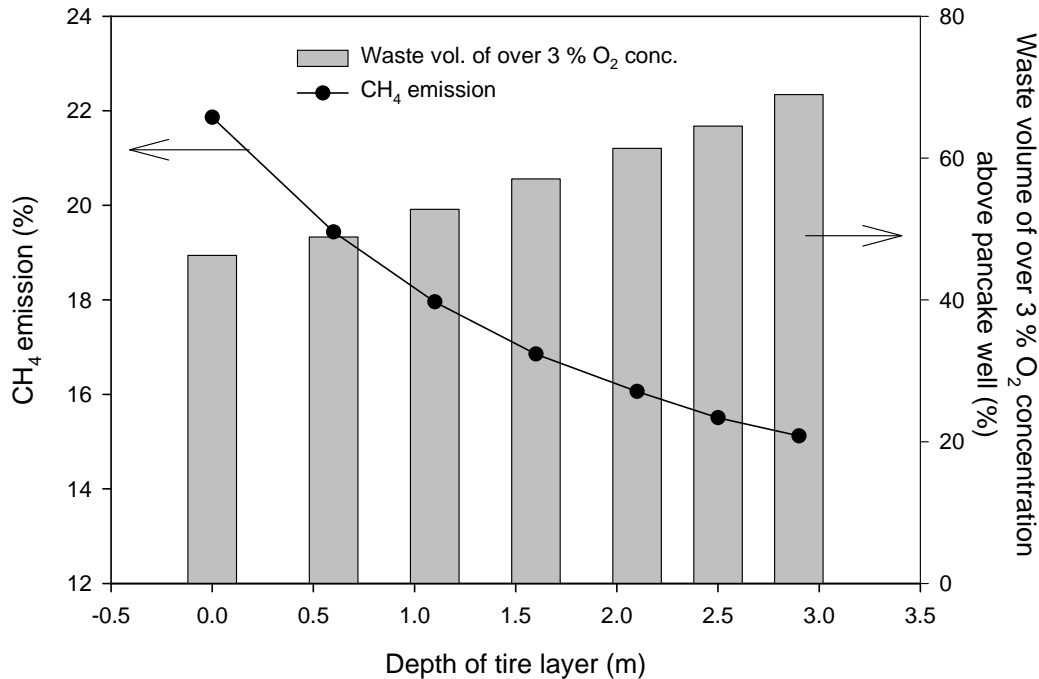
Figure 4-20. Variations of methane emission and waste volume of over 3% of oxygen concentration above the pancake well as a function of depth of tire layer.

Photo Credit: Yolo County Planning & Public Works Department

It is important to note that the installation of a permeable layer right under the landfill cover is not the same as the venting layer of composite landfill cover systems. The latter is used to vent gases generated from underlying wastes into the atmosphere or collect gases in connection with another vacuum pump at the surface (Qian et al. 2002; Zison 1984). But in the present case, the permeable layer only works as a distributor of gases so that all gas flows through the cover layer are uniform. This feature may be useful with biocovers, since it causes even upward flow of gas through the biocover. Because LFG is not directly collected from the permeable layer in the design, the quality of collected LFG may be less affected by barometric pressure changes than in situations where LFG is collected from the venting layer.

4.1.13 Effect of width of tire layer

The influence of the width of the permeable layer was also estimated. The radius of the tire layer was varied from 50 to 100 percent of the domain radius. The lateral condition of the domain was kept as a no-flux boundary condition for comparison with the base case simulations. Figure 4-21 shows the methane emission rate and the oxygen intrusion rate of each simulation. When the coverage of the tire layer was decreased from the whole domain to only half of it, methane emissions increased by less than 2 percent, and oxygen intrusion decreased 6 percent. Compared to the above simulations where the depth of the tire layer was changed, these differences were much smaller. This is a desirable result because the loss in the capacity of

135

landfills by including permeable layers can be reduced by minimizing the area covered by tire layers. This is an important result that should be verified in future field studies.
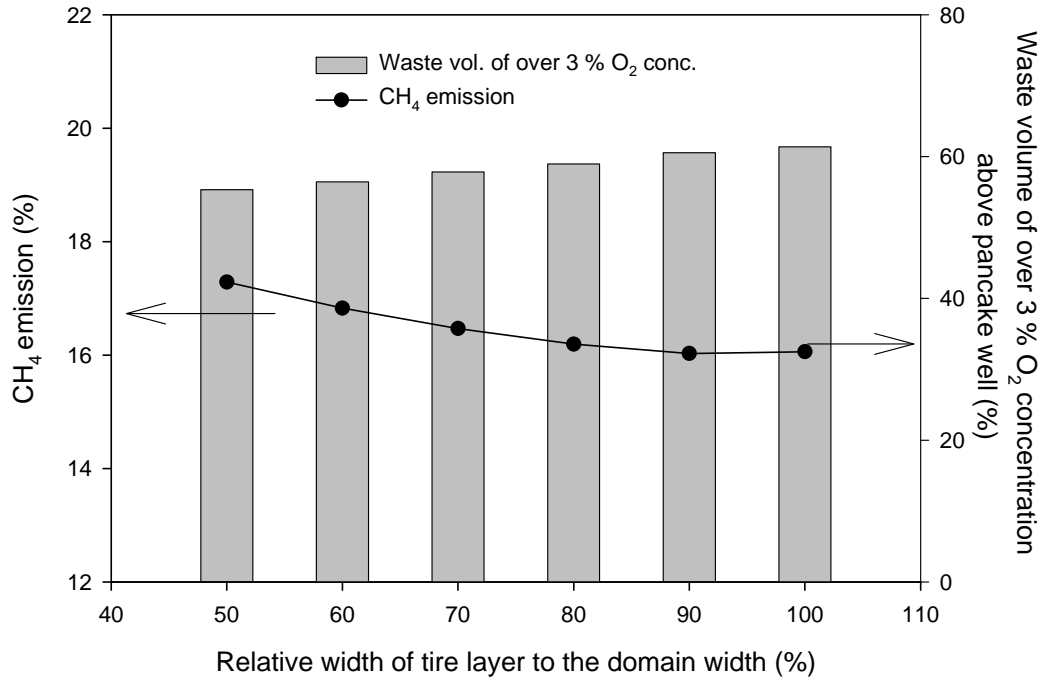
Figure 4-21. Variations of methane emission and waste volume of over 3% of oxygen concentration above the pancake well as a function of width of tire layer.

Photo Credit: Yolo County Planning & Public Works Department

4.1.14 Comparison of simulation results with field data

During March 2007, a field test of peaking power operations was conducted in a new anaerobic test cell constructed at the Yolo County Central Landfill. The field data were compared with simulation results to validate the modeling approach. This landfill was constructed with a horizontal tire layer beneath the top cover, and with a single pancake well installed in the center (approximately) of the cell. Landfill gas composition and landfill gas emissions were measured at two pumping rates: 15 scfm and 65 scfm. Table 4-26 shows the coordinates of measuring locations and Figure 4-22 shows a simplified sketch of the points in elevation and plan view. Figure 4-23 indicates the field data measured for 4 days after reaching a stable condition during peaking power operations. Landfill gas compositions at the pumping well were nearly the same at both extraction rates, suggesting that air intrusion into the landfill was minimal and/or that entering oxygen was quickly oxidized. This result is consistent with the modeling results, which showed negligible fluctuations in LFG quality in the pumping well during peaking power operations.

Table 4-26. Coordinates of measuring locations

Point #	Northing	Easting	Elevation (ft)	Comments
2G-9	1979526.12	6651792	51.6	Pumping well
3-06	1979571	6651765	60.5	
3-11	1979497	6651765	66	
4-05	1979570.6	6651765	76	below 1' soil cover
4-06	1979570.6	6651765	73	

Data collected by Yolo County project team

Elevation View   Plan View
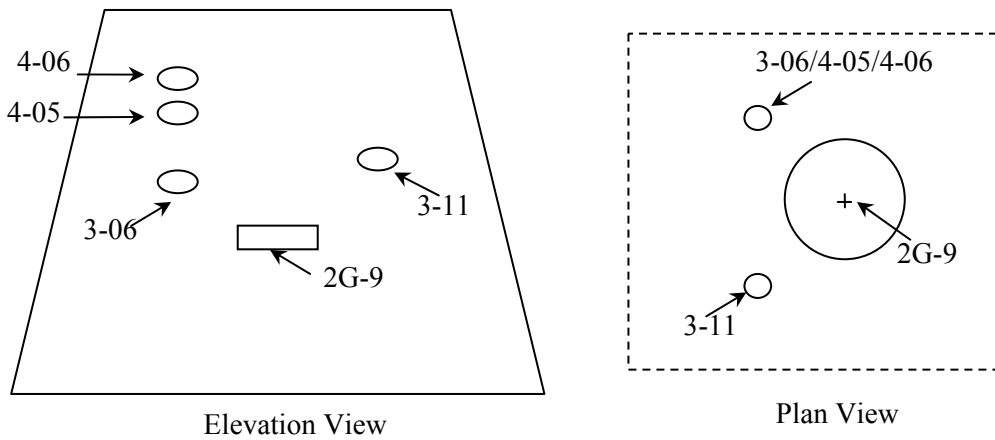
Figure 4-22. Simplified sketch of measuring locations in elevation and plan views.

Photo Credit: Yolo County Planning & Public Works Department
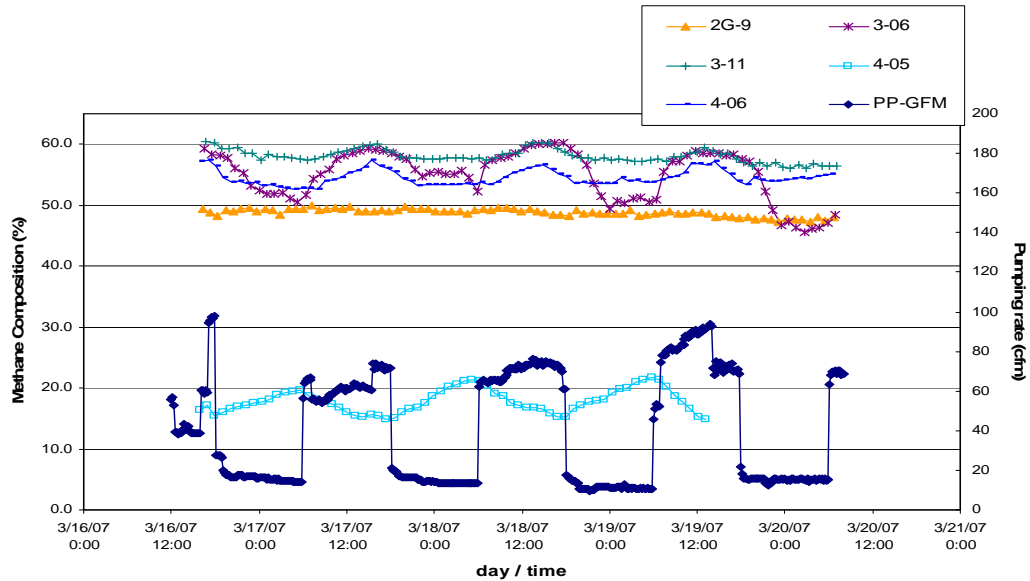
Figure 4-23. Variations of methane composition measured at the Yolo County Central Landfill during March 2007.

Photo Credit: Yolo County Planning & Public Works Department

Methane compositions within the refuse did change during peaking power operations and were correlated with elevation within the waste. At an elevation of 60.5 ft (Point 3-06), the cycle of the methane composition was consistent with the period of the peaking-power operation; the methane content went up while overpulling, and went down while underpulling. This trend was dampened higher in the landfill at elevation 66 ft (Point 3-11) and at 73 ft (Point 4-06), but the fluctuation cycle was still the same. However, the fluctuation cycle of methane composition reversed at 76 ft (Point 4-05), so the methane concentration *decreased* while overpulling and *increased* while underpulling. The methane content at Point 4-05 was much smaller than the concentrations measured at deeper locations. In addition, the data suggest that little oxygen penetrated the landfill: no oxygen was detected at any measurement point except Point 4-05, which was the nearest measuring point to the landfill surface. Even at Point 4-05, the concentration of oxygen was below 1 percent as shown in Figure 4-24. Slight variations in oxygen concentration were observed at Point 4-05 resulting from the peaking-power operation, with concentrations increasing during overpull and decreasing during underpull.
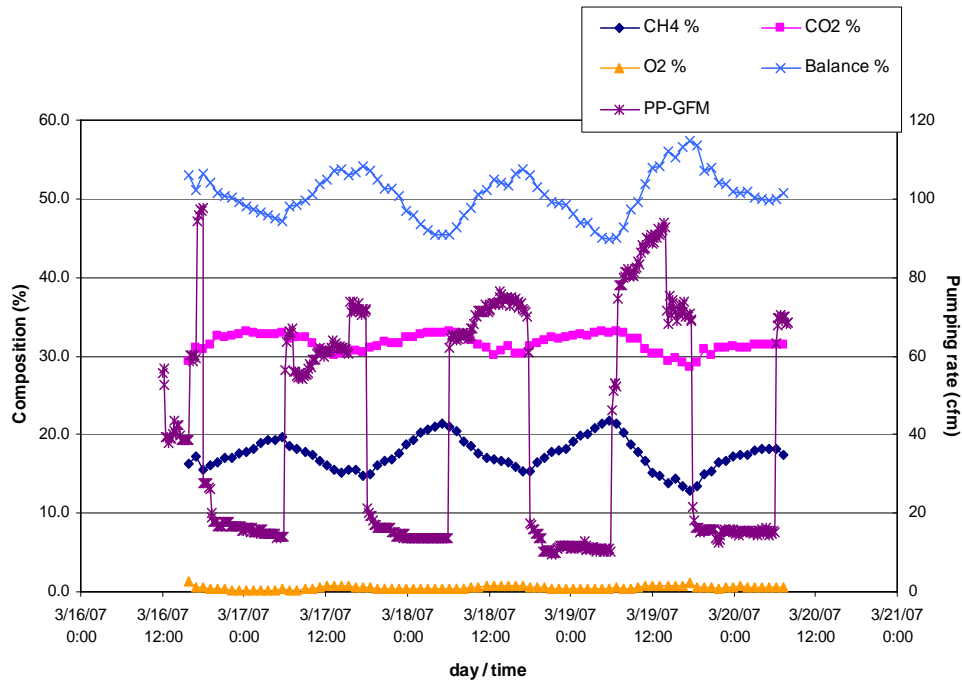
Figure 4-24. Variations of gas composition measured at the Yolo County Central Landfill during March 2007 for measurement location Point 4-05.

Photo Credit: Yolo County Planning & Public Works Department

Similar changes in methane composition with depth were observed in the hypothetical landfill. The simulation results are shown in Figure 4-25. The methane content changed as follows which was in agreement with field measurements: (1) at the pumping well, almost constant methane composition was maintained; (2) at a deeper locations (2.7 m below the biocover), the fluctuation cycle of methane composition followed the pumping cycle, with methane concentrations increasing with overpull and decreasing with underpull; (3) as the measuring location moved up to 1.2 m below the biocover, the gas composition was in an intermediate state in which the influence by the peaking-power operation on methane concentrations changed; and (4) the methane composition was inversely related to the peaking-power operation right below the biocover, with methane concentrations *decreasing* during overpulling and *increasing* during underpulling.

Two important differences were observed between the model simulations and field data. First, in the field data there were less consistent changes in methane concentrations with elevation than in the model simulations: methane concentrations were 20 percent at Point 4-05 (76 ft), but varied only between 50 to 60 percent for measurement points at 73 ft (Point 4-06), 66 ft (Point 3-11), and 60.5 ft (Point 3-06). This difference is partly due to the fact that biological mechanisms that consume oxygen (diluting gas) were not included in the simulations. Natural variability in gas generations rates also likely occurred in the field, while this information was unknown and could not be used in the computer modeling. While the variation in methane concentration with

139

depth was not matched with field data, the general trend of increasing methane concentrations with depth was consistent between the field and model.
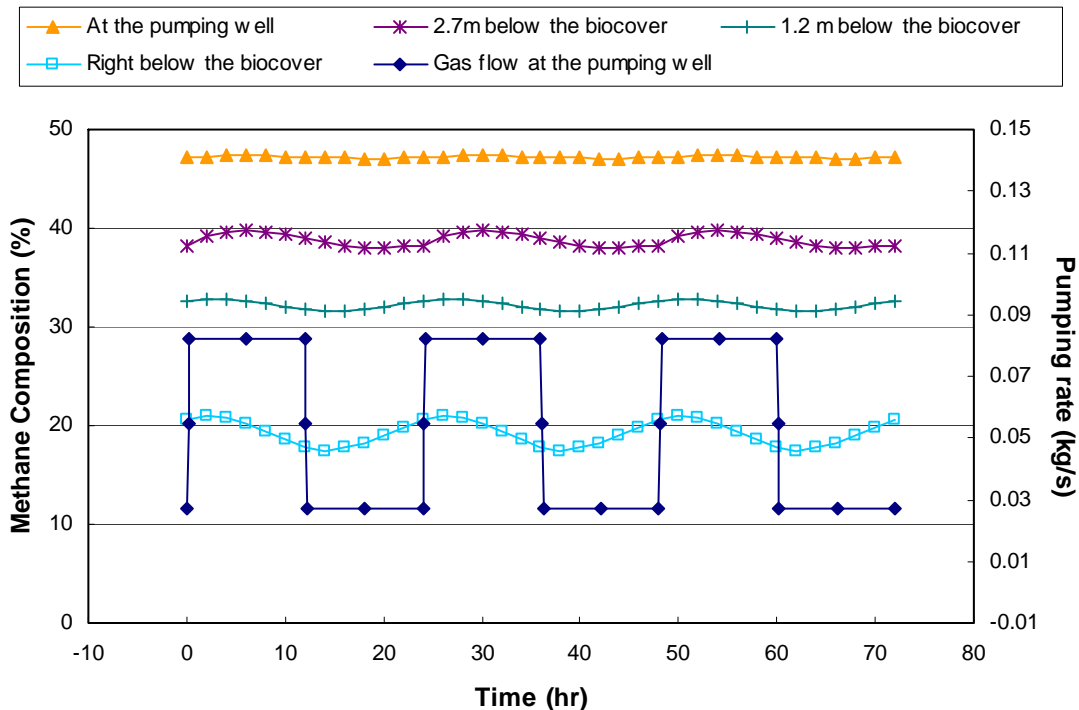
Figure 4-25. Variations of methane composition at the hypothetical landfill

Photo Credit: Yolo County Planning & Public Works Department

A more troubling difference between field and model simulations was observed in the methane concentrations in the pumping well (2G-9). While both model simulations and field data showed gas composition invariant with changes in pumping rates, the field data indicated *smaller* methane concentrations in the pumping well than in measurement points at higher elevations, while in the model simulations methane concentrations were highest in the pumping well (compare Figures 4-23 and 4-25). On the other hand, both field data and model simulations indicate increasing methane concentrations with depth when other sampling points were examined. The authors hypothesize that this unusual result is associated with leakage of air into the pumping well, perhaps through a crack where the gas extraction pipe extends into the pancake well. This particular difference points to possible cracks on the surface cover, which the project team hopes to explore by performing surface scans. It is interesting to note that if such a leak occurs in the system, peaking power operation does not make it any worse. That is, the landfill gas quality in the pumping well in the field test is not affected by peaking power operations (see Figure 4-24). Instead, peaking power operations, with or without a crack, maintain fairly constant gas quality in the gas collection well. This result is consistent with the model simulations.

There is not an exact match between field data and model simulations. This result is expected, since real landfills are heterogeneous with heterogeneous gas generation rates and gas permeabilities, properties that cause spatial variations in gas composition. Current

measurement techniques are not sufficiently accurate to allow such precise characterization of in-place waste properties. However, the general trend of changes in gas composition with depth and with peaking power operation *should match* the computer simulations, if the model is a valid representation of landfill processes. Fortunately, the general trends of the field data match the computer simulations quite well, especially the changing trend of methane composition with switches in the pumping sequence from overpulling to underpulling. This suggests that the results obtained from the model simulations (e.g., effect of waste permeability on peaking power operations) are likely applicable to other landfill sites.
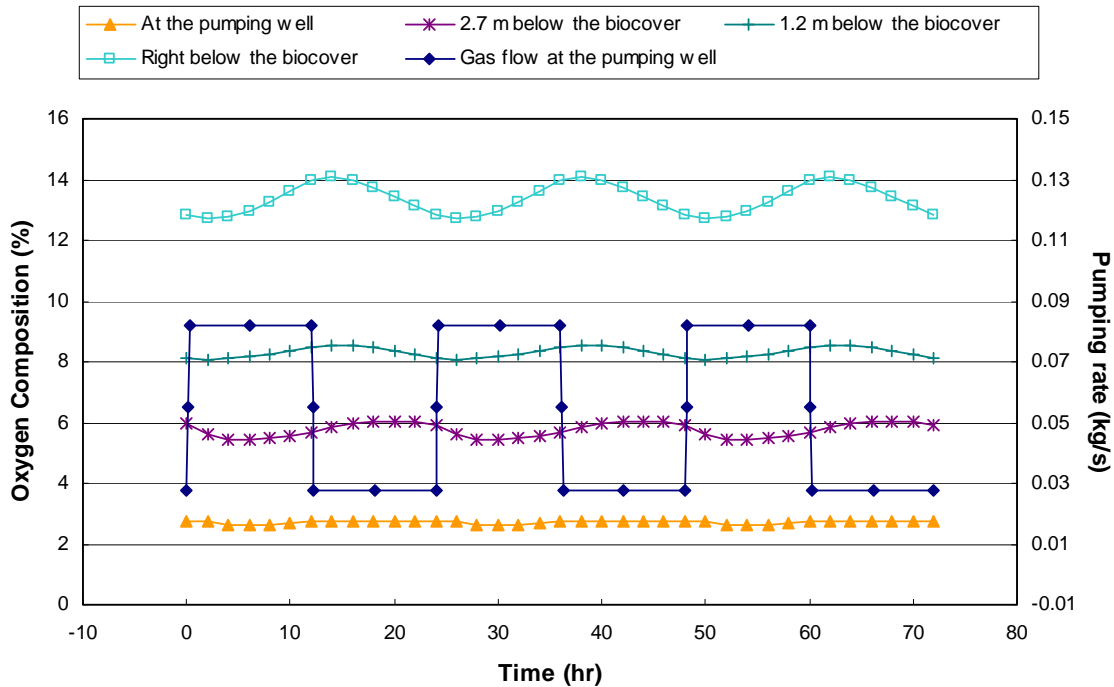
Figure 4-26. Variations of oxygen composition at the hypothetical landfill

Photo Credit: Yolo County Planning & Public Works Department

4.1.15 Conclusions

This study examined the peaking power operation of a model landfill and the influence of various operational parameters on fugitive methane emissions and composition of the collected landfill gas. These model results were compared with field tests conducted in the peaking power test cell at Yolo County Central Landfill. From these analyses, the project team concludes the following:

If a horizontal tire layer is installed at the top of the landfill, the variation in waste conditions has a minimal effect on methane collection efficiency, even if the landfill is operated in peaking power mode.

Atmospheric pressure changes have a minor influence on fugitive methane emissions, likely due to the beneficial effects of the horizontal tire layer at the top of the landfill. This result is the

same for constant gas extraction or peaking power operation of the landfill, as long as the permeable layer is installed at the top of the landfill.

Operating the landfill in peaking power mode results in a 1 percent increase in methane emissions over normal (constant gas extraction) operations. This difference is likely too small to measure in the field and is consistent with field measurements using flux chambers. These simulations did not account for the oxidation of fugitive methane in the biocover, which may reduce fugitive methane emissions even more. Simulations indicate that molecular diffusion is the dominant mechanism controlling upward methane fluxes through the biocover.

When the time-averaged pumping rate is kept constant, it is possible to increase the ratio of overpull/underpull from two to five with minimal effect on oxygen intrusion or methane emissions. Thus, significantly greater overpull might be used to generate more electricity during daytime hours with minimal effect on methane collection efficiency.

The permeable horizontal tire layer near the top of the landfill works as a distributor of gases so that all the gases flowing through the layer become uniform. This feature will help to reduce fugitive methane emissions even if the landfill is not operated in peaking-power mode.

The original landfill design called for a horizontal tire layer near the top of the landfill that completely covers the landfill width. The simulations indicate that the tire layer can be considerable smaller in extent while still mitigating fugitive methane emissions from peaking power operations. Thus, loss in the capacity of landfills by including a permeable layer may be minimized by reducing the area covered by the tire layer.

Simulation results of changing gas composition with depth in the landfill were compared with field measurements. Predicted variations in gas composition with depth and with pumping operations were in good agreement with measured trends in the field, given the unknown variations in gas generation rates and gas permeabilities at the field site. Differences between model predictions and field measurements of methane concentration in the pumping well suggested leakage into the well through a crack or high permeability zone, which might be verified with future gas tracer tests. The computer model is a useful tool for evaluating the effects of various operational conditions on peaking power operations and for suggesting explanations to unusual field results.

From this analysis it seems possible to *increase* the amount of landfill gas collected during peak energy demands above that which was assumed in the base case simulations: the ratio of overpull to underpull pumping might be increased from two up to five with less than 1 percent increase in methane emissions above constant pumping conditions, which would be oxidized by the biocover construction as demonstrated in the field and laboratory experiments. In addition, it is clear that peaking power operation with a horizontal tire layer should result in both *increased* methane collection efficiencies and *reduced* methane emissions, when compared to cases with standard vertical gas collection wells without horizontal tire layers. The comparison of the computer simulations with field data collected to date suggests that the model is a reasonable representation of conditions in the field, thus supporting the results obtained from the modeling exercise.

4.1.16 Modeling and Comparison with Fall 2007 Data

4.1.16.1   *Objectives*

The overall objective of the peaking power project is to evaluate the feasibility of operating landfills in a peaking power mode. The goal of this subtask is to operate and monitor the performance of the constructed permeable layer and gas extraction system in a landfill with biocover. As part of this task the peaking power cell was operated under the on-peaking and off-peaking mode for several months and the collected data was used to determine the performance of the cell as compared to the predicted computer model. Landfill surface scans were performed and gas composition within the landfill, landfill cover and biocover layers were continuously monitored.

Under Section 2.2, computer modeling was performed to help guide the design of the peaking power cell construction followed by field and laboratory testing to determine the performance of the cell under various operating conditions. Further pneumatic pump tests were conducted (Fall 2007) in the peaking power test cell and were "fitted" with the computer model in order to obtain the actual gas permeabilities of the constructed peaking power cell. The results of the modeling were discussed in Section 4.2 and showed that peaking power operations should result in minor increases in methane emissions if a horizontal tire layer is installed near the landfill surface. Model simulations indicated that the construction of a horizontal tire layer can *increase* the methane collection efficiency by 50 percent for conventional (constant) pumping conditions without a tire layer when the horizontal to vertical permeability ratio for refuse was $k_h/k_v = 3$ and $k_h = 10^{-12}$ m², while methane emissions would decreased by 15 percent for the same anisotropy ($k_h/k_v = 3$) but with $k_h = 10^{-11}$ m². A horizontal tire layer also significantly *decreased* the intrusion of oxygen into the landfill. The modeling helped to guide the design of the peaking power landfill test cell constructed at the Yolo County Central Landfill by estimating the influence of different operational parameters.

In addition, beginning with Section 2.2, model simulations were used to help interpret field data. The simulation results were compared with spring 2007 field tests conducted in the peaking power test cell: model-predicted changes in gas composition due to changes in pumping rate at several measurement points within the landfill were consistent with field measurements. The model was also used to interpret pneumatic pump tests conducted in fall 2007. Pneumatic pump tests were conducted to determine the gas flow properties of the waste. By matching the model to field data, insight was gained into the degree of spatial variability of the intrinsic permeability. Model-determined permeabilities were used in all subsequent modeling efforts reported below.

In this report the modeling effort is continued by using the model to interpret field measurements collected in the peaking power test cell in fall 2007. During peaking power operations, changes in gas composition were measured at various locations (see Figure 4-28A, plan view and cross-sections Figures 4-28B and 4-28C) in the peaking power test cell in response to changes in flow rates at the pumping well (2G-9). Methane concentrations varied significantly depending on the measurement location, and high nitrogen (over 20 percent) was observed at the pumping well. Figure 4-27 is a contour map that illustrates the extreme spatial

variability of CH_4 concentrations in Layer 4 during these tests: high CH_4 concentrations occurred in the southeast corner of the cell, with much lower methane concentrations elsewhere. To explain these unusual field data, three hypotheses are proposed:

Hypothesis 1: Air can easily intrude into the landfill through local cracks on the cover layer, and these cracks are the cause of the high levels of nitrogen both in the pumping well and in many measurement locations.

Hypothesis 2: Because of small rainfall during 2007, landfill gas (LFG) generation rates varied widely in the landfill in fall 2007, and these spatially variable LFG generation rates caused the observed field trends in gas composition.

Hypothesis 3: Long cracks/fissures might extend from the landfill surface to the pancake well (2-G9) along well piping. This preferential gas flow path combined with spatially variable LFG generation might have caused the observed field data in fall 2007.

The modeling work reported here was meant to evaluate the reasonableness of these three hypotheses for explaining the fall 2007 field data.
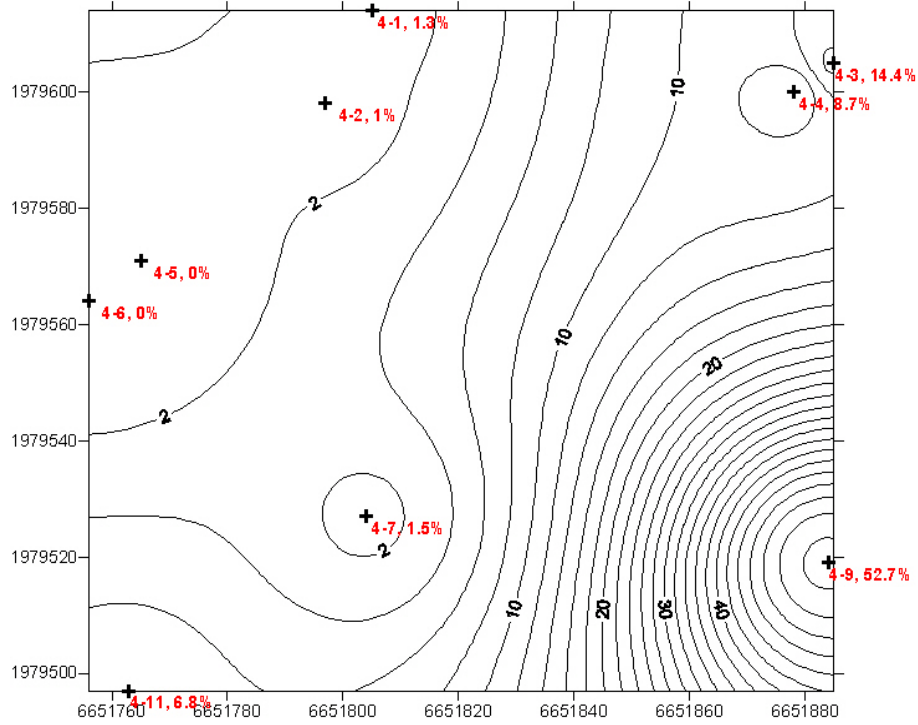
Figure 4-27. Methane concentrations in Layer 4 of the peaking power cell in November 2007. Sampling points are shown along with contoured data. Low methane concentrations exist for much of the cell in Layer 4.

Photo Credit: Yolo County Planning & Public Works Department
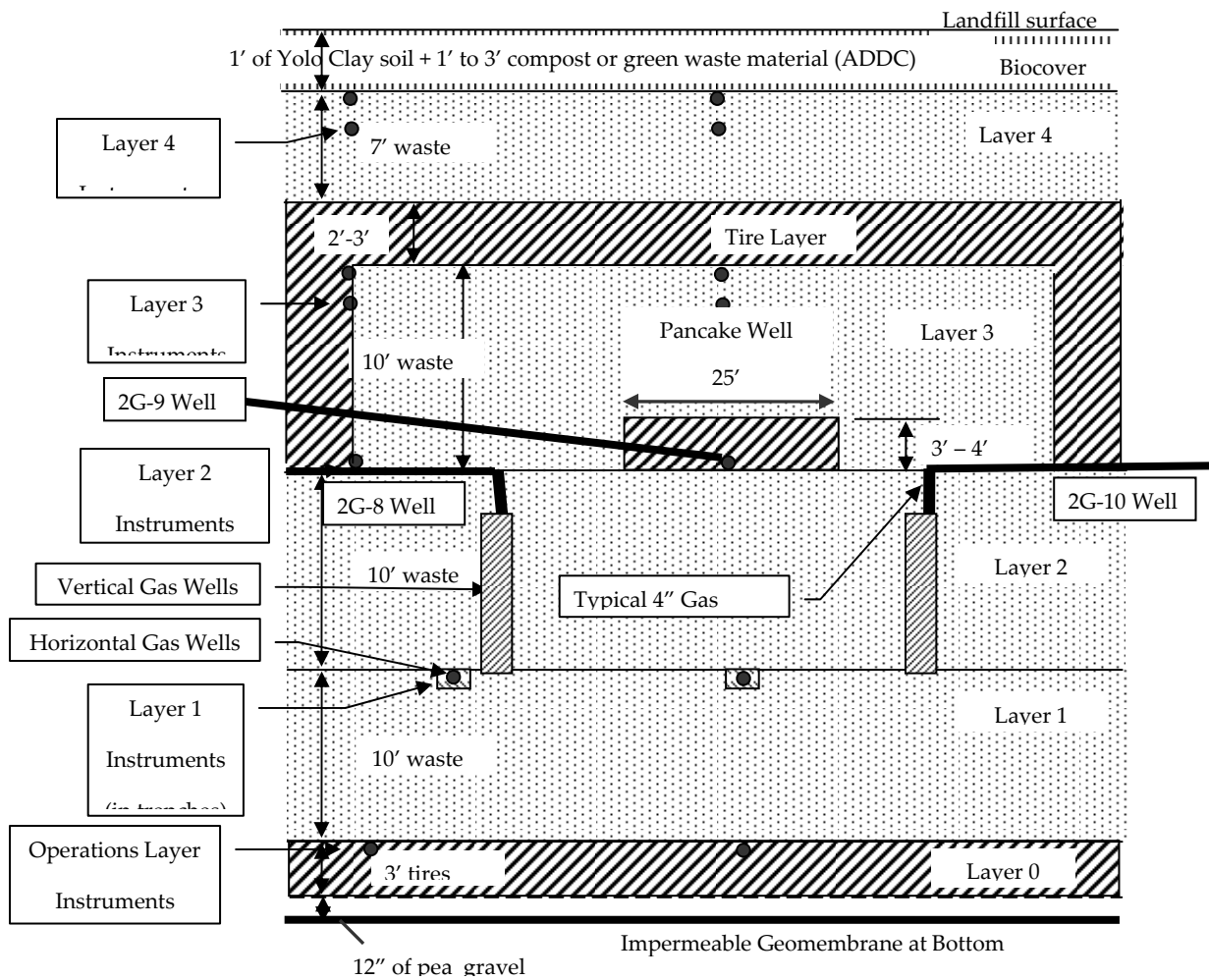
Figure 4-28A. Peaking power landfill cell cross-sectional area

Photo Credit: Yolo County Planning & Public Works Department
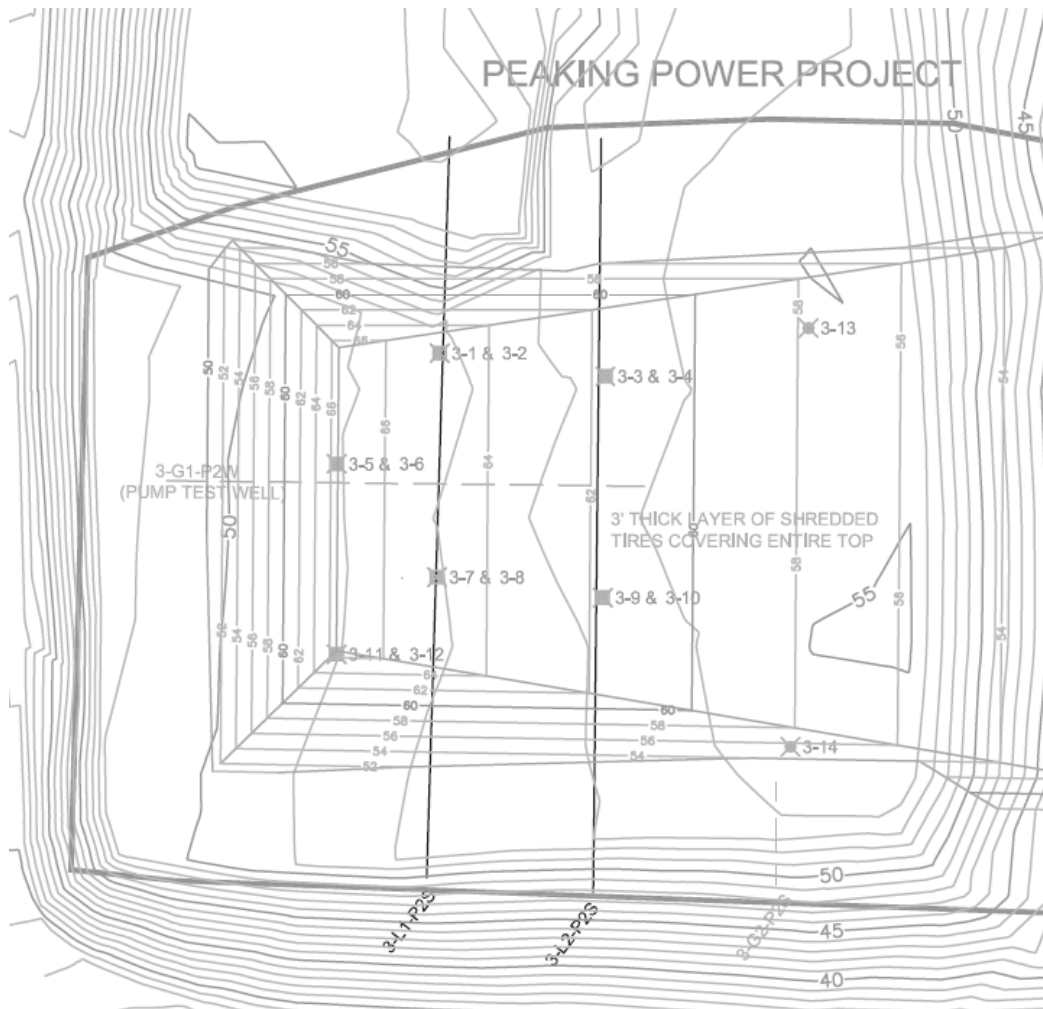
Figure 4-28B. Peaking power landfill cell plan view for Layer 3 instrumentation

Photo Credit: Yolo County Planning & Public Works Department
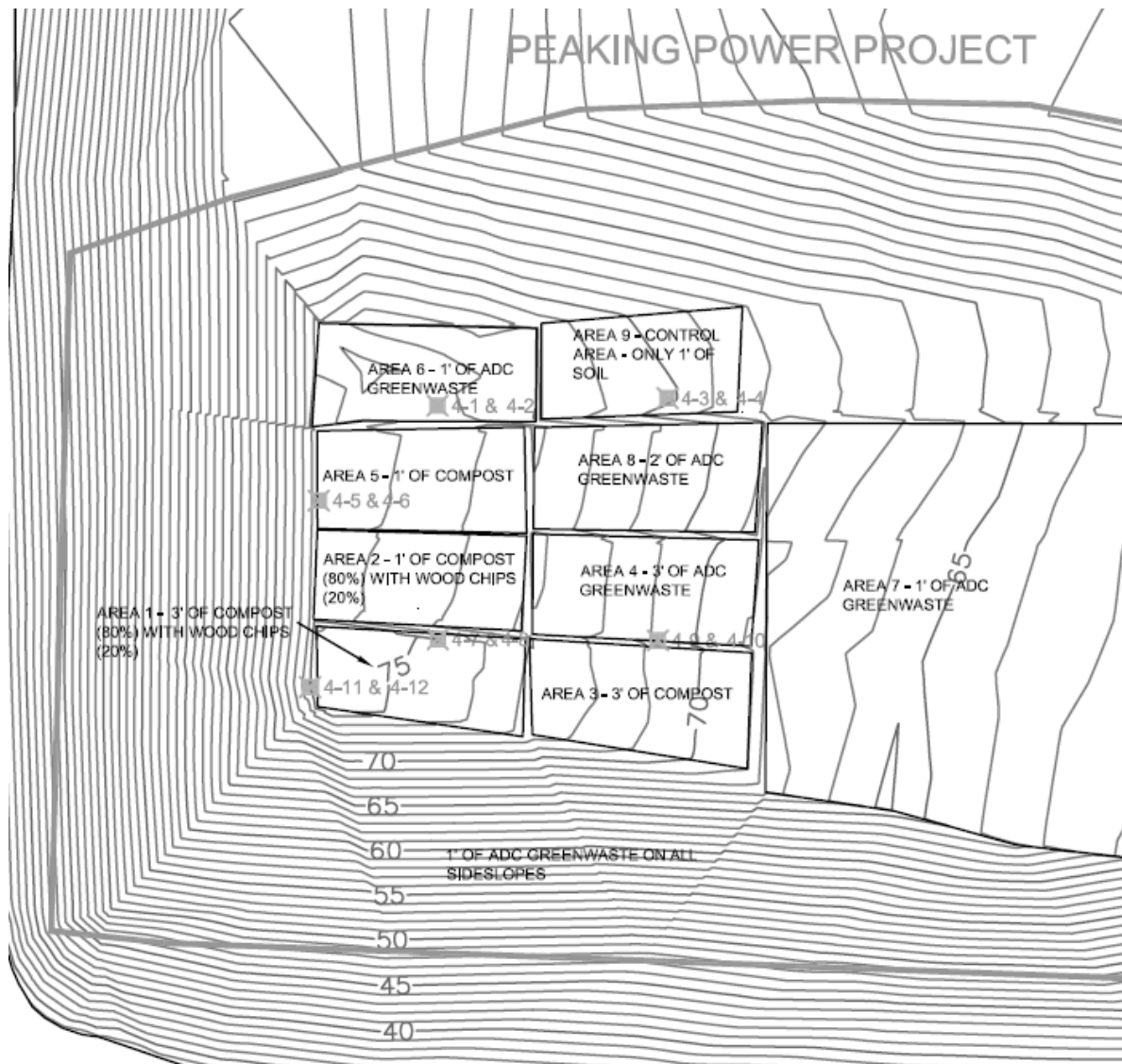
Figure 4-28C. Peaking power landfill cell plan view for Layer 4 instrumentation

Photo Credit: Yolo County Planning & Public Works Department

4.1.17 Methodology

4.1.17.1　　Approach

To test whether or not any of the three hypotheses are valid, a modeling investigation was conducted in concert with careful examination of field data. Several models of gas flow in two-dimensional, rectangular domains were constructed to evaluate the following cases:

Case 1. Cracks were placed in the soil/biocover to determine if cracks alone in the soil/biocover could explain the high nitrogen levels and low CH_4 concentrations in the pumping well and at particular measurement locations.

Case 2. The landfill gas generation rate was varied spatially in an attempt to reproduce the significant variability of CH_4 concentrations at locations in layers 3 and 4 of the peaking power cell and low CH_4 concentrations in the pumping well.

Case 3. Here, the crack introduced in the soil/biocover for Case 1 was extended to the peaking power well. Variable gas generation rates used for Case 2 were also used in this simulation.

The authors begin by discussing the numerical simulator, the model domain and porous medium parameters used for simulating the three Cases, the procedure for generating cracks in the soil/biocover, and the methodology used to select variable gas generation rates to mimic field measurements. The results of simulations for the three Cases are presented in Section 4.3.3. The authors also note that while multiple data sets were collected in fall 2007 from the peaking power landfill cell, the project team focused on the operating period of November 25 through November 28, 2007. Data were only analyzed from this period, but the insights learned from this period are applicable to other test periods in fall 2007.

4.1.17.2　　Numerical Simulator

To simulate LFG transport, a multiphase and multi-component simulator was used, TMVOC (Pruess and Battistelli 2002). TMVOC is an extended version of the TOUGH2 computer code (Pruess et al. 1999) and is capable of modeling multiple gaseous components. A brief description of the governing equations used in TMVOC were presented in previous reports and more detailed information is included in the user's manual (Pruess and Battistelli 2002). One modification was made to TMVOC for calculating diffusive fluxes of LFG for this application. The main purpose of this modification was to improve the estimation of diffusive fluxes at the landfill surface. The details of this modification are discussed by Jung et al. (2007).

4.1.17.3　　Description of Model Domain and Porous Medium Properties

At the Yolo County Central Landfill a new anaerobic test cell was constructed with a horizontal tire layer beneath the top cover and with a single well, referred to as a "pancake" well or pancake layer, installed in the center (approximately) of the cell. In the previous reports considering the characteristics of gas flow, a two-dimensional, axisymmetric, radial domain was used to describe gas flow in this landfill cell. In this study a rectangular model domain, equivalent to the axisymmetric radial domain, was used. A rectangular domain was required in order to create discrete cracks in the soil cover.

Figure 4-29 shows a schematic of the model domain; it is 45 m in width and 12.3 m in depth. The domain includes three major material types: refuse, tire layers (high permeability layers), and soil/biocover. The tire layer is installed between the soil cover and the pumping well and acts as a permeable layer to distribute the gas pressure evenly near the top of the landfill. The tire layer is 0.6 m thick and the permeability of the tire layer is 3×10^{-8} m^2.
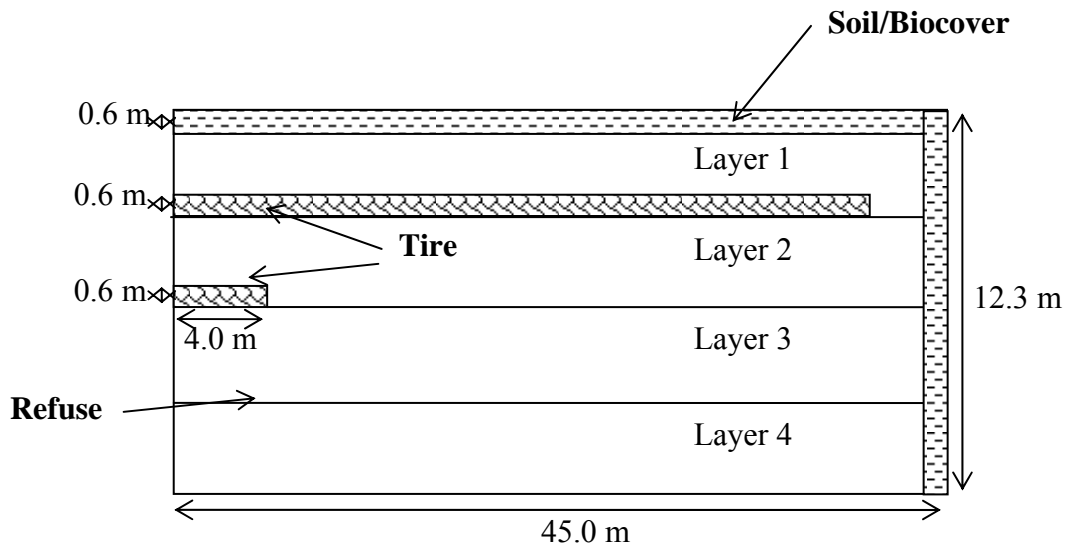
Figure 4-29. Schematic for computer simulations. A rectangular domain was used for all simulations. The thicknesses of layers 1 to 4 are 2.1, 3.0, 3.0, and 3.0 m, respectively. Gas is extracted from the lowest tire layer, which acts as the pumping well.

Photo Credit: Yolo County Planning & Public Works Department

The test cell at the Yolo County Central Landfill has two layers on top of the waste that act as the cover layer: a 0.3 m thick soil layer and an additional biocover material that is usually more permeable than the soil layer. The thickness of the biocover material varies across the landfill as shown Figure 4-30. However, in order to simplify the analysis the authors assumed a constant biocover thickness of 0.3 m for the entire layer in the simulations.
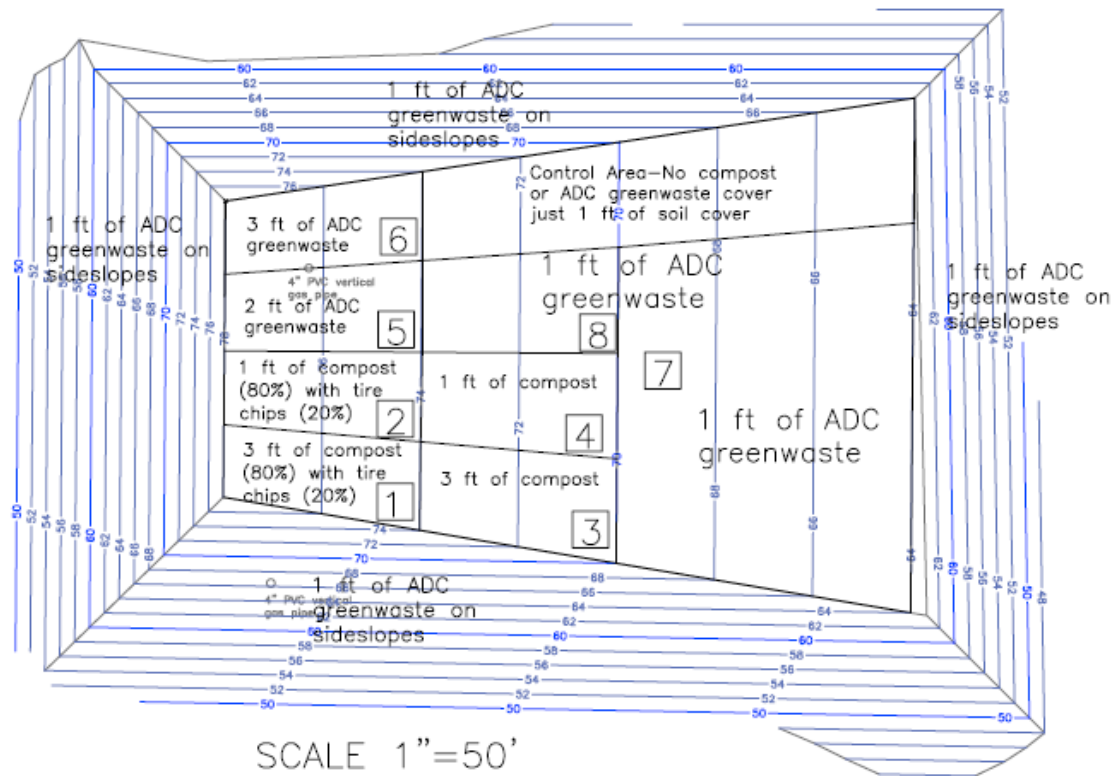
Figure 4-30. Schematic for the types and thickness of the biocover material used on top of the waste at the peaking power test cell.

Photo Credit: Yolo County Planning & Public Works Department

In summer 2007 field tests were conducted by the University of Delaware and Yolo County staff to determine the saturated hydraulic conductivity of the biocover materials on top of the peaking power test cell. A tension disc infiltrometer was used for these measurements. For the 100 percent green waste (ADC), which covers most of the landfill surface, the saturated hydraulic conductivity was approximately 2×10^{-3} cm sec^{-1}. This corresponds to an intrinsic permeability of about 2×10^{-12} m^2. This permeability was assumed to be the same in both the horizontal and vertical directions for the infiltrometer measurements in the field, so the permeabilities in the simulations were also assumed to be isotropic. The soil/biocover layer was set to be 0.6 m thick on top of the waste, and its permeability was 2×10^{-12} m^2.

For the permeabilities of the refuse, the best-fit intrinsic permeabilities from the pneumatic pump tests conducted in fall 2007 were used. Details about these measurements and the matching exercise to determine best-fit permeabilities are described in the previous report. The general properties of each layer used in the simulations are given in Table 4-27.
The van Genuchte–Mualem model (Mualem 1976; van Genuchten 1980) was used for capillary pressure and relative permeability relationships for both the soil/biocover and the refuse. The parameters selected for this model are listed in Table 4-27. The grid used in the simulations

151

consists of 40 and 82 grid elements in the horizontal and vertical directions, respectively. Discretization was finer at material interfaces where significant gradients in concentrations or pressures were expected. The top surface and lateral boundaries for gas flow were a Dirichlet boundary condition of constant pressure (101.3 kPa) and zero methane and carbon dioxide concentrations to represent atmospheric conditions. No flux boundaries were assumed for the bottom border of the simulation domain. The bottom of the model represents the bottom layer to the landfill that is impermeable to both gas and liquid flow. Except for simulations evaluating various LFG generation rates, the best-fit gas generation rate from the previous matching exercise was used, which was 10 m^3/ton/year of landfill gas.

Table 4-27. General properties of model domain for initial simulations. Intrinsic permeabilities were adjusted from values reported here to match field data.

Property		Refuse				Tire	Soil
		Layer					
Bulk Density (kg m^{-3})		1	2	3	4	480	1,700
		632.5	671.3	710.0	758.0		
		Layer					
Porosity		1	2	3	4	0.50	0.35
		0.51	0.48	0.45	0.43		
Aqueous phase saturation		0.21				0.21	0.15
Intrinsic Horizontal Permeability (m^2)		Layer				3.0e-8	2.0e-12
		1	2	3	4		
		1.95e-11	1.39e-11	7.4e-12	6.4e-12		
		Layer					
Intrinsic Vertical Permeability (m^2)		1	2	3	4	3.0e-9	2.0e-13
		1.95e-11	1.39e-11	6.4e-12	6.4e-12		
van Genuchten	Λ	0.59				0.59	0.457
–Mualem parameters	$S_{lr}{}^{a}$	0.21				0.21	0.15
(for relative permeability	$S_{ls}{}^{b}$	1.00				1.00	1.00
function)	$S_{rg}{}^{c}$	0.005				0.005	0.10
	λ^{d}	0.59				0.59	0.457
van Genuchten parameters	S_{lr}	0.20				0.20	0.14
(for capillary pressure	$1/P_0{}^{e}$	8.4e-4				8.4e-4	5.11e-4
Function)	P_{max}	1.0e5				1.0e5	1.0e7
	S_{ls}	1.00				1.00	1.00

a, b, c. Irreducible water saturation, satiated water saturation, and irreducible gas saturation.

d. Pore-size distribution index that determines the shape of the functions.

e. P_o is an air entry pressure.

Data collected by Yolo County project team

For the three Cases reported below, the model was intended to mimic pumping conditions from well 2-G9 during November 25 through November 28, 2007. During this period, the average on-peaking gas flow rate was 15.3 scfm while the off-peaking flow rate was 5.2 scfm. Unless otherwise stated, these two pumping conditions were repeated for 12-hour periods until a quasi-steady state solution was achieved for gas composition in the landfill. The quasi-steady state conditions for gas composition are reported below.

4.1.18 Incorporating Cracks in the Landfill Cover

To examine the influence of cracks/fissures on methane emissions and oxygen intrusion, the equivalent permeability concept was applied. By increasing the permeability of a grid block in the cover layer, a crack can be imaginarily generated in the grid block having a particular aperture. Figure 4-31 shows two equivalent systems: (a) a grid block having a planar crack (fracture) in the landfill cover (matrix) and (b) a homogeneous grid block having an equivalent permeability k_n' to the grid block described in (a).
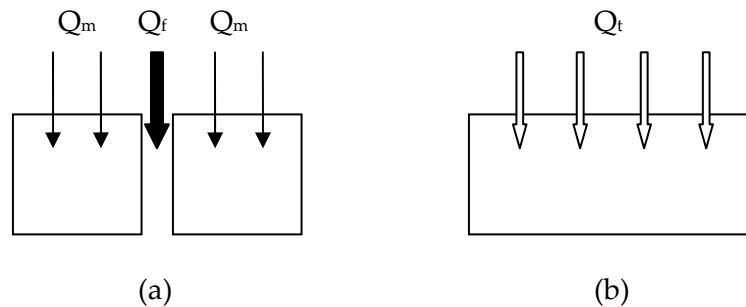
Figure 4-31. Schematic comparison of two equivalent systems. (a) A grid block with a planar crack and (b) a homogeneous grid block equivalent to system (a).

Photo Credit: Yolo County Planning & Public Works Department

The equivalent permeability can be defined in terms of the intrinsic permeability k_n of the matrix in (a) and an amplification factor a_n.

$$k_n' = a_n k_n \qquad (1)$$

a_n is set to be 10^4 in this study, but the value can vary depending on the size of the aperture or the density of cracks. If the total volumetric flow rate in the two systems shown in Figure 4-31 is the same, then the following equation must be satisfied

$$Q_f + Q_m = Q_t \qquad (2)$$

where Q_f and Q_m are the volumetric flow rates through the fracture and the matrix of system (a), and Q_t is the volumetric flow rate through system (b). The width of an aperture in system (a) is calculated using the following equations

$$Q_t = k_n^{'} \frac{k_{rg}}{\mu_g}(\nabla P_g - \rho_g \mathbf{g})w_n l_n \tag{3}$$

$$Q_m = k_n \frac{k_{rg}}{\mu_g}(\nabla P_g - \rho_g \mathbf{g})(w_n - x_n)l_n \tag{4}$$

$$Q_f = k_n^f \frac{k_{rg}}{\mu_g}(\nabla P_g - \rho_g \mathbf{g})x_n l_n \tag{5}$$

where x_n is the width of the crack, and w_n and l_n are the width and length of the grid block n. For the fictitious crack used in this modeling study, w_n and l_n were specified as 0.2 and 0.1 m, respectively. k_{rg} is the relative permeability of gas phase, and k_n^f is the permeability of the planar fracture. μ_c is the viscosity of gas phase, ρ_g is the density of gas phase, P_g is gas pressure, and $\mathbf{g}$ is the vector of gravitational acceleration. Substituting equations (3), (4), and (5) into (2) and canceling out common terms, equation (2) can be simplified to

$$a_n w_n k_n = (w_n - x_n)k_n + \frac{x_n^3}{12} \tag{6}$$

where $k_n^f = \frac{x_n^2}{12}$, which is adopted from the cubic law for laminar flow between two smooth parallel plates (Romm 1966). The first term on the right hand side of equation (6) can be neglected because the coefficient of k_n for this term is much smaller than that for the left hand side of the equation. With this approximation the aperture of the channel was calculated as 0.36 cm, which corresponds to the crack opening size for $a_n = 10^4$ in equation (1). In this way a single crack was included at different positions of the soil cover layer during the simulations. The size of this crack is small, but as will be shown below if such a crack is continuous through the entire soil/biocover and extends into the refuse it can have a significant impact on gas flow.

Matching LFG Generation Rates

For most landfills, the moisture content of waste is the most critical factor in the production of LFG; the higher the moisture content, the greater the gas generation rate (Qian et al. 2002). The moisture content can be significantly different depending on location, even in the same landfill.

To test the validity of Hypothesis No. 1, the authors assumed that the LFG generation rate was not constant in the entire landfill cell. Instead, the LFG generation rate was varied in the model domain until a good match was achieved with measured methane concentrations for six measurement locations in Layers 3 and 4 in the peaking power cell. The problem was approached by determining what spatially uniform gas generation rate would be required to meet the CH_4 concentrations at each of the six measurement points. For instance, one model was used to represent Section O–A shown in Figure 4-32 to estimate the LFG generation associated with measurement location 4-03. The LFG generation rate was varied to match the field measurement of methane at 4-03, keeping the pumping rate at the pancake well equal to the measured flow rate at the field. As in all other simulations, data for all measurement locations

155

and the pumping well were taken from the November 25 to November 28, 2007, time period. During this period, the pumping rate in the pancake well (2-G9) varied between 5.2 scfm for off-peaking and 15.3 scfm for on-peaking.
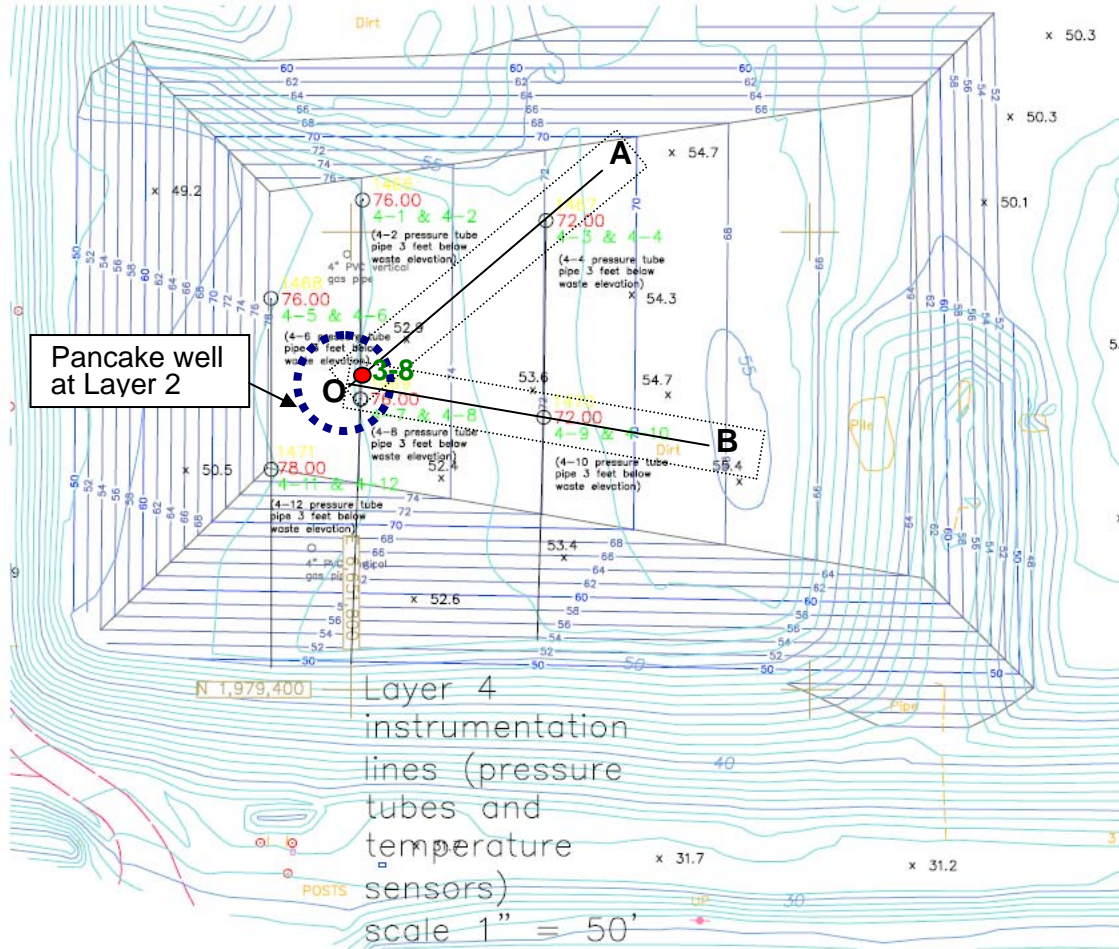
Figure 4-32. Plan view of the test cell. Section O–A represents the rectangular model domain used to estimate the gas generation rate at 4-03. Section O–B is the rectangular model domain used to match gas generation rates at 3-08 (located on Layer 3), 4-07, and 4-09, simultaneously.

It is important to note that this method of determining LFG generation rates only approximates the spatial distribution of generation rates, since the rectangular model domain does not capture all features of the three-dimensional landfill. Future modeling studies will likely require the creation of a three-dimensional model to fully interpret the field data.

4.1.19 Results

Case 1. Influence of Cracks in the Cover Layer

To evaluate the influence of cracks, especially those that might have developed on the side boundary of the landfill, cracks were generated at different positions along the side and top

boundaries of the rectangular domain. Figure 4-33 shows the variation of 24-hour average methane emissions as a function of the crack position. If cracks occurred only in soil/biocover and did not extend through the waste, the position of the crack on the top or side boundary had little impact on fugitive methane emissions. However, cracks on the top of the landfill resulted in about three times as much fugitive methane emissions as cracks through the side slope.
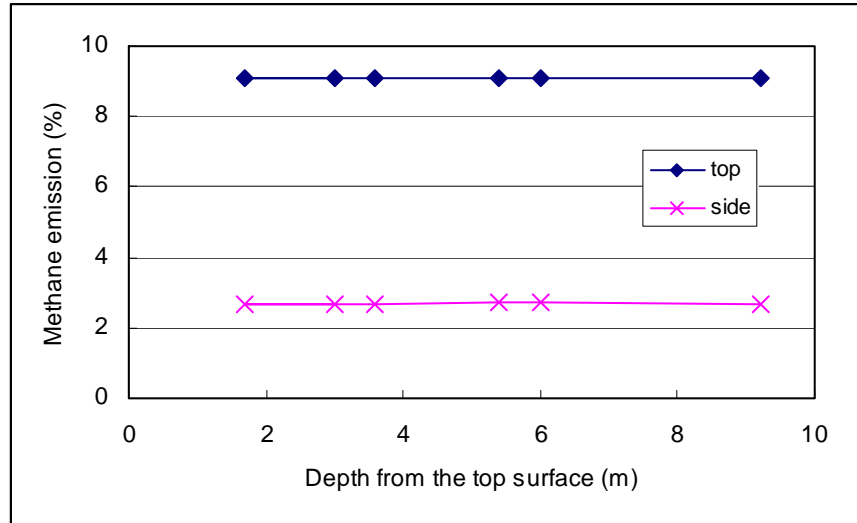
Figure 4-33. Variation of the methane emissions as a function of the position of crack on the top or the side boundary. (a) Top: the methane emission through the top surface boundary and (b) side: the methane emission through the side boundary.

Photo Credit: Yolo County Planning & Public Works Department

Because recent surface scans of the landfill cell suggest that cracks in the side slope might exist, additional focus was given to these cracks. In Table 4-28 the maximum and minimum methane emissions through the side boundary of the domain are shown for different crack positions. These results illustrate that the position of the crack has a minor effect on emissions, and that emissions do not change significantly from the case where no crack exists. Thus, even if a crack occurs in the soil/biocover of the side slope, the effect on methane emissions and air intrusion should be small. Clearly, these model results indicate that if cracking is to have an effect on landfill operations, the cracks must be more than local fissures in the soil/biocover. Additional simulations for Case 3 below explore the impact of a longer crack/fissure on methane emissions.

Table 4-28. Variation of the methane emissions during a 24-hour period through the side boundary during the peaking power operation.

Depth of crack (m)[a]	Average	Maximum	Minimum	Max. – Min.
No crack	2.65	2.93	2.36	0.57
1.7	2.66	2.98	2.34	0.64
3.0[b]	2.68	3.04	2.34	0.70
3.6	2.68	3.01	2.35	0.67
5.4	2.70	3.04	2.37	0.67
6.0[c]	2.71	3.05	2.38	0.67
9.2	2.69	2.99	2.39	0.60

a. Distance from the top surface.
b. The crack is positioned at the same depth with the permeable layer.
c. The crack is positioned at the same depth with the pancake well.
Data collected by Yolo County project team

Case 2. Influence of LFG Generation Rates

Table 4-29 shows the field measurements of CH_4 concentrations and the required LFG generation rates necessary to match these concentrations. As expected, to match the field measurements the LFG generation rates varied greatly depending on the measurement location. For sampling location 4-01 the LFG generation rate was only 1 m^3/ton/year, whereas it was more than 25 m^3/ton/year at 4-09.

Table 4-29. Best-fit values of LFG generation rates

Location	Measured CH_4 concentration (%) (November 25 – 28, 2007 data)	Estimated LFG generation rate (m^3/ton/year)[b]
3-08[a]	24.5 – 38.5	9.0
4-01	0.1 – 1.5	1.0
4-03	11.0 – 17.5	8.0
4-07	0.5 – 2.5	2.0
4-09	50.0 – 53.0	> 25.0
4-11	4.0 – 10.0	5.0

a This measurement point is located on Layer 3.
b These gas generation rates were constant throughout the domain and were selected to fit the measured CH4 concentration data.
Data collected by Yolo County project team

Based on these results, a second matching exercise was conducted. Here, the intent was to determine if spatially varying LFG generation could approximate measured methane concentrations. As shown in Figure 4-30, 4-07, 4-09, and 3-08 are located along Section O–B. These measurement points were assumed to be in the same rectangular domain and were used to evaluate the effect of heterogeneous gas generation rates on the spatial distribution of gas compositions, as observed in the field test. This particular rectangular domain was divided into three regions having different LFG generation rates. Initial LFG generation rates were identical to the best-fit values in Table 7.3-3: (a) Region 1 = 2.0, (b) Region 2 = 9.0, and (c) Region 3 = 25.0 m^3/ton/year. Each region included one measurement point: Region 1–4-07, Region 2–3-08, and Region 3–4-09. However, the simulation with these LFG generation rates did not match field measurements well, since the LFG in Regions 1 and 2 were influenced by the high LFG generation in Region 3. Therefore, generation rates in Regions 1 and 2 were reduced to 1.0, and 5.0 m^3/ton/year.

The results for the steady-state simulation before peaking power operations are shown in Figure 4-34 where the oxygen profiles are drawn. Well pumping is turned off for this plot. Clearly, there are low oxygen and high methane concentrations in Region 3, with higher oxygen and lower methane concentrations in Regions 1 and 2. Note that the model-predicted oxygen concentrations reflect air (i.e., nitrogen) concentrations in the field, since the model did not account for oxygen consumption by methanotrophic bacteria.
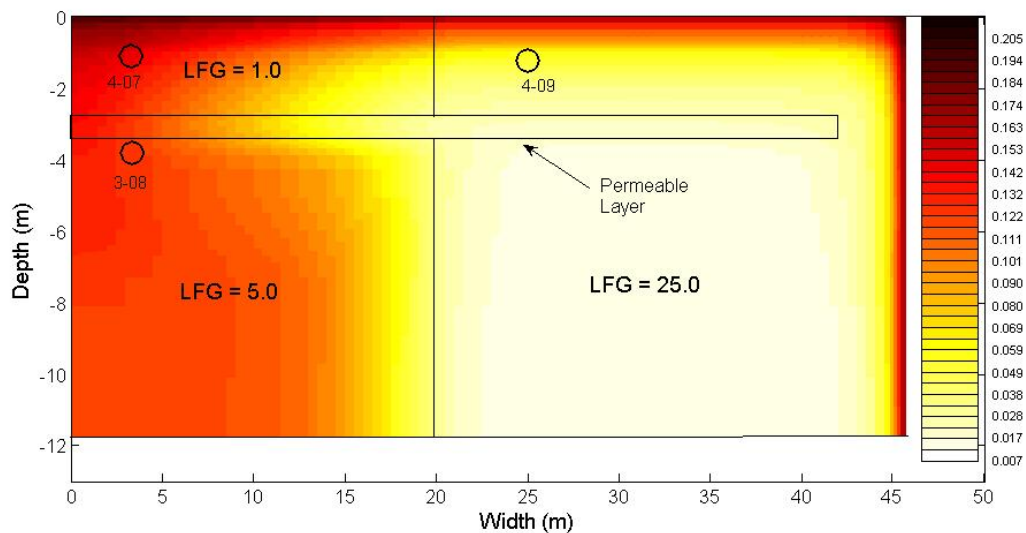
Figure 4-34. Steady-state oxygen profiles (percent by mass) before peaking power operation. Different LFG generation rates were assumed for three regions of the domain and are shown above in units of m^3/ton/year. The approximate locations of 3-08, 4-07, and 4-09 are indicated.

After peaking power operations were initiated, the gas compositions within the landfill eventually reached a quasi-steady state. For this situation the methane concentrations at 4-07

and 3-08 were 21 and 41 percent, respectively, which is much higher than the measured concentrations shown in Table 4-29. On the other hand, the methane concentration at 4-09 was 28 percent, and this value is much lower than the field measurement (~51 percent). Although the gas generation rates near sampling locations 4-07 and 4-09 were significantly different (1.0 vs. 25.0 m^3/ton/year), the effect was evened out when the pump was on. Figure 4-35(a) shows the oxygen profile of the domain and illustrates the role of the permeable layer. The expansion of light color (low oxygen and high methane concentrations) through the permeable layer indicates that the LFG generated in Region 3 was collected through the permeable layer. Because of this gas flow, the permeable layer formed a so-called "buffer zone" and prevented the significant air intrusion observed in Regions 1 and 2 in Figure 7.3-8(a). Also, when the pump was actively operated, the oxygen concentration profiles became much uniform above the permeable layer, explaining the small differences in CH_4 concentrations at 4-07 and 4-09.
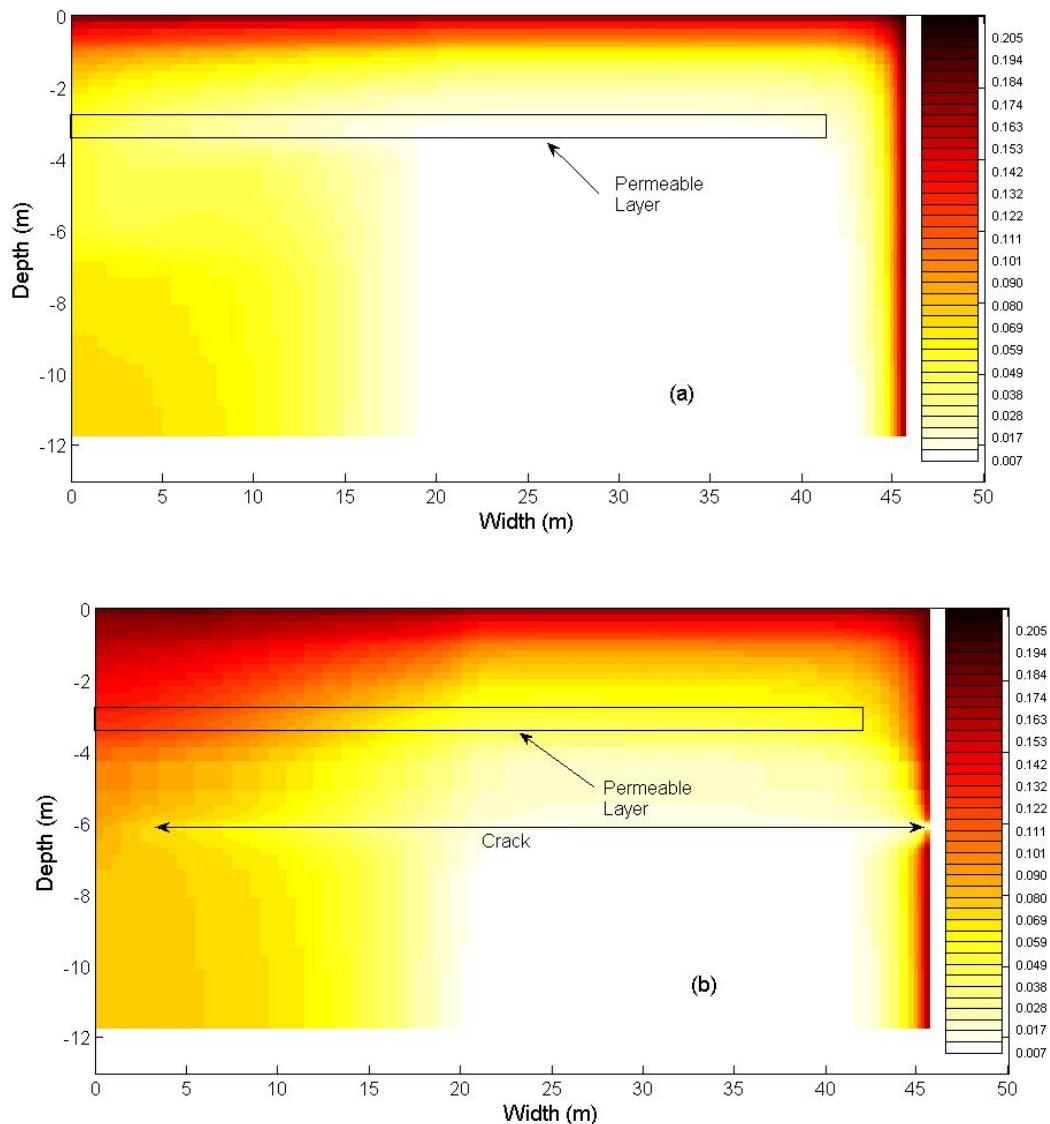
Figure 4-35. Oxygen profiles (percent by mass) throughout the domain for peaking power operations with the spatially variable LFG generation rates shown in Figure 6. (a) With no crack. (b) With a single crack developed from the soil/biocover that extends horizontally through the refuse to near the pancake well.

Photo Credit: Yolo County Planning & Public Works Department

This simulation exercise suggests that it is unlikely that spatially variable LFG generation rates alone could result in the observed spatial distribution of CH_4 concentrations in the sampling tubes. In addition, it is unlikely that spatially variable pumping rates could result in the low CH_4 concentrations (high air content) in the pumping well 2-G9.

161

Case 3. Combined Influence of Cracks and Spatially Variable LFG Generation.

Case 1 and 2 simulations indicate that cracks/fissures in the soil/biocover or spatially variable gas generation rates cannot explain the observed variability in gas composition in the peaking power landfill cell. Case 3 simulations were intended to explore whether or not a long crack that extended from the landfill surface to the pancake well (2-G9) in combination with spatially variable LFG generation might explain observed field data.

Surface scanning was performed using a calibrated TVA-1000B (Toxic Vapor Analyzer) Flame Ionization Device (FID) instrument to measure volatile organic compounds (VOC) concentration in air directly above the surface in the parts per million range. VOC surface concentrations were automatically recorded along a path that traverses the cell at 15 meter intervals.

Surface scans of the landfill surface on November 29, 2007, indicate methane leakage from the side slope in the same vicinity as the horizontal piping to Well 2-G9. This is clearly seen in Figure 4-36, which illustrates the results from this surface scan. It seems quite plausible that cracks/fissures might have formed either around this piping or near this area resulting in a fast gas flow path from the landfill surface to Well 2-G9. In combination with spatially variable LFG generation, this preferential flow path might have resulted in high air content and low CH_4 concentrations in 2-G9, and low CH_4 concentrations at other locations in the landfill

To evaluate this hypothesis, a horizontal crack was extended from the soil/biocover layer to near the pancake well in the model domain. The heterogeneous LFG generation rates shown in Figure 4-34 were used for this simulation, and the same peaking power operations were conducted in the model domain as for Case 2.

The results for the Case 3 simulations are shown in Figure 4-35(b). With the addition of the long crack, the LFG generated in Region 3 was partly collected through the crack. Due to this change the upward flow of LFG in Region 3 was reduced, and the permeable layer played a less important role as collection route for LFG. As a result, the oxygen profiles above the permeable layer were no longer uniform, which is quite apparent in Figure 4-35(b).
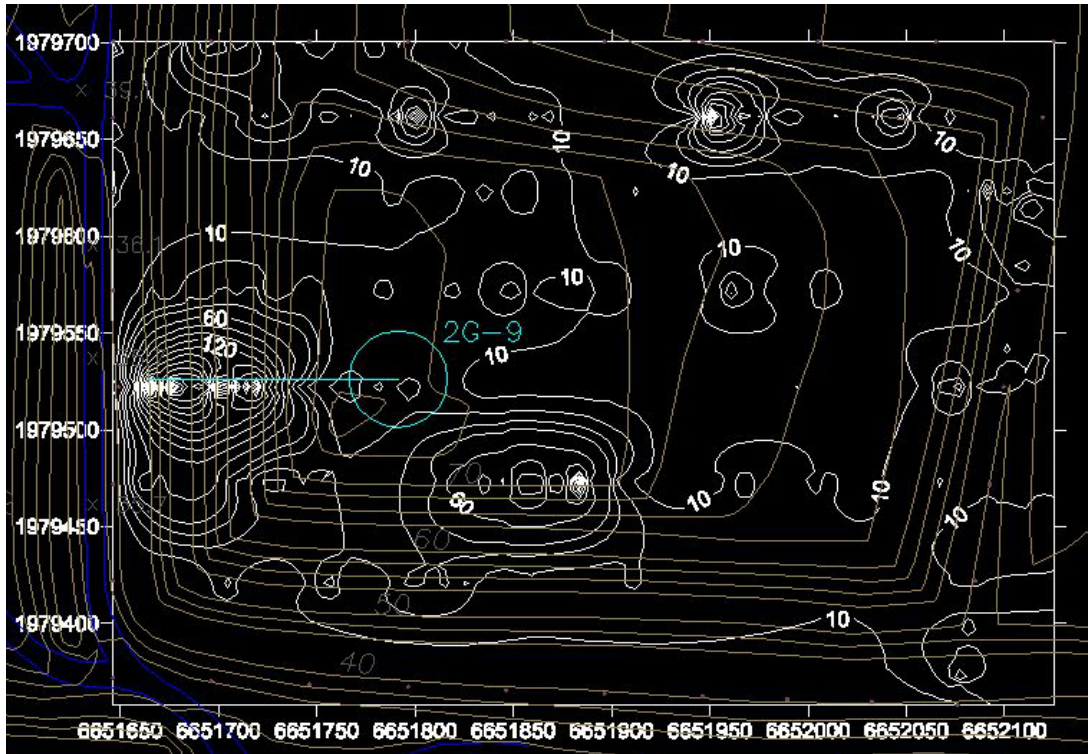
Figure 4-36. Surface scan showing VOC concentrations in ppm along the landfill surface on November 29, 2007. The circle just to the left-of-center in the figure corresponds to well 2G-9, the pancake well. High concentrations near the center of the left boundary suggest leakage where piping enters the side slope.

Photo Credit: Yolo County Planning & Public Works Department

Table 4-30 shows the CH_4 concentrations for the three sampling points for Case 2 (without crack) and Case 3 (with crack) simulations. Clearly, the addition of the long horizontal crack results in lower CH_4 concentrations at all measurement points, with dramatic changes seen for sampling locations 3-08 and 4-07. Here, CH_4 concentrations decrease by 50 percent with the addition of the crack from the landfill surface to pumping well 2-G9. While the CH_4 concentrations in these sampling locations do not match the field data in Table 4-29 exactly, it is apparent that the extension of this crack from the landfill surface to the pancake well will result in dramatic reductions in CH_4 concentrations everywhere. If the crack was made larger and more conductive, the CH_4 concentrations could be reduced even further. The authors postulate that by changing the size of this crack and the spatially variable LFG generation rates, close agreement could be achieved with the field data.

Table 4-30. Gas compositions for simulations with and without crack extending from landfill side to pancake well. Simulations include the spatially variable gas generation rates in Figure 4-33.

Location	24 hour average CH_4 concentration for simulations without crack (%)	24 hour average CH_4 concentration for simulations with crack (%)
3-08[a]	41.0	27.8
4-07	20.5	11.5
4-09	27.6	22.0

a This measurement point is located on Layer 3.

Data collected by Yolo County project team

4.1.20 Discussion

The goal of this subtask was to operate and monitor the performance of the constructed permeable layer and gas extraction system in a landfill with biocover. As part of this task the peaking power cell was operated under the on-peaking and off-peaking mode for several months and the collected data was used to determine the performance of the cell as compared to the predicted computer model. Landfill surface scans were performed and gas composition within the landfill, landfill cover and biocover layers were continuously monitored.

This study shows that the Surface Permeable Layer and Biocover system functioned well in areas with permeable layers. However in areas of the slide slopes below Layer 3, where permeable layers were not constructed landfill surface leaks were discovered where the collected landfill gas was diluted by air through surface leaks. This problem can be mitigated by placing additional cover in these areas or extending the surface permeable layer along the side slopes of the cell to eliminate this problem. Future cell construction will be designed to extend this permeable layer along all side slopes to minimize leaks.

One important limitation of two-dimensional modeling was that it did not describe the behavior of a three-dimensional landfill well. Since a landfill is a non-homogenous mass of refuse with variable moisture content and waste composition it would be very difficult to predict the gas transport behavior and generation rate with any high level of certainty. However, computer models such as the one used in this study provided valuable insight as to what could be expected and gave guidance in the operation of the system to maximize gas collection and reduce surface emissions. Further three-dimensional modeling could improve the predictability of the parameters of interest and provide better modeling results. The field data collected at this landfill site was exhaustive and unique since very few if any other landfills exist in the United States where such detailed data has been collected.

Chapter 5:
Conclusions and Recommendations

5.1   Conclusions

In this study, a peaking power cell was designed, constructed, monitored, and operated at variable extractions by operating on a 12-hour on-off cycle. Computer modeling was used to aid in the design of this project and simulated results were compared with field measurements. It was found that computer simulation results of changing gas composition with depth in the landfill were in excellent agreement with measured trends in the field.

During the diurnal gas extraction, gas output and gas composition were collected and tested from the landfills. Also, gas composition was taken from landfill surface and at different layers within the landfill and close to Surface Permeable Layer and Biocover (SPLAB). Pump tests were conducted to better estimate parameters used for computer modeling. Field data were compared with computer modeling results.

The predicted trends in gas composition were in excellent agreement with measured trends in the field. This suggests that the computer model is a useful tool for evaluating the effects of various operational conditions on peaking power operations. Differences between model predictions and field measurements of methane concentration in the pumping well suggested leakage into the well through side slopes where the surface permeable layer was terminated. This can be mitigated by extending this surface permeable layer on all side slopes.

Field and laboratory experiments were set up to determine methane oxidation rates. In-field static chambers were used to sample emission during rainy and dry seasons. The results of the landfill gas surface emissions testing showed that a maximum oxidation rate of 664.2 gm CH_4/m^2-day was achieved. This average methane oxidation rate is comparable with reported oxidation rates for biocovers and is higher than oxidation rates reported for soil covers. In laboratory columns, methane oxidation decreased as the flux or pressure gradient increased. The methane flux exceeded the oxidation capacity of the system, presumably because there was insufficient retention time in regions where methane and oxygen mixed.

The addition of moisture to the laboratory columns was inhibitory for oxygen diffusion in the compost as evidenced by the reduced oxygen concentrations at depth in the water addition columns. This observation was consistent with the field methane emissions tests where the effect of climate was also significant. In the rainy season tests, there was a statistically significant decrease in methane emissions when the gas system vacuum was increased for the covers with the highest emissions (0.91 m compost + wood chips, 0.31 m compost, soil). In contrast, there was not an increase in methane emissions associated with reduced gas collection system vacuum during the dry season tests.

The results suggest that it would be prudent to operate the gas system to maximize methane collection during periods when then cover soils are saturated with moisture as during this state, CH_4 oxidation will likely be reduced. Further field tests are required to more precisely

determine the extent to which slight reductions in gas collection vacuum may be possible when the cover is saturated.

5.1.1 Commercialization Potential

Peaking power will almost invariably sell at a premium price over "base-load" power that is generated at a constant rate, 24 hours/day. The commercialization and market penetration of LFG fueled peaking power will progress when the premium over baseload power is sufficient to make peaking power from LFG profitable.

Peaking power is defined as power that is dispatchable (capable of being sent out by the LFG to electricity facility) for about 50 percent of each day, year round, at a time that is most convenient for the utility grid to receive it. The premium applies to power generated on this particular part-time schedule.

There are two cases when LFG might be extracted at variable rates to fuel peaking power:

Case 1: When there is surplus generating capacity at the landfill. In the Landfill Gas to Electricity industry experience this is quite common (Augenstein and Pacey 1992). However, data on the "surplus" are anecdotal and it is not clear what fraction of landfills have what is effectively surplus generating capacity, and what fraction of this surplus generating capacity might be realistically tapped.

Case 2: When more generating capacity must be installed specifically to enable peaking. In this case the needed premium over base-load power is highest since it must pay for the excess cost associated with this generation.

The two categories of costs are: (a) Operating (such as extra labor, maintenance etc) and; (b) capital (This is principally the interest and amortization and any desired return on investment of the equipment).

Whether Case 1 or Case 2 is considered above, the total annual operating costs will not change when comparing peaking operation to continuous operation. It is assumed that twice the number of engines or prime movers will operate, but these will operate for only half the 24-hour day. In such a case, total engine operating hours will not change and operating costs per operating hour are not assumed to change materially. In other words, oil changes, consumables, operator costs, etc would remain unchanged (much the case as with motor vehicle engines which starts and stop frequently). The extraction of LFG can be entirely automated as described in earlier reports and should pose no significant additional operational costs. Therefore the extra cost per MWh thus comes back to a very straightforward situation of financing the extra capital costs.

5.1.2 Capital costs

The project team does not attempt to cost out in detail the capital costs of engine-generator sets, as others have more expertise. Instead, the project team relies here on the costs reported by Waste Management, Incorporated (WMI). WMI generates over 600 MWe of electricity from solid waste sites including more than 200 MWe powered by internal combustion (spark-ignited) engines on landfill gas, according to a presentation, "The Energy Value of Landfill Gas", by

Paul Pabor, Vice President, Renewable Energy, Waste Management, Inc. This talk was presented at various symposia including the Recycle Minnesota Symposium in October 2002 and was taken from the website http://www.recycleminnesota.org/2002_conference.htm.

For discussion purposes, Mr. Pabor noted the following parameters for the average or "proxy" landfill gas to energy (LFGTE) Project:

1,600 cubic feet per minute of landfill gas = 400,000 million BTU (mmBTU) per year = 4000 kilowatts of electricity = About 32,000,000 kWh per year

For this size plant: The 2002 capital cost is $3.2 to $5 million ($750 to $1250/kWe). With the cost picture extant in Pabor's analysis in 2002, the total cost to generate power was reported generally in the range of 2.5 to 3.5 c/kWh.

The total cost to generate power consists of these general elements: capital Cost; financing costs; depreciation period; operation and maintenance (O&M) contract; and taxes, administration, permitting.

Costs can vary widely for these items, particularly financing and capital equipment. Thus it is necessary to estimate a range for the necessary premium. An underlying assumption is that base-load electricity from landfill gas is economical with "business as usual" and the premium simply allows the operators of a landfill gas to energy system to make more money.

Another assumption to estimate a "premium" necessary to advance generation of peaking power is that the O&M contract will amount to $0.01 per kilowatt hour. The costs other than O&M (a balance of 1.5 to 2.5 cents/kWh) will increase in proportion from the $800 to $1250/kWh in 2002 to $1,250 to $1,750/kWh in 2008.

The project team estimates that the corresponding capital related costs (financing taxes, permitting) will rise in proportion to the capital cost increase and in addition, about double (reflecting half time power generation). However depreciation per unit power may be somewhat less.

With all of these factors taken into account, it is estimated that the premium necessary to justify peaking power may generally fall between 4.5 and 9 cents/kWh. Although the costs could be broken out in more detail, the summary of cost by Waste Management has the largest experience base in the world, and there are multiple variables.

5.1.3 Economics and Constraints of Other Types of Peaking Plants

Currently, the major resources for peaking electricity are hydro, and natural gas fired plants. There is for practical purposes very little additional (beyond present) near-term hydroelectric potential, either new dams or for pumped storage (Such as Helms). For pumped storage like Helms the cost overruns were in any case severe.

Natural gas peaking plants are mostly older and not very efficient. They consume more natural gas per kWh than the newer combined cycle plants (the combined cycle plants are mostly used for continuous 24 hours/day baseload generation). Due to rise in fuel cost the cost of such natural gas peaking plants are escalating. The availability of natural gas may even become

constraining. The last 12 months' United States' spot (Henry Hub) natural gas price has been near $7/mmBtu and is rising rapidly (March 2008).

Contract prices are most likely to follow spot prices noted above with a one or two year lag. A price of $7/mmBtu sets a fuel-price-alone "floor" under peaking power costs of about $0.07/kWh. Added to generating cost is the incremental cost of incremental plant for peaking. The optimistic projections of natural gas availability and cost of around 2000 (American Petroleum Institute [API], US Geological Survey (USGS), Exxon-Mobil, and others) are being supplanted by dire realities forecast by contrarians (Including Hughes of Canadian Natural Resources, Simmons of Simmons International and Boone Pickens). As to Liquid Natural Gas (LNG) imports, United States terminal construction is blocked. Other countries including Japan and Korea now bid for LNG at landed costs currently over $10/mmbtu and more often around $15/mmBtu. Buyers may be rationed and the Unites States is close to last in line.

Solar photovoltaic systems are a bright spot in the "peaking renewables" picture, but are far short of sufficient. Other peaking options are forestalled by higher costs, environmental constraints, or lack of development. For example, biomass fired plants are too few and may be inconvenient to dispatch to follow need. Battery storage is expensive. Compressed air energy storage needs development and is in any case dependent on natural gas. Flywheels allowing electric energy storage as kinetic energy are developing, but slowly.

An October 2007 Wall Street Journal Article by Rebecca Smith summarizes the industry view that electricity demand is rapidly outpacing new supply (http://online.wsj.com/article/SB119258797074161584.html). The most ominous aspect is that the greatest shortage is seen in peaking plants.

All of the foregoing constraints indicate that the "premium" for peaking power may well be 10 cents or more per kWh, simply reflecting avoided fuel costs. By comparison, natural gas and oil are finite, depleting, and their use to generate electric power may be limited for the electricity sector in the not too distant future.

Though the exact value and market penetration that peaking power will have is necessarily somewhat speculative, it is quite high. Given that the price of oil has topped $100/barrel ($16/mmBtu) and natural gas is currently over $9/mmBtu the best estimate at this point is that 50 percent or more of landfill gas might reasonably be exploited to fuel peaking power. The driving forces include, simply, the need and that fuel cost saving from using landfill gas can economically justify use of this large a fraction of landfill gas for peaking power. For the fairly common cases where other factors (i.e. emission control) are right, and there is surplus generating capacity, the marginal cost for peaking power would be extremely attractive.

In essence, the prospects for peaking LFGTE are good and LFG for peaking power would be a boon to electricity generators and users, but the early stage development must be pursued.

The likely sale price (i.e. premium) for peaking power is likewise subject to a number of variables and factors. The overall conclusion is that the value and purchase price "premium" for peaking power will continue to escalate and is more than adequate to justify peaking landfills.

5.1.4 Recommendations

Yolo County has set up a testing and monitoring section that is unparalleled anywhere else in the world in its capability to test novel and potentially beneficial strategies for landfill gas energy recovery and emission abatement.

The strategies being examined have been applied to "peaking power" for purposes of this project. However the work has much wider value. The measurements and strategies are well suited for the State of California's general objective of landfill methane greenhouse emission control.

The project team recommends additional work that would be valuable to demonstrate the longer term performance and reliability of the peaking approach. This will enable initiation and commercial application with greater confidence by new users.

Although the results from this demonstration project are encouraging, it should be noted that the peaking tests to date have been carried out for a very limited period of time due to the limited project budget. The testing should preferably be extended to a term of years.

The following are recommendations considered important by the project team:

Conduct additional test to increase the ratio of overpull to underpull–Increase the overpull to underpull ratio from 2 to 5 to show the minimal effect on oxygen intrusion or methane emissions. Greater overpull might be used to generate more electricity during daytime hours with minimal effect on methane collection efficiency. Overpull that would lead to a methane content of about 45 percent is the lowest level that is suitable for energy applications.

Vary cycle time for extraction profile–The extraction cycle operated to date has been 12 hours on-12 hours off using an overpull to underpull ratio of 2. While this operational period is representative for weekday operations, can landfill gas be stored (to some extent) during weekends and delivered for use during weekdays?

Test efficacy of greenhouse gas control–Given California's recognition of the importance of climate problems, an objective of equal importance to "peaking" is controlling greenhouse (methane) emissions. Two categories of greenhouse emissions observed in the tests at Yolo are top cover emissions and dealing with "hot spots." Top cover emissions were small while emissions from "hot spots" outside of the influence of the SPLAB were significant, but still under the maximum allowable by the U.S. EPA.

Continue novel in-situ gas composition and pressure measurements–The combination of interior gas composition measurements and flow measurements within the waste are unique to this experimental investigation. The authors recommend that these very informative and valuable measurements be continued. The in-situ gas composition measurements have proven extremely helpful in tracking how interior gas compositions and emissions respond to changes in extraction rate and also barometric pressure. In-situ pressure measurements thus far have been revealing and are integral in the flow modeling process.

Continue modeling–The modeling thus far by the University of Delaware, with assistance from Hydro Geo Chem., Inc., has proven to be extremely helpful. In fact the value of the modeling cannot be overstated. The modeling results can be refined and verified as more field data are obtained. Not only will the modeling permit better understanding and "zeroing in" on best possible designs, but the models will be usable worldwide in the future by landfills desiring to conduct either peaking or gas control.

Continue advanced automation strategies–A very significant aspect of the project has been its very successful automation. The amenability of the peaking process thus far to automation indicates that automation can minimize the labor required to operate the system, and for this experimental project, to take data. Experience with peaking and gas flow control and automated sampling indicates two things: (1) Peaking operation and its monitoring need not impose an undue or extra burden compared to conventional landfill operation and (2) The automation of landfill operations, in combination with better design may generally allow more efficient greenhouse emission control at less cost than now experienced by landfills. All of the experience and strategies being developed with respect to automation are extraordinarily valuable and should be continued.

Optimize biocover designs–Further work is appropriate to optimize the composition of biocovers to balance porosity and infiltration capacity with the potential for emissions associated with cracks. In laboratory column experiments, evidence of decreasing methane oxidation capacity was observed at higher pressure gradients. Further research should be performed to characterize this effect through modeling. The effects of gas flow rate, compost moisture content, retention time, and compost porosity should be addressed in the modeling to optimize cover design.

5.1.5 Benefits to California

California's renewable portfolio standard mandates increasing amounts of electricity derived from renewable resources in the electrical generation mix. The peaking landfill would be an exceptionally attractive way to meet the increasing need for renewable electricity in the renewable portfolio standard. In addition, in the United States in general and California specifically, the general energy situation is seen by many experts as becoming increasingly precarious in terms of oil and natural gas reserves. To the extent possible, California electricity is generated within the state, however a major fraction of California power, above 40 percent, is natural gas fueled (Energy Commission data for 2006). The natural gas fired generation may be subject to increasing fuel costs and constraints.

Projections of future power demand and time-of day load profiles are necessarily uncertain but estimates of these are still helpful in evaluating benefits. Based on the above and information on the Energy Commission website, and the authors presume here that total time-averaged California electricity year-round will average about 35,000 MWe in 2012. Profiles in summer are assumed to have an estimated peak demand reaching an average of 50,000 MWe for 3 months in summer daytime (25,000 nighttime minimum) and 45,000 daytime load (still 25,000 nighttime minimum) in the nine months of off-peak use. Any power source that supplements peak use

will basically supplement other peaking options such as hydropower, conserving and extending this valuable resource.

5.1.6 Avoidance of Transmission Constraints

In California, another severe constraining factor in meeting peak load has been congestion of the long distance transmission system. The grid congestion is greatest at times of peak load. In fact, during the rolling blackouts of 2000-2001, peaking power was often available but could not be distributed because of grid congestion.

A virtue of supplemental peaking power from landfill gas is that landfills are by and large distributed generation systems. The landfill gas fueled power enters the transmission grid near the populated areas that use the electricity. Thus landfill gas peaking power lessens electricity grid congestion and also, assures the highest fractional delivery of the "busbar" electricity to customers by avoiding transmission resistance losses. It is not possible at this point to quantify monetary value of this benefit, except to say that it is significant.

5.1.7 Contribution of Peaking Landfill Gas to Electricity Generation

Based on information in the section on commercialization potential, and the presumption that economics are favorable, the authors make the judgment that methane from about 50 percent of waste placed in California's landfills might be recovered at variable rates to fuel peaking power. It is then possible to use California's official waste statistics and methane yield based on experience to determine how much "peaking power" might be derived from California's municipal waste.

Based on California Integrated Waste Management website, California's landfilled waste tonnage for 2006 was about 42 million tons. Assuming that the recovery yield of methane with use of the highly efficient permeable layer will be 3,000 cubic feet per ton of "gate waste" as received at the landfill and that the heat rate of the GenSet prime mover is 12,000 Btu/kWh, it is estimated that each ton of waste can fuel 0.25 MWh (250 kWh) or 4 tons of waste would yield one MWh.

If half of California's landfills were to elect to operate in peaking power mode, the total amount of power that can be generated in California from 20 million tons of waste is 5 million MWh (5000 GWh). Assuming the recovery of this power over half days throughout the year, (4380 hours/year) the contribution of the "peaking landfill" is 1141 MW or about 1100 MWe. While this comprises a relatively small number in the mix of total generation this would provide over 10 percent of the daytime excess of power requirement over minimum nighttime use. This is enough daytime power increment to satisfy the total electrical needs of 4 million Californians (out of a population near 40 million in 2012).

5.1.8 Economic benefits

Economic benefits are difficult to determine because of the wide distribution of site characteristics and circumstances of individual landfills. The values of gross revenue from peaking power if sale price were: a) 10 cents/kWh ($100/MWh) and b) 15centskWh (150/MWh). are straightforwardly calculated as $500 million and $750 million per year for California, respectively.

5.1.9 Methane GHG Emission Avoidance

Other things being equal, the fueling of peaking power, relative to constant rate baseload generation, might not have much of an effect "up or down" on greenhouse gas emissions. The natural gas fueled peaking plants tend to be older and less efficient, so the avoided CO_2 emissions from substituting LFG fueled peaking power for natural gas fueled peaking plants would be better than its substitution for conventional baseload power. Offsetting this is the fact that the peaking approach might lead to some limited, additional CO_2 emission relative to constant-rate baseload power generation. The modeling and field data from this project shows that peaking may increase the incremental emissions but the biocover used will eliminate this increase in methane emissions relative to conventional generation.

The most promising for abatement of greenhouse gases is the overall design incorporating permeable layers. Based on modeling and field measurements the permeable layers can reduce emissions whether the extraction is for conventional baseload power or for peaking. Thus the permeable layer itself is worth pursuing on its own merits independent from peaking power.

REFERENCES

Abichou, T.; Chanton, J.; Powelson, D.; Fleiger, J.; Escoriaza, S.; Lei, Y.; Stern, J. 2006 (a). Methane flux and oxidation at two types of intermediate landfill covers. *Waste Management* 26 (11):1305-1312.

Abichou, T.; Powelson, D.; Chanton, J.; Escoriaza, S.; Stern, J. 2006 (b). Characterization of methane flux and oxidation at a solid waste landfill. *Journal of Environmental Engineering* 132 (2):220-228.

API Division of Refining. 1977. *Technical Data Book, Petroleum Refining*. Washington: American Petroleum Institute, Refining Department.

Augenstein, D. 1992. The Greenhouse Effect and US Landfill Methane. Global Environmental Change. 2(4): 311-328.

Augenstein, D. 1999. Landfill Operation for Carbon Sequestration and Maximum Methane Emission Control. Cost effectiveness and potential: Controlled landfilling for greenhouse gas abatement. Institute for Environmental Management (IEM). Final Report on Contract DE-AC26 98FT40422 to National Energy Technology Laboratory, U.S. Department of Energy, Pittsburgh, PA.

Augenstein, D., Yazdani, R., Moore, R. and K. Dahl. 1998. Yolo County Controlled Landfill Project. Proceedings, California Integrated Waste Management Board (CIWMB) Symposium on Landfill Gas Assessment and Management April 8-9 1998.

Augenstein, D., Wise, D.L, Wentworth, R.L., and C.L.Cooney. 1976. Fuel Gas Recovery from Controlled Landfilling of Municipal Waste. Resource Recovery and Conservation. 2(2): 103-117.

Barlaz, M. A.; Green, R. B.; Chanton, J. P.; Goldsmith, C. D.; Hater, G. R. (2004). "Evaluation of a biologically active cover for mitigation of landfill gas emissions." Environmental Science & Technology 38, (18), 4891-4899.

Bergamaschi, P.; Lubina, C.; Konigstedt, R.; Fischer, H.; Veltkamp, A. C.; Zwaagstra, O. (1998). "Stable isotopic signatures (delta C-13, delta D) of methane from European landfill sites." Journal of Geophysical Research-Atmospheres 103, (D7), 8251-8265.

Berger, J.; Fornes, L. V.; Ott, C.; Jager, J.; Wawra, B.; Zanke, U. (2005). "Methane oxidation in a landfill cover with capillary barrier." Waste Management 25, (4), 369-373.

Bird, R., Stewart, W.E. and Lightfoot, E.N. (1960). "Transport phenomena." John Wiley & Sons, New York, NY

Bogner, J.; Spokas, K. (1993). "Landfill CH4 - rates, fates, and role in global carbon-cycle." Chemosphere 26, (1-4), 369-386.

Borjesson, G.; Chanton, J.; Svensson, B. H. (2001). "Methane oxidation in two Swedish landfill covers measured with carbon-13 to carbon-12 isotope ratios." Journal of Environmental Quality 30, (2), 369-376.

Borjesson, G.; Svensson, B. H. (1997). "Effects of a gas extraction interruption on emissions of methane and carbon dioxide from a landfill, and on methane oxidation in the cover soil." Journal of Environmental Quality 26, (4), 1182-1190.

Borjesson, G.; Svensson, B. H. (1997). "Seasonal and diurnal methane emissions from a landfill and their regulation by methane oxidation." Waste Management & Research 15, (1), 33-54.

California Regional Water Quality Control Board, Central Valley Region. 2000. Waste Discharge Requirements for the Yolo County Central Landfill. No. 5-00-134.

Carson, D. and R. Green. 2003. title. Proceedings of U.S. EPA Workshop on Bioreactor Landfills. Arlington, VA.

Chanton, J. P.; Rutkowski, C. M.; Mosher, B. (1999). "Quantifying methane oxidation from landfills using stable isotope analysis of downwind plumes." Environmental Science & Technology 33, (21), 3755-3760.

Chanton, J.; Liptay, K. (2000). "Seasonal variation in methane oxidation in a landfill cover soil as determined by an in situ stable isotope technique." Global Biogeochemical Cycles 14, (1), 51-60.

Chen, Y. C., Chen, K. S., and Wu, C. H. (2003). "Numerical simulation of gas flow around a passive vent in a sanitary landfill." Journal of Hazardous Materials B100, 39-52.

Colberg, P. 1988. Anaerobic microbial degradation of cellulose, lignin, oligolignols, and monoaromatic lignin derivatives. In A.J.B. Zehnder (ed.), Biology of Anaerobic Microorganisms. John Wiley & Sons. New York.

Corey, A. T. (1954). "The interrelation between gas and oil relative permeabilities." Producers Monthly, November, 38-41.

Croft, B. and T. Fawcett. 1993. Landfill Gas Enhancement Studies – The Brogborough Test Cells ETSU B/B5/00080/REP. Final Report, Environmental Safety Center.

Czepiel, P.M., Shorter, J.H., Mosher, B., Allwine, E., McManus, J.B., Harriss, R.C., Kolb, C.E. and Lamb, B.K. (2003). "The influence of atmospheric pressure on landfill methane emissions." Waste Management 23, 593-598.

De Baere, L. 2004. State of the Art of Anaerobic Digestion. International Conference on Anaerobic Digestion, Montreal, Canada.

Das, K., and Keener, H. M. (1997). "Moisture effect on compaction and permeability in composts" J. Environ. Eng. 123(3), 275-281.

Davis, M. W. (1998). "A rapid modified method for compositional carbohydrate analysis of lignocellulosics by high pH anion-exchange chromatography with pulsed amperometric detection (HPAEC/PAD)." Journal of Wood Chemistry and Technology 18, (2), 235-252.

Eleazer, W. E.; Odle, W. S.; Wang, Y. S.; Barlaz, M. A. (1997). "Biodegradability of municipal solid waste components in laboratory-scale landfills." Environmental Science & Technology 31, (3), 911-917.

EMCON Associates. 1975. Results of Sonoma County Stabilization Project. Report for the U.S. Environmental Protection Agency, Washington, DC.

EMCON Associates. 1987. Final Report on the Mountain View Controlled Landfill Demonstration Project, Mountain View, CA. Available from National Technical Information Service.

EMCON Associates and J. Pacey. 1985. Controlled Landfill Project: Mountain View, California. Fifth Annual Report available from National Technical Information Service.

Falta, R.W., Pruess, K., Finsterle, S. and Battistelli, A. (1995). T2VOC User's Guide, Lawrence Berkeley Laboratory Report LBL-36400. Lawrence Berkeley National Laboratory, Berkeley, CA

Fen, C.S. and Abriola, L.M. (2004). "A comparison of mathematical model formulations for organic vapor transport in porous media." Advances in Water Resources 27, 1005-1016.

Giroud, J.P. and R. Bonaparte, R. 1989. Leakage Through Liners Constructed With Geomembranes – Part I. Geomembrane Liners. Geotextile and Geomembranes. 8(1): 27-67.

Golder Associates. 1999. Final Report, Construction Quality Assurance, Yolo County Central Landfill, WMU 6, Module D, Phase 1 Expansion. Report for Yolo County.

Hilger, H. A.; Wollum, A. G.; Barlaz, M. A. (2000). "Landfill methane oxidation response to vegetation, fertilization, and liming." Journal of Environmental Quality, 29, (1), 324-334.

Humer, M.; Lechner, P. (2001). "Design of a Landfill cover layer to enhance methane oxidation-results of a two year field investigation." In Eighth International Waste Management and Landfill Symposium, Cagliari, Italy.

Humer, M.; Lechner, P. (1999). "Methane oxidation in compost cover layers on Landfills." In Seventh International Waste Management and Landfill Symposium, Cagliari, Italy.

IPCC (2001). Intergovernmental Panel on Climate Change, Climate Change 2001: The Scientific Basis, Cambridge University Press, United Kingdom.

Jain, P., Powell, J., Townsend, T.G and Reinhart, D.R. (2005). "Air permeability of waste in a municipal solid waste landfill." Journal of Environmental Engineering-Asce 131, 1565-1573.

Jones, H. A.; Nedwell, D. B. (1993). Methane Emission And Methane Oxidation In Land-Fill Cover Soil FEMS Microbiology Ecology 102, (3-4), 185-195.

Jones, H. A.; Nedwell, D. B. (1990). "Soil atmosphere concentration profiles and methane emission rates in the restoration covers above landfill sites-equipment and preliminary-results." Waste Management & Research, 8, (1), 21-31.

Jung, Y. and Imhoff, P.T., Influence of high-permeability layer on methane emission and air intrusion at bioreactor landfills, in preparation.

Jung, Y., Imhoff, P. T., Augenstein, D. C., R. Yazdani (2007). "Influence of high-permeability layers for enhancing landfill gas capture and reducing fugitive methane emissions from landfills." submitted to Journal of Environmental Engineering.

175

Kightley, D.; Nedwell, D. B.; Cooper, M. (1995). "Capacity for methane oxidation in landfill cover soils measured in laboratory-scale soil microcosms." Applied and Environmental Microbiology 61, (2), 592-601.

Kjeldsen, P.; Dalager, A.; Broholm, K. (1997). "Attenuation of methane and nonmethane organic compunds in landfill gas affected soils." J. of Air Waste Management Association 47, 1268-1275.

Klinkenberg, L.J. (1941). "The permeability of porous media to liquids and gases." in API Drilling and Production Practice, 200-213.

Kunz, C. O., and Lu, A. H. (1980). "Methane production rate studies and gas flow modeling for the Fresh Kills Landfill." New York State Energy Res. & Dev. Admin. Rep. No. 80-21., N. Y. State Dep. Of Health, Div. of Lab. And res., Albany, NY.

Leckie, J. and J. Pacey. 1979. Landfill Management with Moisture Control. Journal of the Environmental Engineering Division, ASCE. 105(2): 337-355.

Liptay, K.; Chanton, J.; Czepiel, P.; Mosher, B., (1998). "Use of stable isotopes to determine methane oxidation in landfill cover soils." Journal of Geophysical Research-Atmospheres 103, (D7), 8243-8250.

Moore, R., Dahl, K., and R. Yazdani. 1997. Hydraulic Characteristics of Municipal Solid Waste Findings of the Yolo County Bioreactor Landfill Project. Thirteenth International Conference on Solid Waste Technology and Management, Philadelphia, PA.

Mualem, Y. A. (1976). "A new model for predicting the hydraulic conductivity of unsaturated porous media." Water Resour. Res., 12(3), 513-522.

O'Leary, P. and Walsh, P. (1991). "Landfill gas movement, control, and uses." Waste Age, 114, 114-124.

Oonk, H. and H. Woelders. 2000. Full-scale demonstration of treatment of mechanically separated organic residue in a bioreactor at VAM. Wijster Waste Management and Research. 17(2): 535.

Pacey, J. 1987. title. SWANA Gas Conference Proceedings.

Poulsen, T.G., Christophersen, M., Moldrup, P., and Kjeldsen, P. (2003). "Relating landfill gas emissions to atmospheric pressure using numerical modelling and state-space analysis." Waste Management & Research 21, 356-366.

Pruess, K. and Battistelli, A. (2002). "TMVOC, A numerical simulator for three-phase non-isothermal flows of multicomponent hydrocarbon mixtures in saturated-unsaturated heterogeneous media." Report LBNL-49375, Lawrence Berkeley National Laboratory, Berkeley, CA.

Pruess, K., Oldenburg, C., and Moridis, G. (1999). "TOUGH2 User's Guide, Version 2.0." Report LBNL-43134, Lawrence Berkeley National Laboratory Berkeley, CA.

Qian, X., Koerner, R. M., and Gray, D. H. (2002). "Geotechnical aspects of landfill design and construction." Prentice Hall, Upper Saddle River, New Jersey.

Reinhart, D. and T. Townsend. 1997. Landfill Bioreactor Design and Operation. Lewis Publishing. New York, NY.

Reinhart, D., Pradeep, J., Townsend, T., and J. Arnold. 2004. Update on New River Bioreactor Landfill Demonstration. SWANA Landfill Symposium, Monterey, CA.

Romm, E. S. (1966). Flow characteristics of fractured rocks (in Russian), Nedra, Moscow.

van Genuchten, M. T. (1980). "A closed-form equation for predicting the hydraulic conductivity of unsaturated soils." Soil Sci. Soc. Am. J., 44, 892-898.

Schuetz, C.; Bogner, J.; Chanton, J.; Blake, D.; Morcet, M.; Kjeldsen, P. (2003). "Comparative oxidation and net emissions of methane and selected non-methane organic compounds in landfill cover soils." Environmental Science & Technology 37, (22), 5150-5158.

Stein V.B.: Hettiaratchi J.P.A. (2000). "Methane oxidation in three Alberta soils: Influence of soil parameters and methane flux rates." Environmental Technology 22, (1), 101 – 111.

Tchobanoglous, G., H. Theisen, and S. Vigil. 1993. Integrated Solid Waste Management: Engineering Principle and Management Issues. Irwin/McGraw-Hill. New York. pp: 418-420.

U.S. EPA. 1997. Statistics for Waste Management in the United States: Summary for the Year.

U.S. EPA (2003). Inventory of U.S. Greenhouse Gas Emissions and Sinks: 1990-2001, U.S. Environmental Protection Agency, Washington, DC.

Van Genuchten, M. Th. (1980). "A closed-form equation for predicting the hydraulic conductivity of unsaturated soils." Soil Sci. Soc. Am. J., 44, 892-898.

Vasuki, N. 1993. Practical Experiences with Landfill Leachate Recirculation in Pilot and Field Scale Units. 31st Annual International Solid Waste Exposition, SWANA.

Vector Engineering. 2001. Design Report for the Surface Liners of the Module D Phase 1 Bioreactors at the Yolo County Central Landfill. Report for Yolo County.

Verma, S. 2002. Anaerobic Digestion of Municipal Solid Waste Organic to Methane, M. S. Thesis. Columbia University. New York.

Vogt, G. and D. Augenstein. 1996. Comparison of Models for Predicting Methane Recovery from Landfills. Solid Waste Association of North America and U.S. Department of Energy.

Vogt, G. and D. Augenstein. 1997. A Comparison of Landfill Methane Recovery Models. Prepared for the Solid Waste Association of North America (SWANA) and the National Renewable Energy Laboratory (NREL) of the USDOE.

Warith, M.A., Evgin, E., and Benson, P.A.S. (2004). Suitability of shredded tires for use in landfill leachate collection systems. Waste Management 24, 967-979.

Wu, J. S. (1999). "Methanotrophic activities in tropical landfill cover soils: effects of temperature, moisture content and methane concentration." Waste Management & Research 17, (4), 313-323.

Yazdani, R. 1997. Methane Enhancement by Accelerated Anaerobic Composting at the Yolo County Central Landfill. Report to the California Energy Commission Sacramento, CA.

Yazdani, R. 2003. Yolo County Accelerated Anaerobic And Aerobic Composting (bioreactor) -- EPA Project XL. EPA Workshop on Bioreactor Landfills, Arlington, VA.

Yazdani, R. and D. Augenstein. 2001. U. S. EPA Project XL: Yolo County's Accelerated Anaerobic and Aerobic Composting (Full-scale Controlled Landfill Bioreactor) Project. SWANA Annual Landfill Symposium. San Diego, CA.

Yazdani, R., Moore, R., Dahl, K. and D. Augenstein. 1998. Yolo County Controlled Landfill Bioreactor Project. Yolo County Public Works and I E M, Inc. report to the Urban Consortium Energy Task Force and the Western Regional Biomass Energy.

Yildiz, E.D., Ünlü, K., and Rowe, R.K. (2004). Modeling leachate quality and quantity in municipal solid waste landfills. Waste Management & Research 22, 78-92.

Zison, S.W. (1984). "Landfill gas recovery method." U.S. Patent 4,442,901

GLOSSARY

API	American Petroleum Institute
C	Celsius
CH:L	cellulose + hemicellulose to lignin ratio
CH4	Methane
CIMIS	California Irrigation Management Information System
Cm	Centimeter
CO2	Carbon Dioxide
DWR	Department of Water Resources
FID	Flame Ionization Detector
Ft	Feet/foot
GC	Gas Chromatograph
GEM 2000	LandTec Landfill Gas Estraction Monitor 2000
GW	Gigawatt
GWe	Gigawatts of energy
H2O	Water
H_2SO_4	Sulfuric Acid
HDPE	High Density Polyethylene
kW	Kilowatt
kWh	Kilowatt-hour
LBNL	Lawrence Berkeley National Laboratory
LFG	Landfill Gas
LFGTE	Landfill Gas to Energy
LNG	Liquid Natural Gas
M	Meter
mL	Milliliter
MSW	Municipal Solid Waste
MW	Megawatt
MWe	Megawatts of energy
MWh	Megawatt-hour
NAPLs	non-aqueous phase liquids

NOAA	National Oceanic and Atmospheric Administration
NOx	Nitrous Oxide
O&M	Operations & Maintenance
O2	Oxygen
PIER	Public Interest Energy Research
Ppm	Parts Per Million
PVC	Polyvinyl Chloride
SCFM	Standard Cubic Feet per Minute
SD	Standard Deviation
SMUD	Sacramento Municipal Utility District
SPLAB	Surface Permeable Layer and Biocover
STP	Standard Temperature and Pressure
TCD	Thermal Conductivity Detector
TOUGH2	Transport of Unsaturated Groundwater and Heat
U.S. DOE	United States Department of Energy
U.S. EPA	United States Environmental Protection Agency
USGS	United States Geological Survey
VICI	Valco Instruments Co. Inc.
VOC	Volatile Organic Compound
WMI	Waste Management Incorporated

Appendix A

Yolo County Central Landfill **SMUD Re-GEN Program**

Peaking Power Project As-Built Plans

S:\PM\AutoCAD\Peaking Power Topo-as built\instrumentsonly_with_details.dwg   3-19-06   09:56:09 AM   kstead

YOLO COUNTY CENTRAL LANDFILL
WASTE MANAGEMENT UNIT 6, MODULE D PHASE 2
YOLO COUNTY, CALIFORNIA

SMUD RE-GEN PROGRAM
PEAKING POWER PROJECT

SHEET NO.	TITLE
1	COVER
2	BASE LINER INSTRUMENTATION
3	LAYER 1 PIPING AND INSTRUMENTATION
4	LAYER 2 PIPING AND INSTRUMENTATION
5	LAYER 3 PIPING AND INSTRUMENTATION
6	LAYER 4 INSTRUMENTATION AND BIOCOVER

AS BUILT PLANS

SOLANO COUNTY

DAVIS

SOLANO

SACRAMENTO COUNTY

WEST SACRAMENTO

SITE

LOCATION MAP

YOLO COUNTY

DEPARTMENT APPROVAL

DESIGN ENGINEER
R.C.E. NO.

DATE

	BY	DATE
DESIGN	RY	03/22/2006
DRAWN	MW,KS,JK	03/22/2006
SCALE: NONE		

YOLO COUNTY CENTRAL LANDFILL
SMUD Re – Gen Program
PEAKING POWER PROJECT
COVER

YOLO COUNTY
Department of Planning and Public Works
292 West Beamer Street
Woodland, 95695–2598
Phone: (530) 666–8775   FAX: (530) 666–8728

SHEET No. 1

PROJECT
YOLO COUNTY CENTRAL LANDFILL
SMUD Re – Gen Program

SHEET 1 OF 6

PEAKING POWER PROJECT

AS BUILT PLANS

SCALE: 1" = 50'

INSTRUMENTATION SUMMARY

DESCRIPTION	NORTHING	EASTING	ELEVATION
B-01	1979968	6651699	31.4
B-02	1979968	6651885	26.6
B-03	1979968	6652116	31.4
B-04	1979968	6652303	26.6
B-05	1979709	6651899	31.4
B-06	1979709	6651885	26.6
B-07	1979709	6652116	31.4
B-08	1979709	6652302	26.6
B-09	1979450	6651699	31.4
B-10	1979450	6651865	26.6
B-11	1979450	6652116	31.4
B-12	1979450	6652301	26.6

All base layer locations have a bare thermister, a PVC moisture sensor, and a tube.
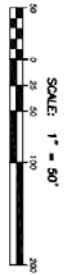
LEGEND

B-01 ✕ BASE LAYER INSTRUMENT LOCATION

THERMISTER (QUALITY THERMISTER, 10,000 OHM RESISTANCE AT 25°C TOLERANCE ±0.2°C) SHIELDED TUBE, 1/4 INCH DIA BY 36 DEG LONG, AND PVC MOISTURE SENSOR.

YOLO COUNTY CENTRAL LANDFILL
SMUD Re-Gen Program
PEAKING POWER PROJECT
BASE LINER INSTRUMENTATION

YOLO COUNTY
PLANNING AND PUBLIC WORKS
DIVISION OF INTEGRATED WASTE MANAGEMENT
292 West Beamer Street
Woodland, CA 95695-2598
Phone: (530) 666-8852   FAX: (530) 666-8853

DESIGN BY	RY	03/22/2006
DRAWN BY	MW,KS,JK	03/22/2006
CHECK BY	RY	03/22/2006

SCALE: 1" = 50'

REVISIONS

SHEET NUMBER 2

YOLO COUNTY CENTRAL LANDFILL
SMUD Re-Gen Program

PEAKING POWER PROJECT

AS BUILT PLANS

INSTRUMENTATION SUMMARY

DESCRIPTION	NORTHING	EASTING	ELEVATION	COMMENTS
1-01	1980050	6651698	41.0	No conduit or tube.
1-02	1980090	6651838	43.0	No conduit or tube.
1-03	1980017	6651710	40.0	No conduit or tube.
1-04	1980015	6651765	41.0	No conduit or tube.
1-05	1979913	6651669	38.0	No conduit or tube. Extra thermistor.
1-06	1979905	6651768	40.0	No conduit or tube. Extra thermistor.
1-07	1979897	6651898	41.0	No conduit or tube.
1-08	1979889	6651888	42.0	No conduit or tube.
1-09	1979824	6651667	41.0	No conduit or tube.
1-10	1979812	6651768	42.0	No conduit or tube.
1-11	1979801	6651898	43.0	No conduit or tube.
1-12	1979746	6651664	40.0	No conduit or tube.
1-13	1979737	6651764	41.0	No conduit, Extra thermistor.
1-14	1979726	6651863	42.0	No conduit or tube.
1-15	1979669	6651660	41.0	Silicone.
1-16	1979660	6651760	41.0	Silicone, No tube.
1-17	1979649	6651849	42.0	Silicone, Extra thermistor.

DESCRIPTION	NORTHING	EASTING	ELEVATION	COMMENTS
1-18	1979579	6651980	40.0	Silicone, No tube.
1-19	1979571	6651769	40.0	Silicone.
1-20	1979563	6651849	41.0	Silicone, Extra thermistor.
1-21	1979504	6651980	40.0	Silicone.
1-22	1979486	6651770	40.0	Silicone.
1-23	1979489	6651850	40.0	Silicone.
1-24	1979418	6651685	40.0	Silicone.
1-25	1979414	6651775	40.0	Silicone.
1-26	1979411	6651865	41.0	Silicone.
1-27	1979450	6652141	41.0	Silicone.
1-28	1979444	6652218	41.0	Silicone.
1-29	1979444	6652287	41.0	Silicone.
1-30	1979508	6652144	42.0	Silicone.
1-31	1979528	6652218	42.0	Silicone.
1-32	1979528	6652291	42.0	Silicone.
1-33	1979616	6652240	45.0	Silicone.
1-34	1979603	6652294	45.0	Silicone.

DESCRIPTION	NORTHING	EASTING	ELEVATION	COMMENTS
1-35	1979707	6652256	44.0	Silicone.
1-36	1979685	6652304	44.0	Silicone.
1-37	1979783	6652259	43.0	Silicone.
1-38	1979764	6652305	44.0	Silicone.
1-39	1979874	6652224	43.0	Silicone.
1-40	1979869	6652291	42.0	Silicone.
1-41	1980004	6652228	43.0	Silicone.
1-42	1980002	6652298	44.0	Silicone.
1-43	1979846	6652261	44.0	Silicone.
1-44	1979822	6652133	43.0	Silicone.
1-45	1979727	6652103	43.0	Silicone.
1-46	1979789	6652189	43.0	Silicone.
1-47	1979603	6652064	43.0	Silicone.
1-48	1979489	6652064	42.1	Silicone.
1-49	1979419	6652068	40.6	Silicone.
1-50	1980063	6652217	46.0	Silicone.
1-51	1980063	6652794	44.0	Silicone.

Unless otherwise noted, all layer 1 locations include conduit with a bare thermistor, a PVC metallic sensor, and a tube. "Silicone" refers to a silicone protected thermister.

LEGEND

HORIZONTAL GAS COLLECTION PIPE

HORIZONTAL LEACHATE INJECTION PIPE, LOW 30, SDR 11 HDPE WITH 1/8" DIA HOLES @ 10' OC

SCALE: 1" = 30'

SITE

YOLO COUNTY CENTRAL LANDFILL
SMUD Re-Gen Program
PEAKING POWER PROJECT
LAYER 1 PIPING AND INSTRUMENTATION

YOLO COUNTY
PLANNING AND PUBLIC WORKS
DIVISION OF INTEGRATED WASTE MANAGEMENT
292 West Beamer Street
Woodland, CA 95695-2598
Phone: (530) 666-8852   FAX: (530) 666-8853

DESIGN BY RY	03/22/2006	
DRAWN BY MW,KS,JK	03/22/2006	
CHECK BY RY	03/22/2006	

SCALE: 1" = 30'

SHEET NUMBER 3

A-4

LEGEND

HORIZONTAL GAS COLLECTION LINE

HORIZONTAL LEACHATE INJECTION LINE, CSP 2, SDR 11 HDPE WITH 1/2" OR DRILLED HOLES @ 18" O/C.

INSTRUMENT LOCATION #

THERMISTOR QUALITY THERMISTOR WIRE PROBE, 10,000 OHM RESISTANCE AT 25°C, TOLERANCE ±0.2°C (±0.36°F), THERMISTOR SENSING TUBE THREADED BY 3/4" OD LLDPE, AND PVC MOISTURE SENSOR.

2-01   LEVEL 2 INSTRUMENT LOCATION #

2-L-P2W   LEVEL 2, LEACHATE INJECTION LINE 1, PHASE 2 MODULE, WEST END

2-G1-P2W   LEVEL 2, GAS EXTRACTION LINE 1, PHASE 2 MODULE, WEST END

SCALE: 1" = 30'

30 0 15 30 60 120

PEAKING POWER PROJECT

2-G7-P2W

2-G8-P2W (VERTICAL WELL)

2-G9-P2W (PANCAKE WELL)

2-G10-P2W (VERTICAL WELL)

2-L4-P2W

2-L5-P2W

4" THICK LAYER OF SHREDDED TIRES. LARGE/WHOLE TIRES PLACED AROUND PERIMETER

8" HDPE Gas Header Pipe

AS BUILT PLANS

INSTRUMENTATION SUMMARY

DESCRIPTION	NORTHING	EASTING	ELEVATION	DESCRIPTION	NORTHING	EASTING	ELEVATION
2-01	1962248	6651765	71.0	2-17	1979792	6651834	53.0
2-02	1962236	6651849	68.0	2-18	1979731	6651714	48.0
2-03	1962115	6651734	52.0	2-19	1979725	6651769	50.0
2-04	1960111	6651824	54.0	2-20	1979720	6651824	50.0
2-05	1960107	6651904	56.0	2-21	1979625	6651724	49.5
2-06	1960052	6651735	54.0	2-22	1979614	6651805	52.0
2-07	1960043	6651825	56.0	2-23	1979625	6651685	53.7
2-08	1960036	6651905	56.0	2-24	1979535	6651724	53.2
2-09	1979971	6651737	52.0	2-25	1979627	6651804	52.0
2-10	1978657	6651826	52.0	2-26	1979618	6651616	53.5
2-11	1978645	6651965	54.0	2-27	1979460	6651724	50.5
2-12	1978886	6651734	51.0	2-28	1979453	6651802	52.2
2-13	1978806	6651814	52.0	2-29	1979446	6651883	53.2
2-14	1978877	6651883	54.0	2-30	1979698	6651665	54.5
2-15	1979799	6651724	48.0	2-31	1979611	6651664	54.4
2-16	1979796	6651779	50.0	2-32	1979439	6651662	54.0

All layer 2 locations include a thermister in silicone, a PVC moisture sensor, and a tube. 2-32 was covered with tires, not waste.

YOLO COUNTY CENTRAL LANDFILL
SMUD Re-Gen Program
PEAKING POWER PROJECT
LAYER 2 PIPING AND INSTRUMENTATION

YOLO COUNTY
PLANNING AND PUBLIC WORKS
DIVISION OF INTEGRATED WASTE MANAGEMENT
292 West Beamer Street
Woodland, CA 95695-2598
Phone: (530) 666-8852   FAX: (530) 666-8853

DESIGN BY	RY	03/22/2006
DRAWN BY	MW,KS,JK	03/22/2006
CHECK BY	RY	03/22/2006

SCALE: 1" = 30'

REVISIONS

PROJECT
YOLO COUNTY CENTRAL LANDFILL
SMUD Re-Gen Program

SHEET NUMBER
4

SHEET 4 OF 6

AS BUILT PLANS

SCALE: 1" = 30'

PEAKING POWER PROJECT

3' THICK LAYER OF SHREDDED TIRES COVERING ENTIRE TOP

LEGEND

INSTRUMENTATION SUMMARY				
DESCRIPTION	NORTHING	EASTING		ELEVATION
3-1	1979614	6651805		65.0
3-2	1979614	6651805		60.5
3-3	1979605	6651989		61.0
3-4	1979605	6651989		59.0
3-5	1979571	6651785		66.0
3-6	1979571	6651785		60.5
3-7	1979627	6651804		65.0
3-8	1979627	6651804		60.5
3-9	1979619	6651888		61.0
3-10	1979619	6651888		58.5
3-11	1979497	6651888		66.0
3-12	1979497	6651785		60.5
3-13	1979624	6651948		56.0
3-14	1979481	6651941		56.0

YOLO COUNTY CENTRAL LANDFILL
SMUD Re-Gen Program
PEAKING POWER PROJECT
LAYER 3 PIPING AND INSTRUMENTATION

YOLO COUNTY
PLANNING AND PUBLIC WORKS
DIVISION OF INTEGRATED WASTE MANAGEMENT
292 West Beamer Street
Woodland, CA 95695-2598
Phone: (530) 666-8852   FAX: (530) 666-8853

DESIGN BY	RY	03/22/2006	REVISIONS
DRAWN BY	MW,KS,JK	03/22/2006	
CHECK BY	RY	03/22/2006	
SCALE: 1" = 30'			

PROJECT
YOLO COUNTY CENTRAL LANDFILL
SMUD Re-Gen
Program

SHEET NUMBER: 5

North Carolina State University

Laboratory Column Study

Table A1. Gas composition profiles at different depths of the columns on the 4th day of the experiment at a gas flow rate of 5 mL/min and air flow rate of 50 mL/min

Column[*]	Depth Below Top of the Compost (cm)	CO_2	O_2	N_2	CH_4
1	5.1	22.0	10.7	50.7	16.6
	20.3	44.5	1.4	8.6	45.4
	35.6	43.2	2.2	8.3	46.3
	50.8	45.6	1.1	3.7	49.6
2	5.1	11.7	12.6	70.0	5.7
	20.3	34.8	2.7	30.2	32.4
	35.6	43.0	1.2	9.1	46.6
	50.8	44.0	1.3	6.7	48.0
3	5.1	20.9	11.8	50.6	16.6
	20.3	42.1	1.9	16.8	39.2
	35.6	43.8	1.6	9.9	44.7
	50.8	45.3	1.1	4.9	48.7
5	5.1	22.6	11.4	47.5	18.6
	20.3	41.4	2.4	17.3	38.9
	35.6	44.5	1.4	7.9	46.2
	50.8	45.0	1.2	4.9	48.8
7	5.1	33.6	6.2	31.0	29.3

	20.3	44.6	1.5	5.3	48.6
	35.6	44.3	1.6	5.2	48.8
	50.8	45.7	1.1	3.0	50.3
	5.1	16.5	11.5	61.5	10.5
8	20.3	33.9	4.0	32.6	29.5
	35.6	43.0	1.2	11.7	44.1
	50.8	43.2	1.5	8.9	46.3

*No column 6 data due to problems with mass flow controller

Table A2. Gas composition profiles at different depths of the columns on the 55th day of the experiment at a gas flow rate of 5 mL/min and air flow rate of 50 mL/min

Column	Depth Below Top of the Compost (cm)	CO2	O2	N2	CH4
1	5.1	41.5	6.1	37.0	15.3
	20.3	46.8	1.5	5.0	46.7
	35.6	44.8	1.8	7.3	46.1
	50.8	46.9	0.9	3.3	48.9
2	5.1	17.1	11.2	64.5	7.3
	20.3	0.3	21.5	77.9	0.3
	35.6	47.4	0.7	3.0	49.0
	50.8	46.7	0.8	3.0	49.5
3	5.1	47.6	0.6	1.7	50.2
	20.3	47.1	0.6	1.8	50.4
	35.6	47.7	0.7	2.0	49.6
	50.8	47.4	0.7	2.0	49.9

Column	Depth Below Top of the Compost (cm)	CO2	O2	N2	CH4
	5.1	27.9	6.2	49.6	16.2
5	20.3	39.8	2.7	23.2	34.2
	35.6	46.8	0.6	6.7	45.9
	50.8	47.3	0.6	3.5	48.6
	5.1	19.3	9.1	63.3	8.3
6	20.3	28.2	7.0	44.6	20.2
	35.6	38.9	3.5	22.4	35.2
	50.8	36.1	5.4	23.3	35.2
	5.1	47.1	0.7	1.9	50.4
7	20.3	47.5	0.7	1.9	49.9
	35.6	47.7	0.6	1.6	50.2
	50.8	47.9	0.6	1.6	49.9
	5.1	46.9	0.7	2.1	50.3
8	20.3	47.6	0.6	1.6	50.2
	35.6	46.7	0.9	2.7	49.7
	50.8	47.5	0.6	1.5	50.4

Table A3. Gas composition profiles at different depths of the columns on the 62nd day of the experiment at a gas flow rate of 10 mL/min and air flow rate of 50 mL/min

Column	Depth Below Top of the Compost (cm)	CO2	O2	N2	CH4
	5.1	35.9	5.3	32.0	26.8
1	20.3	46.7	1.5	5.0	46.8
	35.6	44.5	2.4	8.4	44.6
	50.8	47.9	0.9	2.4	48.8
2	5.1	27.7	8.8	44.5	19.0

	20.3	NA	NA	NA	NA
	35.6	48.4	0.8	2.1	48.7
	50.8	47.9	0.9	2.5	48.7
3	5.1	49.0	0.6	1.7	48.6
	20.3	48.9	0.6	1.5	49.0
	35.6	48.6	0.7	1.7	49.0
	50.8	48.0	0.8	2.1	49.1
5	5.1	40.1	3.3	26.5	30.1
	20.3	47.0	1.3	6.4	45.3
	35.6	48.2	0.8	2.6	48.4
	50.8	48.4	0.7	1.7	49.2
6	5.1	32.0	5.5	41.0	21.5
	20.3	38.4	4.6	21.7	35.3
	35.6	46.5	1.5	5.9	46.1
	50.8	NA	NA	NA	NA
7	5.1	48.6	0.8	2.2	48.4
	20.3	48.6	0.8	1.9	48.8
	35.6	48.2	0.9	2.2	48.7
	50.8	48.2	0.8	1.8	49.2
8	5.1	48.8	0.7	1.9	48.6
	20.3	48.6	0.7	1.6	49.1
	35.6	NA	NA	NA	NA
	50.8	48.2	0.7	1.7	49.3

NA = Data were not available due to sampling problems

Table A4. Gas composition profiles at different depths of the columns on the 90th day of the experiment at a gas flow rate of 10 mL/min and air flow rate of 85 mL/min

Column	Depth Below Top of the Compost (cm)	CO2	O2	N2	CH4
	5.1	33.6	6.9	34.6	25.0
1	20.3	41.1	4.1	14.9	39.9
	35.6	44.6	2.8	10.0	42.6
	50.8	49.6	0.7	1.8	47.9
	5.1	20.7	11.4	50.3	17.7
2	20.3	NA	NA	NA	NA
	35.6	49.5	0.7	2.1	47.7
	50.8	49.3	0.7	2.0	47.9
	5.1	48.8	0.7	2.1	48.4
3	20.3	49.0	0.7	1.8	48.5
	35.6	49.8	0.7	1.5	48.0
	50.8	49.3	0.7	2.0	47.9
	5.1	36.0	6.7	33.0	24.3
5	20.3	43.1	3.1	11.4	42.4
	35.6	49.7	0.6	1.8	47.8
	50.8	49.4	0.6	1.7	48.2
	5.1	31.6	6.2	40.8	21.4
6	20.3	45.7	1.8	10.2	42.3
	35.6	48.3	1.2	4.3	46.3
	50.8	28.0	9.5	35.3	27.2
	5.1	48.4	0.9	2.4	48.3
7	20.3	49.0	0.7	1.6	48.7
	35.6	49.5	0.7	1.8	48.1
	50.8	49.5	0.6	1.4	48.5

A-11

Column	Depth Below Top of the Compost (cm)				

	5.1	48.7	0.7	1.9	48.6
8	20.3	48.9	0.7	1.5	48.9
	35.6	NA	NA	NA	NA
	50.8	49.4	0.6	1.4	48.6

NA = Data were not available due to sampling problems

Table A5. Gas composition profiles at different depths of the columns on the 121st day of the experiment at a gas flow rate of 15 mL/min and air flow rate of 85 mL/min

Column	Depth Below Top of the Compost (cm)	CO2	O2	N2	CH4
1	5.1	31.4	6.4	32.3	29.8
	20.3	NA	NA	NA	NA
	35.6	39.8	4.2	16.1	39.9
	50.8	49.3	0.6	1.9	48.1
2	5.1	26.5	9.8	43.2	20.6
	20.3	NA	NA	NA	NA
	35.6	48.7	0.6	1.9	48.8
	50.8	50.0	0.5	1.5	48.0
3	5.1	48.7	0.5	1.3	49.5
	20.3	48.8	0.6	1.4	49.2
	35.6	49.2	0.6	1.4	48.9
	50.8	49.3	0.7	2.0	47.9
5	5.1	36.0	6.7	33.0	24.3
	20.3	36.7	7.6	18.5	37.2
	35.6	48.6	0.7	2.1	48.5
	50.8	49.6	0.5	1.3	48.6

	5.1	36.7	4.7	29.0	29.6
6	20.3	44.0	2.4	9.6	43.9
	35.6	45.3	2.1	7.5	45.2
	50.8	22.3	11.4	44.6	21.7
	5.1	48.4	0.6	1.6	49.3
7	20.3	48.2	0.6	2.3	48.9
	35.6	48.7	0.7	1.9	48.7
	50.8	49.5	0.5	1.3	48.6
	5.1	47.9	0.8	2.4	48.9
8	20.3	48.8	0.6	1.4	49.3
	35.6	NA	NA	NA	NA
	50.8	50.2	0.4	1.0	48.4

NA = Data were not available due to sampling problems

Table A6. CH$_4$ emissions for alternate covers during the rainy season (gm CH$_4$/m^2-day)

Area	0.91 m compost + wood chips	0.31 m compost + wood chips	0.91 m compost	0.31 m compost	0.91 m green waste	0.61 m green waste	0.31 m green waste	0.31 m soil
	Gas System at Low Vacuum (47-63 cfm)							
1/23/06	21.5	0.0	0.3	14.1	3.9		0.0	23.6
1/24/06	27.8	0.0	0.2	22.4	3.2	0.3	0.0	19.1
1/24/06					5.3			9.4
1/25/06	21.9	0.0	0.1	20.3	6.8	2.0	0.0	13.5
1/25/06	21.2	0.0	0.1	23.8	9.4	0.3	0.5	1.1
1/25/06	11.8	0.0		21.5	3.6		0.4	
	Gas System at High Vacuum (117 cfm)							
1/30/06	6.39	0.00	0.25	4.09	6.25	0.61	0.00	1.71
1/30/06	5.69	0.00		2.54	3.33			1.99
1/31/06	0.40	0.00	0.24	0.69	1.69	0.01	0.00	2.12
1/31/06	0.63	0.00	0.00	1.78	2.10	0.00	0.00	0.90

1/31/06			0.07				0.00	
1/31/06							0.00	

Table A7. CH$_4$ emissions for alternate covers during the dry season (gm CH$_4$/m^2-day)

Area	0.91 m compost + wood chips	0.31 m compost + wood chips	0.91 m compost	0.31 m compost	0.91 m green waste	0.61 m green waste	0.31 m green waste	0.31 m soil	Side Slope green waste and shredded tires	Side Slope close to bottom, green waste only
	Gas System at Low Vacuum (30 cfm)									
11/15/06	0	0.014	0.005	0	0.039	0.02	2.07	22.97		
11/16/06	0	0	0	0	0.037	0	3.30	1.22		
11/16/06	0	0.012	-0.013	-0.017	0	0	0.00	0.29		
11/16/06	0	0	0.010	0	0	-0.01	2.78	0.27		
11/16/06	0	0	0	0	0	0	1.84	1.52		
	Gas System at High Vacuum (60 cfm)									
11/29/06	0.008	0	0	0	0	0	0	-0.62	0	0
11/29/06	0	0	0	0	0.051	0	2.130	1.32	0	0.90
11/30/06	0	0	0	0	0.020	0.010	2.522	2.12	0.01	1.50
11/30/06	0	0	0	-0.010	0.016	0	2.276	2.79	-0.31	1.16
11/30/06	0	-0.002	0	0	0.019	0	1.316	0	0.06	2.84